

SATURN

MPR-SAT-FE-74-1

JANUARY 31, 1974

SATURN IB LAUNCH VEHICLE FLIGHT EVALUATION REPORT-SA-208

SKYLAB-4

(NASA-TM-X-72019) SATURN IB LAUNCH
VEHICLE FLIGHT EVALUATION REPORT SA-208
(SKYLAB-4) (NASA) 250 p HC \$7.50

N75-10140

CSCCL 22C

Unclas
G3/15 52706

PREPARED BY

SATURN FLIGHT EVALUATION WORKING GROUP



NATIONAL AERONAUTICS AND SPACE ADMINISTRATION

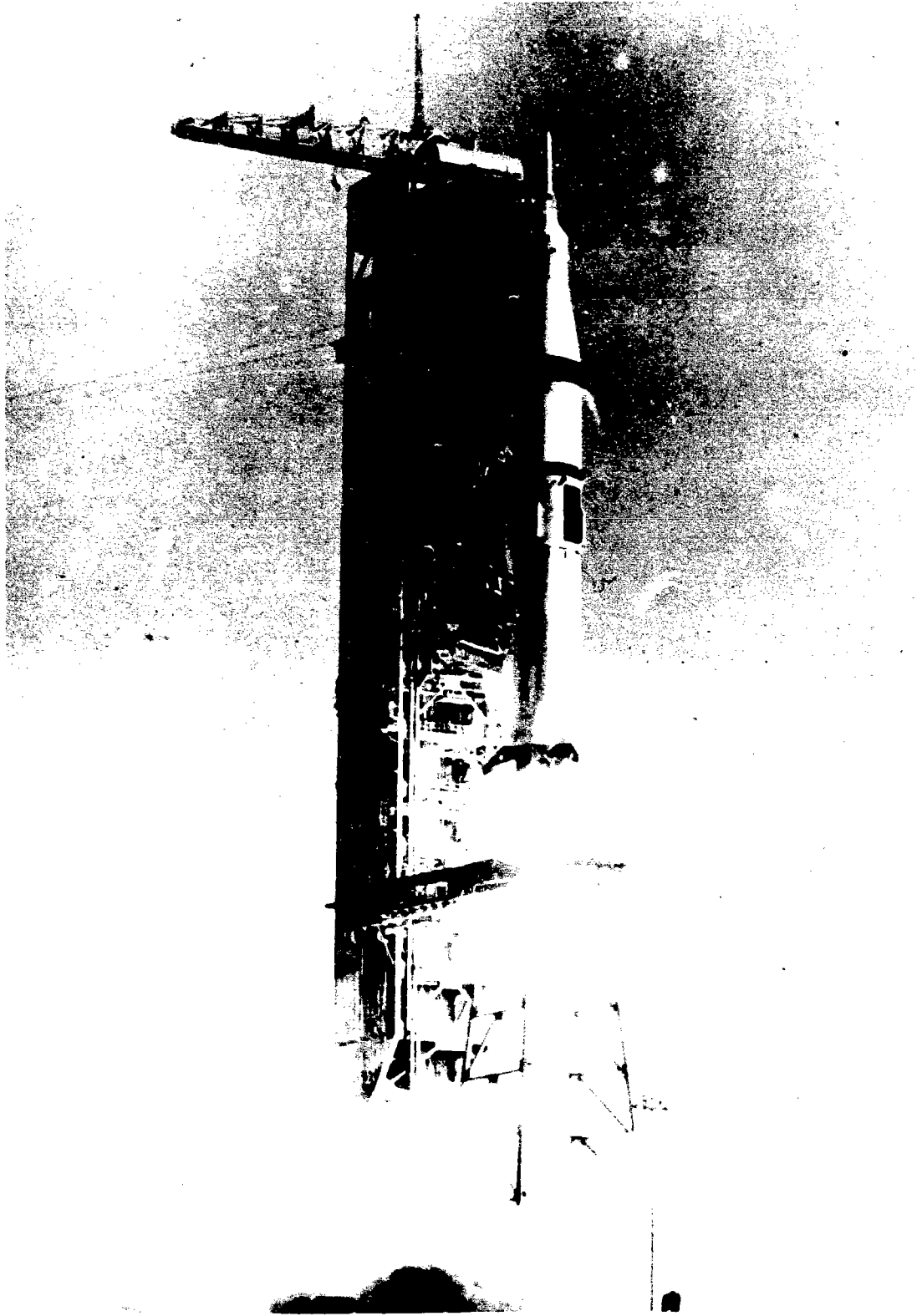
GEORGE C. MARSHALL SPACE FLIGHT CENTER

MPR-SAT-FE-74-1

JANUARY 31, 1974

**SATURN IB LAUNCH VEHICLE
FLIGHT EVALUATION
REPORT-SA-208
SKYLAB-4**

**PREPARED BY
SATURN FLIGHT EVALUATION
WORKING GROUP**



MPR-SAT-FE-74-1

SATURN IB LAUNCH VEHICLE FLIGHT EVALUATION REPORT - SA-208

SKYLAB-4

BY

Saturn Flight Evaluation Working Group

George C. Marshall Space Flight Center

ABSTRACT

The Saturn IB, SA-208 Launch Vehicle was launched on November 16, 1973 from Kennedy Space Center and placed the Command and Service Module containing three crew members into an 150.10 x 227.08 km altitude earth orbit. No anomalies occurred that seriously affected the mission.

Any questions or comments pertaining to the information contained in this report should be directed to:

Director, George C. Marshall Space Flight Center
Huntsville, Alabama 35812
Attention: Chairman, Saturn Flight Evaluation Working
Group, SAT-E (Phone 205-453-1030)

PRECEDING PAGE BLANK NOT FILMED

TABLE OF CONTENTS

	Page		Page
TABLE OF CONTENTS	iii	5.4 Impact	5-2
LIST OF ILLUSTRATIONS	v	SECTION 6 - S-IB PROPULSION	6-1
LIST OF TABLES	viii	6.1 Summary	6-1
ACKNOWLEDGEMENT	ix	6.2 S-IB Ignition Transient Performance	6-1
ABBREVIATIONS	xi	6.3 S-IB Mainstage Performance	6-2
MISSION PLAN	xv	6.4 S-IB Shutdown Transient Performance	6-6
FLIGHT SUMMARY	xvii	6.5 S-IB Stage Propellant Management	6-6
MISSION OBJECTIVES ACCOMPLISHMENT	xxi	6.6 S-IB Pressurization System	6-13
FAILURES AND ANOMALIES	xxiii	6.6.1 Fuel Pressurization System	6-13
		6.6.2 LOX Pressurization System	6-15
SECTION 1 - INTRODUCTION	1-1	6.7 S-IB Pneumatic Control Pressure System	6-18
1.1 Purpose	1-1	6.8 S-IB Hydraulic System	6-18
1.2 Scope	1-1	SECTION 7 - S-IVB PROPULSION	7-1
1.3 Performance Predictions Baseline	1-1	7.1 Summary	7-1
SECTION 2 - EVENT TIMES	2-1	7.2 S-IVB Chilldown and Buildup Transient Performance	7-2
2.1 Summary of Events	2-1	7.3 S-IVB Mainstage Performance	7-2
2.2 Variable Time and Commanded Switch Selector Events	2-1	7.4 S-IVB Shutdown Transient Performance	7-12
SECTION 3 - LAUNCH OPERATIONS	3-1	7.5 S-IVB Stage Propellant Management	7-12
3.1 Summary	3-1	7.6 S-IVB Pressurization System	7-13
3.2 Prelaunch Milestones	3-1	7.6.1 S-IVB Fuel Pressurization System	7-13
3.3 Terminal Countdown	3-1	7.6.2 S-IVB LOX Pressurization System	7-15
3.4 Propellant Loading	3-1	7.7 S-IVB Pneumatic Control Pressure System	7-20
3.4.1 RP-1 Loading	3-1	7.8 S-IVB Auxiliary Propulsion System	7-20
3.4.2 LOX Loading	3-3	7.9 S-IVB/IU Stage Deorbit Propellant Dump	7-25
3.4.3 LH ₂ Loading	3-3	7.10 S-IVB Orbital Coast and Safing	7-28
3.5 Ground Support Equipment	3-4	7.10.1 Fuel Tank Orbital Coast and Safing	7-28
3.5.1 Ground/Vehicle Interface	3-4	7.10.2 LOX Tank Orbital Coast and Safing	7-34
3.5.2 MSFC Furnished Ground Support Equipment	3-4	7.10.3 Cold Helium Dump	7-35
SECTION 4 - TRAJECTORY	4-1	7.10.4 Stage Pneumatic Control and Engine Control Sphere Safing	7-35
4.1 Summary	4-1		
4.2 Trajectory Evaluation	4-1		
4.2.1 Ascent Phase	4-1		
4.2.2 Orbital Phase	4-9		
SECTION 5 - S-IVB/IU DEORBIT TRAJECTORY	5-1		
5.1 Summary	5-1		
5.2 Deorbit Maneuvers	5-1		
5.3 Deorbit Trajectory Evaluation	5-2		

TABLE OF CONTENTS (CONTINUED)

	Page		Page
7.11 S-IVB Hydraulic System	7-35	11.4.1 Prelaunch Power Transfer Test Anomaly	11-13
SECTION 8 - STRUCTURES	8-1	11.5 Emergency Detection System	11-14
8.1 Summary	8-1	SECTION 12 - VEHICLE PRESSURE ENVIRONMENT	12-1
8.2 Total Vehicle Structures	8-1	12.1 S-IB Base Pressure	12-1
8.2.1 Longitudinal Loads	8-1	SECTION 13 - VEHICLE THERMAL ENVIRONMENT	13-1
8.2.2 Bending Moments	8-4	13.1 S-IB Base Heating	13-1
8.2.3 Combined Loads	8-8	SECTION 14 - ENVIRONMENTAL CONTROL SYSTEMS	14-1
8.2.4 Vehicle Dynamic Characteristics	8-8	14.1 Summary	14-1
8.3 Structural Assessment	8-17	14.2 S-IB Environmental Control	14-1
8.3.1 Fuel Tank Forward Bulkhead Damage	8-17	14.3 IU Environmental Control	14-1
8.3.2 Stress Corrosion Cracking	8-17	14.3.1 Thermal Conditioning System (TCS)	14-1
SECTION 9 - GUIDANCE AND NAVIGATION	9-1	14.3.2 Gas Bearing System (GBS)	14-2
9.1 Summary	9-1	14.3.3 Component Temperatures	14-2
9.2 Guidance Comparisons	9-1	SECTION 15 - DATA SYSTEMS	15-1
9.3 Guidance and Navigation Scheme Evaluation	9-6	15.1 Summary	15-1
9.3.1 First Stage Boost	9-6	15.2 Vehicle Measurement Evaluation	15-1
9.3.2 Second Stage Boost	9-6	15.3 Airborne Telemetry System Evaluation	15-1
9.3.3 Orbital Phase	9-6	15.3.1 IU DP-1 Telemetry Link RF Power Output Variations	15-2
9.3.4 Deorbit Phase	9-10	15.4 C-Band Radar System Evaluation	15-7
9.4 Guidance and Navigation System Components	9-10	15.5 Secure Range Safety Command Systems Evaluation	15-9
9.4.1 ST-124M Stabilized Platform System	9-10	15.6 Digital Command System Evaluation	15-9
9.4.2 Guidance Computer	9-12	15.7 Ground Engineering Cameras	15-9
SECTION 10 - CONTROL AND SEPARATION	10-1	SECTION 16 - MASS CHARACTERISTICS	16-1
10.1 Summary	10-1	16.1 Summary	16-1
10.2 S-IB Control System Evaluation	10-1	16.2 Mass Evaluation	16-1
10.3 S-IVB Control System Evaluation	10-2	SECTION 17 - SPACECRAFT SUMMARY	17-1
10.3.1 S-IVB Control System Evaluation During Burn	10-8	APPENDIX A - ATMOSPHERE	A-1
10.3.2 S-IVB Control System Evaluation During Orbit	10-8	APPENDIX B - SA-208 SIGNIFICANT CONFIGURATION CHANGES	B-1
10.3.3 S-IVB Control System Evaluation During Deorbit	10-14		
10.4 Instrument Unit Control Components Evaluation	10-19		
10.5 Separation	10-19		
10.5.1 S-IB/S-IVB Separation	10-19		
10.5.2 S-IVB/CSM Separation	10-19		
SECTION 11- ELECTRICAL NETWORKS AND EMERGENCY DETECTION SYSTEM	11-1		
11.1 Summary	11-1		
11.2 S-IB Stage Electrical System	11-1		
11.3 S-IVB Electrical System	11-4		
11.4 Instrument Unit Electrical System	11-9		

LIST OF ILLUSTRATIONS

Figure	Page	Figure	Page
2-1	LVDC Clock/Ground Time Difference	2-2	2-2
4-1	Ascent Trajectory Position Comparison	4-3	4-3
4-2	Ascent Trajectory Space-Fixed Velocity and Flight Path Angle Comparison	4-4	4-4
4-3	Ascent Trajectory Acceleration Comparison	4-5	4-5
4-4	Ascent Trajectory Dynamic Pressure and Mach Number Comparison	4-8	4-8
4-5	Launch Vehicle Ground Track	4-12	4-12
5-1	S-IVB/IU Stage Deorbit Altitude History (No Breakup Assumed)	5-3	5-3
5-2	S-IVB/IU Ground Track Dump to Impact	5-4	5-4
6-1	S-IB Engine Thrust Buildup	6-3	6-3
6-2	S-IB Stage Propulsion Performance	6-4	6-4
6-3	S-IB LOX Flowrate	6-5	6-5
6-4	S-IB Fuel Flowrate	6-5	6-5
6-5	S-IB Inboard Engines Total Thrust Decay	6-8	6-8
6-6	S-IB Outboard Engine Total Thrust Decay	6-9	6-9
6-7	S-IB LOX Mass Above Main LOX Valve	6-12	6-12
6-8	S-IB Fuel Mass Above Main Fuel Valve	6-12	6-12
6-9	S-IB Fuel Tank Ullage Pressure	6-14	6-14
6-10	S-IB Fuel Tank Helium Pressurization Sphere Pressure	6-16	6-16
6-11	S-IB Center LOX Tank Ullage Pressure	6-17	6-17
6-12	S-IB Center LOX Tank Ullage Pressure	6-19	6-19
6-13	S-IB GOX Flow Control Valve Position	6-20	6-20
6-14	S-IB Pneumatic Control Pressure	6-21	6-21
6-15	S-IB Maximum Gimbal Angle	6-23	6-23
7-1	S-IVB Start Box and Run Requirements	7-3	7-3
7-2	S-IVB Steady-State Performance	7-5	7-5
7-3	S-IVB Engine Control Bottle Pressure	7-6	7-6
7-4	S-IVB Gas Generator Chamber Pressure (D010)	7-8	7-8
7-5	S-IVB Gas Generator Valve Position	7-9	7-9
7-6	S-IVB Engine Regulator Outlet Pressure (D018)	7-10	7-10
7-7	S-IVB Engine Pneumatic System Pre-Start of Cutoff Mode	7-11	7-11
7-8	S-IVB LH ₂ Ullage Pressure - Preliftoff, Boost and Burn	7-14	7-14
7-9	S-IVB Fuel Pump Inlet Conditions	7-16	7-16
7-10	S-IVB LOX Tank Ullage Pressure - Boost Phase	7-17	7-17
7-11	S-IVB LOX Pump Inlet Conditions - Burn	7-18	7-18
7-12	S-IVB Cold Helium Supply History	7-19	7-19
7-13	S-IVB APS Module No. 1 Propellant Usage	7-21	7-21
7-14	S-IVB APS Module No. 2 Propellant Usage	7-22	7-22
7-15	S-IVB APS Chamber Pressure (Spacecraft Separation Disturbance)	7-24	7-24
7-16	S-IVB APS Valve, Injector, Thrust Chamber Assembly	7-26	7-26
7-17	S-IVB Deorbit Propellant Dump and Safing Sequence	7-27	7-27
7-18	S-IVB LOX Dump Parameter Histories	7-29	7-29
7-19	S-IVB LH ₂ Dump	7-30	7-30
7-20	S-IVB LH ₂ Ullage Pressure - Orbital Coast	7-31	7-31
7-21	S-IVB LH ₂ NPV Nozzle Pressure Oscillations	7-33	7-33
7-22	S-IVB LOX Tank Ullage Pressure - Orbit, Dump, and Safing	7-36	7-36
8-1	Longitudinal Acceleration During Thrust Buildup and Launch	8-2	8-2
8-2	Longitudinal Load from Strain Data at Station 942	8-2	8-2
8-3	Longitudinal Load Distribution at Time of Maximum Bending Moment and IECC	8-3	8-3
8-4	Longitudinal Acceleration During Cutoffs	8-4	8-4
8-5	Pitch Bending Moment Distributions at Time of Maximum Resultant Moment	8-5	8-5
8-6	Yaw Bending Moment Distributions at Time of Maximum Resultant Moment	8-6	8-6
8-7	Resultant Bending Moment Distributions at Time of Maximum Resultant Moment	8-7	8-7
8-8	Combined Loads Producing Minimum Safety Margin During SA-208 Flight	8-9	8-9

LIST OF ILLUSTRATIONS (CONTINUED)

Figure	Page	Figure	Page
8-9	Minimum Factor of Safety During SA-208 S-IB Flight	8-10	
8-10	Vibration Measured During First Stage Burn	8-11	
8-11	Vehicle Bending Frequencies	8-12	
8-12	Vehicle Bending Amplitudes	8-13	
8-13	Low Frequency Vibration and Pressure Oscillations Measured During S-IVB Stage Burn	8-14	
8-14	Low Frequency Analysis of Vibration and Engine Pressures	8-15	
8-15	S-IVB Engine Cutoff Transients	8-16	
8-16	S-IB Outrigger Assembly Channel Repair	8-18	
8-17	S-IB Fin Reinforcing Block Installation	8-19	
8-18	S-IB/S-IVB Interstage Reaction Beam	8-20	
9-1	SA-208 Trajectory and ST-124M Platform Velocity Comparisons (OMPT Minus LVDC)	9-2	
9-2	Roll Command During Boost	9-7	
9-3	Pitch Command During Boost	9-8	
9-4	Yaw Command During Boost	9-9	
9-5	SA-208 Inertially-Referenced Velocity Changes in Earth Orbit	9-11	
10-1	Pitch Plane Dynamics During S-IB Burn	10-3	
10-2	Yaw Plane Dynamics During S-IB Burn	10-4	
10-3	Roll Plane Dynamics During S-IB Burn	10-5	
10-4	Pitch and Yaw Plane Free Stream Angle of Attack During S-IB Burn	10-7	
10-5	Pitch Plane Dynamics - S-IVB Burn	10-9	
10-6	Yaw Plane Dynamics - S-IVB Burn	10-10	
10-7	Pitch Plane Dynamics During Orbit (Sheet 1 of 2)	10-12	
10-8	SA-208 Vehicle Dynamics During LH ₂ NPV Relief Venting	10-15	
10-9	Vehicle Dynamics During Deorbit (Sheet 1 of 2)	10-16	
10-10	S-IB/S-IVB Longitudinal Acceleration	10-20	
10-11	Angular Velocities During S-IB/S-IVB Separation	10-21	
11-1	S-IB 1D10 Battery Voltage and Current	11-2	
11-2	S-IB 1D20 Battery Voltage and Current	11-3	
11-3	S-IVB Stage Forward No. 1 Battery Voltage, Current, and Temperature	11-5	
11-4	S-IVB Stage Forward No. 2 Battery Voltage, Current, and Temperature	11-6	
11-5	S-IVB Stage Aft No. 1 Battery Voltage, Current, and Temperature	11-7	
11-6	S-IVB Stage Aft No. 2 Battery Voltage, Current, and Temperature	11-8	
11-7	IU 6D10 Battery Parameters	11-10	
11-8	IU 6D30 Battery Parameters	11-11	
11-9	IU 6D40 Battery Parameters	11-12	
12-1	S-IB Stage Heat Shield Pressure	12-2	
12-2	S-IB Stage Flame Shield Pressure	12-3	
12-3	S-IB Stage Heat Shield Loading	12-4	
12-4	S-IB Stage Base Drag Coefficient	12-5	
13-1	S-IB Stage Heat Shield Inner Region Total Heating Rate	13-2	
13-2	S-IB Stage Heat Shield Inner Region Radiation Heating Rate	13-3	
13-3	S-IB Stage Heat Shield Inner Region Gas Temperature	13-4	
13-4	S-IB Stage Heat Shield Outer Region Gas Temperature	13-5	
13-5	S-IB Stage Flame Shield Total Heating Rate	13-6	
13-6	S-IB Stage Flame Shield Gas Temperature	13-7	
13-7	S-IB Stage Flame Shield Radiation Heating Rate	13-8	
13-8	Variation of S-IB Flame Shield Radiant Heating with Inboard Engine Thrust	13-10	
13-9	Comparison of S-IB Stage Flame Shield Radiant Heating Data	13-11	
14-1	IU Sublimator Start Up Parameters for Initial Cycle	14-3	
14-2	IU TCS Coolant Control Parameters	14-4	
14-3	IU TCS Hydraulic Performance	14-5	
14-4	IU TCS GN ₂ Sphere Pressure (D25-601)	14-6	
14-5	IU Inertial Platform Internal Gas Bearing GN ₂ Pressure	14-7	

LIST OF ILLUSTRATIONS (CONTINUED)

Figure		Page
14-6	IU GBS GHz Sphere Pressure (D10-603)	14-8
14-7	Selected IU Component Temperatures	14-9
14-8	Selected IU Component Temperatures	14-10
15-1	SA-208 Telemetry Ground Station Coverage	15-5
15-2	SA-208 DP-1 Link RF Power Output	15-6
15-3	SA-208 C-Band Acquisition and Loss Times	15-8
A-1	Surface Weather Map Approximately 2 Hours Before Launch of SA-208/SL-4	A-2
A-2	500 Millibar Map Approximately 2 Hours Before Launch of SA-208/SL-4	A-4
A-3	Scalar Wind Speed at Launch Time of SA-208/SL-4	A-7
A-4	Wind Direction at Launch Time of SA-208/SL-4	A-9
A-5	Pitch Wind Velocity Component (W_x) at Launch Time of SA-208/SL-4	A-10
A-6	Yaw Wind Velocity Component (W_z) at Launch Time of SA-208/SL-4	A-11
A-7	Pitch (S_x) and Yaw (S_z) Component Wind Shears at Launch Time of SA-208/SL-4	A-12
A-8	Relative Deviation of Temperature and Pressure from the PRA-63 Reference Atmosphere, SA-208/SL-4	A-15
A-9	Relative Deviation of Density and Absolute Deviation of the Index of Refraction from the PRA-63 Reference Atmosphere, SA-208/SL-4	A-16

LIST OF TABLES

Table	Page	Table	Page	
1	Mission Objective Accomplishment	xxi	10-1 Liftoff Misalignment Summary	10-1
2	Summary of Failures and Anomalies	xxiii	10-2 Maximum Control Variables During S-IB Burn	10-6
2-1	Time Base Summary	2-2	10-3 Maximum Control Variables During S-IVB First Burn	10-11
2-2	Significant Event Times Summary	2-3	11-1 S-IB Stage Battery Power Consumption	11-4
2-3	Variable Time and Commanded Switch Selector Events	2-10	11-2 S-IVB Stage Battery Power Consumption	11-9
3-1	SA-208/Skylab-4 Prelaunch Milestones	3-2	11-3 IU Battery Power Consumption	11-13
4-1	Tracking Data Summary	4-2	15-1 SA-208 Measurement Summary	15-2
4-2	Comparison of Significant Trajectory Events	4-6	15-2 SA-208 Flight Measurements Waived Prior to Flight	15-3
4-3	Comparison of Cutoff Events	4-7	15-3 SA-208 Measurement Malfunctions	15-3
4-4	Comparison of Separation Events	4-7	15-4 SA-208 Launch Vehicle Telemetry Links Performance Summary	15-4
4-5	Comparison of S-IB Spent Stage Impact	4-10	15-5 SA-208 IU Commands	15-10
4-6	S-IB Spent Stage Impact Envelope	4-10	16-1 Vehicle Masses (Kilograms)	16-2
4-7	Comparison of Orbit Insertion Conditions	4-11	16-2 Vehicle Masses (Pounds)	16-3
5-1	S-IVB-208 Propellant Dump Desorbit Velocity	5-1	16-3 Vehicle Masses (Kilograms)	16-4
5-2	S-IVB-208 Impact Dispersion Limits	5-2	16-4 Vehicle Masses (Pounds)	16-5
6-1	S-IB Engine Start Characteristics	6-2	16-5 Flight Sequence Mass Summary	16-6
6-2	S-IB Individual Engine Propulsion Performance	6-7	16-6 Mass Characteristics Comparison	16-8
6-3	S-IB Stage Propellant Usage	6-10	A-1 Surface Observations at SA-208 Launch Time	A-3
6-4	Cutoff Level Sensor Actuation Characteristics	6-11	A-2 Solar Radiation at SA-208 Launch Time, Launch Pad 39B	A-5
6-5	S-IB Stage Propellant Mass History	6-11	A-3 Systems Used to Measure Upper Air Wind Data for SA-208	A-6
6-6	S-IB Actuator Maximum Performance Data	6-23	A-4 Maximum Wind Speed in High Dynamic Pressure Region for Saturn Launch Vehicles 201 through 208	A-13
7-1	S-IVB Steady State Performance (STDV Open +60 Second Time Slice at Standard Altitude Conditions)	7-4	A-5 Extreme Wind Shear Values in the High Dynamic Pressure Region for Saturn Launch Vehicles 201 through 208	A-14
7-2	S-IVB Stage Propellant Mass History	7-13	A-6 Selected Atmospheric Observations for Saturn Launch Vehicles 201 through 208 at Kennedy Space Center, Florida	A-18
7-3	S-IVB APS Propellant Consumption	7-23	B-1 S-IB Significant Configuration Changes	B-1
9-1	SA-208 Inertial Platform Velocity Comparisons	9-3	B-2 S-IVB Significant Configuration Changes	B-2
9-2	Navigation Position and Velocity Comparison (PACCS-12)	9-4	B-3 IU Significant Configuration Changes	B-2
9-3	SA-208 Boost Terminal Conditions	9-5		
9-4	SA-208 Orbital Phase Flight Program Attitude Commands	9-10		

ACKNOWLEDGEMENT

This report is published by the Saturn Flight Evaluation Working Group, composed of representatives of Marshall Space Flight Center (MSFC), Kennedy Space Center, and MSFC's prime contractors, and in cooperation with the Johnson Space Center. Significant contributions to the evaluation have been made by:

George C. Marshall Space Flight Center

Science and Engineering

Aero-Astroynamics Laboratory

Astrionics Laboratory

Computation Laboratory

Astronautics Laboratory

Saturn Program Office

John F. Kennedy Space Center

Lyndon B. Johnson Space Center

Chrysler Corporation

McDonnell Douglas Astronautics Company

International Business Machines Corporation

Rockwell International Corporation

General Electric Company

The Boeing Company

ABBREVIATIONS

A_B	Base Area	ECO	Engine Cutoff
ACN	Ascension Island	ECS	Environmental Control System
A_E	Engine Exit Area	EDS	Emergency Detection System
AOS	Acquisition of Signal	EST	Eastern Standard Time
APS	Auxiliary Propulsion System	EMR	Engine Mixture Ratio
ARIA	Apollo Range Instrumented Aircraft	EMRC	Engine Mixture Ratio Change
ASAP	Auxiliary Storage and Playback	EPO	Earth Parking Orbit
ASI	Augmented Spark Igniter	ESC	Engine Start Command
AUX	Auxiliary	FCC	Flight Control Computer
BDA	Bermuda	FM	Frequency Modulation
C_{DB}	Base Drag Coefficient	GBS	Gas Bearing System
CDDT	Countdown Demonstration Test	GCS	Guidance Cutoff Signal
CG	Center of Gravity	GDS	Goldstone
CIF	Central Instrumentation Facility	GFCV	GOX Flow Control Valve
CM	Command Module	GG	Gas Generator
C_p	Pressure Coefficient	GN ₂	Gaseous Nitrogen
C_{pB}	Base Pressure Coefficient	GRR	Guidance Reference Release
CSM	Command and Service Module	HAW	Hawaii
CYI	Canary Island	HE	Helium
DCS	Digital Command System	H ₂	Hydrogen
DOD	Department of Defense	HSK	Honeysuckle
EBW	Explosive Bridge Wire	Hz	Hertz
		I	Inclination

ABBREVIATIONS (CONTINUED)

IAPX	Power Transfer Test	Misc.	Miscellaneous
IBM	International Business Machines	ML	Mobile Launcher
ICD	Interface Control Document	MOV	Main Oxidizer Valve
IECO	Inboard Engine Cutoff	MR	Mixture Ratio
IGM	Iterative Guidance Mode	MSFC	Marshall Space Flight Center
IU	Instrument Unit	#, NO.	Number
JSC	Johnson Space Center	NASA	National Aeronautics and Space Administration
KSC	Kennedy Space Center	NPSH	Net Positive Suction Head
KWJ	Kwajalein	NPSP	Net Positive Suction Pressure
LH ₂	Liquid Hydrogen	OAT	Overall Test
LOS	Loss of Signal	OEEO	Outboard Engine Cutoff
LOX	Liquid Oxygen	OMPT	Observed Mass Point Trajectory
LSA	Level Sensor Actuation	OT	Operational Trajectory
LUT	Launch Umbilical Tower	OTBV	Oxidizer Turbine By-Pass Valve
LV	Launch Vehicle	OWS	Orbital Workshop (Modified S-IVB Stage)
LVDA	Launch Vehicle Data Adapter	Oxid.	Oxidizer
LVDC	Launch Vehicle Digital Computer	P _A	Ambient Pressure
MAD	Madrid	PACSS	Project Apollo Coordinate System Standard
Manf	Manifold	P _B	Base Pressure
MAX Q	Maximum Dynamic Pressure	PCM	Pulse Code Modulation
MCC-H	Mission Control Center - Houston	PEA	Platform Electronics Assembly
MILA	Merritt Island Launch Area	PWA	Printed Wiring Assembly

ABBREVIATIONS (CONTINUED)

Press.	Pressure	TAN	Tananarive
PSD	Power Spectral Density	TB	Time Base
PTCS	Propellant Tanking Computer System	TCS	Terminal Countdown Sequencer or Thermal Conditioning System
PU	Propellant Utilization	TEX	Corpus Christi, Texas
Qty.	Quantity	TM	Telemetry
q	Dynamic Pressure	TVC	Thrust Vector Control
R	Radius	UCR	Unsatisfactory Condition Report
RDSM	Remote Digital Sub- Multiple	US	United States
RF	Radio Frequency	UT	Universal Time
RFI	Radio Frequency Interference	VAB	Vertical Assembly Building
RLH	Petrograde Local Horizontal	V	Velocity
S/A	Service Arm	WLP	Wallops Island
SACS	Service Arm Control Switch	λ	Descending Node
SC	Spacecraft	θ	Path Angle
SCFM	Standard Cubic Feet per Minute		
SCIM	Standard Cubic Inches Per Minute		
SL	Skylab		
SLA	Spacecraft Lunar Module Adapter		
SM	Service Module		
S_{ref}	Reference Area		
SV	Space Vehicle		
SWS	Saturn Workshop		

SA-208 MISSION PLAN

The Saturn IP SA-208 (SL-4 Launch) is to place the Command and Service Module (CSM-118) in a 150 x 224 km (81 x 121 n.mi.) orbit coplanar with the orbiting Saturn Work Shop (SWS). SA-208 is comprised of the S-IB-8, S-IVB-208, and Instrument Unit (IU)-207. This is the third and final manned flight of the Skylab Program.

Launch is scheduled to occur on the 16th of November 1973 from Launch Complex 39, Pad B of the Kennedy Space Center (KSC) at 9:01 a.m. Eastern Standard Time (EST). Flight will be along an azimuth dependent on launch time. The nominal flight azimuth will be 53.781 degrees measured east of north. The launch window duration is 13 minutes. Vehicle weight at ignition is nominally 594,214 kg (1,310,021 lbm).

The S-IB stage powered flight will last approximately 141 seconds. The S-IVB stage will provide powered flight for approximately 434.7 seconds inserting the CSM into a phasing orbit for rendezvous with the orbiting SWS. Then the S-IVB/IU will separate from the CSM.

On the fourth revolution, residual S-IVB stage propellants will be dumped through the J-2 engine to produce a deorbit impulse. By controlling vehicle attitude, and time and duration of propellant dump, the spent S-IVB/IU will be directed towards impact in an island-free area of the Pacific Ocean.

After rendezvous, the crew will transfer from the CSM to the SWS to perform the on-orbit scheduled mission activities. These activities currently call for inhabiting the SWS for a maximum period of 84 days. After completion of these activities, the SWS will be prepared for long duration orbital storage. The crew will transfer to the CSM and the SWS will be left in a solar inertial attitude. The CSM will undock and deorbit for re-entry.

REPRODUCIBILITY OF THE
ORIGINAL PAGE IS POOR

FLIGHT SUMMARY

The space vehicle was launched at 09:01:23 Eastern Standard Time (EST) on 16 November, 1973 from pad 39B of the Kennedy Space Center (KSC), and placed the Command Service Module containing three crew members into earth orbit for rendezvous with the orbiting Saturn Work Shop. The performance of ground systems supporting the SA-208/Skylab-4 countdown and launch was satisfactory. Some concern was expressed during prelaunch countdown about stress-corrosion in the launch vehicle. The launch was re-scheduled from a November 10, 1973 date to replace all eight fins on the S-IB stage after post Countdown Demonstration Test inspections revealed cracks in the fin attachment fittings.

The vehicle was launched on an azimuth of 90 degrees east of north. A roll maneuver was initiated at approximately 10 seconds that placed the vehicle on a flight azimuth of 53.781 degrees east of north. The down range pitch program was also initiated at this time. The reconstructed flight trajectory (actual) was very close to the Post Launch Predicted Operational Trajectory (nominal). The S-IB stage Outboard Engine Cutoff (OECO) was 0.31 seconds later than nominal. The total space-fixed velocity at this time was 0.82 m/s greater than nominal. After separation, the S-IB stage continued on a ballistic trajectory until earth impact. The S-IVB burn terminated with guidance cutoff signal and was followed by parking orbit insertion, both events being 2.17 seconds earlier than nominal. An excess velocity of 0.73 m/s at insertion resulted in an apogee 2.84 km higher than nominal. The parking orbit portion of the trajectory from insertion to Command and Service Module/S-IVB separation was close to nominal. The crew-initiated separation of the CSM from the S-IVB stage occurred 20.45 seconds later than nominal.

All aspects of the S-IVB/IU deorbit were accomplished successfully. The propellant dump was performed as planned with impact occurring in the primary disposal area. Honeysuckle confirmed that the vehicle was safed following the propellant dump. Although breakup occurred after loss of signal at Kwajalein, Department of Defense sources confirmed the deorbit.

The S-IB stage propulsion system performance was satisfactory throughout flight. Stage longitudinal site thrust averaged 0.13 percent lower than predicted. Stage LOX, fuel, and total flowrates averaged 0.10 percent, 0.18 percent, and 0.13 percent lower than predicted, respectively. Stage mixture ratio averaged 0.08 percent higher than predicted. Stage specific impulse was within 0.04 percent of predicted. Inboard Engine Cutoff (IECO) occurred at 137.82 seconds (0.16 seconds earlier than predicted). OECO occurred 3.47 seconds after IECO at 141.29 seconds. OECO was initiated by LOX starvation, as planned. At OECO, the LOX residual was 2925 lbm compared to the predicted 3287 lbm, and the fuel residual was 6878 lbm compared to the predicted 5989 lbm. The stage hydraulic system performed satisfactorily.

The S-IVB propulsion system performed satisfactorily throughout the operational phase of burn and had normal start and cutoff transients. S-IVB burn time was 432.22 seconds, 2.46 seconds shorter than predicted for the actual flight azimuth of 53.8 degrees. This difference is composed of -0.07 second due to S-IB/S-IVB separation velocity, orbital radius, and weight and -2.39 seconds due to higher than predicted S-IVB performance. The engine performance during burn, as determined from standard altitude reconstruction analysis, deviated from the predicted Start Tank Discharge Valve (STDV) open +60 second time slice by +0.26 percent for thrust. Specific impulse was as predicted. The engine control system performed within expected limits. However, a helium leak was evidenced by greater than expected helium usage during mainstage. The S-IVB stage engine cutoff (ECO) was initiated by the Launch Vehicle Digital Computer (LVDC) at 577.18 seconds. The S-IVB residuals at engine cutoff were near nominal. The best estimate of the residuals at engine cutoff is 1581 lbm for LOX and 2093 lbm for LH₂ as compared to the predicted values of 2137 lbm for LOX and 1727 lbm for LH₂. The propellant tanks were vented satisfactorily following engine cutoff. During orbital coast, the LOX tank pressure increased more rapidly than predicted and went above the predicted limits. This was probably a result of the greater-than-expected LOX boiloff indicated by reconstruction of the orbital coast phase and the LOX dump. The increased LOX boiloff is an effect of the increased LOX tank wetted area resulting from propellant slosh. LOX slosh could have been induced by Auxiliary Propulsion System (APS) engine firing activity during LH₂ tank cyclic relief venting. The fuel tank nonpropulsive vent (NPV) system satisfactorily controlled fuel ullage pressure during earth orbit. Throughout the flight, APS Module No. 1 performed nominally. Module No. 2 functioned nominally except for the pitch engine. The pitch engine thrust was approximately 30% of nominal. This lower thrust level resulted in longer pitch engine on-time to provide the required attitude control system total impulse. This reduced performance has been attributed to partial blockage of the oxidizer injector area. During orbital coast, the APS responded to a disturbing force on the S-IVB/IU stage. LH₂ NPV venting cycles were time correlated with this disturbance. The APS activity and resulting propellant consumption on both modules was greater than expected. During this time period, 4200 seconds to 6000 seconds, the LH₂ NPV system was venting in a cyclic manner. Although the precise nature of the mechanism has not been established, similar response seems to be characteristic of the S-IVB/IU stage under certain conditions. There was no mission impact, and since the disturbing forces are small no further corrective action is planned other than allowing for additional APS propellant consumption in future predictions. The impulse derived from the LOX and fuel dumps was sufficient to satisfactorily deorbit the S-IVB/IU. The total impulse provided, 66,975 lbf-sec, was in good agreement with the real time nominal predicted value of 70,500 lbf-sec. The APS satisfied control system demands throughout the deorbit sequence. Propellant tank safing after fuel dump was satisfactory.

The structural loads experienced during the SA-208 flight were well below design values. The maximum bending moment was 10.3×10^6 in-lbf (approximately 18.5 percent of design) at vehicle station 942. The S-IB thrust cutoff transients experienced by SA-208 were comparable to those of the SA-207. The S-IVB engine cutoff transients did not produce the 55 Hz oscillations noted on the SA-207 flight. All vibration and pressure oscillations were nominal during the entire launch and there was no indication of any POGO instability. The maximum ground wind experienced during the prelaunch period was 21 knots and during launch was 7 knots. Both values were well below the allowable limits. There was no evidence during flight of any compromise of structural integrity due to either the prelaunch RP-1 tank bulkhead reversal or the stress corrosion incidents associated with the S-IB E-Beam, S-IB fin rear spar fitting, and S-IB/S-IVB interstage reaction beam.

The stabilized platform and the guidance computer successfully supported the accomplishment of the SA-208 Launch Vehicle mission objective. Targeted conditions at orbit insertion were attained with insignificant error. No anomalies nor deviations from nominal performance were noted. The stabilized platform indicated unplanned velocity changes between 3440 and 5735 seconds. The control and separation systems functioned correctly throughout the powered and coast flight of SA-208. Engine gimbal deflections were nominal. Bending and slosh dynamics were adequately stabilized during boost flight. Separation dynamics were normal.

The electrical systems and Emergency Detection System (EDS) of the SA-208 launch vehicle performed satisfactorily during the flight. Battery performance (including voltages, currents, and temperatures) was satisfactory and remained within acceptable limits. Operation of all power supplies, inverters, Exploding Bridge Wire (EBW) firing units, and switch selectors were nominal. During the countdown at T minus 75 minutes, an out-of-tolerance indication terminated the Instrument Unit (IU) internal power test by switching power to external.

Base pressure data obtained from SA-208 have been compared with preflight predictions and/or previous flight data and show good agreement.

Data from the seven SA-208 S-IB stage base thermal measurements have been compared with corresponding data from the flights of SA-203 through SA-207. These comparisons indicate an SA-208 base region thermal environment of comparable magnitude, with the flame shield radiant data trend being similar to that recorded on SA-207. All measured thermal environment data were well below S-IB stage design levels.

The S-IB stage engine compartment and instrument compartment require environmental control during prelaunch operations, but are not actively controlled during S-IB boost. The desired temperatures were maintained in both compartments during the prelaunch operation. The IU stage Environmental Control System (ECS) exhibited satisfactory performance for the duration of the IU mission. Coolant temperatures, pressures, and flowrates were continuously maintained within the required ranges and design limits.

The vehicle data systems performed satisfactorily except for a problem with the IU DP-1 telemetry link. This problem resulted in the loss of some IU and S-IVB data, but sufficient data were recovered to reconstruct all important flight information and to provide real time mission support. The overall measurement system reliability was 100 percent. The usual telemetry interference due to flame effects and staging was experienced. Usable telemetry data were received until 20,460 seconds (05:41:00). Good tracking data were received from the C-Band radar, with Kwajalein (KWJ) indicating final Loss of Signal (LOS) at approximately 21,180 seconds (05:53:00). The Secure Range Safety Command Systems on the S-IB and S-IVB stages were ready to perform their functions properly, on command, if flight conditions during launch phase had required destruct. The Digital Command System (DCS) performed satisfactorily from liftoff through deorbit. In general, ground engineering camera coverage was good.

Total vehicle mass, determined from post-flight analysis, was within 1.47 percent of predicted from ground ignition through S-IVB/spacecraft separation. Hardware weights, propellant loads and propellant utilization were close to predicted values during flight.

The SA-208/Skylab-4 space vehicle on the third visit to the Saturn Work Shop (SWS), was manned by Lieutenant Colonel Gerald P. Carr, Commander; Doctor Edward D. Gibson, Science Pilot; and Lieutenant Colonel William R. Pogue, Pilot. The Command and Service Module (CSM) was inserted into earth orbit approximately 9 minutes and 47 seconds after liftoff. The orbit achieved was 227.08 by 150.10 kilometers. Stationkeeping with the SWS began approximately 7.5 hours after liftoff. A hard dock was achieved at approximately 8 hours after liftoff following two unsuccessful docking attempts. Activation of the SWS was accomplished during visit days 2 through 4.

Undocking, CSM deorbit, and command module landing is planned for visit day 85, February 8 at 20:15:00 UT in the Pacific Ocean, southwest of San Diego, California.

MISSION OBJECTIVES ACCOMPLISHMENT

Table 1 presents the MSFC Launch Vehicle objective for Skylab-4 as defined in the "Saturn Mission Implementation Plan SL-4/SA-208," MSFC Document PM-SAT-8010.24, Revision A, dated July 20, 1973. An assessment of the degree of accomplishment can be found in other sections of this report as shown in Table 1.

Table 1. Mission Objective Accomplishment

NO.	LAUNCH VEHICLE OBJECTIVE	DEGREE OF ACCOMPLISHMENT	DISCREPANCIES	SECTION IN WHICH DISCUSSED
1	Launch and insert a manned CSM into the earth orbit targeted for during the final launch countdown. [SL-4 was targeted for an 81 x 121 n.mi. (150 x 224 km) orbit].	Complete	None	4.2

REPRODUCIBILITY OF THIS
ORIGINAL PAGE IS POOR

REPRODUCIBILITY OF THE ORIGINAL PAGE IS POOR

FAILURES AND ANOMALIES

Evaluation of the launch vehicle and launch vehicle ground support equipment data revealed the following five anomalies, none of which are considered significant.

Table 2. Summary of Failures and Anomalies

ITEM	SYSTEM	ANOMALY (PROBABLE CAUSE)	SIGNIFICANCE	CORRECTIVE ACTION	SECTION REFERENCE
1	S-1VB J-2 ENGINE	CONTROL HELIUM CONSUMPTION INCREASED TO AN ABNORMAL RATE AT 292 SECONDS AND REMAINED ABNORMAL UNTIL ENGINE CUTOFF (COMPONENT LEAKAGE DOWNSTREAM OF THE MAIN OXIDIZER VALVE SEQUENCE VALVE)	NONE. SUFFICIENT HELIUM AVAILABLE FOR ALL REQUIREMENTS. (APD 19C ANOMALY)	NONE. PREVIOUSLY IMPLEMENTED CHANGE COMBINED WITH SYSTEM INSPECTION PROVIDE ASSURANCE THAT REPEATITION IS UNLIKELY. CLOSED.	7.3
2	S-1VB AUXILIARY PROPULSION SYSTEM (APS)	MODULE NO. 2 TOTAL FUEL USAGE WAS APPROXIMATELY TWICE PREDICTED WHILE THE OXIDIZER USAGE WAS NEAR NOMINAL. (PARTIAL BLOCKAGE OF THE OXIDIZER SUPPLY DUE TO CORROSION CAUSED BY OXIDIZER SEEPING THROUGH THE QUAD VALVE).	NONE. SUFFICIENT PROPELLANTS AVAILABLE FOR NORMAL MISSION REQUIREMENTS. (APD 19C ANOMALY).	IMPLEMENT SPECIAL FLOW TEST PRIOR TO HYPERGOL LOADING TO ASSURE NO SYSTEM RESTRICTION. PERFORM HAZARDOUS GAS "SNIFF" TESTS TO DETECT LEAKAGE AFTER HYPERGOL LOADING. CLOSED.	7.8
3	GROUND SUPPORT SOFTWARE	IU 6D10 BATTERY CURRENT OUT OF TOLERANCE WHEN CHECKED BY THE POWER TRANSFER TEST (IAPX) SOFTWARE AT 7-75 MINUTES. (TEST TOO STRINGENT FOR BATTERY THAT HAD BEEN INACTIVE FOR SEVERAL HOURS).	NONE. IU CONSOLE ENGINEERS VERIFIED ACCEPTABLE INTERNAL POWER CONDITIONS BY MANUAL TESTS AND NO COUNT-DOWN DELAY WAS EXPERIENCED. (APD 19C ANOMALY).	1. POWER TRANSFER TEST LIMITS FOR THE IAPX HAVE BEEN REVISED. 2. MANUAL POWER TRANSFER TEST HAS BEEN MOVED FROM 7-7:00 TO THE 7-3:30 HOLD, REDUCING PERIOD OF BATTERY INACTIVITY. CLOSED.	3.3, 11.4.1
4	IU DP-1 TELEMETRY LINK	BETWEEN 600 AND 5400 SECONDS THERE WERE THREE UNEXPECTED SHIFTS IN THE RF POWER OUTPUT. AFTER 5400 SECONDS THE POWER OUTPUT REMAINED LOW. (INTERMITTENT OPEN CIRCUIT IN THE COAXIAL CONNECTORS DUE TO MECHANICAL INTERFERENCE IN MATING THE COAXIAL CONNECTORS AT THE POWER AMPLIFIER, OR OPEN/SHORT CIRCUIT IN TRANSMITTER SUB-ASSEMBLY).	NONE. SOME IU AND S-1VB TELEMETRY DATA WERE LOST, BUT SUFFICIENT DATA WERE RECOVERED TO RECONSTRUCT ALL IMPORTANT FLIGHT INFORMATION. (APD 19C ANOMALY).	SA-209 IU PCM RF ASSEMBLIES HAVE BEEN REMOVED TO REMOVE THE LOCK WASHER UNDER THE COAXIAL CONNECTOR JAM NUT ON THE POWER AMPLIFIER AND SECURE THE JAM NUT WITH LOCKING COMPOUND. ADDITIONAL REMARK INCLUDING INSPECTION AND REFLASHERMENT OF RF TRANSMITTER IS PLANNED FOR A3P. CLOSED.	15.3
5	S-1VB/IU	UNANTICIPATED VELOCITY CHANGES WERE INDICATED BY THE ST-124 STABLE PLATFORM ACCELEROMETERS DURING THE 3440 TO 5735 SECOND TIME PERIOD. (NOT FULLY EXPLAINED, BUT CLEARLY RELATED TO FUEL TANK VENTING CYCLES).	NO MISSION IMPACT (APD 19C ANOMALY).	NONE REQUIRED, BECAUSE THE SYSTEMS INVOLVED ARE PASSIVE AND THE FORCES SMALL.	7.10.1 10.3.2

SECTION 1

INTRODUCTION

1.1 PURPOSE

This report provides the National Aeronautics and Space Administration (NASA) Headquarters, and other interested agencies, with the results of the SA-208 launch vehicle flight evaluation (Skylab-4 launch). The basic objective of flight evaluation is to acquire, reduce, analyze, evaluate and report on flight data to the extent required to assure future mission success and vehicle reliability. To accomplish this objective, actual flight problems are identified, their causes determined, and recommendations made for appropriate corrective action.

1.2 SCOPE

This report contains the performance evaluation of the launch vehicle systems with special emphasis on problems. Summaries of launch operations and spacecraft performance are included.

The official George C. Marshall Space Flight Center (MSFC) position at this time is represented by this report. It will not be followed by a similar report unless continued analysis or new information should prove the conclusions presented herein to be significantly incorrect.

1.3 PERFORMANCE PREDICTIONS BASELINE

Unless otherwise noted, all performance predictions quoted herein for comparison purposes are those used in or generated by the Skylab-4 (SA-208) Post Launch Predicted Operational Trajectory (OT) S&E-AERO-MFP-162-73, dated November 28, 1973.

SECTION 2

EVENT TIMES

2.1 SUMMARY OF EVENTS

Range zero occurred at 09:01:23 Eastern Standard Time (EST) (14:01:23 Universal Time [UT]) November 16, 1973. Range time is the elapsed time from range zero, which, by definition, is the nearest whole second prior to liftoff signal, and is the time used throughout this report unless otherwise noted. Time from base time is the elapsed time from the start of the indicated time base. Table 2-1 presents the time bases used in the flight sequence program.

The start of Time Bases T₀ and T₁ were near nominal. T₂ and T₃ were initiated approximately 0.2 second early and 0.3 second late, respectively. These variations are functions of S-IB stage cutoff times discussed in Section 6 of this document. T₄ was initiated 2.2 seconds early, consistent with the early S-IVB engine cutoff discussed in Section 7. Start of T₅ was initiated by the receipt of a ground command, 1.9 seconds earlier than scheduled as discussed in Section 5.2.

Figure 2-1 shows the difference between telemetry signal receipt at a ground station and vehicle (Launch Vehicle Digital Computer [LVDC] clock) time. This difference between ground and vehicle time is a function of LVDC clock speed.

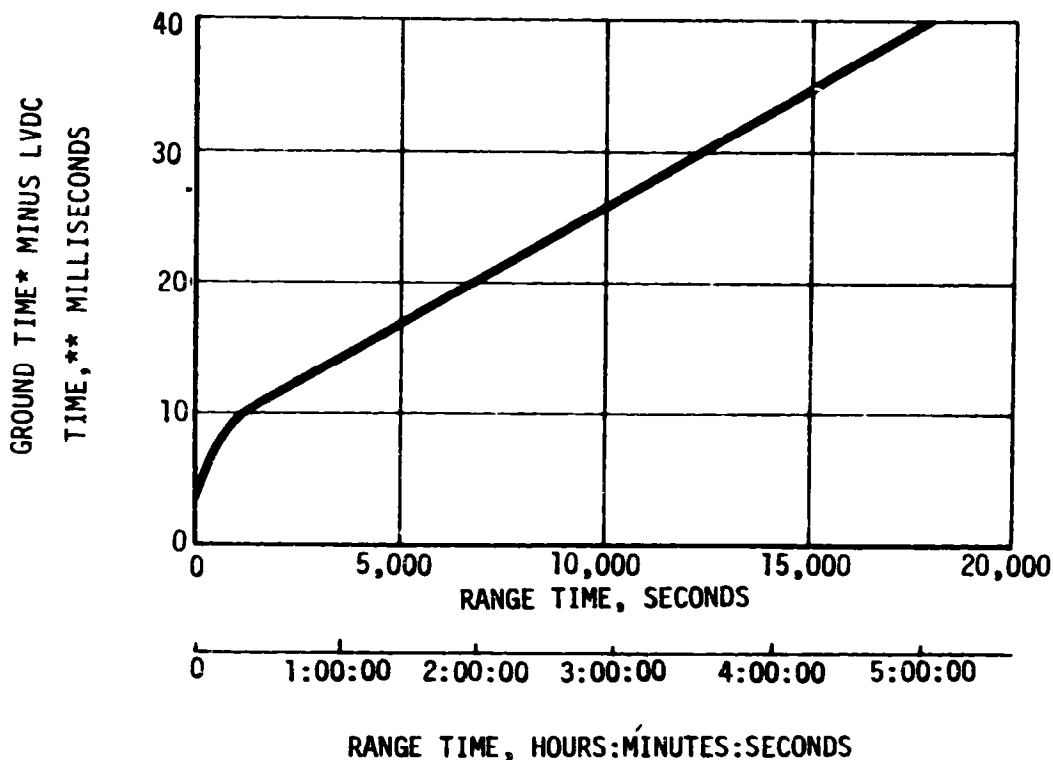
A summary of significant event times for SA-208 is given in Table 2-2. The preflight predicted times were adjusted to match the actual first motion time. The predicted times for establishing actual minus predicted times in Table 2-2 were taken from 68M00001C, "Interface Control Document Definition of Saturn SA-207 and Subs Flight Sequence Program" and from the Skylab-4 (SA-208) Post Launch Predicted Operational Trajectory (OT) S&E-AERO-MFP-162-73, dated November 28, 1973, unless otherwise noted.

2.2 VARIABLE TIME AND COMMANDED SWITCH SELECTOR EVENTS

Table 2-3 lists the switch selector events which were issued during the flight, but were not programmed for specific times.

Table 2-1. Time Base Summary

TIME BASE	RANGE TIME SECONDS	SIGNAL START
T ₀	-16.954	Guidance Reference Release
T ₁	0.471	IU Umbilical Disconnect Sensed by LVDC
T ₂	134.839	S-IB Low Level Sensors Dry Sensed by LVDC
T ₃	141.287	S-IB OECD Sensed by LVDC
T ₄	577.379	S-IVB ECO (Velocity) Sensed by LVDC
T ₅	18,637.674	Initiated by Receipt of Ground Command



- * RANGE TIME OF GROUND RECEIPT OF TELEMETERED SIGNAL FROM VEHICLE
- ** RANGE TIME OF OCCURENCE AS INDICATED BY UNCORRECTED LVDC CLOCK

Figure 2-1. LVDC Clock/Ground Time Difference

REPRODUCIBILITY OF THE
ORIGINAL PAGE IS POOR

Table 2-2. Significant Event Times Summary

ITEM	EVENT DESCRIPTION	RANGE TIME		TIME FROM BASE	
		ACTUAL SEC	ACT-PRED SEC	ACTUAL SEC	ACT-PRED SEC
1	GUIDANCE REFERENCE RELEASE (GRF)	-17.0	-0.1	-17.4	0.0
2	S-1H ENGINE START COMMAND	-3.1	-0.1	-3.5	0.0
3	S-1H START SIGNAL ENGINE NO. 7	-3.0	-0.1	-3.4	0.0
4	S-1H START SIGNAL ENGINE NO. 5	-3.0	-0.1	-3.4	0.0
5	S-1H START SIGNAL ENGINE NO. 6	-2.9	-0.1	-3.3	0.0
6	S-1H START SIGNAL ENGINE NO. 4	-2.9	-0.1	-3.3	0.0
7	S-1H START SIGNAL ENGINE NO. 2	-2.8	-0.1	-3.2	0.0
8	S-1B START SIGNAL ENGINE NO. 4	-2.8	-0.1	-3.2	0.0
9	S-1H START SIGNAL ENGINE NO. 3	-2.7	-0.1	-3.1	0.0
10	S-1H START SIGNAL ENGINE NO. 1	-2.7	-0.1	-3.1	0.0
11	RANGE ZERO	0.0		-0.5	
12	FIRST MOTION	0.3	0.0	-0.2	0.0
13	TO UMBILICAL DISCONNECT, START OF TIME BASE 1 (T1) LIFTOFF	0.5	0.0	0.0	0.0
14	SINGLE ENGINE CUTOFF ENABLE	3.4	-0.1	3.0	0.0
15	LOX TANK PRESSURIZATION SHUTOFF VALVES CLOSE	6.4	-0.1	6.0	0.0
16	BEGIN PITCH, YAW AND ROLL MANEUVER	10.3	-0.5	9.9	-0.4
17	MULTIPLE ENGINE CUTOFF ENABLE #1	10.4	-0.1	10.0	0.0
18	MULTIPLE ENGINE CUTOFF ENABLE #2	10.5	-0.1	10.1	0.0
19	TELEMETER CALIBRATE ON	20.4	-0.1	20.0	0.0
20	TELEMETER CALIBRATE OFF	25.4	-0.1	25.0	0.0
21	TELEMETRY CALIBRATOR IN-FLIGHT CALIBRATE ON	27.4	-0.1	27.0	0.0
22	TELEMETRY CALIBRATOR IN-FLIGHT CALIBRATE OFF	32.4	-0.1	32.0	0.0
23	LAUNCH VEHICLE ENGINES EDS CUTOFF ENABLE	40.4	-0.1	40.0	0.0

REPRODUCIBILITY OF THE
ORIGINAL PAGE IS POOR

Table 2-2. Significant Event Times Summary (Continued)

ITEM	EVENT DESCRIPTION	RANGE TIME		TIME FROM BASE	
		ACTUAL SEC	ACT-PRED SEC	ACTUAL SEC	ACT-PRED SEC
24	END ROLL MANEUVER	48.4	1.4	48.0	1.5
25	MACH 1	59.5	0.1	59.0	0.1
26	MAXIMUM DYNAMIC PRESSURE (MAX Q)	69.5	-4.9	69.0	-4.4
27	TELEMETRY CALIBRATION IN-FLIGHT CALIBRATE ON	90.0	-0.1	90.2	0.0
28	TELEMETRY CALIBRATION IN-FLIGHT CALIBRATE OFF	95.6	-0.1	95.2	0.0
29	FLIGHT CONTROL COMPUTER SWITCH POINT NO. 1	100.4	-0.1	100.0	0.0
30	FLIGHT CONTROL COMPUTER SWITCH POINT NO. 2	100.6	-0.1	100.2	0.0
31	TELEMETER CALIBRATION ON	120.2	-0.1	119.8	0.0
32	FLIGHT CONTROL COMPUTER SWITCH POINT NO. 3	120.4	-0.1	120.0	0.0
33	I/O CONTROL ACCEL. PWR OFF	120.7	0.0	120.2	0.0
34	TELEMETER CALIBRATION OFF	125.2	-0.1	124.8	0.0
35	TELEMETER CALIBRATE ON	126.4	-1.1	126.5	-1.0
36	TELEMETER CALIBRATE OFF	127.9	-1.1	127.4	-1.1
37	EXCESS RATE (P.Y.M) AUTO-ABORT INHIBIT ENABLE	128.0	-1.2	127.6	-1.1
38	EXCESS RATE (P.Y.M) AUTO-ABORT INHIBIT AND SWITCH RATE GYROS SC INDICATION 'A'	129.3	-0.1	128.9	0.0
39	S-18 TWO ENGINES OUT AUTO- ABORT INHIBIT ENABLE	129.6	0.0	129.1	0.0
40	S-18 TWO ENGINES OUT AUTO- ABORT INHIBIT	129.7	-0.1	129.3	0.0
41	PROPELLANT LEVEL SENSORS ENABLE	129.9	-0.1	129.5	0.0
42	TILT ARREST	130.9	0.1	130.5	0.2
43	S-18 PROPELLANT LEVEL SENSOR ACTUATION	134.8	-0.2	134.4	-0.1
44	START OF TIME BASE 2 (T2)	134.8	-0.2	0.0	0.0

Table 2-2. Significant Event Times Summary (Continued)

ITEM	EVENT DESCRIPTION	RANGE TIME		TIME FROM BASE	
		ACTUAL SEC	ACT-PRED SEC	ACTUAL SEC	ACT-PRED SEC
45	EXCESS RATE (HULL) AUTO-ABORT INHIBIT ENABLE	135.0	-0.2	0.2	0.0
46	EXCESS RATE (HULL) AUTO-ABORT INHIBIT AND SWITCH RATE GYROS SC INDICATION "H"	135.2	-0.2	0.4	0.0
47	INBOARD ENGINES CUTOFF (IECU)	137.92	-0.16	2.98	-0.02
48	AUTO-ABORT ENABLE RELAYS RESET	138.2	-0.2	3.4	0.0
49	CHARGE ULLAGE IGNITION FOR FIRING UNITS	138.4	-0.2	3.6	0.0
50	PREVALVES OPEN	139.1	-0.2	4.3	0.0
51	LOR DEPLETION CUTOFF ENABLE	139.3	-0.2	4.5	0.0
52	FUEL DEPLETION CUTOFF ENABLE	139.8	-0.2	5.0	0.0
53	S-1B OUTBOARD ENGINES CUTOFF (OECU)	141.29	0.31	6.45	0.45
54	START OF TIME BASE 3 (13)	141.3	0.3	0.0	0.0
55	LOR TANK PRESSURIZATION SHUTOFF VALVES OPEN	141.5	0.3	0.2	0.0
56	LOR TANK FLIGHT PRESSURE SYSTEM ON	141.6	0.3	0.3	0.0
57	S-1VB ENGINE CUTOFF NO. 1 OFF	141.7	0.3	0.4	0.0
58	S-1VB ENGINE CUTOFF NO. 2 OFF	141.8	0.3	0.5	0.0
59	MIXTURE RATIO CONTROL VALVE OPEN (4.851 EMM)	142.1	0.3	0.8	0.0
60	MIXTURE RATIO CONTROL VALVE BACKUP OPEN	142.2	0.3	0.9	0.0
61	ULLAGE MOTORS IGNITION	142.4	0.3	1.1	0.0
62	S-1B/S-1VB SEPARATION SIGNAL ON	142.5	0.2	1.3	0.0
63	S-1B/S-1VB PHYSICAL SEPARATION	142.9	0.5	1.6	0.2
64	S-1VB ENGINE START COMMAND	144.0	0.3	2.7	0.0
65	MAINSTAGE ENABLE ON (S-1VB STDV OPEN)	145.0	0.3	3.7	0.0
66	LMP TANK PRESSURIZATION CONTROL SWITCH ENABLE	146.6	0.3	5.3	0.0

REPRODUCIBILITY OF THE ORIGINAL PAGE IS POOR

Table 2-2. Significant Event Times Summary (Continued)

ITEM	EVENT DESCRIPTION	RANGE TIME		TIME FROM BASE	
		ACTUAL SEC	ACT-PRED SEC	ACTUAL SEC	ACT-PRED SEC
67	S-IVB MAINSTAGE OK PRESSURE SWITCH 1	146.8	0.4	5.5	0.1
68	S-IVB MAINSTAGE OK PRESSURE SWITCH 2	146.8	0.3	5.5	0.0
69	S-IVB MAINSTAGE	147.4	0.3	6.1	0.0
70	MIXTURE RATIO CONTROL VALVE CLOSE (5.5:1 EMR)	150.4	0.7	7.7	-1.0
71	CHARGE ULLAGE JETTISON EBW FIRING UNITS	151.4	0.2	10.2	0.0
72	ULLAGE MOTORS JETTISON	154.6	0.3	13.3	0.0
73	ENGINE MAINSTAGE ENABLE OFF	154.9	0.2	13.7	0.0
74	ULLAGE EBW FIRING UNITS RESET	159.5	-0.8	18.2	-1.1
75	ULLAGE MOTORS IGNITION AND JETTISON RELAYS RESET	160.8	0.3	19.5	0.0
76	HEAT-EXCHANGER BYPASS VALVE CONTROL ENABLE	165.2	0.2	24.0	0.0
77	TELEMETRY CALIBRATOR IN-FLIGHT CALIBRATE ON	166.7	0.3	25.4	0.0
78	TELEMETRY CALIBRATOR IN-FLIGHT CALIBRATE OFF	171.7	0.3	30.4	0.0
79	COMMAND ACTIVE GUIDANCE	177.6	0.6	36.3	0.3
80	FLIGHT CONTROL COMPUTER SWITCH POINT NO. 4	181.6	-1.4	40.3	-1.7
81	FLIGHT CONTROL COMPUTER SWITCH POINT NO. 5	343.2	-1.5	201.9	-1.8
82	TELEMETRY CALIBRATOR IN-FLIGHT CALIBRATE ON	346.7	0.3	205.4	0.0
83	TELEMETRY CALIBRATOR IN-FLIGHT CALIBRATE OFF	351.6	0.2	210.4	0.0
84	LM2 TANK PRESSURIZATION CONTROL SWITCH DISABLE	444.1	0.2	302.9	0.0
85	MIXTURE RATIO CONTROL VALVE OPEN (4.8:1 EMR)	469.3	0.2	328.1	0.0
86	S-IVB MIXTURE RATIO CONTROL VALVE OPEN	469.4	0.3	328.1	0.0
87	BEGIN IGM PHASE 2	471.2	0.3	329.9	-0.1

REPRODUCIBILITY OF THE ORIGINAL PAGE IS POOR

REPRODUCIBILITY OF THE
ORIGINAL PAGE IS POOR

Table 2-2. Significant Event Times Summary (Continued)

ITEM	EVENT DESCRIPTION	RANGE TIME		TIME FROM BASE	
		ACTUAL SEC	ACT-PRED SEC	ACTUAL SEC	ACT-PRED SEC
88	TELEMETRY CALIBRATOR INFLIGHT CALIBRATE ON	496.7	0.3	355.4	0.0
89	TELEMETRY CALIBRATOR INFLIGHT	499.9	-1.5	356.6	-1.6
90	PROPELLANT DEPLETION CUTOFF ARM	541.3	0.3	400.0	0.0
91	BEGIN TERMINAL GUIDANCE	553.0	-4.0	411.7	-4.3
92	GUIDANCE CUTOFF SIGNAL (GCS) ECU	577.16	-2.17	435.88	-2.49
93	S-IVB SOLENOID ACTIVATION SIGNAL	577.2	-2.3	435.9	-2.6
94	START OF TIME BASE 4 (14)	577.4	-2.2	0.0	0.0
95	S-IVB MAINSTAGE OK PRESSURE SWITCH DROPOUT #1	577.4	-2.3	0.0	-0.1
96	#2 INERTIAL ATTITUDE FREEZE	577.4	-2.3	0.0	-0.1
97	S-IVB ENGINE CUTOFF NO. 1 ON	577.5	-2.2	0.1	0.0
98	S-IVB ENGINE CUTOFF NO. 2 ON	577.6	-2.2	0.2	0.0
99	PNEUMATICS CLOSE	577.7	-2.2	0.3	0.0
100	LOX TANK NPV VALVE OPEN ON START LOX VENT	577.9	-2.3	0.6	0.0
101	LOX TANK PRESSURIZATION SHUT- OFF VALVES CLOSE ON	578.1	-2.3	0.8	0.0
102	LOX TANK FLIGHT PRESS SYSTEM OFF	578.3	-2.3	1.0	0.0
103	PROPELLANT DEPLETION CUTOFF DISARM	579.1	-2.3	1.8	0.0
104	S-IVB MIXTURE RATIO CONTROL VALVE CLOSE	579.6	-2.2	2.2	0.0
105	S-IVB MIXTURE RATIO CONTROL VALVE BACKUP CLOSE	579.7	-2.3	2.4	0.0
106	FLIGHT CONTROL COMPUTER S-IVB BURN MODE OFF 'A'	580.8	-2.3	3.5	0.0
107	FLIGHT CONTROL COMPUTER S-IVB BURN MODE OFF 'B'	581.0	-2.3	3.7	0.0
108	AUX HYDRAULIC PUMP FLIGHT MODE OFF	581.2	-2.3	3.9	0.0

Table 2-2. Significant Event Times Summary (Continued)

ITEM	EVENT DESCRIPTION	RANGE TIME		TIME FROM BASE	
		ACTUAL SEC	ACT-PRED SEC	ACTUAL SEC	ACT-PRED SEC
109	S/C CONTROL OF SATURN ENABLE	582.3	-2.3	5.0	0.0
110	MATE MEASUREMENTS SWITCH	583.3	-2.3	6.0	0.0
111	ORBIT INSERTION	587.2	-2.2	9.8	0.0
112	S-1VB ENGINE EDS CUTOFF DISABLE	587.3	-2.3	10.0	0.0
113	LH2 TANK LATCHING RELIEF VALVE OPEN ON	587.7	-2.3	10.4	0.0
114	LH2 TANK LATCHING RELIEF VALVE LATCH ON	589.7	-2.3	12.4	0.0
115	LH2 TANK LATCHING RELIEF VALVE OPEN OFF	591.0	-2.2	13.6	0.0
116	LH2 TANK LATCHING RELIEF VALVE LATCH OFF	592.1	-2.3	14.8	0.0
117	CHILLDOWN SHUTOFF VALVES CLOSE	597.3	-2.3	20.0	0.0
118	PITCH MANEUVER TO LOCAL HORIZ NOSE LEADING	598.5	-1.1	21.1	1.1
119	P.U. INVERTER AND DC POWER OFF	607.4	-2.2	30.0	0.0
120	LOX TANK NPV VALVE OPEN OFF END LOX VENT	607.9	-2.2	30.6	0.0
121	LOX TANK VENT AND NPV VALVES BOOST CLOSE ON	610.9	-2.3	33.6	0.0
122	LOX TANK VENT AND NPV VALVES BOOST CLOSE OFF	612.9	-2.3	35.6	0.0
123	CSM SEPARATION	1080.0	20.4	502.6	22.6
124	PREVALVES OPEN	1257.3	-2.3	680.0	0.0
125	CHILLDOWN SHUTOFF VALVES OPEN	1257.5	-2.3	680.2	0.0
126	LH2 TANK LATCHING RELIEF VALVE OPEN ON	1257.8	-2.2	680.4	0.0
127	LH2 TANK LATCHING RELIEF VALVE OPEN OFF	1258.7	-2.3	681.4	0.0
128	LH2 TANK VENT AND LATCHING RELIEF VALVES BOOST CLOSE ON	1261.7	-2.3	684.4	0.0
129	LH2 TANK VENT AND LATCHING RE- LIEF VALVES BOOST CLOSE OFF	1263.7	-2.3	686.4	0.0

ORIGINAL PAGE IS POOR

Table 2-2. Significant Event Times Summary (Continued)

ITEM	EVENT DESCRIPTION	RANGE TIME		TIME FROM BASE	
		ACTUAL SEC	ACT-PRED SEC	ACTUAL SEC	ACT-PRED SEC
130	PITCH MANEUVER TO LOCAL HORIZ TAIL LEADING	1334.5	54.9	757.1	57.1
131	IU/S-IVB DEORBIT COMMAND	15897.5	-102.8	15320.1	-100.5
132	START OF TIME BASE 5 (TS)	18637.7	-1.9	0.0	0.0
133	ENGINE HE CONTROL VALVE OPEN ON (START LOX DUMP)	18671.3	-1.9	33.6	0.0
134	ENGINE MAINSTAGE CONTROL VALVE OPEN OFF (END LOX DUMP)	19146.3	8.1	508.6	10.0
135	ENGINE HE CONTROL VALVE OPEN ON (START H2 DUMP)	19176.3	8.1	538.5	9.9
136	START SEQUENCE C STOP H2 DUMP START SIVB SAMING	19262.3	-0.9	624.6	1.0
137	S-IVB/IU IMPACT	21714.0	127.7	3076.3	129.6

Table 2-3. Variable Time and Commanded Switch Selector Events

FUNCTION	STAGE	RANGE TIME (SEC)	TIME FROM BASE (SEC)	REMARKS
Telemetry Calibrator In-Flight Calibrate On	IU	660.691	T4 + 83.312	Bermuda Revolution 1
TM Calibrate On	S-IVB	663.691	T4 + 86.312	" " "
TM Calibrate Off	S-IVB	664.692	T4 + 87.313	" " "
Telemetry Calibrator In-Flight Calibrate Off	IU	665.699	T4 + 88.320	" " "
Telemetry Calibrator In-Flight Calibrate On	IU	1244.710	T4 + 667.331	Madrid Revolution 1
TM Calibrate On	S-IVB	1247.720	T4 + 670.341	" " "
TM Calibrate Off	S-IVB	1248.726	T4 + 671.347	" " "
Telemetry Calibrator In-Flight Calibrate Off	IU	1249.710	T4 + 672.331	" " "
TM Calibrator In-Flight Calibrate On	IU	6716.716	T4 + 6139.337	Madrid Revolution 2
TM Calibrate On	S-IVB	6719.717	T4 + 6142.338	" " "
TM Calibrate Off	S-IVB	6720.718	T4 + 6143.339	" " "
Telemetry Calibrator In-Flight Calibrate Off	IU	6721.717	T4 + 6144.338	" " "
Water Coolant Valve Open	IU	6780.175	T4 + 6780.175	LVDC Function
Telemetry Calibrator In-Flight Calibrate On	IU	10980.765	T4 + 10403.386	Goldstone Revolution 2
TM Calibrate On	S-IVB	10983.756	T4 + 10406.377	" " "
TM Calibrate Off	S-IVB	10984.756	T4 + 10407.377	" " "
Telemetry Calibrator In-Flight Calibrate Off	IU	10985.765	T4 + 10408.386	" " "

Table 2-3. Variable Time and Commanded Switch Selector Events (Continued)

FUNCTION	STAGE	RANGE TIME (SEC)	TIME FROM BASE (SEC)	REMARKS
Telemetry Calibrator In-Flight Calibrate On	IU	12252.729	T4 + 11675.350	Madrid Revolution 3
TM Calibrate On	S-IVB	12256.729	T4 + 11679.349	
TM Calibrate Off	S-IVB	12257.728	T4 + 11680.350	
Telemetry Calibrator In-Flight Calibrate Off	IU	12257.05	T4 + 11679.68	TM Dropout, Timed From Compressed Data
Telemetry Calibrator In-Flight Calibrate On	IU	14756.761	T4 + 14179.382	Honeysuckle Revolution 3
TM Calibrate On	S-IVB	14759.750	T4 + 14182.371	
TM Calibrate Off	S-IVB	14760.750	T4 + 14183.371	
Telemetry Calibrator In-Flight Calibrate Off	IU	14761.750	T4 + 14184.371	
Telemetry Calibrator In-Flight Calibrate On	IU	15948.761	T4 + 15371.382	Hawaii Revolution 3
TM Calibrate On	S-IVB	15951.766	T4 + 15374.387	" " "
TM Calibrate Off	S-IVB	15952.761	T4 + 15375.382	" " "
Telemetry Calibrator In-Flight Calibrate Off	IU	15953.05	T4 + 15375.67	TM Dropout, Timed From Compressed Data
Telemetry Calibrator In-Flight Calibrate On	IU	17748.807	T4 + 17731.835	*
TM Calibrate On	S-IVB	17751.774	T4 + 17734.820	*
TM Calibrate Off	S-IVB	17752.782	T4 + 17735.828	*
TM Calibrator In-Flight Calibrate Off	IU	(17753)		**

* Telemetry dropout caused data processing problems. These commands were received by CYI Rev. 4 and are shown with the same Ground Range Times as in Table 3-3.

** This command occurred at a time when the quality of the data received was so poor it was not processed.

13-00000

SECTION 3

LAUNCH OPERATIONS

3.1 SUMMARY

The space vehicle was launched at 09:01:23 Eastern Standard Time (EST) on 16 November, 1973 from pad 39B of the Kennedy Space Center (KSC), Saturn Complex. Damage to the pad, Launch Umbilical Tower (LUT) and support equipment was considered minimal.

The performance of ground systems supporting the SA-208/Skylab-4 countdown and launch was satisfactory. Some concern was expressed during prelaunch countdown about stress-corrosion in the launch vehicle. The launch was rescheduled from a November 10, 1973 date to replace all eight fins on the S-IB stage after post Countdown Demonstration Test (CDDT) inspections revealed cracks in the fin attachment fittings.

3.2 PRELAUNCH MILESTONES

A chronological summary of prelaunch milestones is contained in Table 3-1. The fuel tank damage problem is discussed in paragraphs 3.4.1 and 8.3.1. The stress corrosion problem is discussed in Paragraph 8.3.2.

3.3 TERMINAL COUNTDOWN

The SA-208/Skylab-4 terminal countdown was interrupted to allow for removal and replacement of the S-IB fins (see paragraph 3.4.1). The countdown was resumed on 14 November with the space vehicle countdown start at T-42.5 hours. Scheduled holds were initiated at T-3 hours 30 minutes for a duration of 60 minutes and at T-15 minutes for a duration of 2 minutes. During the countdown power transfer test (IAPX) the IU internal power was automatically returned to external indicating an out-of-tolerance IU Power measurement. The IU console engineers verified acceptable IU internal power conditions by manual tests immediately after the IAPX test was completed. The power transfer by terminal countdown sequencer at T-50 seconds was accomplished smoothly and no countdown delay was experienced (see paragraph 11.4.1). The space vehicle was launched at 09:01:23 EST on 16 November, 1973.

3.4 PROPELLANT LOADING

3.4.1 RP-1 Loading

The RP-1 system successfully supported countdown and launch. Fuel was initially placed onboard the S-IB stage October 23, 1973. During a normal gravity drain to the 600-inch level, the bulkheads were subjected to a negative pressure because the vent covers had not been removed.

Table 3-1. SA-208/Skylab-4 Prelaunch Milestones

DATE	ACTIVITY OR EVENT
November 4, 1971	S-IVB-208 Stage Arrival
June 12, 1973	Instrument Unit (IU) S-IU-207 Arrival
June 20, 1973	S-IB-8 Stage Arrival
July 31, 1973	S-IB Erection on Mobile Launcher (ML)-1
July 31, 1973	S-IVB Erection
August 1, 1973	IU Erection
August 4, 1973	Launch Vehicle (LV) Electrical Systems Test Complete
August 14, 1973	LV Transfer to Pad B
August 20, 1973	LV Propellant Dispersion/Malfunction Overall Test (OAT)
August 22, 1973	SV OAT 1 (Plugs In)
August 30, 1973	Space Vehicle (SV) Electrical Mate
October 11, 1973	SV Flight Readiness Test (FRT) Complete
October 23, 1973	RP-1 Loaded (forward fuel tank bulkhead damage)
October 25, 1973	S-IB Forward fuel tank bulkhead re-formed
November 2, 1973	Countdown Demonstration Test (CDDT) Completed (Wet)
November 7, 1973	RP-1 Drain (for fin replacement)
November 13, 1973	S-IB Fin Replacement Complete
November 14, 1973	RP-1 Reloaded
November 14, 1973	Launch Countdown Begun
November 16, 1973	SL-4 Launch

This resulted in localized curvature reversal of the upper bulkheads of tanks F3 and F4. The bulkheads were returned to flight-worthy configuration by applying a positive pressure to the fuel ullage (see paragraph 8.3.1). On November 7, 1973 the fuel was drained from the S-IB stage to reduce the load on the fins to allow their removal and replacement (see paragraph 8.3.2).

Fuel was again placed onboard the S-IB stage November 14, 1973. Tail service mast fill and replenish was accomplished at T-8 hours and level adjust/line inert at about T-1 hour. Both operations were completed satisfactorily as planned. Launch countdown support consumed 41,522 gallons of RP-1.

The fuel temperature was monitored during the launch countdown and at T-1 hour, a final fuel temperature of 57°F was projected to ignition. The final fuel density was obtained using the projected temperature. When the fuel level was raised to the overfill sensor level 8-1/2 hours prior to launch, the Propellant Tanking Computer System (PTCS) mass readout indicated no error in the fuel height. No error correction was required to the final PTCS number.

3.4.2 LOX Loading

The LOX loading system successfully supported countdown and launch. The fill sequence began with S-IB chilldown November 16 at 12:42:00 A.M. EST and was completed 1 hour 50 minutes later with all stage replenish. Replenish was automatic through the Terminal Countdown Sequencer (TCS) without incident. LOX consumption during launch countdown was 133,000 gallons.

LOX was reported emanating occasionally from the four outboard tank vent valves during the countdown. The magnitude and frequency of these discharges were considered to be less than those observed during the countdown of SA-207.

The LOX vent valves were closed for three periods during the countdown to preclude the possibility of safety hazards to personnel from LOX discharges. Each of the three vent closure periods was approximately two minutes in duration.

3.4.3 LH₂ Loading

The LH₂ system successfully supported countdown and launch. The fill sequence began at 02:20:22 EST and normal S-IVB replenish was established at 03:15:28 EST. Replenish was nominal and was terminated at the start of terminal countdown sequence. Launch countdown support consumed about 125,000 gallons of LH₂.

3.5 GROUND SUPPORT EQUIPMENT

3.5.1 Ground/Vehicle Interface

In general, performance of the ground service systems supporting all stages of the launch vehicle was satisfactory. Overall damage to the pad, LUT, and support equipment from blast and flame impingement was considered minimal. Detailed discussion of the Ground Support Equipment is contained in KSC Skylab/Saturn IB (SA-208) "Ground Support Evaluation Report".

The Propellant Tanking Computer Systems (PTCS) adequately supported all countdown operations and there was no launch damage.

The Environmental Control System (ECS) performed satisfactorily through the countdown and launch. Changeover from air to GN₂ occurred at 23:56:00 EST on November 15, 1973.

The Service Arm Control Switches (SACS) satisfactorily supported SL-4 countdown and launch. Readjustment was required after S-IB fin replacement. Launch damage was minimal.

The hydraulic charging unit and service arms 1A, 6, 7 and 8 satisfactorily supported the SL-4 countdown and launch. Performance was nominal during terminal count and liftoff.

The damping systems supported the countdown and launch. There were no system failures.

The Digital Event Evaluator -3 and -6 systems satisfactorily supported all countdown operations. There was no system damage.

3.5.2 MSFC Furnished Ground Support Equipment

All ground power and battery equipment supported the prelaunch operations satisfactorily. All systems performed within acceptable limits. The hazardous gas detection system successfully supported SL-4 countdown.

SECTION 4

TRAJECTORY

4.1 SUMMARY

The Skylab-4 vehicle was launched at 09:01:23 Eastern Standard Time (Range Zero), November 16, 1973, from Pad 39B at Kennedy Space Center. The vehicle was launched on an azimuth of 90 degrees east of north. A roll maneuver was initiated at approximately 10 seconds that placed the vehicle on a flight azimuth of 53.781 degrees east of north. The down range pitch program was also initiated at this time.

The reconstructed flight trajectory (actual) was very close to the Post Launch Predicted Operational Trajectory (nominal). The S-IB stage Out-board Engine Cutoff (OECO) was 0.31 seconds later than nominal. The total space-fixed velocity at this time was 0.82 m/s greater than nominal. After separation, the S-IB stage continued on a ballistic trajectory until earth impact. The S-IVB burn terminated with guidance cutoff signal and was followed by parking orbit insertion both 2.17 seconds earlier than nominal. An excess velocity of 0.73 m/s at insertion resulted in an apogee 2.84 km higher than nominal.

The parking orbit portion of the trajectory from insertion to Command and Service Module (CSM)/S-IVB separation was close to nominal. The crew-initiated separation of the CSM from the S-IVB stage occurred 20.45 seconds later than nominal.

4.2 TRAJECTORY EVALUATION

The standard coordinate systems used in the following paragraphs are defined in S&E-AERO-MFT-10-74, "SL-4 (SA-208) Launch Vehicle Postflight Trajectory".

4.2.1 Ascent Phase

The ascent phase spans the interval from guidance reference release through parking orbit insertion. The ascent trajectory was established from telemetered guidance velocity data and tracking data from five C-Band stations and one S-Band station listed in Table 4-1. Approximately 2 percent of the tracking data was rejected due to inconsistencies. The initial launch phase trajectory (from first motion to 20 seconds) was established by a least squares curve fit of the initial portion of the ascent trajectory developed above. Comparisons between the resultant best estimate trajectory and the available tracking data show consistency and good agreement.

Table 4-1. Tracking Data Summary

DATA SOURCE, TYPE	PHASE	RANGE TIME INTERVAL (SEC)
BERMUDA, C-BAND	ASCENT	290 - 620
BERMUDA, C-BAND	ORBITAL	577 - 709
BERMUDA, S-BAND	ASCENT	413 - 620
BERMUDA, S-BAND	ORBITAL	597 - 747
CAPE KENNEDY, C-BAND	ASCENT	1 - 418
HAWAII, C-BAND	ORBITAL	15,997 - 16,195
MERRITT ISLAND, C-BAND	ASCENT	6 - 524
PATRICK, C-BAND	ASCENT	25 - 514
TANANARIVE, C-BAND	ORBITAL	7807 - 8167
TANANARIVE, C-BAND	ORBITAL	13,333 - 13,693
WALLOPS ISLAND, C-BAND	ASCENT/ORBITAL	210 - 620

Telemetered guidance data were used as a model for obtaining proper velocity and acceleration profiles through the transient areas of Mach 1, maximum dynamic pressure, S-IB thrust decay and S-IVB thrust decay.

Actual and nominal altitude, cross range, and surface range for the boost phase are presented in Figure 4-1. Figure 4-2 presents similar comparisons of space fixed velocity and flight path angle. Comparisons of actual and nominal non-gravitational accelerations are displayed in Figure 4-3. Inspection shows the actuals were very close to the nominal values.

Trajectory parameters at significant events are presented in Table 4-2. Table 4-3 presents the trajectory conditions at engine cutoffs. Table 4-4 presents significant parameters at the S-IB/S-IVB and S-IVB/CSM separation events

The S-IB stage OECO was a result of LOX depletion. The S-IVB cutoff signal was issued by the guidance computer when end conditions were satisfied.

ε-t

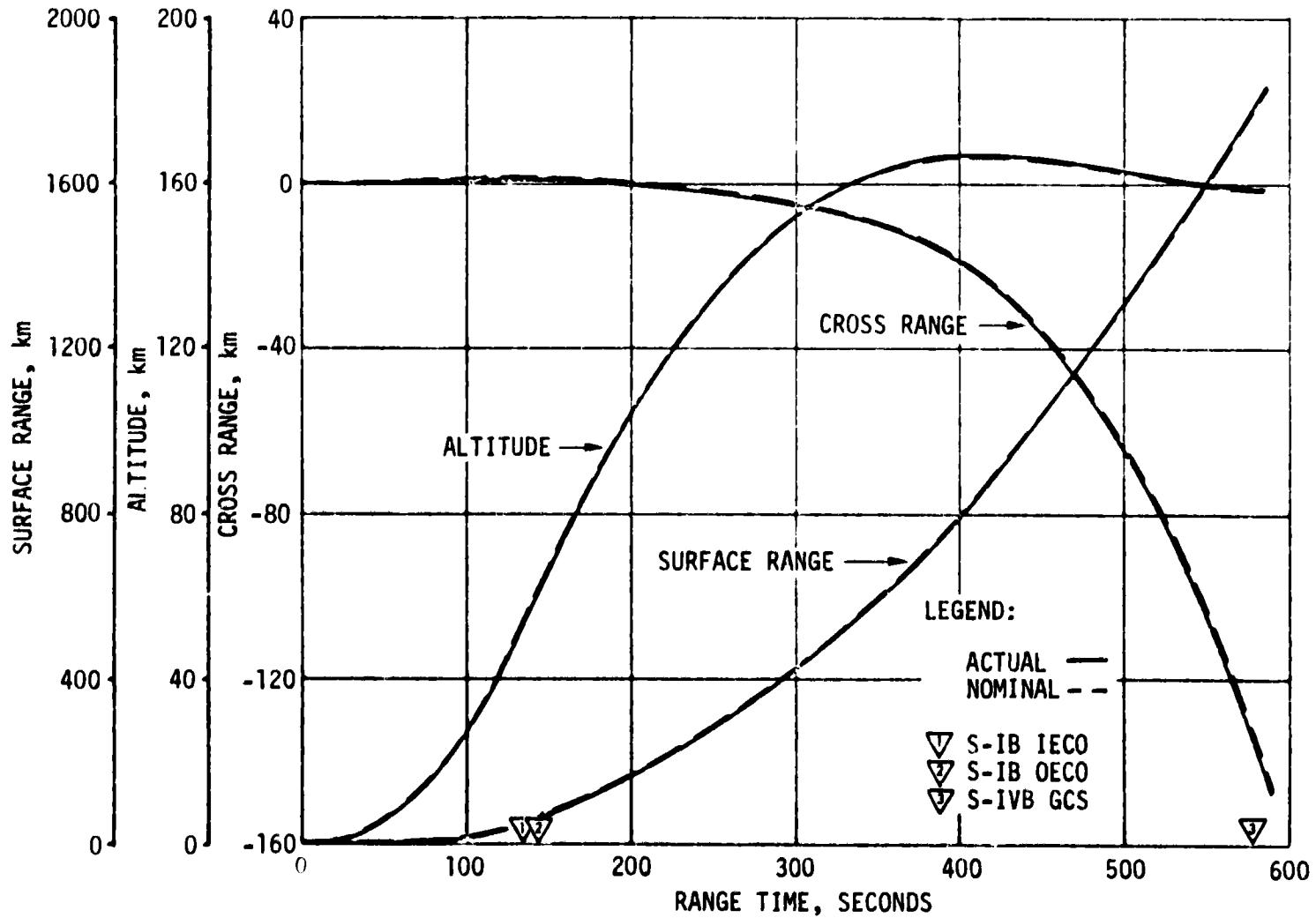


Figure 4-1. Ascent Trajectory Position Comparison

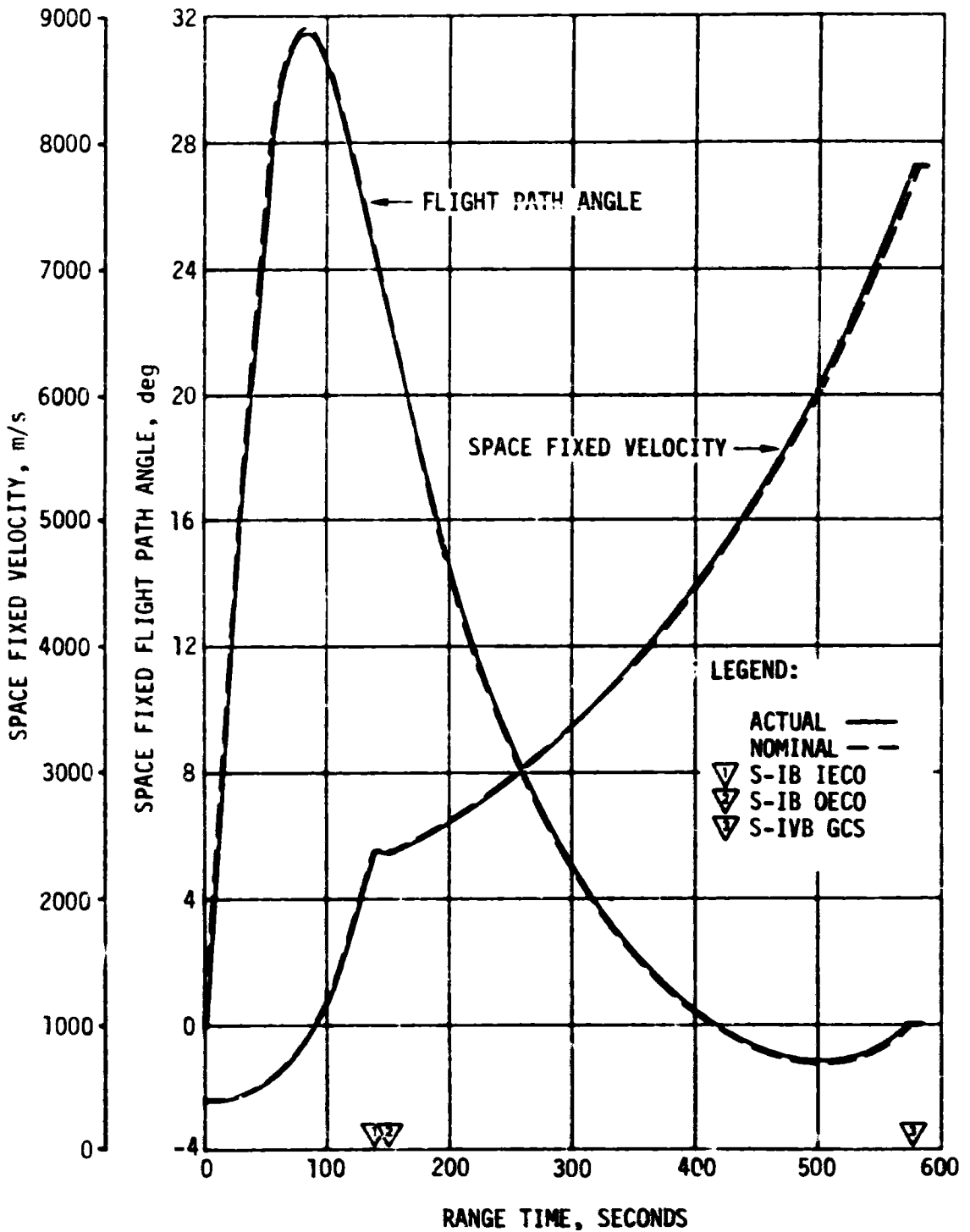


Figure 4-2. Ascent Trajectory Space-Fixed Velocity and Flight Path Angle Comparison

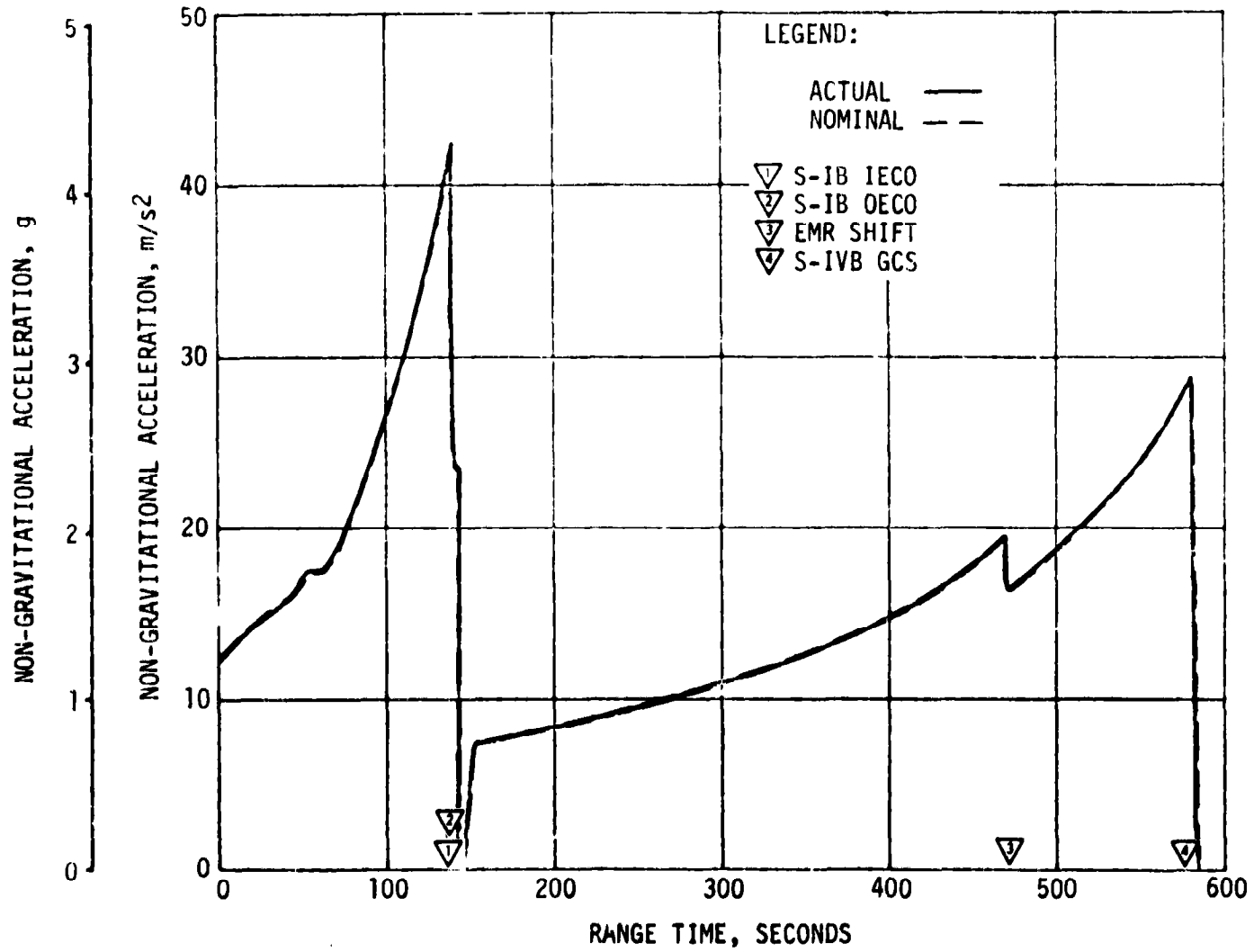


Figure 4-3. Ascent Trajectory Acceleration Comparison

Table 4-2. Comparison of Significant Trajectory Events

EVENT	PARAMETER	ACTUAL	NOMINAL	ACT-NOM
First Motion	Range Time, sec	0.271	0.271	0.000
	Non-Gravitational Acceleration, m/s ²	12.347	12.218	0.129
Mach 1	Range Time, sec	59.500	59.372	0.128
	Altitude, km	7.48	7.47	0.01
Maximum Dynamic Pressure	Range Time, sec	69.500	74.358	-4.858
	Dynamic Pressure, N/cm ²	3.258	3.337	-0.079
	Altitude, km	10.72	12.59	-1.87
* Maximum Non-Gravitational Acceleration: S-IB	Range Time, sec	137.814	137.975	-0.161
	Acceleration, m/s ²	42.198	42.642	-0.444
S-IVB	Range Time, sec	577.176	579.351	-2.175
	Acceleration, m/s ²	28.742	28.588	0.154
* Maximum Earth-Fixed Velocity: S-IB	Range Time, sec	141.500	141.271	0.229
	Velocity, m/s	2037.59	2037.27	0.32
S-IVB	Range Time, sec	581.000	581.271	-0.271
	Velocity, m/s	7534.33	7533.52	0.81
*Nearest Time Points Available				

Mach number and dynamic pressure history comparisons are shown in Figure 4-4. These parameters were calculated using measured meteorological data to an altitude of 59 km. Above this altitude the U.S. Standard Reference Atmosphere was used.

A theoretical free-flight trajectory was computed for the spent S-IB stage, using initial conditions from the actual trajectory at S-IB/S-IVB separation signal. Three trajectories were integrated from that point to impact using nominal retro-motor performance and outboard engine decay data. The three trajectories incorporate three different drag conditions

Table 4-3. Comparison of Cutoff Events

PARAMETER	S-IB IECD			S-IB OECD			S-IVB GCS		
	ACTUAL	NOMINAL	ACT-NOM	ACTUAL	NOMINAL	ACT-NOM	ACTUAL	NOMINAL	ACT-NOM
Range Time (sec)	137.82	137.98	-0.16	141.29	140.98	0.31	577.18	579.35	-2.17
Altitude (km)	54.08	54.46	-0.38	57.35	57.31	0.04	158.18	158.08	0.10
Space-Fixed Velocity (m/s)	2279.83	2287.15	-7.32	2345.48	2344.66	0.82	7829.82	7829.46	0.36
Flight Path Angle (deg)	24.236	24.300	-0.064	23.682	23.821	-0.138	-0.006	-0.008	0.002
Heading Angle (deg)	60.160	60.201	-0.041	59.927	49.988	-0.061	54.426	54.506	-0.080
Surface Range (km)	59.55	59.67	-0.12	65.64	64.95	0.69	1747.44	1757.89	-10.45
Cross Range (km)	0.69	0.82	-0.13	0.63	0.77	-0.14	-133.63	-134.91	1.28
Cross Range Velocity (m/s)	-16.80	-14.87	-1.93	-18.91	-16.98	-1.93	-1205.77	-1200.90	-2.87

Table 4-4. Comparison of Separation Events

PARAMETER	S-IB/S-IVB			S-IVB/CSM		
	ACTUAL	NOMINAL	ACT-NOM	ACTUAL	NOMINAL	ACT-NOM
Range Time (sec)	142.54	142.28	0.26	1080.00	1059.55	20.45
Altitude (km)	58.54	58.54	0.00	169.62	168.74	0.88
Space-Fixed Velocity (m/s)	2345.79	2344.93	0.86	7825.58	7826.21	-0.63
Flight Path Angle (deg)	23.449	23.576	-0.127	0.201	0.188	0.013
Heading Angle (deg)	59.918	59.983	-0.065	87.334	85.614	1.720
Geodetic Latitude (deg, North)	28.984	28.980	0.004	50.165	50.067	0.098
Longitude (deg, West)	80.055	80.060	-0.005	21.767	23.936	2.169
Surface Range (km)	67.89	67.27	0.62	--	--	--
Cross Range (km)	0.60	0.75	-0.15	--	--	--
Cross Range Velocity (m/s)	-19.12	-17.07	-2.05	--	--	--

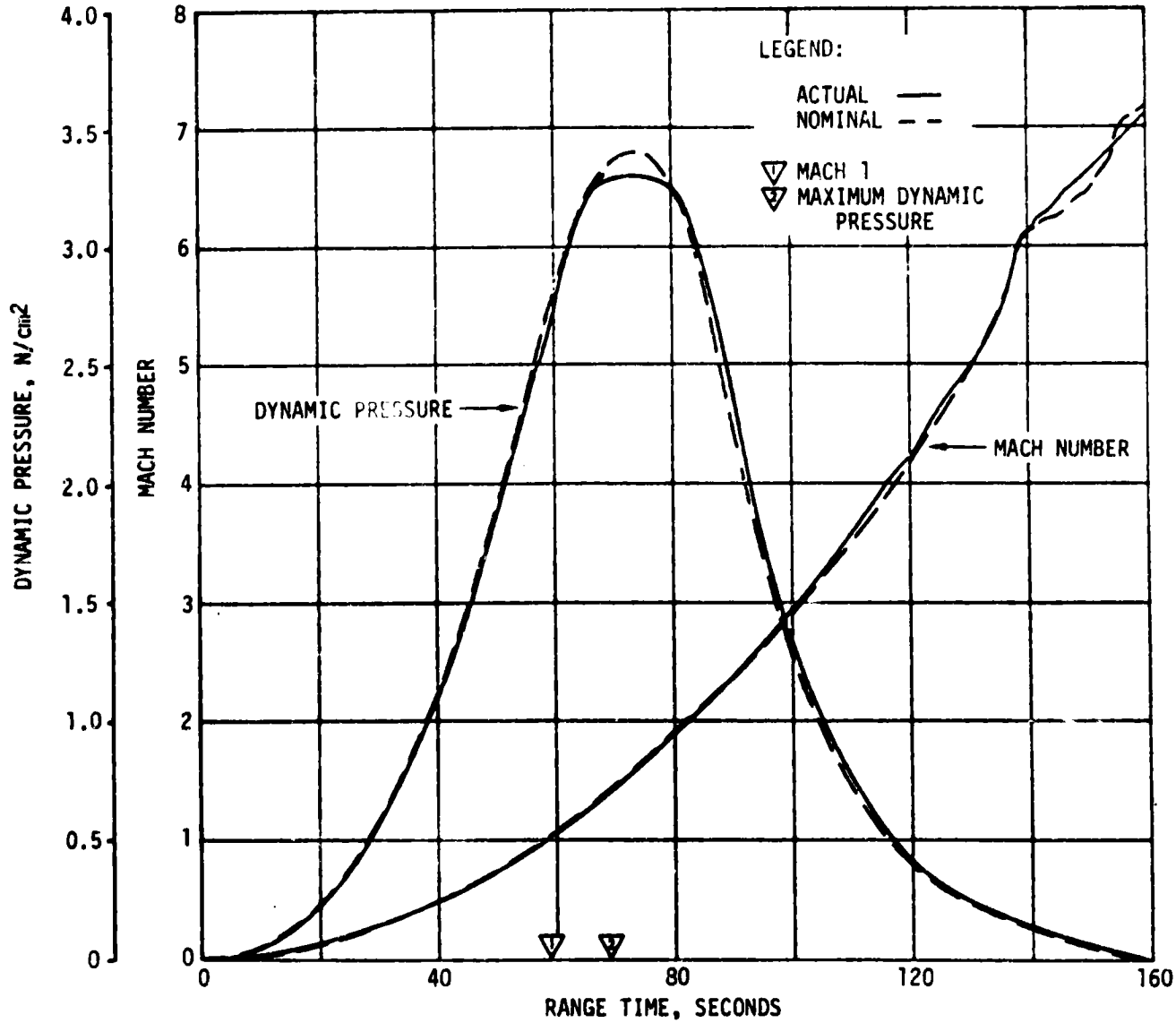


Figure 4-4. Ascent Trajectory Dynamic Pressure and Mach Number Comparison

for 1) stabilized at zero angle of attack (nose forward), 2) tumbling stage, and 3) stabilized at 90 degree angle of attack (broadside). Tables 4-5 and 4-6 summarize the results of these simulations and present the impact envelope. Tracking data were not available, but previous flight data indicates the tumbling drag trajectory to be a close approximation to actual flight conditions. The calculated impact for this case was 31.19 degrees north latitude, 76.46 degrees west longitude.

4.2.2 Orbital Phase

Orbital tracking was conducted by the National Aeronautics and Space Administration (NASA) Space Tracking and Data Network. One C-Band (Bermuda) and one S-Band station (Bermuda) were available for tracking coverage during the first revolution. Tananarive provided second and third revolution coverage while Hawaii afforded additional third revolution coverage. Some high speed tracking data beyond insertion were available from Wallops Island. These data were edited to provide additional orbital tracking information. The trajectory parameters at orbital insertion were established by adjusting the preliminary estimate of the insertion conditions to fit the orbital tracking data. A comparison of the actual and nominal parking orbit insertion parameters are delineated in Table 4-7. Figure 4-5 presents the SL-4 ground track from lift-off through CSM separation.

Table 4-5. Comparison of S-IB Spent Stage Impact

PARAMETER	ACTUAL	NOMINAL	ACT-NOM
Range Time (sec)	534.26	534.78	-0.52
Surface Range (km)	492.58	494.65	-2.07
Cross Range (km)	-0.51	1.53	-2.04
Geodetic Latitude (deg, North)	31.193	31.187	0.006
Longitude (deg, West)	76.455	76.425	0.030
NOTE: Data reflects simulation of tumbling stage			

Table 4-6. S-IB Spent Stage Impact Envelope

PARAMETER	DRAG SIMULATION		
	NOSE FORWARD	TUMBLING	BROADSIDE
Range Time (sec)	472.67	534.26	575.39
Surface Range (km)	505.91	492.58	483.07
Cross Range (km)	-0.43	-0.51	-0.55
Geodetic Latitude (deg, North)	31.26	31.19	31.14
Longitude (deg, West)	76.34	76.46	76.54

Table 4-7. Comparison of Orbit Insertion Conditions

PARAMETER	ACTUAL	NOMINAL	ACT-NOM
Range Time (sec)	587.18	589.35	-2.17
Altitude (km)	158.33	158.22	0.11
Space-Fixed Velocity (m/s)	7836.82	7836.09	0.73
Flight Path Angle (deg)	0.006	0.003	0.003
Heading Angle (deg)	54.853	54.935	-0.082
Cross Range (km)	-145.68	-146.92	1.24
Cross Range Velocity (m/s)	-1199.93	-1196.74	-3.19
Inclination (deg)	50.048	50.033	0.015
Descending Node (deg)	156.979	156.966	0.013
Eccentricity	0.0059	0.0057	0.0002
Apogee Altitude (km)	227.08	224.24	2.84
Perigee Altitude (km)	150.10	149.96	0.14
Period (min)	88.26	88.23	0.03
Geodetic Latitude (deg, North)	28.432	38.487	-0.055
Longitude (deg, West)	64.841	64.744	0.097

REPRODUCIBILITY OF THE ORIGINAL PAGE IS POOR

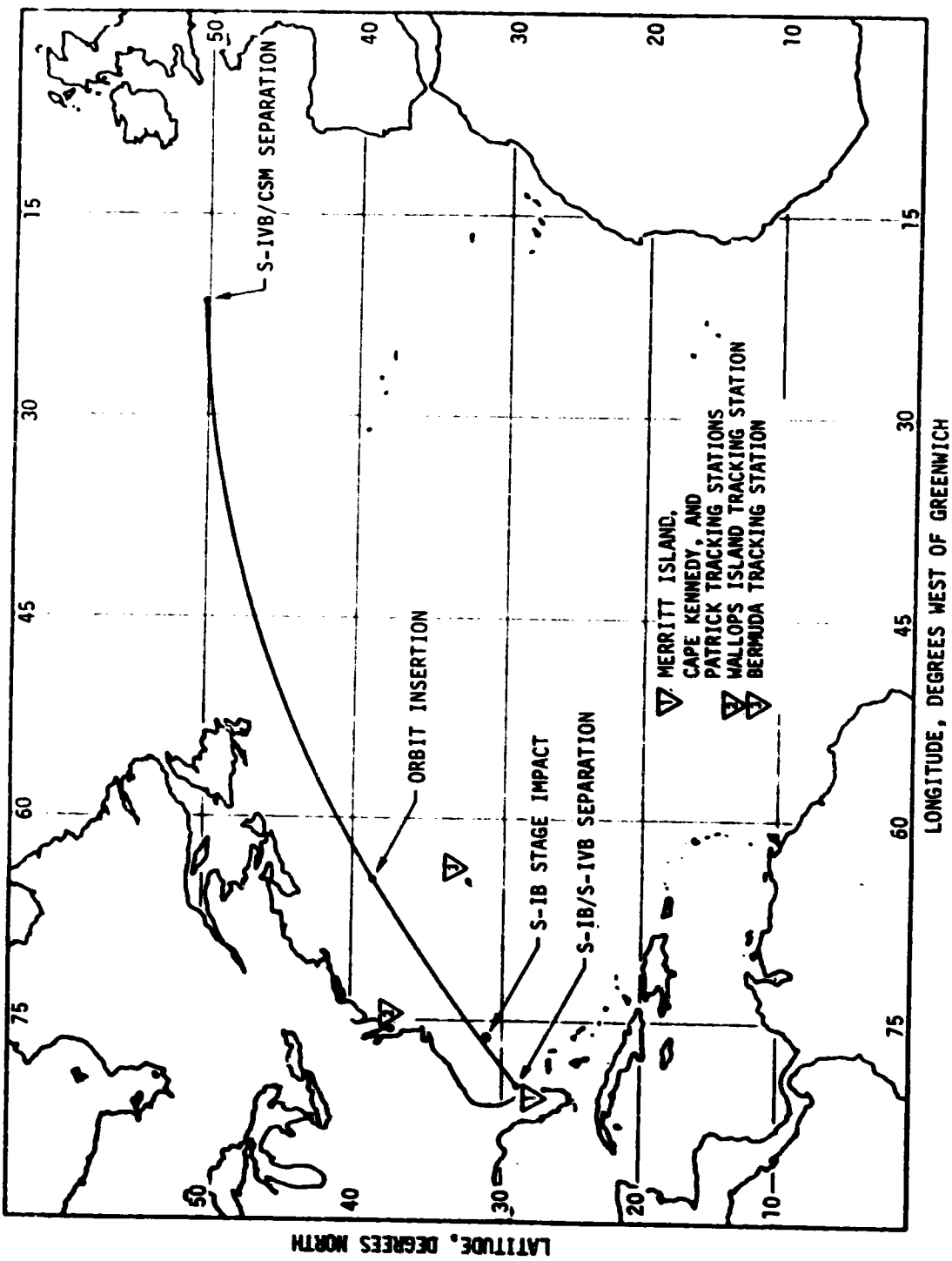


Figure 4-5. Launch Vehicle Ground Track

SECTION 5

S-IVB/IU DEORBIT TRAJECTORY

5.1 SUMMARY

All aspects of the S-IVB/IU deorbit were accomplished successfully. The propellant dump was performed as planned with impact occurring in the primary disposal area. Honeysuckle confirmed that the vehicle was safed following the propellant dump. Although breakup occurred after loss of signal at Kwajalein, Department of Defense (DOD) sources confirmed the deorbit.

5.2 DEORBIT MANEUVERS

Timebase 5 (start of S-IVB/IU deorbit events) was initiated at 18,637.7 seconds (301 minutes past Timebase 4) with the vehicle already in the retrograde attitude. A deorbit LOX dump of 475 seconds duration and an LH₂ dump of 86 seconds were implemented. Remaining pneumatic pressure was sufficient for vehicle safing.

The retrograde velocity increments achieved from the LOX and LH₂ tank dumps are presented in Table 5-1, and compared with the real time predictions. The actual total dump velocity was slightly less than nominal, but well within the -3 sigma prediction.

Table 5-1. S-IVB-208 Propellant Dump Deorbit Velocity

	ACTUAL	REAL-TIME PREDICTED	ACT-RT
LOX Dump ΔV (m/s)	17.93	19.17	-1.24
LH ₂ Dump ΔV (m/s)	2.61	2.70	-0.09
Total Dump ΔV (m/s)	20.54	21.87	-1.33
LOX Dump Duration = 475 Seconds			
LH ₂ Dump Duration = 86 Seconds			

5.3 DEORBIT TRAJECTORY EVALUATION

A timebase 5 state vector, obtained from the orbit trajectory reconstruction (actual) discussed in Section 4, was utilized to initialize the reentry trajectory which terminates with breakup. The LOX and LH₂ dump data used in determining this trajectory were taken from the telemetered accelerometer data. The altitude profile developed differs only slightly from the real time prediction, as shown in Figure 5-1. The difference in altitude is attributable to the slightly lower than nominal (real time prediction) retrograde velocities mentioned above.

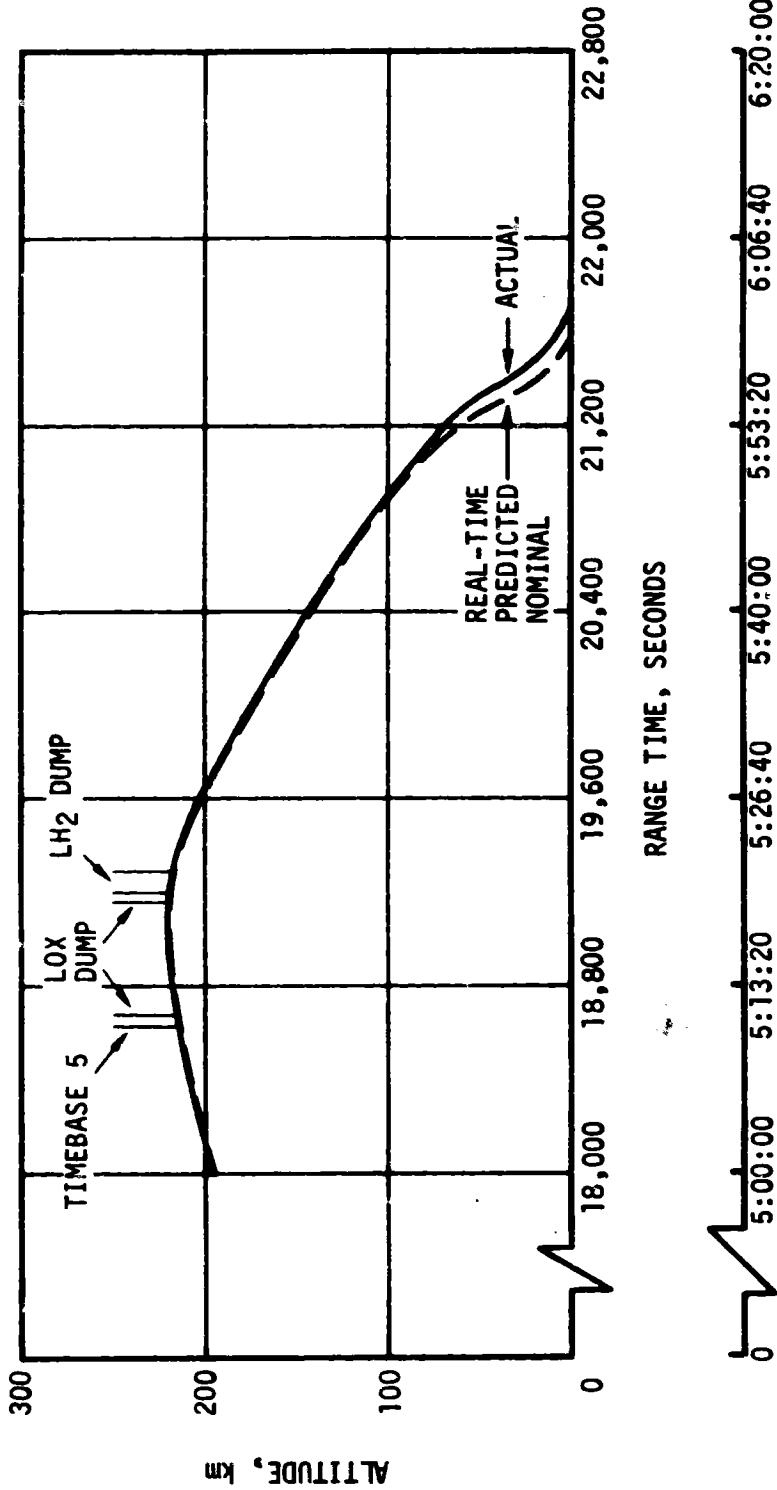
Honeysuckle verified that the vehicle was safed following the propellant dump. Kwajalein radar tracked the S-IVB/IU, but did not establish breakup since it occurred after loss of signal. Other DOD sources did confirm deorbit. A breakup altitude of 81.7 km was assumed for the concluding part of the reentry simulation. This altitude was selected since it was observed by Kwajalein as the actual breakup altitude during the SA-207 flight.

5.4 IMPACT

The impact area of the S-IVB/IU is illustrated in Figure 5-2, which also shows the ground track past Kwajalein. The limits of the impact area were defined by simulation, assuming a range of ballistic coefficients from 47 to 650 kg/m². Table 5-2 presents the short range, nominal, and long range impact point coordinates as they occurred in the plane of the trajectory. These data show that the impact area was approximately 925 km (500 n.mi.) in length and well within the planned disposal area.

Table 5-2. S-IVB-208 Impact Dispersion Limits

	SHORT RANGE	NOMINAL	LONG RANGE
Range Time (sec)	21,836	21,732	21,672
Latitude (deg), N	24.5	26.5	30.1
Longitude (deg), W	172.3	170.3	166.2



RANGE TIME, HOURS:MINUTES:SECONDS

Figure 5-1. S-IVB/IU Stage Deorbit Altitude History (No Breakup Assumed)

REPRODUCIBILITY OF THE ORIGINAL PAGE IS POOR

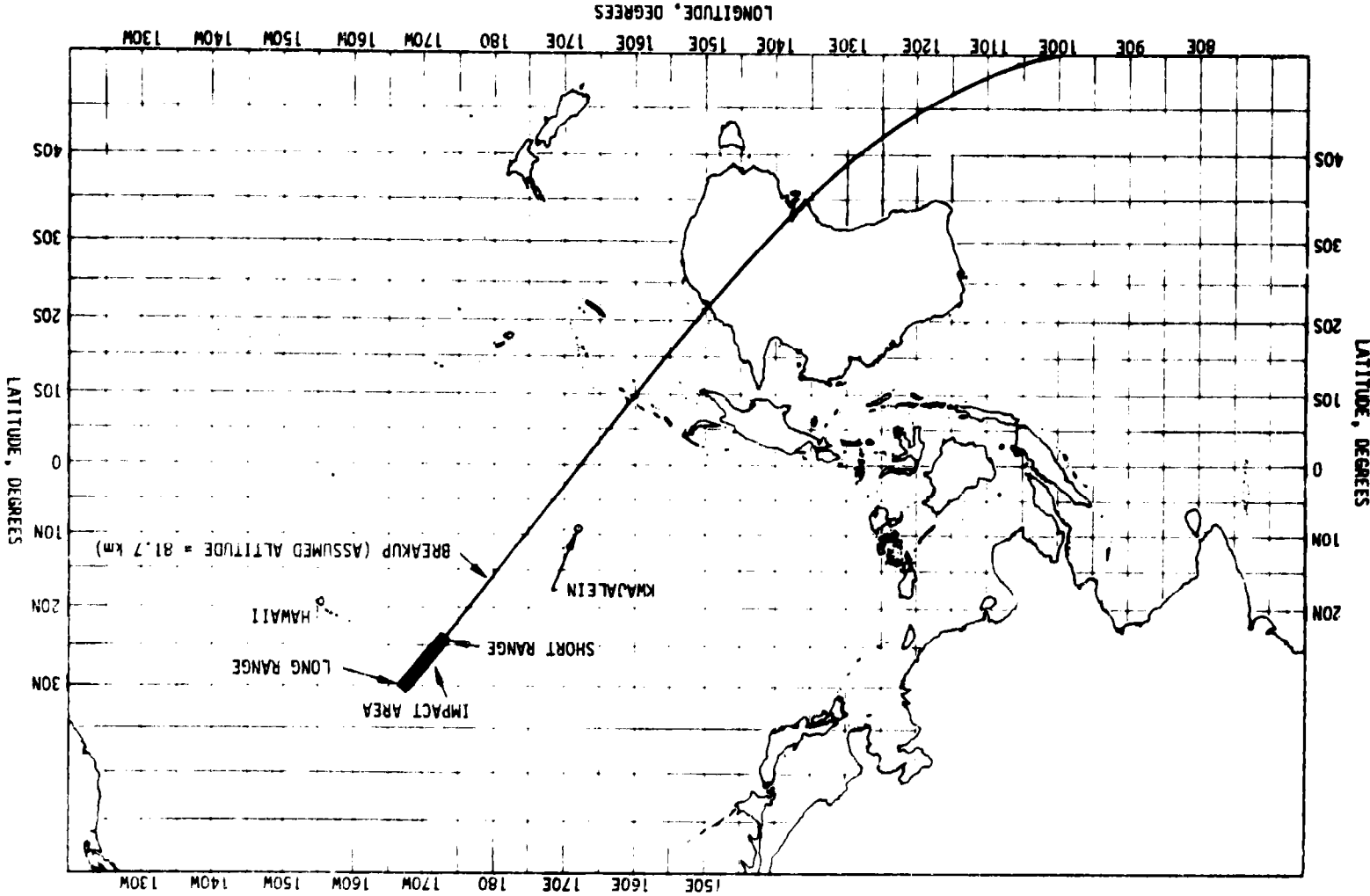


Figure 5-2. S-IVB/IU Ground Track Dump to Impact

SECTION 6

S-IB PROPULSION

6.1 SUMMARY

The S-IB stage propulsion system performance was satisfactory throughout flight. Stage longitudinal site thrust averaged 0.13 percent lower than predicted. Stage LOX, fuel, and total flowrates averaged 0.10 percent, 0.18 percent, and 0.13 percent lower than predicted, respectively. Stage mixture ratio averaged 0.08 percent higher than predicted. Stage specific impulse was within 0.04 percent of predicted. Inboard Engine Cutoff (IECO) indicated by measurement VK0001-012 occurred at 137.82 seconds (0.16 seconds earlier than predicted). Outboard Engine Cutoff (OECO) indicated by measurement VK0003-012 occurred 3.47 seconds after IECO at 141.29 seconds (0.31 seconds later than predicted). OECO was initiated by engine no. 1 thrust OK pressure switch deactuation (LOX starvation). At OECO, the LOX residual was 2925 lbm compared to the predicted 3287 lbm, and the fuel residual was 6878 lbm compared to the predicted 5989 lbm. The stage hydraulic system performed satisfactorily.

6.2 S-IB IGNITION TRANSIENT PERFORMANCE

All eight H-1 engines ignited satisfactorily. The automatic ignition sequence, which schedules the engines to start in pairs with a 100-millisecond delay between each pair, began with the time for ignition command at -3.050 seconds range time. The start sequence that occurred was close to optimum. The maximum spread in the start time, defined by the intersection of the extrapolated maximum slope of chamber pressure or thrust buildup with the zero line (P_c prime times) of engines within a pair was 25 milliseconds and was between engines 2 and 4 (third pair of engines). The smallest interval in the planned 100-millisecond sequence between pairs was 75 milliseconds and was between the third pair's later engine and the fourth pair's earlier engine (specifically, between engines 2 and 3).

Table 6-1 compares predicted and actual start event times. The individual engine thrust buildup curves are shown in Figure 6-1. The thrust values shown are the engine chamber thrusts and do not account for cant angles or turbine exhaust thrust.

Table 6-1. S-IB Engine Start Characteristics

ENGINE POSITION AND SERIAL NUMBER		TIME, IGNITION COMMAND TO ENGINE IGNITION SIGNAL (msec)		TIME, ENGINE IGNITION SIGNAL TO THRUST CHAMBER IGNITION (msec)		TIME, ENGINE IGNITION SIGNAL TO P _c PRIME (msec)	
		ACTUAL (1)	PROGRAMMED	ACTUAL	NOMINAL	ACTUAL	NOMINAL
5	H-4077	102	100	548	554 (2)	833	833 (2)
7	H-4079	102	100	548		833	
6	H-4073	201	200	544		844	
8	H-4080	201	200	544		842	
2	H-7079	303	300	527		862	
4	H-7098	300	300	532		837	
1	H-7092	402	400	505		844	
3	H-7081	402	400	513		838	

(1) Values referenced to Terminal Countdown Sequencer (TCS) event "Time for Ignition Command"

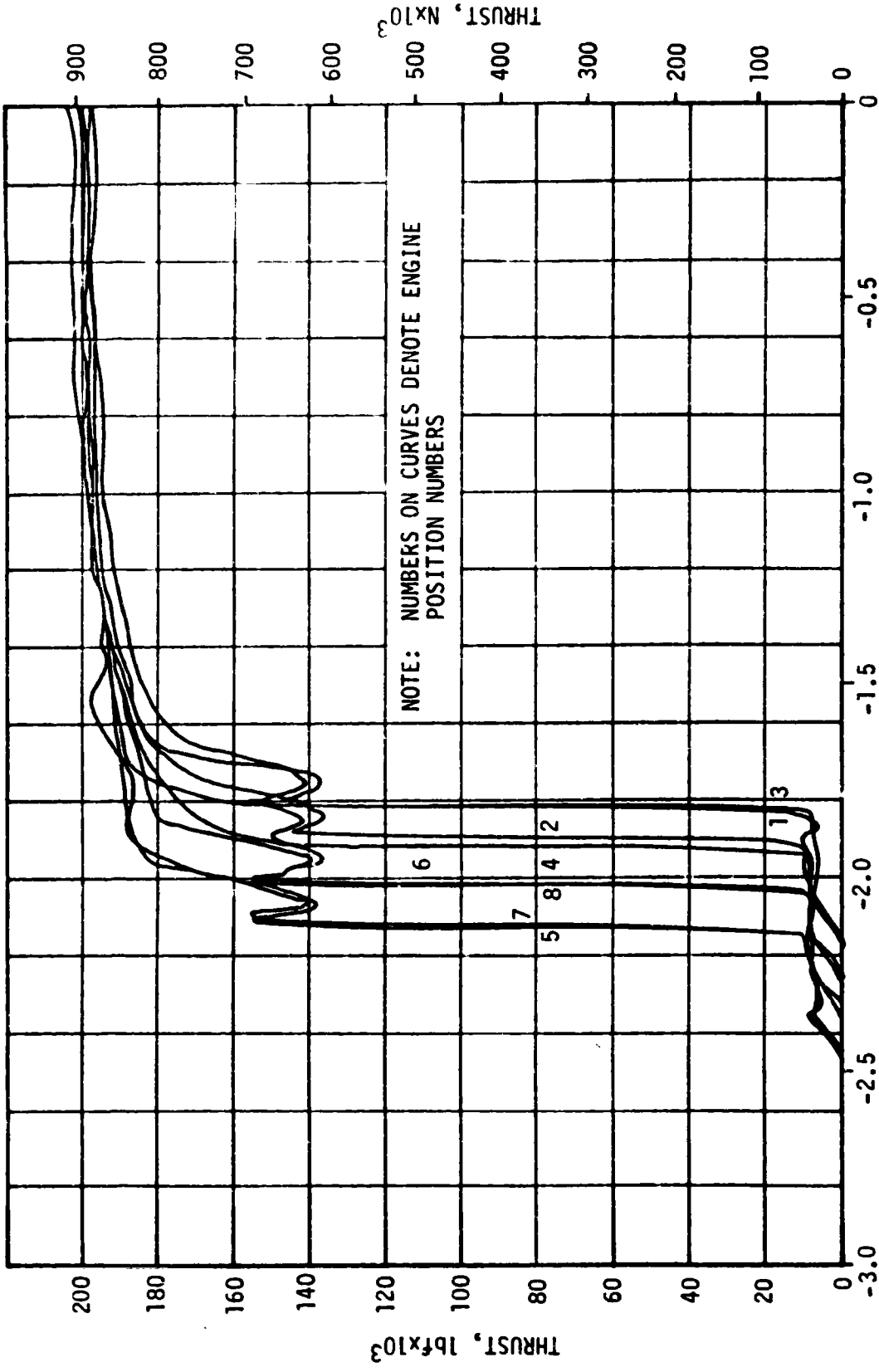
(2) Values presented are mean values S-IB-6 through S-IB-12 static test, Technical Bulletin - P&VE-65-148, Revision D. Sample means and standard deviations were: Time to thrust chamber ignition 583.7 msec and 18.4 msec; time to P_c prime 874.6 msec and 22.6 msec.

6.3 S-IB MAINSTAGE PERFORMANCE

S-IB mainstage flight performance, Figure 6-2, was satisfactory. Stage longitudinal site thrust averaged 2330 pounds (0.13 percent) lower than predicted. The stage specific impulse during flight was within 0.04 percent of predicted. Stage mixture ratio averaged 0.0019 (0.08 percent) higher than predicted. Total flowrate averaged 8.0 lbm/sec (0.13 percent) lower than predicted. Stage LOX and fuel flowrate, Figures 6-3 and 6-4, averaged 4.5 lbm/sec (0.10 percent) and 3.5 lbm/sec (0.18 percent) lower than predicted, respectively. These average deviations were taken between first motion and IEEO.

The fuel temperature was 5.4°F lower than predicted which normally would have significantly decreased thrust and total flowrates; however, the effects of the more dense fuel were almost entirely compensated for by a slightly higher LOX tank pressure and a lower LOX temperature than predicted.

Early IEEO (0.16 seconds earlier than predicted) and late OEEO (0.31 seconds later than predicted) were primarily the result of a greater than predicted level difference between the outboard LOX tank number 2 (O-2), which signalled level sensor actuation and the other four tanks, particularly, the center tank. The lower than predicted level in the O-2 tank caused less LOX to be consumed by the inboard engines before



RANGE TIME, SECONDS

Figure 6-1. S-IB Engine Thrust Buildup

▽ IECO
▽ OECO

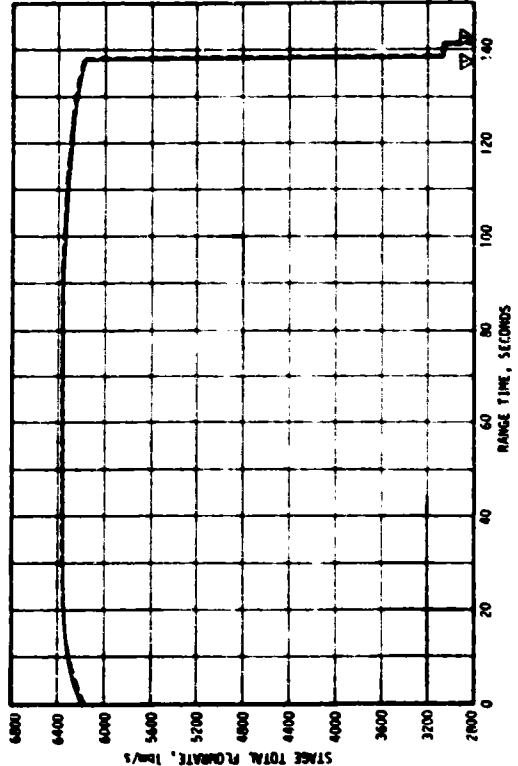
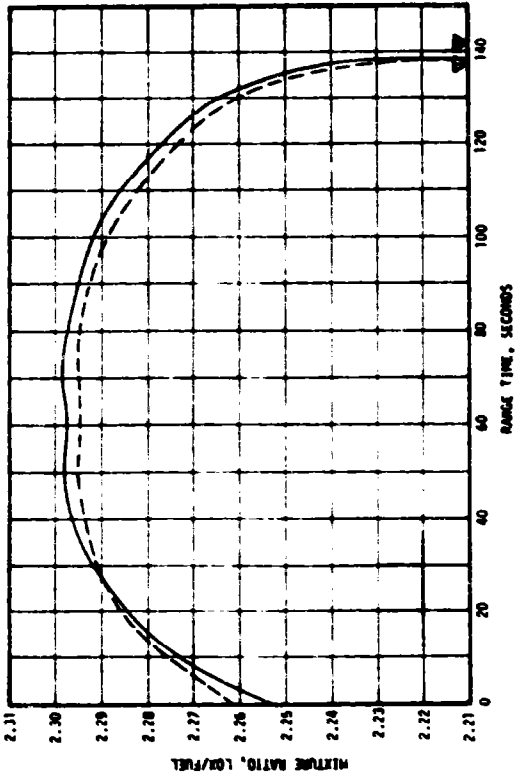
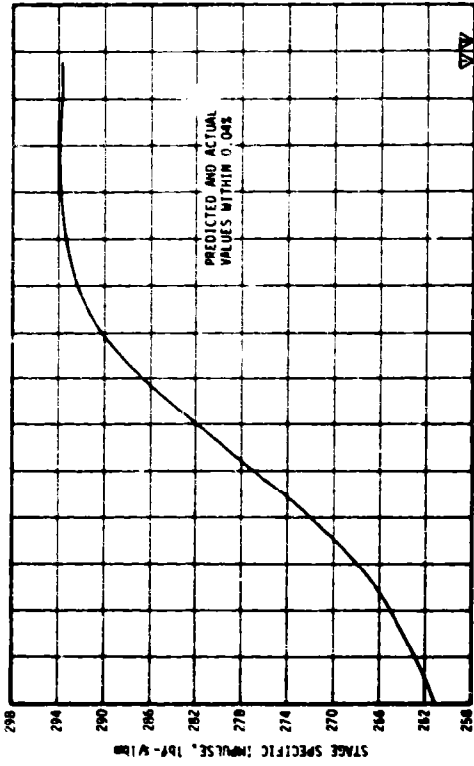
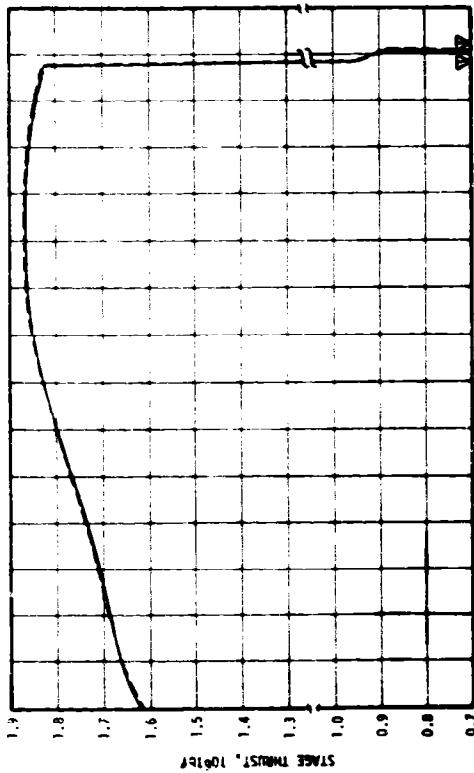


Figure 6-2. S-1B Stage Propulsion Performance

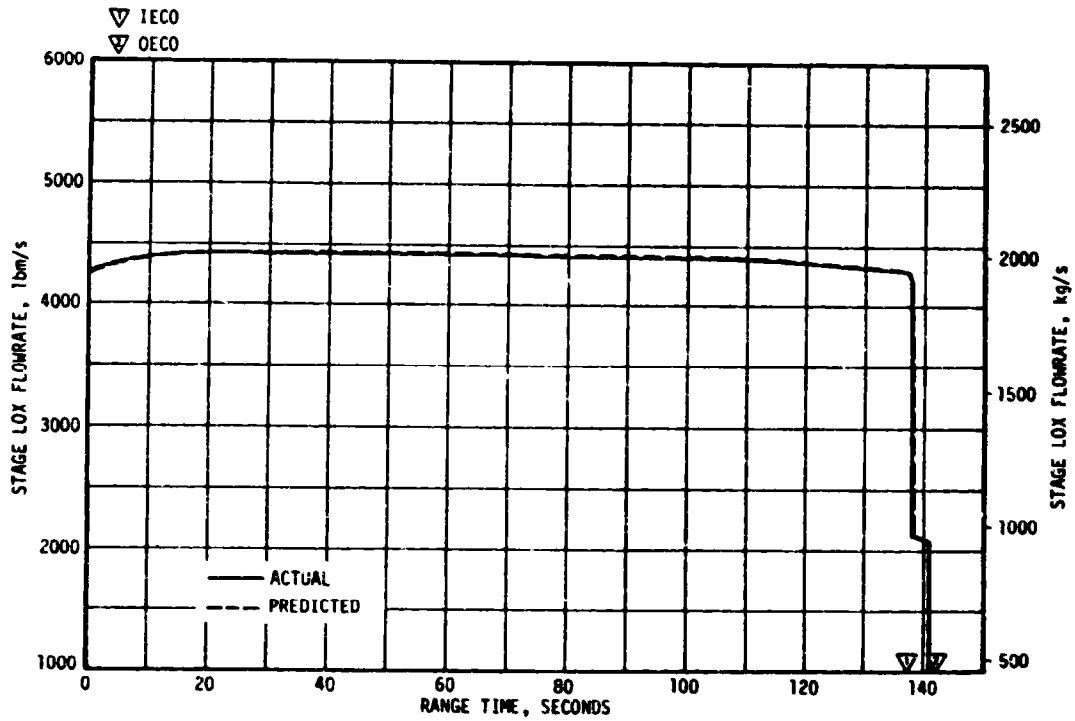


Figure 6-3. S-IB LOX Flowrate

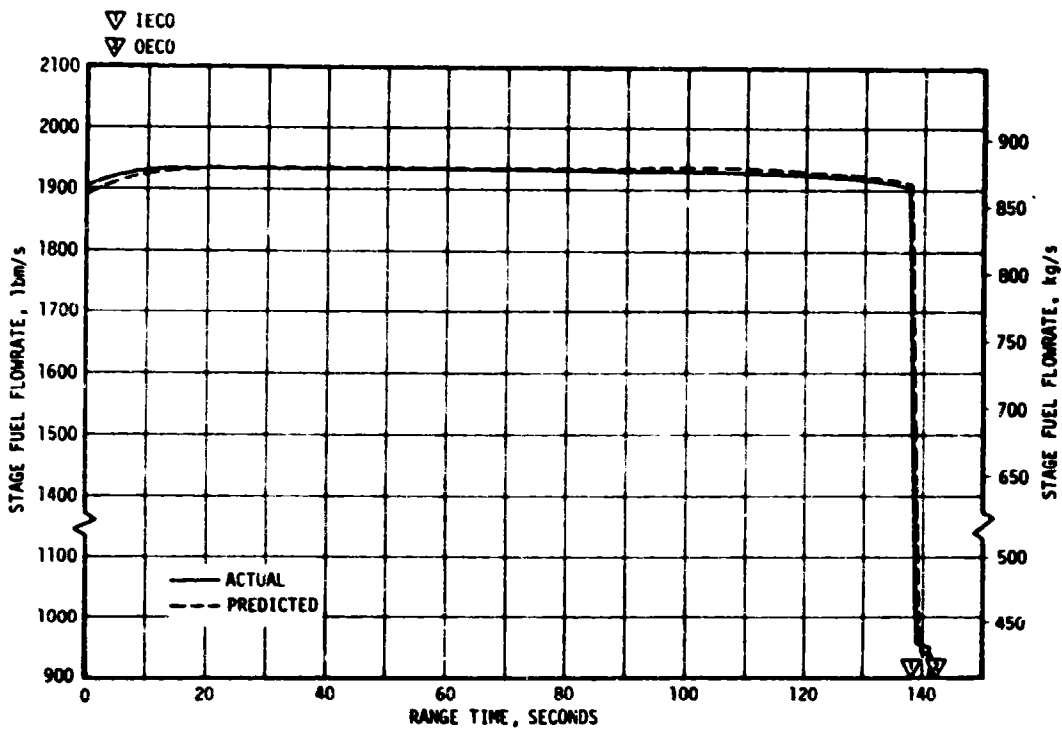


Figure 6-4. S-IB Fuel Flowrate

LOX depletion occurred. The predicted performance was determined before any stages with 205Klbf thrust engines had flown. Since the flight of S-IB-6, it was expected that the fuel and LOX tank pressures would be higher, the fuel temperature lower, and the LOX level in O-2 lower than predicted for S-IB-7 and S-IB-8. The combined effects of these small deviations do not significantly affect stage performance and prediction updates were not considered necessary.

Table 6-2 compares individual S-IB engine propulsion performance to predicted values when reduced to standard sea level conditions.

The predicted sea level values for the S-IB-8 engines were calculated in a similar manner to the sea level values for the S-IB-7 engine prediction data. The predicted thrusts, turbine speeds and flowrate sea level data were derived by increasing the engine manufacturer's acceptance test data to be consistent with the trends noted during the flights of S-IB-1 through S-IB-5 with 200Klbf thrust engines. The 8-engine average sea level thrust, LOX flowrate, and specific impulse were within 0.1 percent of those predicted. The average sea level fuel flowrate and mixture ratio were within 0.26 percent of those predicted.

6.4 S-IB SHUTDOWN TRANSIENT PERFORMANCE

The cutoff sequence began at 134.88 seconds with the actuation of the low level sensor in LOX tank O-2 as indicated by measurement VK00015-002. It should be noted that this measurement has an 83 millisecond sampling rate, therefore, this event could be as much as 0.083 seconds earlier than indicated by this measurement. IECO was initiated 2.94 seconds later by the Launch Vehicle Digital Computer (LVDC) at 137.82 seconds as indicated by measurement VK0001-012. Thrust of each inboard engine was normal. The total IECO impulse was 238,258 lbf-sec. Inboard engine total thrust decay is shown in Figure 6-5.

LOX starvation occurred in the four outboard engines as planned. Outboard engine total thrust decay is shown in Figure 6-6. The total OECO impulse was 181,550 lbf-sec. Each engine has three thrust OK pressure switches, and as engine performance decays during LOX starvation, the first outboard engine to lose thrust OK signal from two-out-of-three switches, will simultaneously cut off all outboard engines. Engine 1 initiated OECO which occurred at 141.29 seconds range time as indicated by measurement VK0003-012.

6.5 S-IB STAGE PROPELLANT MANAGEMENT

The effectiveness of propellant management may be measured by the ratio of propellant consumed to propellant loaded which is an indication of the capability of predicting mixture ratio and of the propellant loading system to load the proper propellant masses. The predicted and actual (reconstructed) percentages of loaded propellants utilized during the flight are shown in Table 6-3.

Table 6-2. S-1B Individual Engine Propulsion Performance*

ENG NO.	THRUST (lbf)			SPECIFIC IMPULSE (lbf-sec/lbm)			LOX FLOWRATE (lbm/sec)			FUEL FLOWRATE (lbm/sec)			MIXTURE RATIO O/F		
	PRED	ACTUAL	%DIFF	PRED	ACTUAL	% DIFF	PRED	ACTUAL	% DIFF	PRED	ACTUAL	% DIFF	PRED	ACTUAL	%DIFF
1	206,629	207,254	0.302	262.68	262.92	0.053	545.27	547.03	0.323	241.35	241.55	0.083	2.2593	2.2647	0.239
2	206,562	208,595	0.994	262.28	262.64	0.137	545.35	550.42	0.930	242.22	243.90	0.652	2.2515	2.2577	0.275
3	205,167	204,326	-0.410	262.77	262.67	-0.038	539.95	538.17	-0.311	240.95	239.70	-0.519	2.2405	2.2452	0.210
4	204,787	204,862	0.037	262.13	262.19	0.023	539.67	540.14	0.087	241.58	241.22	-0.149	2.2339	2.2392	0.237
5	208,732	206,966	-0.846	264.08	263.85	-0.087	547.74	543.89	-0.703	242.66	240.53	-0.978	2.2572	2.2612	0.177
6	203,105	203,747	0.316	262.70	262.86	0.061	536.57	539.35	0.332	236.57	236.76	0.080	2.2682	2.2739	0.251
7	205,906	204,150	-0.853	263.33	263.09	-0.091	541.98	538.15	-0.707	239.95	237.80	-0.896	2.2588	2.2630	0.186
8	205,601	204,994	-0.295	263.78	263.73	-0.019	539.89	538.76	-0.209	239.55	238.52	-0.430	2.2538	2.2587	0.217
AVG	205,811	205,612	-0.096	262.97	262.98	0.005	542.04	541.86	-0.032	240.60	239.98	-0.257	2.2529	2.2580	0.224

*Standard Sea Level Conditions at 30 Sec

LOX density 70.79 lbm/ft³
 Fuel density 50.45 lbm/ft³
 Ambient Pressure 14.696 psia

Fuel pump inlet pressure 57 psia
 LOX pump inlet pressure 65 psia
 Fuel temperature 60°F

REPRODUCIBILITY OF THE ORIGINAL PAGE IS POOR

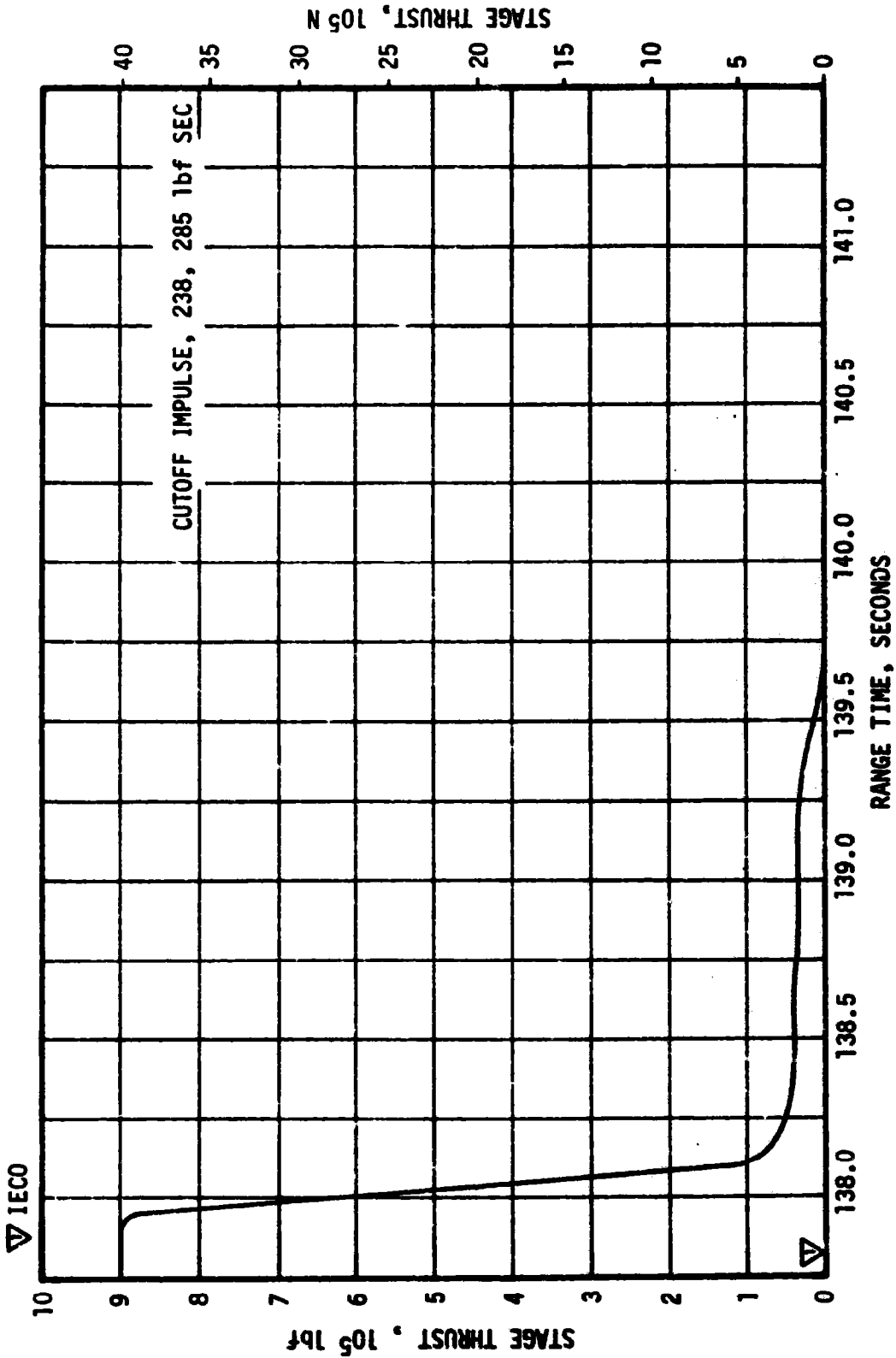


Figure 6-5. S-1B Inboard Engines Total Thrust Decay

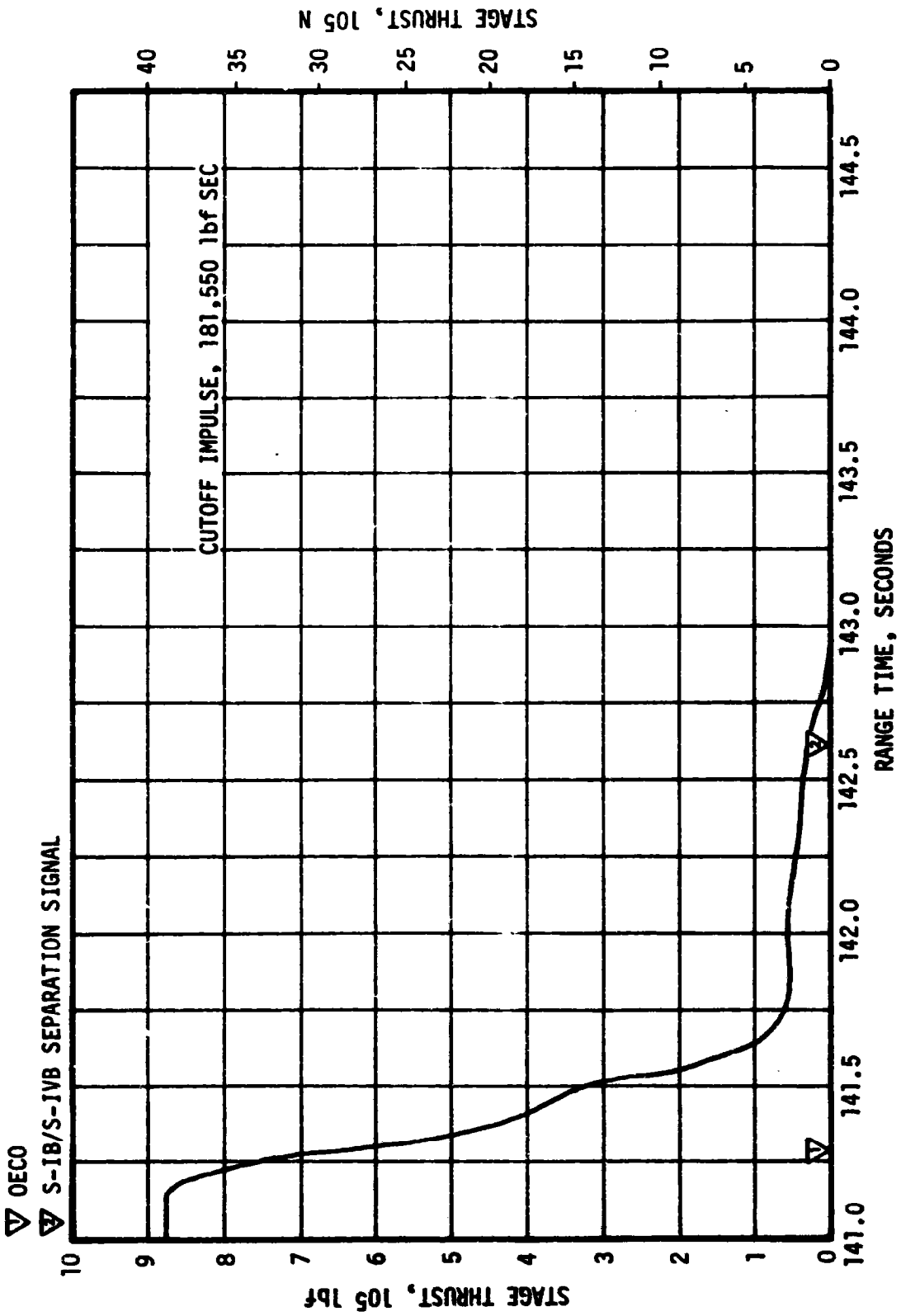


Figure 6-6. S-IB Outboard Engine Total Thrust Decay

Table 6-3. S-IB Stage Propellant Usage

PROPELLANT	PREDICTED (%)	ACTUAL (%)
Total	99.20	99.12
Fuel	98.34	98.02
LOX	99.58	99.61

The center LOX tank sump orifice was 19.0 (+0.005) inches in diameter, and a liquid level height differential of approximately 3.0 inches between the center and outboard LOX tanks was predicted at IECO (center tank level higher). The LOX and fuel level cutoff sensor heights and flight sequence settings were determined for a 3.00-second time interval between cutoff sensor actuation and IECO. The planned time interval between IECO and OECO was 3.00-seconds. The planned mode of OECO was by LOX starvation. OECO was to be initiated by the deactuation of two of the three thrust OK pressure switches on any outboard engine as a result of LOX starvation and the subsequent thrust decay. It was assumed that approximately 271 gallons of LOX in the outboard suction lines were usable. The backup timer (flight sequencer) was set to initiate OECO 13.00 seconds after level sensor actuation.

To prevent fuel starvation, fuel depletion cutoff sensors were located in the F2 and F4 container sumps. The fuel bias for S-IB-8 was 1550 lbm. This fuel mass, included in the predicted residual, was available for consumption to minimize propellant residual due to off-nominal conditions and is not expected to be used during a nominal flight.

The cutoff sequence on S-IB-8 was initiated by a signal from the cutoff level sensor in tank 0-2 at 134.88 seconds. The IECO signal was received 2.94 seconds later at 137.82 seconds. OECO occurred 3.47 seconds after IECO at 141.29 seconds. OECO was initiated by engine no. 1 thrust OK pressure switch deactuation. Fuel depletion probes in the fuel tank sumps were not actuated prior to retrorocket ignition.

Based on discrete probe data, liquid levels in the fuel tanks were nearly equal and approximately 24.7 inches above theoretical tank bottom at IECO. This level represents a mass of 11,580 lbm of fuel onboard. At that time, 11,033 lbm of LOX remained onboard. Corresponding liquid height in the center tank was approximately 14.7 inches and average height in the outboard tanks was approximately 10.3 inches above theoretical tank bottom. Propellants remaining above the main valves after outboard engine decay were 2,390 lbm of LOX and 5,549 lbm of fuel. Predicted values for these

quantities were 2,642 lbm of LOX and 4,628 lbm of fuel.

Cutoff level sensor signal times and setting heights from theoretical tank bottom are shown in Table 6-4.

Table 6-4. Cutoff Level Sensor Actuation Characteristics

TANK	HEIGHT (inches)	ACTUATION TIME (seconds)
O2	27.5	134.88*
O4	27.5	135.05
F2	31.4	136.36
F4	31.4	136.44
* 83 millisecond sampling rate		

Total LOX and fuel masses above the main propellant valves beginning at ignition command are shown in Figure 6-7 and 6-8. A summary of the propellants remaining at major event times is presented in Table 6-5.

Table 6-5. S-IB Stage Propellant Mass History

EVENT	PREDICTED (lbm)			RECONSTRUCTED (lbm)		
	FUEL	LOX	TOTAL	FUEL	LOX	TOTAL
Ignition Command	279,594	632,015	911,609	280,540	632,415	912,955
IU Umbilical Disconnect	275,625	620,632	896,257	276,709	619,910	896,619
IECO	10,247	10,437	20,684	11,580	11,033	22,613
DECO	5,989	3,287	9,276	6,878	2,925	9,803
Separation Command	4,900	2,725	7,592	5,823	2,473	8,296
Zero Thrust	4,628	2,642	7,270	5,549	2,390	7,939

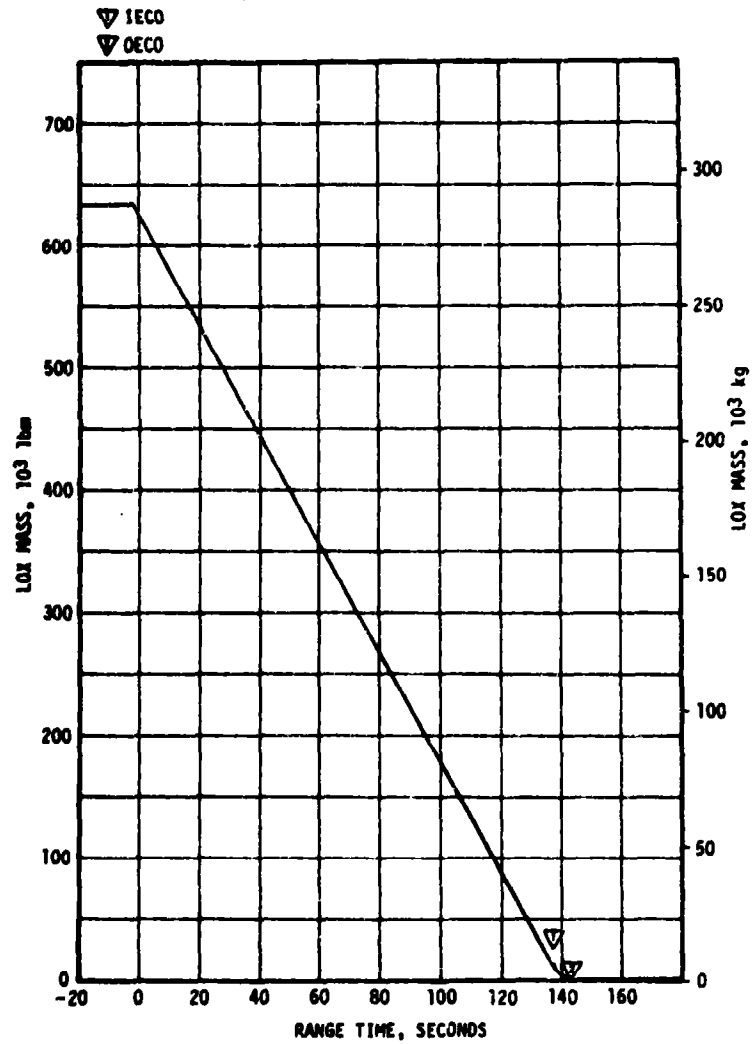


Figure 6-7. S-IB LOX Mass Above Main LOX Valve

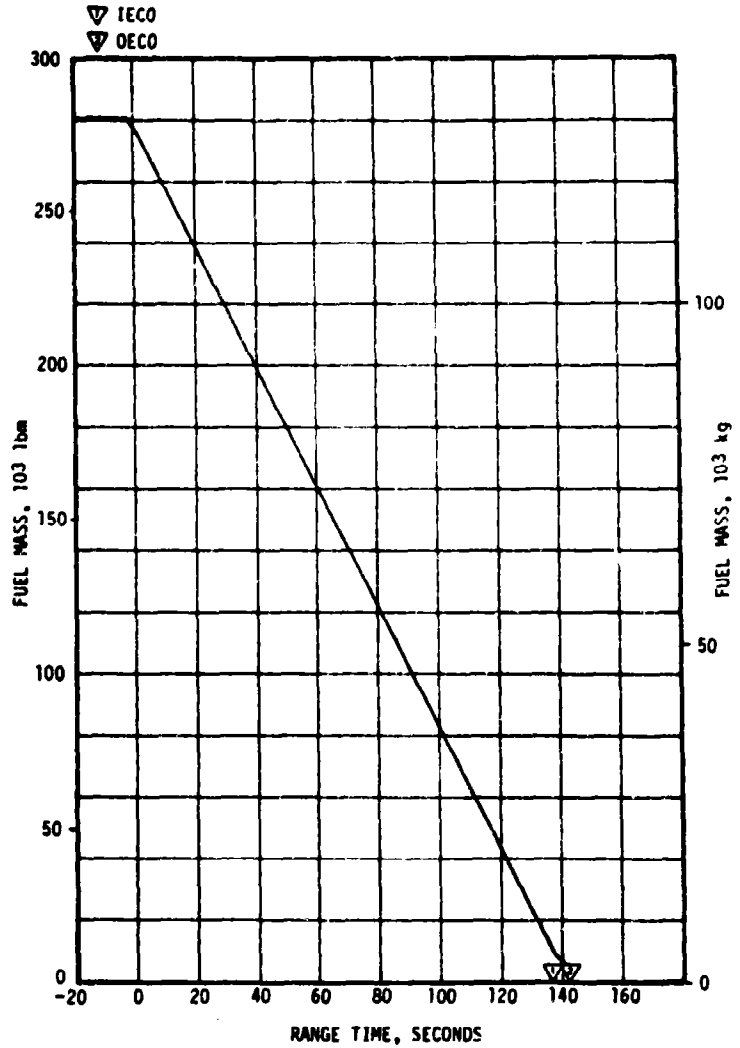


Figure 6-8. S-IB Fuel Mass Above Main Fuel Valve

6.6 S-IB PRESSURIZATION SYSTEM

6.6.1 Fuel Pressurization System

The fuel tank pressurization system performed satisfactorily during the entire flight and no anomalies were observed. With the exception of a change in the vent valve relief pressure setting and minor changes in the vent valve sensing lines, the pressurization system was the same as on S-IB-7 and included the two 19.28 ft³ high-pressure helium spheres, light weight tanks and fuel vent valves. Because of the accidental damage to the upper bulkheads on fuel tanks F3 and F4 during prelaunch activities (see Section 3.4.1), the vent valve relief pressure was lowered from the normal 21.0/21.5 psig to 19.0/19.1 psig to maintain adequate structural margin. In addition, expansion loops were added to the vent valve sensing lines on the upper bulkheads to relieve the strain on the sensing system caused by the increased bulkhead deflection. To reduce the peak pressure during tank prepressurization, a pressure switch was selected which showed the lowest actuation pressure during pressure switch calibration tests. The switch installed on S-IB-8 actuated at 31.5 psia and deactivated at 30.3 psia during calibration.

Helium flow into the fuel tank ullage is metered by a sonic nozzle between the high-pressure spheres and the tanks. The orifice diameter of the sonic nozzle was 0.220/0.221 inches. Sufficient pressure must be provided by this system to meet Fuel Net Positive Suction Head (NPSH) requirements at the end of flight and maintain structural integrity throughout flight. Both requirements were met. The pressures that define the operating band are 10 psig minimum for structural integrity and the minimum vent valve relief pressure of 19.0 psig. Fuel ullage pressure remained within these limits.

A comparison of measured ullage pressure and predicted ullage pressure is presented in Figure 6-9. Measured ullage pressure compared favorably with predicted ullage pressure during the flight and at no time exceeded a difference of 1.0 psia from the predicted value.

The Digital Events Evaluator showed that fuel vent valves 1 and 2 closed at the beginning of the pressurization sequence and remained closed until liftoff. No vent valve position instrumentation is available during flight but inspection of the fuel tank ullage pressure history reveals no reason to suspect that the vents opened during flight.

Tank pressurization began at T-159.86 seconds. The 1527-gallon (3.61 percent) ullage volume was pressurized to 32.2 psia in 2.43 seconds. Due to the ullage cooling, the pressurization valves opened again at T-135.73 seconds for a period of 0.23 seconds to repressurize the fuel tank ullage. This is about 15 seconds earlier than in previous flights and results from the increased ullage pressure decay rate due to fuel vent and relief valve

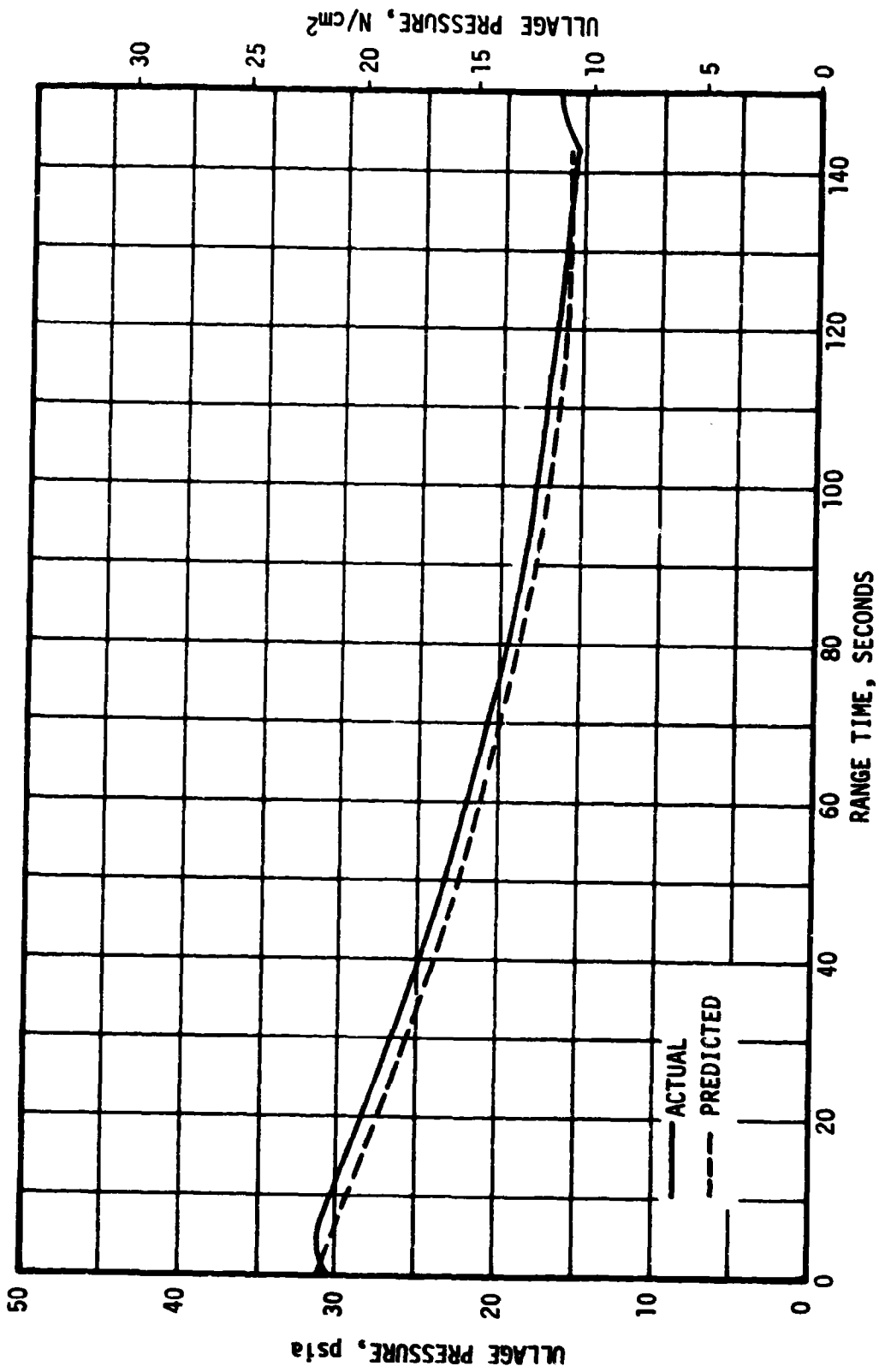


Figure 6-9. S-1B Fuel Tank Ullage Pressure

pilot valve leakage, and from the tighter operating band on the pressure switch.

S-IB-8 was the first stage to have noticeable pilot valve leakage because the pilot valve assembly is normally adjusted to provide relief actions at 21.0/21.5 psig and poppet reseating at 19.0 psig. The valves used on S-IB-8 differed from the normally qualified valves in that the relief setting was reduced to 19.0/19.1 psig to accommodate a lowered proof pressure for the tanks. The effect of the reduction of relief pressure was also to reduce reseat pressure to approximately 17.0 psig. Pilot valve leakage was then approximately 4000 SCIM per valve at a tank ullage pressure of 18.0 psig, whereas there was zero leakage at 18.0 psig for valves qualified to relieve at 21.0/21.5 psig.

The Digital Events Evaluator shows that the pressurizing valves opened three times to repressurize the fuel tank. Two of these repressurization cycles occurred during the engine start sequence.

Telemetry data show helium sphere pressure to be 2903 psia at liftoff which is slightly higher than it was on S-IB-7. The sphere pressure is shown in Figure 6-10.

Because the fuel temperature and ullage pressure were different in each of the tanks, the liquid levels were different. The maximum difference between tanks F1 and F3, determined from recorded discrete probe data, was 10.2 inches at 8.2 seconds. The levels converged to a difference of 0.6 inches at approximately 138.0 seconds.

6.6.2 LOX Pressurization System

The LOX tank pressurization system performed satisfactorily during the entire flight.

Following the LOX bubbling test at T-4 hours, 8 minutes; the LOX vents were closed on three occasions prior to prepressurization as a personnel safety procedure against LOX spillage through the vents. The vents were closed at T-4 hours, 2 minutes; T-2 hours, 40 minutes; and T-55 minutes for durations of 129 seconds, 135 seconds, and 150 seconds, respectively.

Prepressurization began with the helium pressurizing valve opening at T-102.893 seconds as shown in Figure 6-11, and was accomplished in 55.21 seconds, compared to 73.3 seconds for S-IB-7. The faster pressurizing rate occurred because of increasing the ground pressurizing orifice diameter from 0.100 to 0.114 inch.

With the additional 18 seconds for ullage decay, the pressure switch cycled 6 times prior to ignition, which is 3 more than S-IB-7. The switch actuated at approximately 57.7 psia and deactuated at 56.2 psia, which is within the switch limits. The bypass orifice flow was initiated at T-2.387

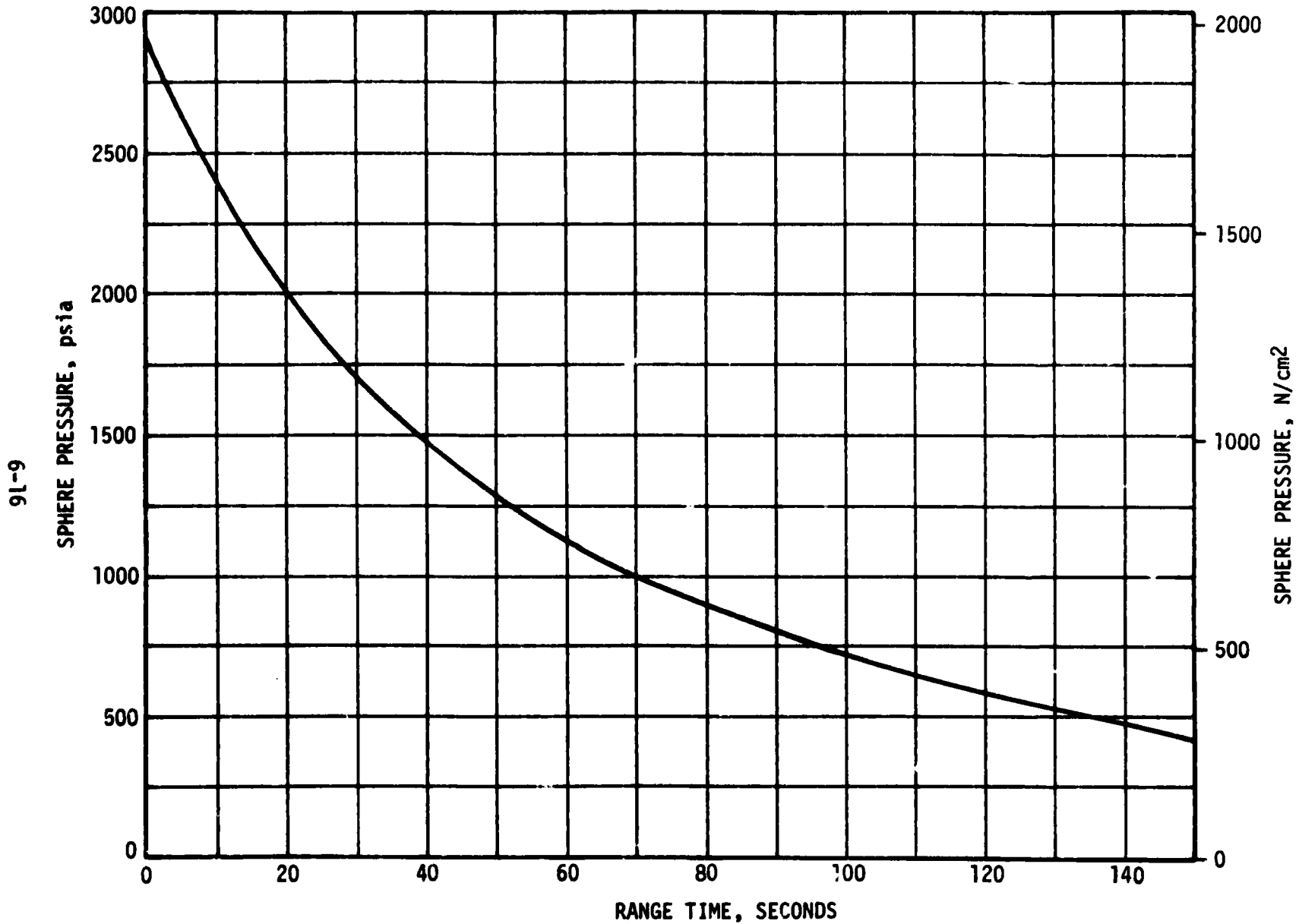


Figure 6-10. S-1B Fuel Tank Helium Pressurization Sphere Pressure

- ▽ START HELIUM BUBBLING
- ▽ START PRESSURIZATION
- ▽ IGNITION
- ▽ BYPASS OFF

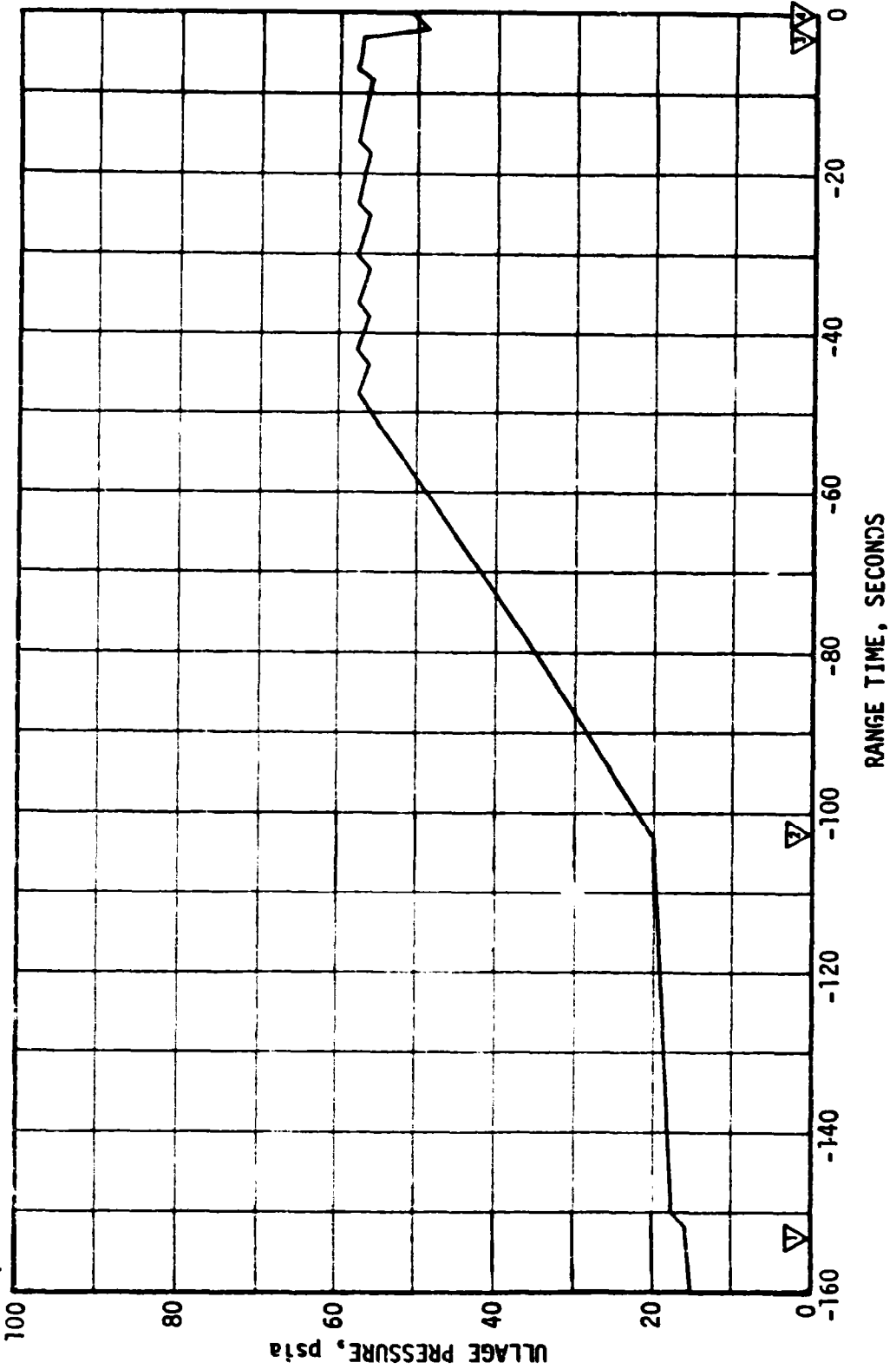


Figure 6-11. S-IB Center LOX Tank Ullage Pressure

seconds, while the pressurizing valve was open during the final cycle. The reconstructed LOX ullage volume prior to vent closure of 994 gallons (1.48 percent) was the same as that on S-IB-7.

The ullage pressure during flight is compared with the predicted pressure in Figure 6-12. The minimum pressure of 47.2 psia occurred during the engine start transient and the maximum pressure of 52.7 psia occurred at 33 seconds. The GOX Flow Control Valve (GFCV) started to close at ignition, and after the normal hesitations during the start transient, reached the fully closed position at 20 seconds and remained closed until 50 seconds as shown in Figure 6-13. The predicted GFCV position is not shown because the valve was originally installed on S-IB-6 and removed after the stage test.

The GFCV moved off the minimum position at 50 seconds, which was 22 seconds earlier than S-IB-7. The earlier opening time is attributed to a lower ullage pressure than on S-IB-7, because GFCV opened at an ullage pressure of approximately 52 psia on both flights. The GFCV continued to open gradually for the remainder of the flight to 21 percent open at IECO, while the ullage pressure decayed to 49.5 psia.

6.7 S-IB PNEUMATIC CONTROL PRESSURE SYSTEM

The S-IB pneumatic control pressure system supplied GN₂ at a regulated pressure of 769 to 686 psia to pressurize the H-1 engine turbopump gearboxes and to purge the LOX and lube seal cavities and the two radiation calorimeters. This regulated pressure was also used to close the LOX and fuel prevalves at IECO and OECO. The actual sphere pressure history recorded by measurement XD0040-009 remained within the acceptable band as shown in Figure 6-14.

6.8 S-IB HYDRAULIC SYSTEM

The system hydraulic pressures were satisfactory during flight and were similar to those of the SA-207 flight. At zero seconds the system pressures ranged from 3190 to 3250 psig. The pressure decreased approximately 50 psi on each engine during flight. This normal pressure decrease was due to the main pump temperature increase during the flight.

Reservoir oil levels were also similar to those of the SA-207 flight. There was a rise of approximately 2 percent in each level during flight indicating about 7°C rise in each hydraulic system's average oil temperature (not reservoir oil temperature).

The reservoir oil temperatures were satisfactory during flight. The temperature at liftoff averaged 44°C compared to an average of 51°C for the four S-IB-7 hydraulic systems. The average temperature decrease during the flight was 7°C for S-IB-8 compared to a decrease of 9°C for the four S-IB-7 hydraulic systems.

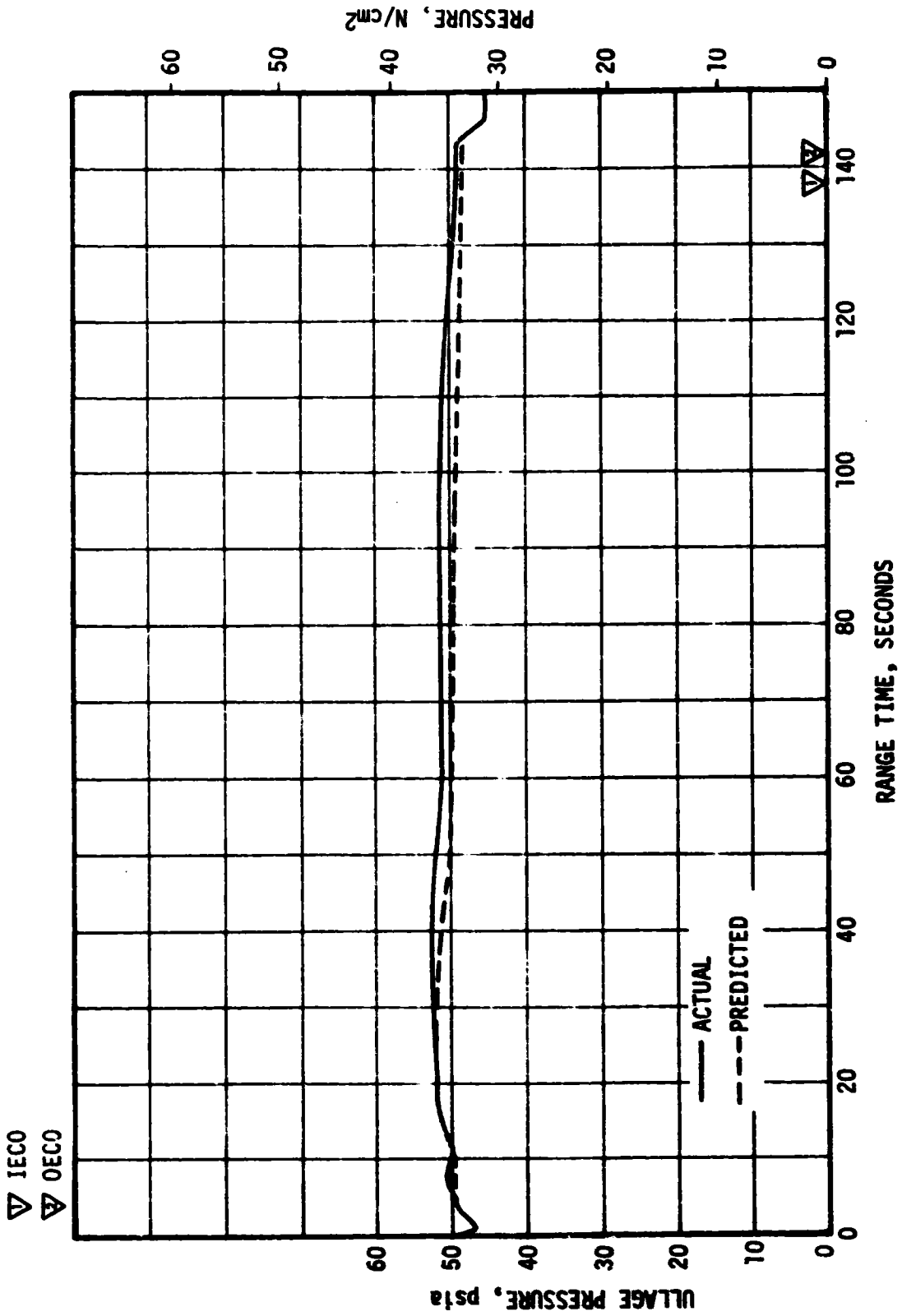


Figure 6-12. S-IB Center LOX Tank Ullage Pressure

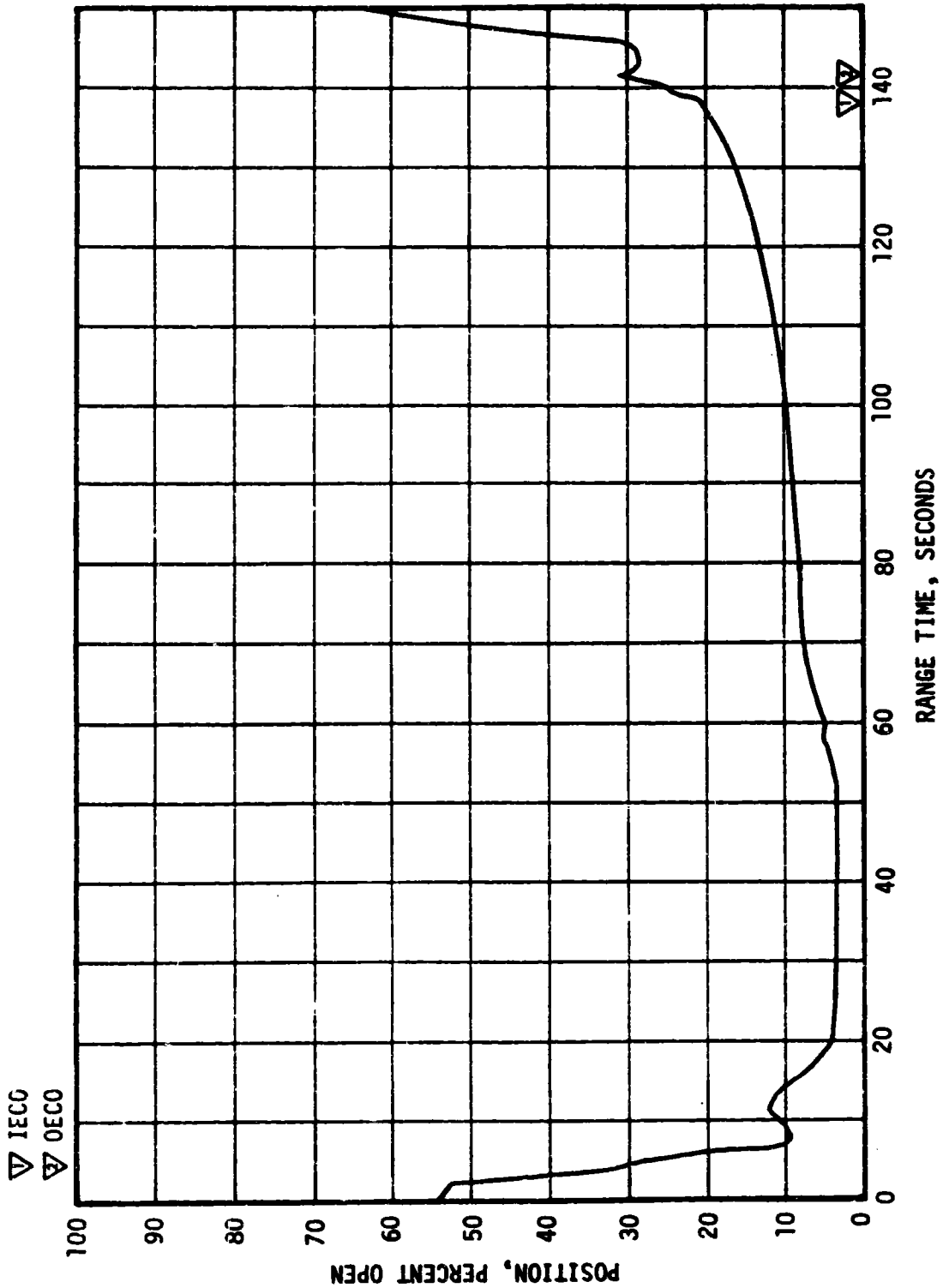


Figure 6-13. S-1B GOX Flow Control Valve Position

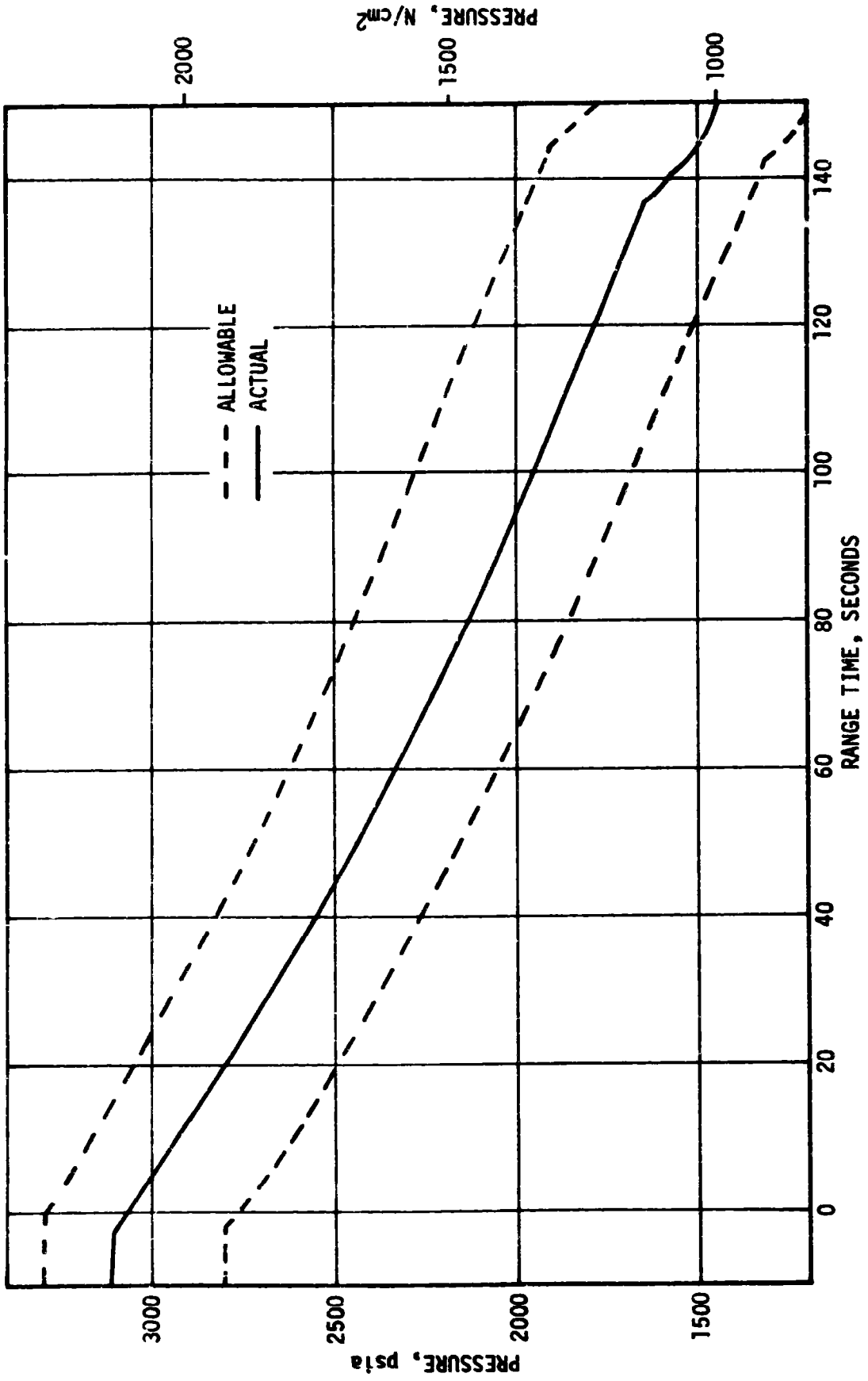


Figure 6-14. S-IB Pneumatic Control Pressure

All eight actuators performed smoothly during S-IB stage flight. In general, individual actuator activity was less than on previous flights. The maximum pitch gimbal angle of 1.5 degrees occurred on engines No. 1 and 3 at 58 seconds, which is approximately 19 percent of the maximum possible deflection. Engine No. 2 yaw actuator represents the largest yaw gimbal angle of 1.6 degrees at 58 seconds or approximately 20 percent of the maximum possible deflection. Figure 6-15 is a comparison of the maximum individual actuator gimbal angles for all S-IB flights. The gimbal rates observed on SA-208 are comparable to previous flights. The greatest gimbal rate observed for SA-208 flight was 1.7 deg/sec on engine No. 1 yaw actuator at 58 seconds. This rate is approximately 5 percent of the actuator's maximum rate.

The differential currents to the servo valves ranged from 0 to 14 percent of rated current during S-IB stage flight. The largest differential current observed was on engine No. 1 yaw actuator and was 1.7 mA at 58 seconds. The maximum value of each performance parameter for any actuator during liftoff, max Q, OECO and for S-IB stage flight are given in Table 6-6.

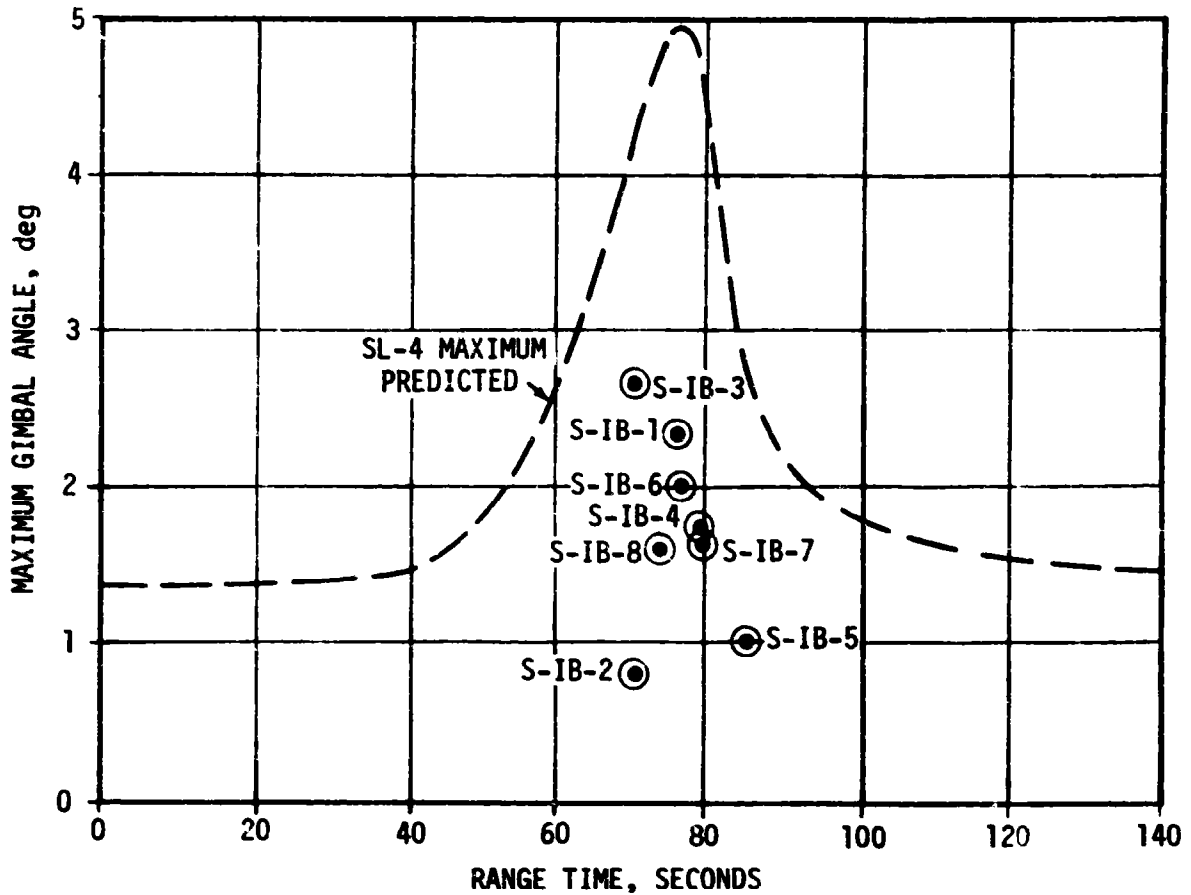


Figure 6-15. S-IB Maximum Gimbal Angle

Table 6-6. S-IB Actuator Maximum Performance Data

PARAMETERS	UNITS	AXIS	LIFTOFF	MAX q	OECO	FLIGHT
Gimbal Angle	deg	Pitch	0.3	1.5	0.3	1.5
		Yaw	0.3	1.5	0.4	1.6
Gimbal Rate	deg/sec	Pitch	0.2	1.2	0.2	1.2
		Yaw	0.8	1.7	0.3	1.7
Valve Current	mA	Pitch	0.3	1.7	0.2	1.7
		Yaw	0.3	0.5	0.2	0.6

SECTION 7

S-IVB PROPULSION

7.1 SUMMARY

The S-IVB propulsion system performed satisfactorily throughout the operational phase of burn and had normal start and cutoff transients. S-IVB burn time was 432.22 seconds, 2.46 seconds shorter than predicted for the actual flight azimuth of 53.8 degrees. This difference is composed of -0.07 second due to S-IB/S-IVB separation velocity, orbital radius, and weight and -2.39 seconds due to higher than predicted S-IVB performance. The engine performance during burn, as determined from standard altitude reconstruction analysis, deviated from the predicted Start Tank Discharge Valve (STDV) open +60 second time slice by +0.26 percent for thrust. Specific impulse was as predicted. The engine control system performed within expected limits. However, a helium leak was evidenced by greater than expected helium usage during mainstage. The S-IVB stage engine cutoff (ECO) was initiated by the Launch Vehicle Digital Computer (LVDC) at 577.18 seconds. The S-IVB residuals at engine cutoff were near nominal. The best estimate of the residuals at engine cutoff is 1581 lbm for LOX and 2093 lbm for LH₂ as compared to the predicted values of 2137 lbm for LOX and 1727 lbm for LH₂.

The propellant tanks were vented satisfactorily as sequenced following engine cutoff. During orbital coast, the LOX tank pressure increased more rapidly than predicted and went above the predicted limits. This was probably a result of the greater-than-expected LOX boiloff indicated by reconstruction of the orbital coast phase and the LOX dump. The increased LOX boiloff is an effect of the increased LOX tank wetted area resulting from propellant slosh. LOX slosh could have been induced by Auxiliary Propulsion System (APS) engine firing activity during LH₂ tank cyclic relief venting. The fuel tank nonpropulsive vent (NPV) system satisfactorily controlled fuel ullage pressure during earth orbit.

Throughout the flight, APS Module No. 1 performed nominally. Module No. 2 functioned nominally except for off nominal performance of the pitch engine. The pitch engine chamber pressure and thrust was approximately 30% of nominal. This lower thrust level resulted in longer pitch engine on-time to provide the required attitude control system total impulse. This reduced performance has been attributed to partial blockage of the oxidizer injector area.

During orbital coast, the APS responded to a disturbing force on the S-IVB/IU stage. LH₂ NPV venting cycles were time correlated with this disturbance. The APS activity and resulting propellant consumption on both modules

was greater than expected. During this time period, 4200 seconds to 6000 seconds, the LH₂ NPV system was venting in a cyclic manner. Although the precise nature of the mechanism has not been established, similar response seems to be characteristic of the S-IVB/IU stage under certain conditions. There was no mission impact, and since the disturbing forces are small no further corrective action is planned other than allowing for additional APS propellant consumption in future predictions.

The impulse derived from the LOX and fuel dumps was sufficient to satisfactorily deorbit the S-IVB/IU. The total impulse provided, 66,975 lbf-sec, was in good agreement with the real time nominal predicted value of 70,500 lbf-sec. The APS satisfied control system demands throughout the deorbit sequence.

Propellant tank safing after fuel dump was satisfactory.

7.2 S-IVB CHILLDOWN AND BUILDUP TRANSIENT PERFORMANCE

The thrust chamber temperature at liftoff was -221°F, which was below the maximum allowable redline limit of -185°F. At S-IVB STDV open signal, the temperature was -192°F, which was within the requirements of -225 +75°F.

The chilldown and loading of the engine GH₂ start tank and pneumatic control bottle prior to liftoff was satisfactory. At liftoff, the engine control sphere pressure and temperature were 3070 psia and -170°F and the start tank pressure and temperature were 1340 psia and -185°F. At STDV open the engine control sphere pressure and temperature were 2899 psia and -182°F. The start tank conditions were 1354 psia and -181.5°F, which were within the start box.

Propellant tank prepressurizations were satisfactory. The propellant recirculation system operation was satisfactory and operated continuously from before liftoff until just prior to Engine Start Command (ESC). Start and run box requirements for both fuel and LOX were met, as shown in Figure 7-1. At STDV open the LOX pump inlet temperature was -294.8°F and the pump inlet pressure was 41.5 psia. At STDV open the fuel pump inlet temperature was -421.8°F and the pump inlet pressure was 32.0 psia.

Fuel lead followed the expected pattern and resulted in satisfactory conditions as indicated by the fuel injector temperature.

The engine start transient was satisfactory, and the thrust buildup was within the limits set by the engine manufacturer. This buildup was similar to the thrust buildups observed during previous flights. The Mixture Ratio Control Valve (MRCV) was in the closed position, 4.8 Engine Mixture Ratio (EMR), during the buildup. The total impulse from STDV open to STDV open +2.4 seconds was 165,726 lbf-s.

7.3 S-IVB MAINSTAGE PERFORMANCE

The propulsion reconstruction analysis verified that the stage performance during mainstage operation was satisfactory. A comparison of predicted

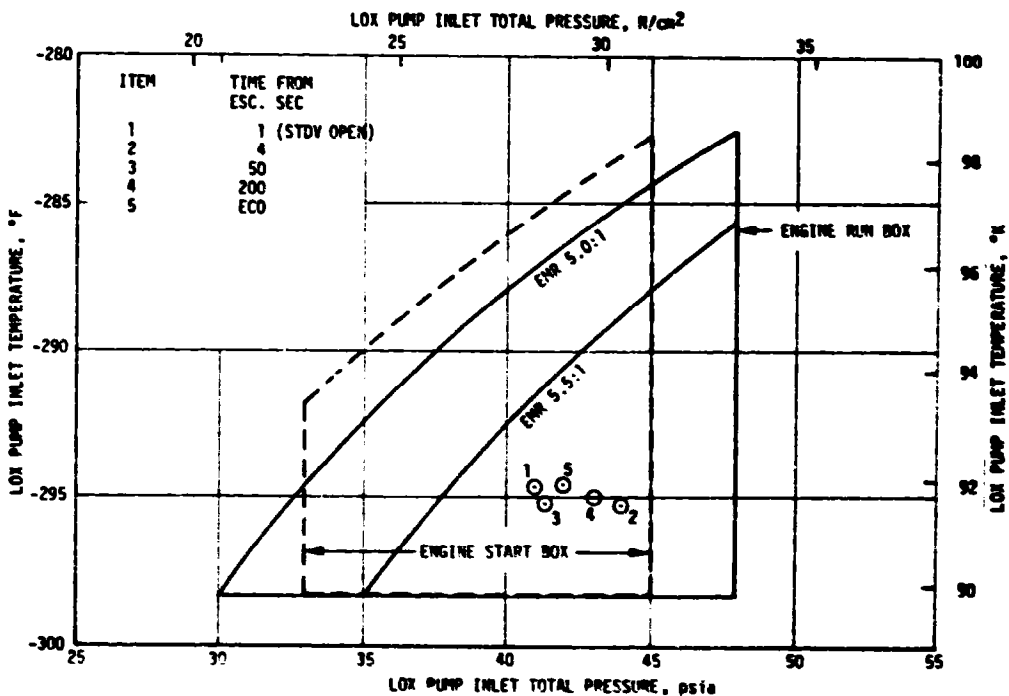
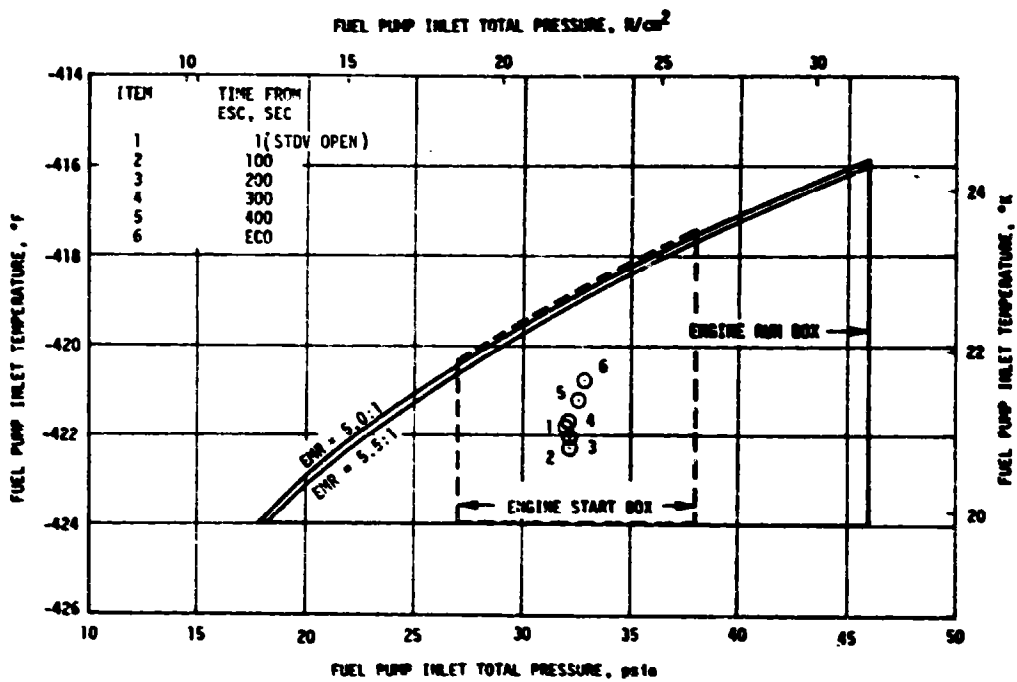


Figure 7-1. S-IVB Start Box and Run Requirements

and actual performance of thrust, specific impulse, total flowrate, and EMR versus time is shown in Figure 7-2. Table 7-1 shows the thrust, specific impulse, flowrate, and EMR deviations from predicted at the STDV open +60 second time slice at standard altitude conditions.

Table 7-1. S-IVB Steady State Performance (STDV Open +60 Second Time Slice at Standard Altitude Conditions)

	PREDICTED	ACTUAL (RECONSTRUCTED)	FLIGHT DEVIATION (ACT-PRED)	PERCENT DEVIATION FROM PREDICTED
Thrust, lbf	233,600	234,200	600	0.26
Specific Impulse, lbf-s/lbm	425.3	425.3	0	0
LOX Flowrate, lbm/s	465.29	466.61	1.32	0.28
Fuel Flowrate, lbm/s	84.00	84.06	0.06	0.07
Engine Mixture Ratio, LOX/Fuel	5.540	5.551	0.011	0.20

Engine burn time was 432.22 seconds which was 2.46 seconds less than predicted for the actual flight azimuth of 53.8 degrees. Of this difference 2.39 seconds was due to higher than predicted S-IVB thrust and flowrate.

The engine control system performed within expected limits during mainstage operation. However, the helium usage during mainstage was greater than expected. Helium usage was nominal up to ESC +148 sec. At that time, there was a transient response in the regulator outlet pressure resulting in a net drop of 2 psi. At that time a helium leak was evidenced when the engine and stage helium bottle pressures began to decrease at an increased rate of about 20 Standard Cubic Feet per Minute (SCFM) (Figure 7-3).

Helium usage during LOX and LH₂ dump was near nominal. The computed usage rates were slightly less than predicted. After adjusting for ground and

▽ S-IVB ESC
 ▽ S-IVB ECO

5.5 PREDICTED = 425.6 ± 2 SEC
 4.8 PREDICTED = 429.4 ± 2 SEC

—— ACTUAL
 - - - PREDICTED

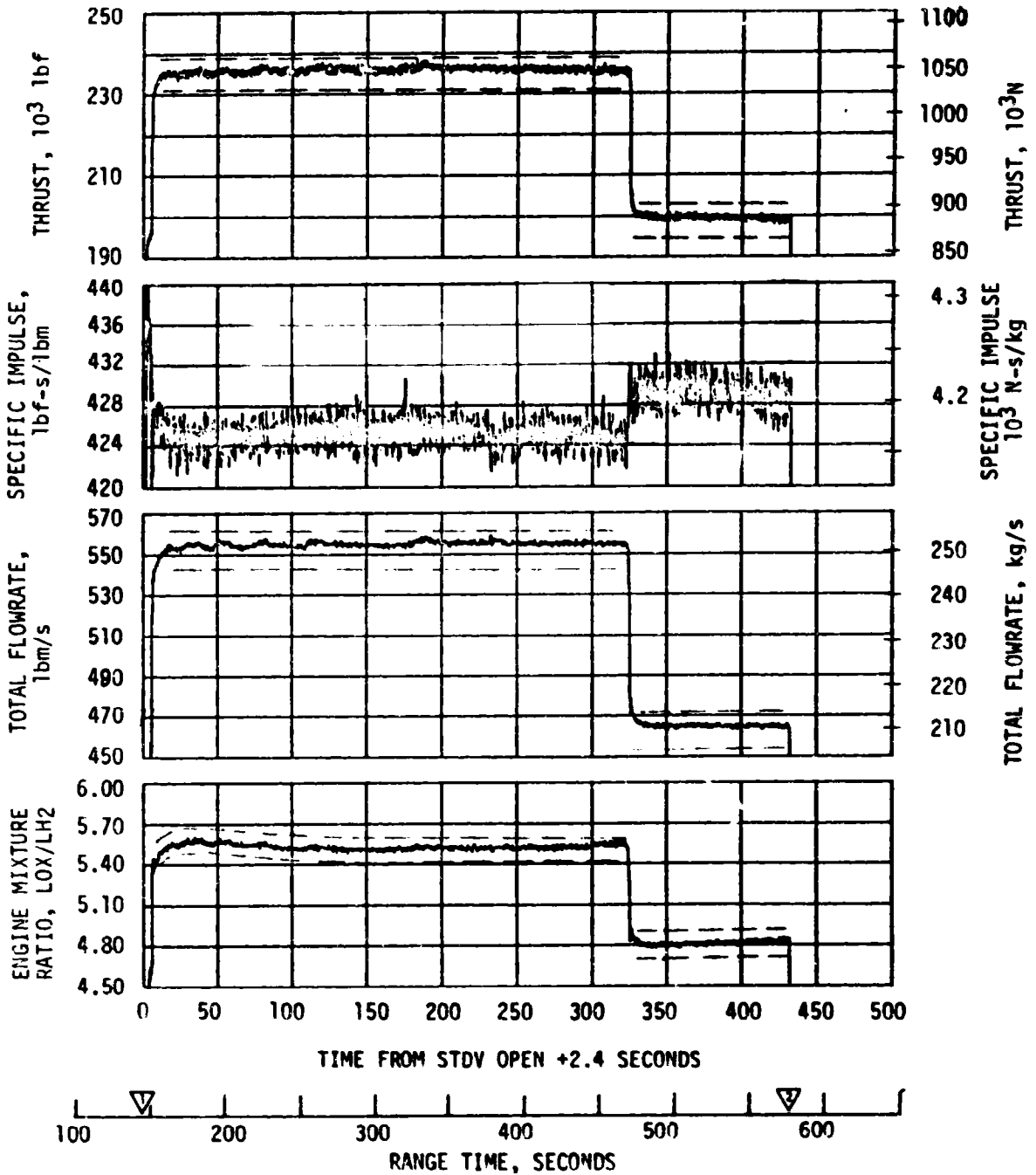


Figure 7-2. S-IVB Steady-State Performance

▽ ENGINE START
▽ ENGINE CUTOFF

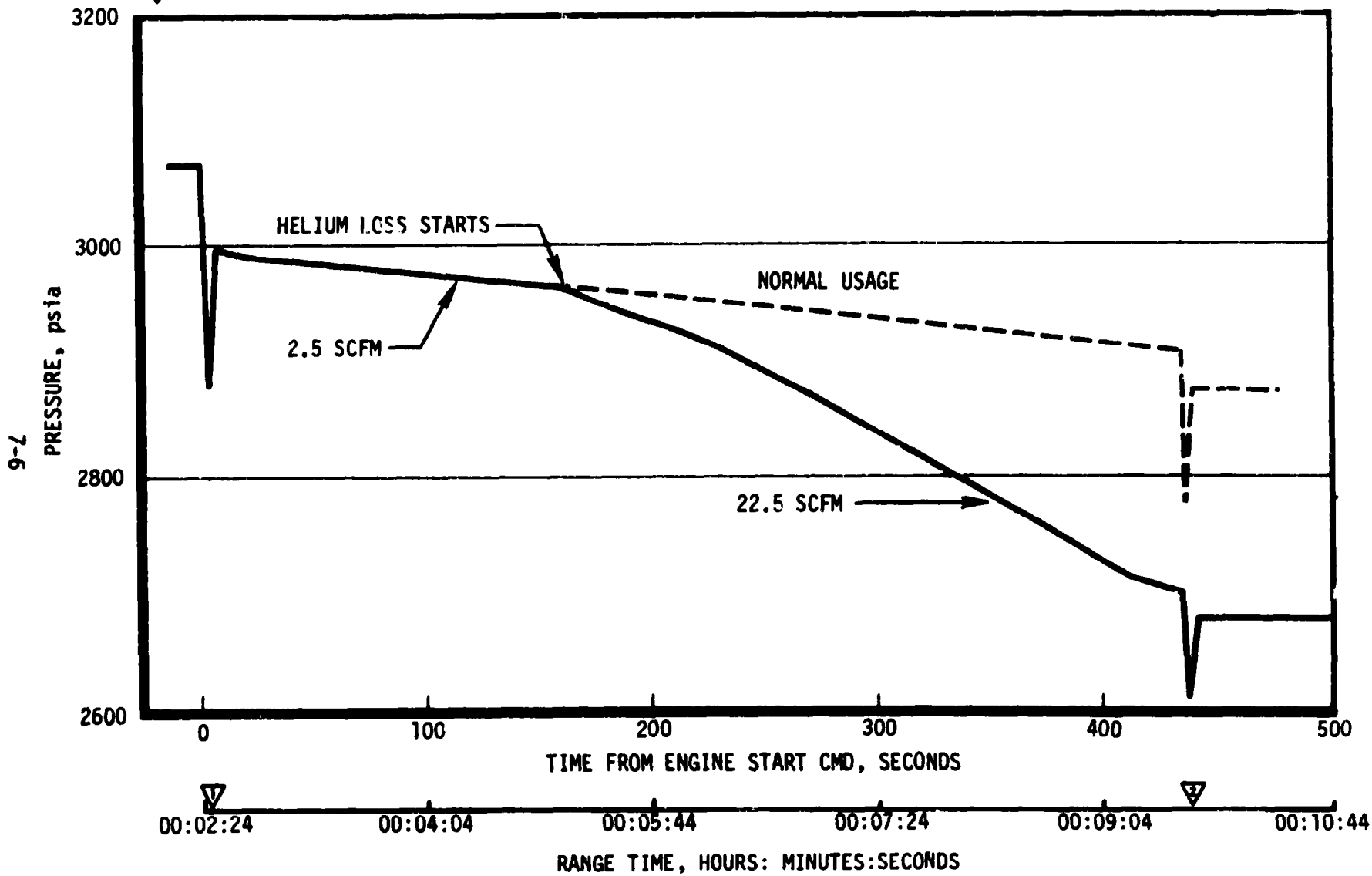


Figure 7-3. S-IVB Engine Control Bottle Pressure

flight temperature differences, the usage rates during flight LOX and LH₂ dumps were found to agree very closely with the rates observed during the Flight Readiness Test (FRT). This indicates that there was no helium leakage during LOX or LH₂ dump. Also, there was no indication of any leakage during orbital coast. Therefore, the leakage appears to only be present during mainstage operation.

In an attempt to further isolate the leakage source, a comparison was made between pertinent acceptance and flight data. Figure 7-4 shows that the Gas Generator (GG) chamber pressure for flight and acceptance tests prior to EMR shift were similar. However, the GG valve position (G005 and G509) were not similar (Figure 7-5). The acceptance data indicated a tendency for the valve to go more open while the flight data indicated a tendency for the valve to go more closed. Also, the regulator outlet pressures (D018) were not similar (Figure 7-6). As expected, the acceptance data indicated no rapid shifts in regulator outlet pressure while the flight data showed a 2 psi shift in regulator pressure at ESC +148 sec.

The 2 psi decrease in flight regulator outlet pressure indicates an increased helium usage downstream of the regulator. The tendency of the GG valve to move in the closed direction for flight, when acceptance data showed movement in the open direction for the same GG chamber pressure trend, indicated a high probability of decreased pressure downstream of the Main Oxidizer Valve (MOV) sequence valve resulting from helium leakage.

Because of reconfiguration of the engine pneumatic system during mainstage, orbital coast, and propellant dumps the helium leak has been isolated to that part of the pneumatic system downstream of the MOV sequence valve as shown in Figure 7-7. The potential leakage sources in this part of the system are: pneumatic line sleeve weld failure; Oxidizer Turbine Bypass Valve (OTBV); fast shutdown valve; MOV sequence valve; or GG.

A pneumatic line sleeve weld failure could result in a 60 SCFM helium leak using maximum tolerance in fit between line and sleeve if weld material does not restrict the passage. However, allowing for restriction by weld material and considering samples of actual fits between line and sleeve a much lower leakage rate would be possible. This failure mode could be the cause of the high helium usage but should not be a concern for future flights since ECP-517, providing improved welding procedures, was implemented on S-IVB-209.

OTBV actuator seal leakage was considered and ruled out due to a 0.015 inch diameter orifice located in the upstream line which would cause a considerable change in the OTBV opening time at engine cutoff. Valve operation on SA-208 at engine cutoff was normal.

A fast shutdown valve diaphragm failure would give a maximum leakage rate of 0.58 SCFM due to diaphragm restriction in the seal cavity and, therefore, could not account for the observed leakage.

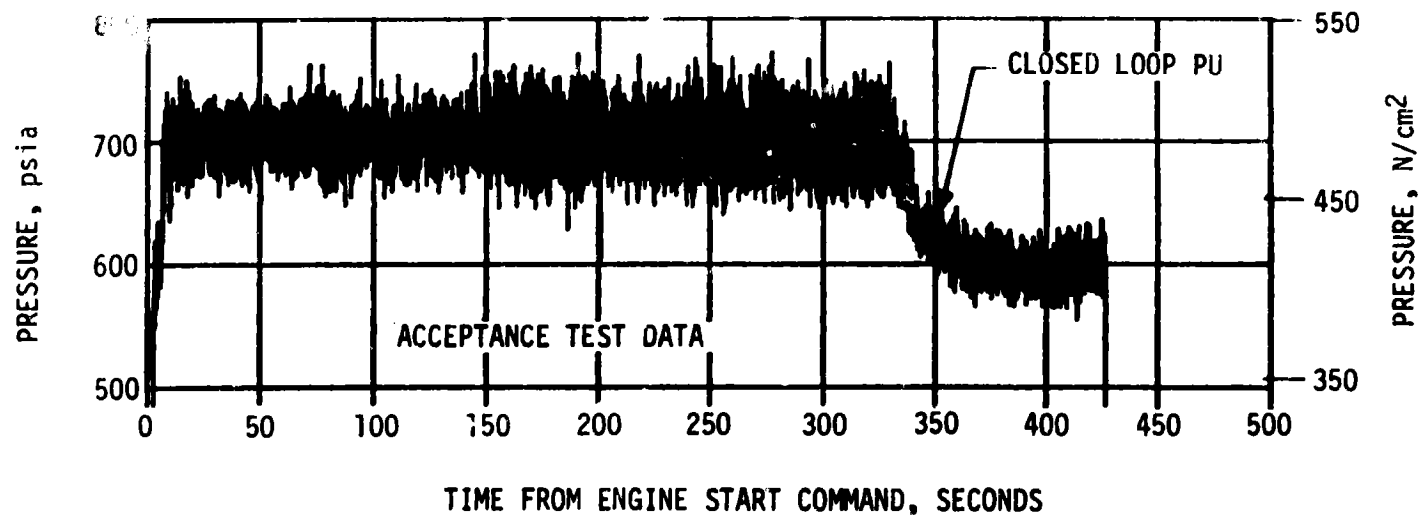
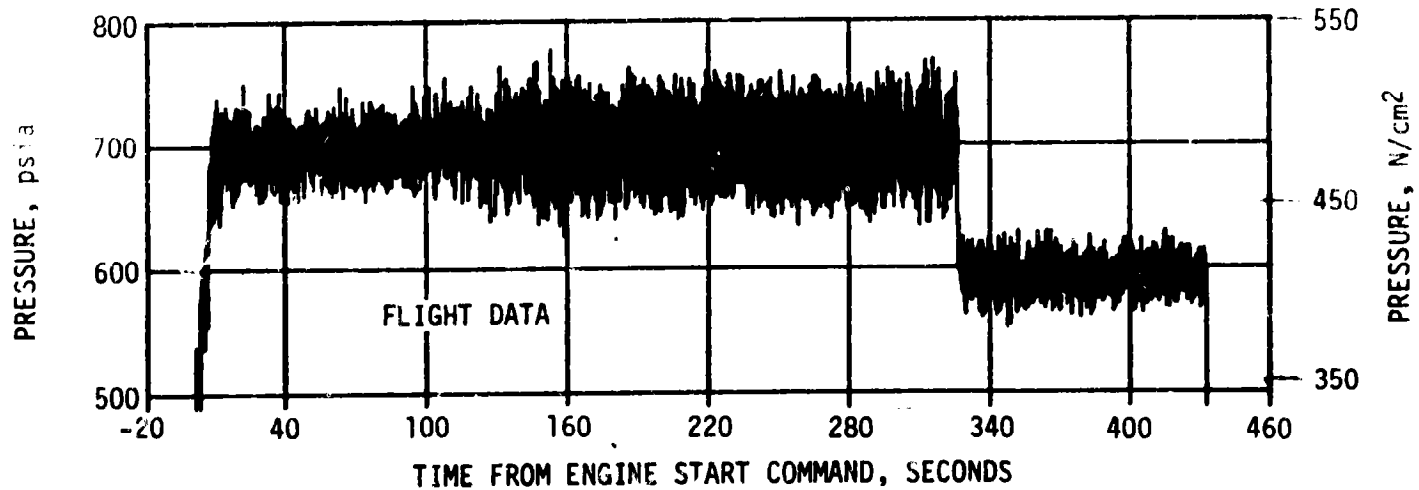


Figure 7-4. S-IVB Gas Generator Chamber Pressure (D010)

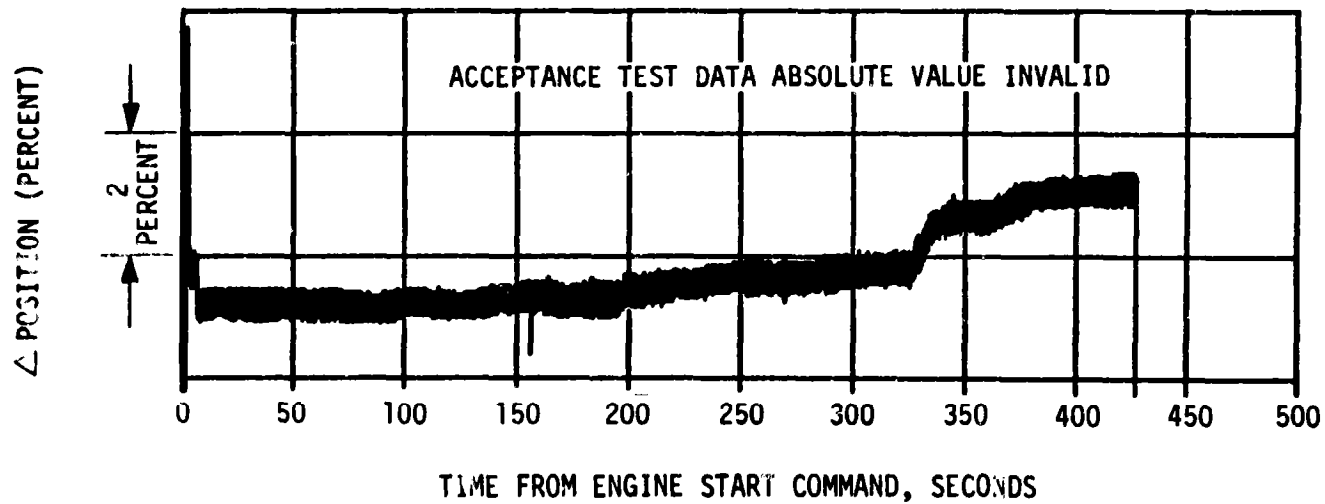
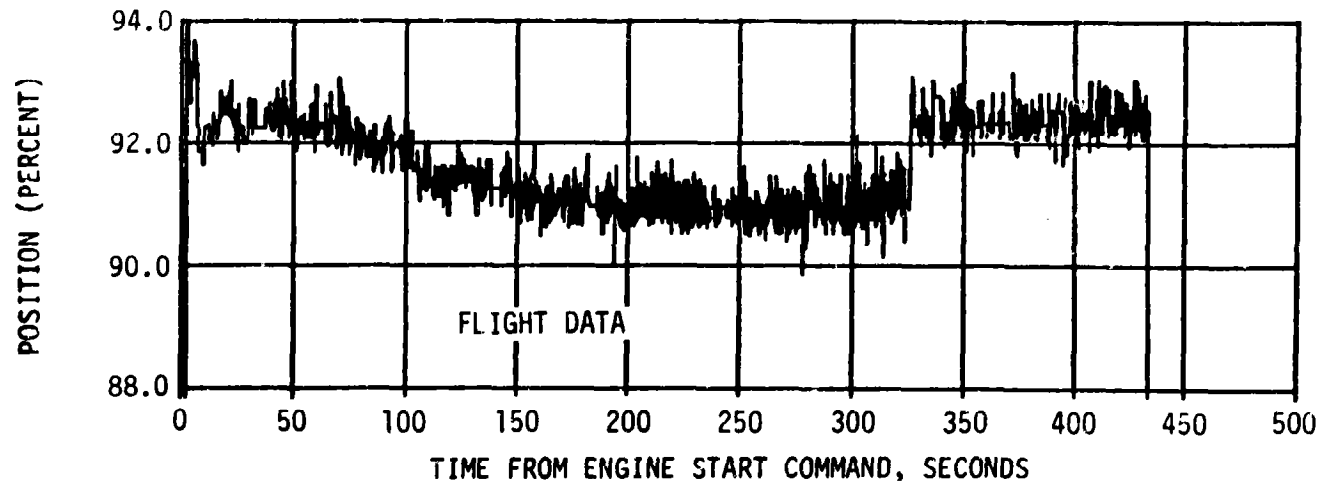


Figure 7-5. S-IVB Gas Generator Valve Position

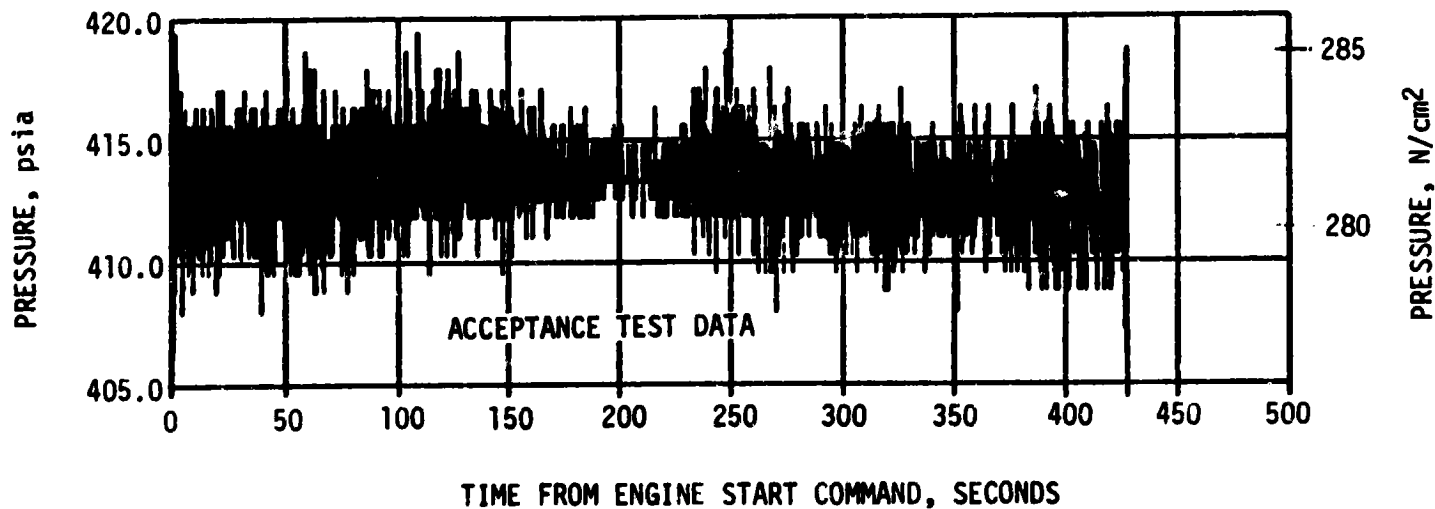
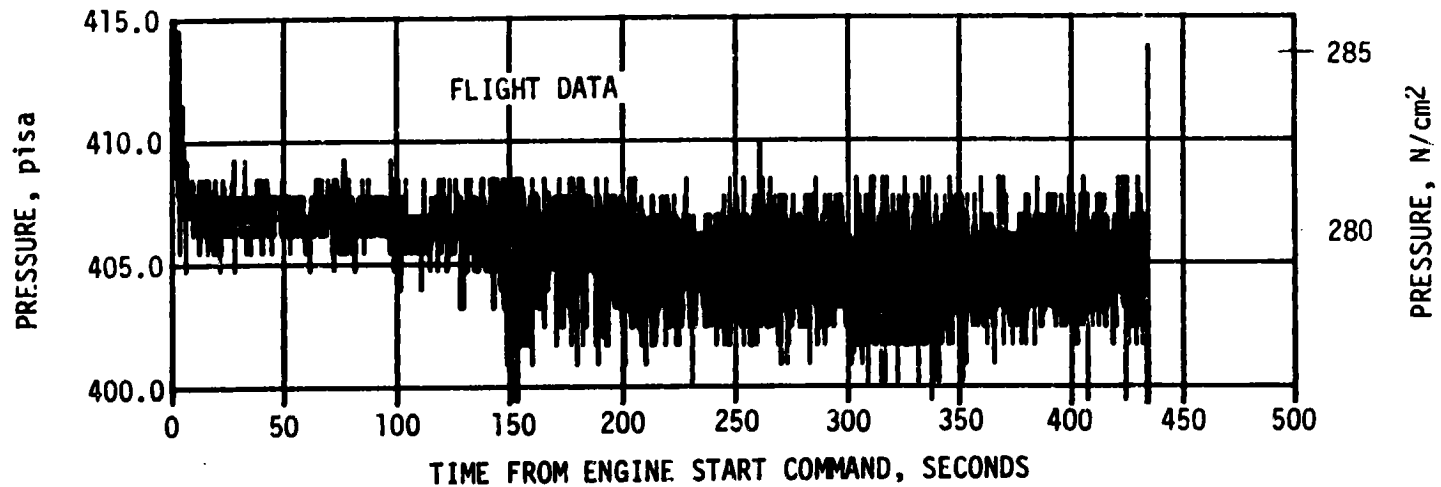


Figure 7-6. S-IVB Engine Regulator Outlet Pressure (D018)

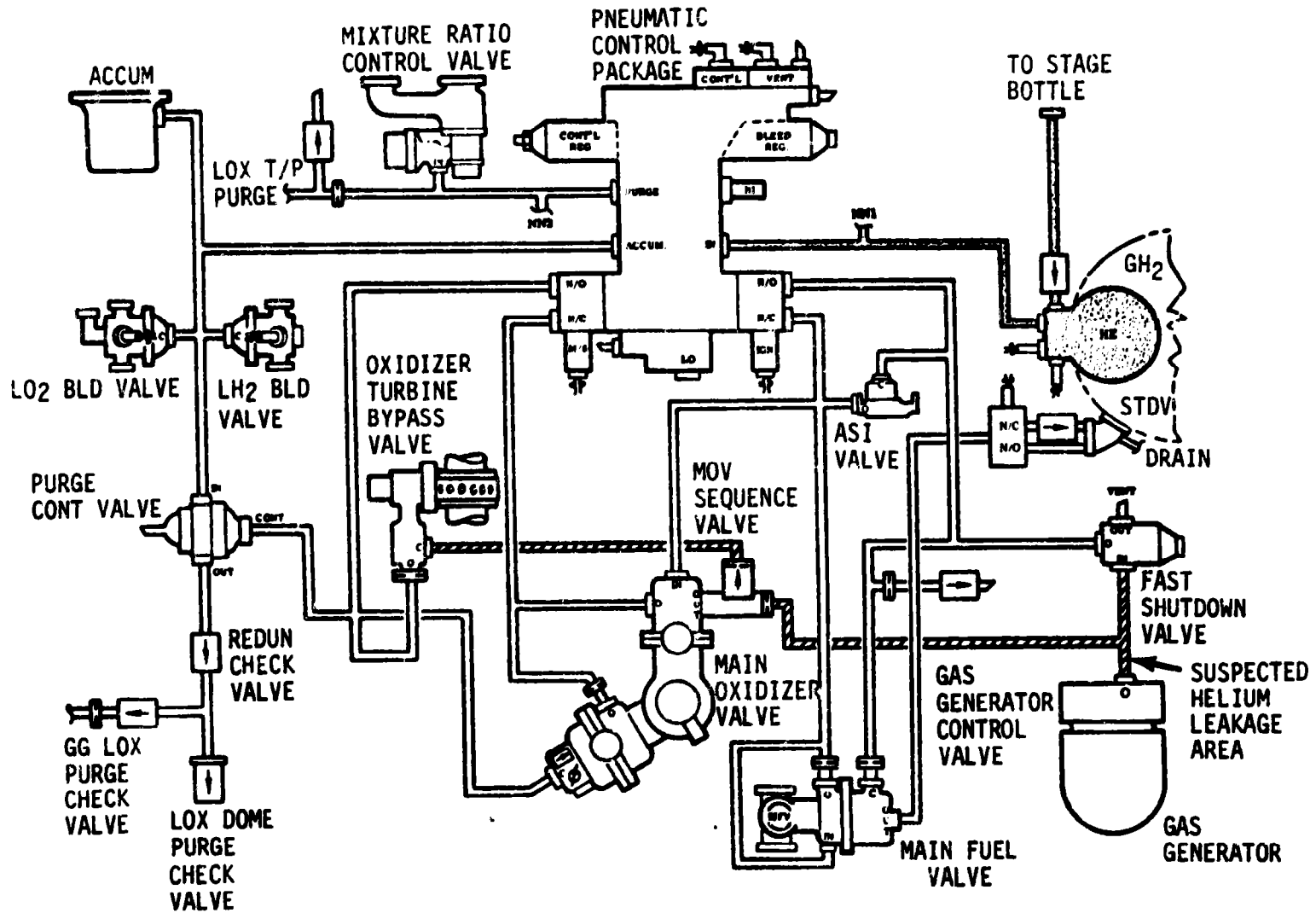


Figure 7-7. S-IVB Engine Pneumatic System Pre-Start or Cutoff Mode

The MOV sequence valve failure mode is at the seal between the sequence valve outlet and balance port. This failure could pass the required flow; however, the lack of MOV valve motion at time of failure, and no previous failure history, tend to rule out this potential failure.

The GG has two failure modes; leakage due to corrosion of the GG valve solar braze joint or leakage due to cracked bellows. There have been two cases of corrosion on earlier stages but with no associated leakage. This failure mode is a possible cause of the high helium usage observed on S-IVB-208. The S-IVB-209 stage has been field checked for corrosion of this joint with negative results. There is no failure history of fatigue cracks in the valve bellows; however, a cracked bellows simulator test did duplicate the effects observed during flight. In particular, previous experience with bellows failures shows that a crack will propagate with time. This could explain the increase in leakage rate, as seen in Figure 7-3, during main-stage after the initial leak started. It is possible, therefore, that a cracked bellows could be the cause of helium leakage.

7.4 S-IVB SHUTDOWN TRANSIENT PERFORMANCE

S-IVB ECO was initiated at 577.18 seconds by guidance velocity cutoff command. The ECO transient was satisfactory. The total cutoff impulse to zero thrust was 42,806 lbf-s which was 459 lbf-s lower than the nominal predicted value of 43,265 lbf-s and within the +4,373 lbf-s predicted band. Cutoff occurred with the MRCV in the 4.8 EMR position.

7.5 S-IVB STAGE PROPELLANT MANAGEMENT

Comparison of propellant masses at critical flight events, as determined by various analyses, is presented in Table 7-2. The best estimate full load propellant mass for LOX is 194,753 + 458 lbm and the best estimate full load propellant mass for LH₂ is 38,488 + 181 lbm. The best estimate full load propellant masses were 0.09 percent less for LOX and 0.61 percent greater for LH₂ than predicted. This deviation was well within the required loading accuracy. The best estimate for propellant residuals at end of thrust decay were 1,521 lbm for LOX and 2,071 lbm for LH₂. Cutoff transient propellant consumption was 60 lbm for LOX and 22 lbm for LH₂.

Extrapolation of best estimate residuals data to depletion, using the propellant flow rates, indicated that a LOX depletion (320 lbm) would have occurred approximately 3.3 seconds after the velocity cutoff.

The pneumatically controlled two position MRCV was commanded to the 4.8 EMR engine start position 1.9 seconds prior to ESC. The MRCV does not respond until it receives engine pneumatic power which becomes available at ESC.

The MRCV was commanded to the closed position at ESC +6.0 seconds (approximately 5.5 EMR) and indicated closed at ESC +6.9 seconds. The MRCV was commanded to 4.8 EMR (open) position at ESC +325.4 seconds indicating open at ESC +325.8 seconds where it remained for the duration of powered flight.

Table 7-2. S-IVB Stage Propellant Mass History

EVENT	UNITS	PREDICTED		PU INDICATED (CORRECTED)		PU VOLUMETRIC		FLOW INTEGRAL		BEST ESTIMATE	
		LOX	LM ₂	LOX	LM ₂	LOX	LM ₂	LOX	LM ₂	LOX	LM ₂
S-IB Liftoff	lbm	194,958	38,197	194,814	38,396	194,814	38,431	194,632	38,558	194,753	38,488
S-IVB ESC	lbm	194,958	38,197	194,814	38,391	194,814	38,426	194,632	38,553	194,753	38,488
S-IVB Cutoff	lbm	2,137	1,727	1,633	2,051	1,588	1,983	1,581	2,093	1,581	2,093

The masses shown do not include mass below the main engine valves, as represented in Section i6.

The MRCV was commanded to the closed position at ECO +2.4 seconds. The MRCV indicated closed 484 milliseconds after the command was received. No further activities were planned for the MRCV during the rest of the mission.

7.6 S-IVB PRESSURIZATION SYSTEM

7.6.1 S-IVB Fuel Pressurization System

The LH₂ pressurization system met all of its operational requirements. The LH₂ pressurization system indicated acceptable performance during prepressurization, boost, burn, earth orbit and deorbit.

The LH₂ tank prepressurization command was received at -119.4 seconds and the tank pressurized signal was received 31.7 seconds later. The ullage pressure reached relief conditions (approximately 31.7 psia) at liftoff, as shown in Figure 7-8.

The LH₂ ullage pressure was 31.6 psia at ESC. The average pressurization flowrate was 0.68 lbm/s until step pressurization, when it increased to 9.95 lbm/s. The total mass used for pressurization during burn was 324 lbm. Throughout the burn, the ullage pressure was at relief (31.6 psia), as predicted.

LH₂ tank relief venting during boost included periods of vent valve chatter similar to those which occurred during orbital coast (see Section 7.10.1) and during SA-206 flight. The ullage pressure cycled between 32.1 and 31.1 psia, as shown in Figure 7-8. Chatter of the LH₂ vent and relief valve and the LH₂ latching vent valve occurred during the vent portion of the ullage pressure cycle, as evidenced by the valve position microswitches and the NPV nozzle pressure oscillations. The valves were closed during the self-

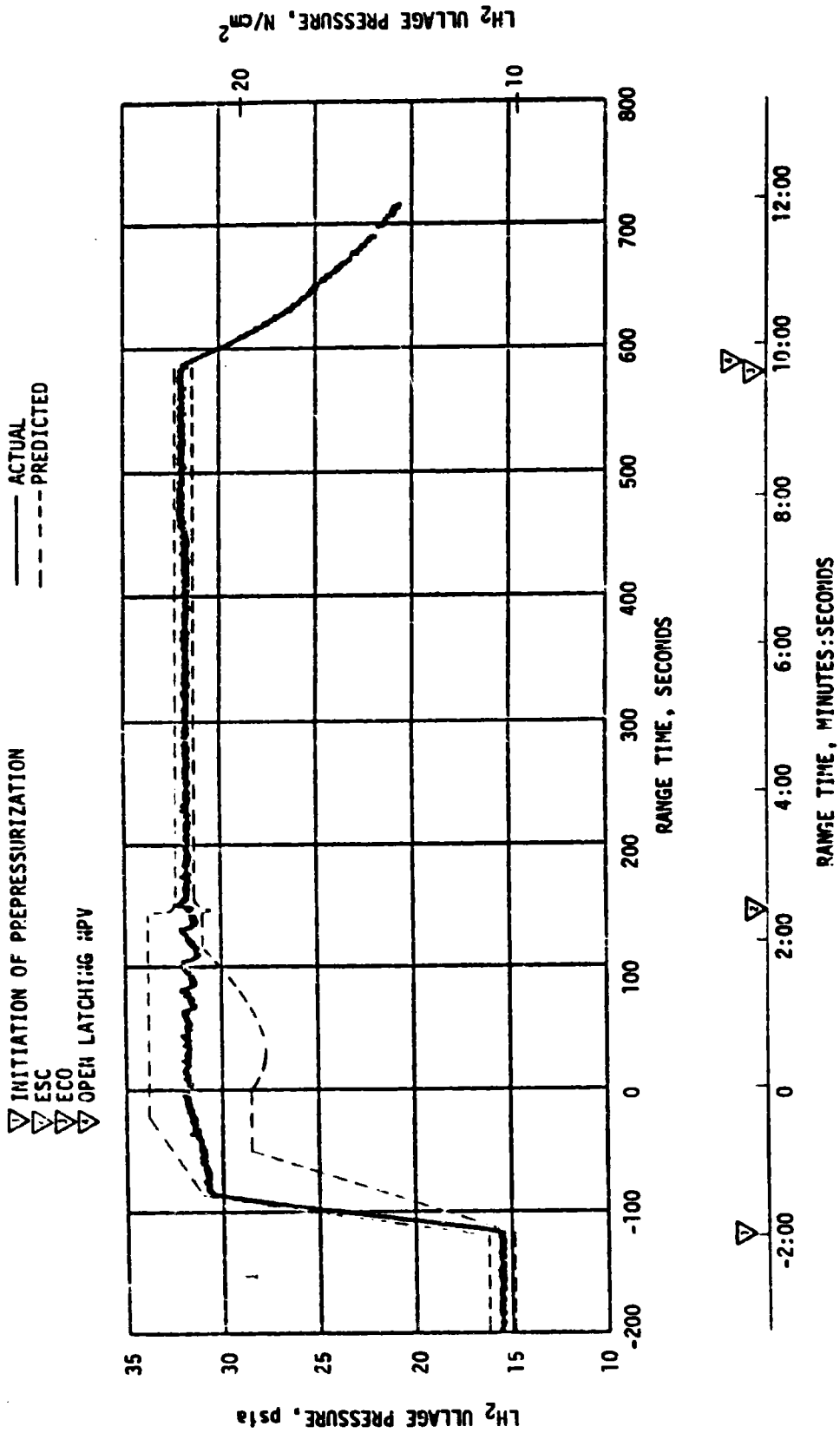


Figure 7-8. S-IVB LH₂ Ullage Pressure - Preliftoff, Boost and Burn

pressurization portion of the cycle. The valve chatter during boost had no effect on tank conditions.

LH₂ tank relief during burn was accomplished by an open/close mode, similar to that experienced on SA-207, until the venting requirement increased at step pressurization. The open/close venting mode had no effect on tank conditions or pressurization system performance.

The LH₂ pump inlet Net Positive Suction Pressure (NPSP) was calculated from the pump interface temperature and total pressure. These values indicated that the NPSP at STDV was 13.2 psi. At the minimum point, the NPSP was 6.0 psi above the minimum required value. Throughout the burn, the NPSP had satisfactory agreement with the predicted values. Figure 7-9 summarizes the fuel pump inlet conditions during burn.

7.6.2 S-IVB LOX Pressurization System

LOX tank prepressurization was initiated at -167 seconds and increased the LOX tank ullage pressure from ambient to 39.8 psia in 13.5 seconds, as shown in Figure 7-10. Two makeup cycles were required to maintain the LOX tank ullage pressure before the ullage temperature stabilized. A total of 5.42 lbm of helium were required for LOX tank prepressurization. At -119 seconds, fuel tank prepressurization and the vent valve purge caused the LOX tank pressure to increase from 39.6 to 41.0 psia at liftoff.

During boost there was a nominal rate of ullage pressure decay caused by tank volume increase (acceleration effect) and ullage temperature decrease. No makeup cycles could occur because of an inhibit from liftoff +6.0 seconds until ESC -2.5 seconds. LOX tank ullage pressure was 36.4 psia just prior to separation and was increasing at ESC due to a makeup cycle.

During burn, six over-control cycles were initiated, including the programmed over-control cycle initiated prior to ESC. The LOX tank pressurization flowrate variation was 0.24 to 0.41 lbm/s during under-control and 0.30 to 0.51 lbm/s during over-control system operation. This variation is normal and is caused by temperature effects. Heat exchanger performance during burn was satisfactory.

The LOX NPSP calculated at the interface was 24.0 psi at ESC. This was 11.2 psi above the NPSP minimum requirement for start. The LOX pump static interface pressure during burn follows the cyclic trends of the LOX tank ullage pressure. Figure 7-11 summarizes the LOX pump conditions for burn. The LOX pump run requirements for burn were satisfactorily met.

The cold helium supply was adequate to meet all flight requirements. At ESC, the cold helium spheres contained 257 lbm of helium. At the end of burn, the helium mass had decreased to 94 lbm. Figure 7-12 shows helium supply pressure history.

▽ S-IVB ESC
 ▽ S-IVB STDV OPEN
 ▽ S-IVB ECO

— ACTUAL
 - - - PREDICTED

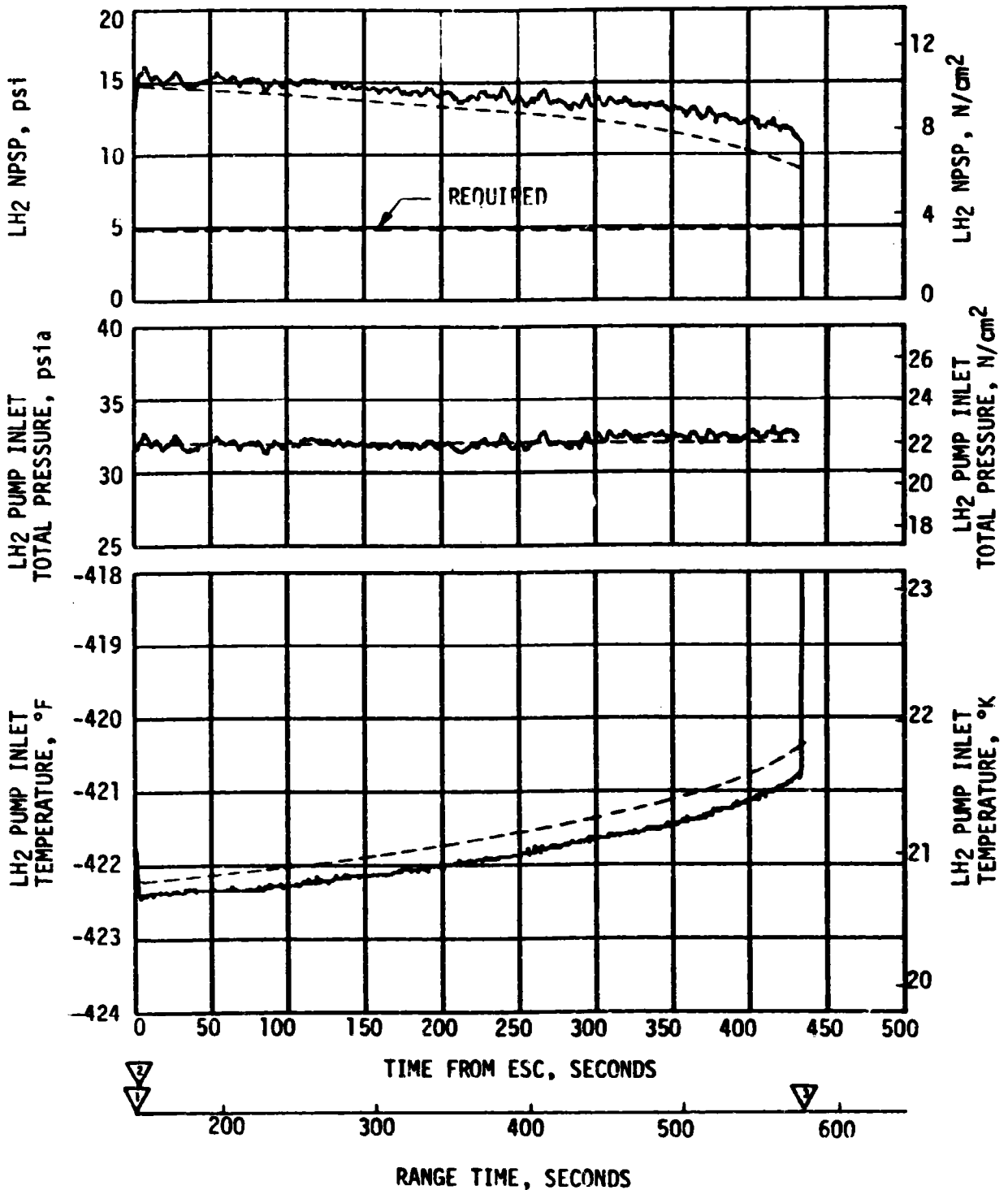


Figure 7-9. S-IVB Fuel Pump Inlet Conditions

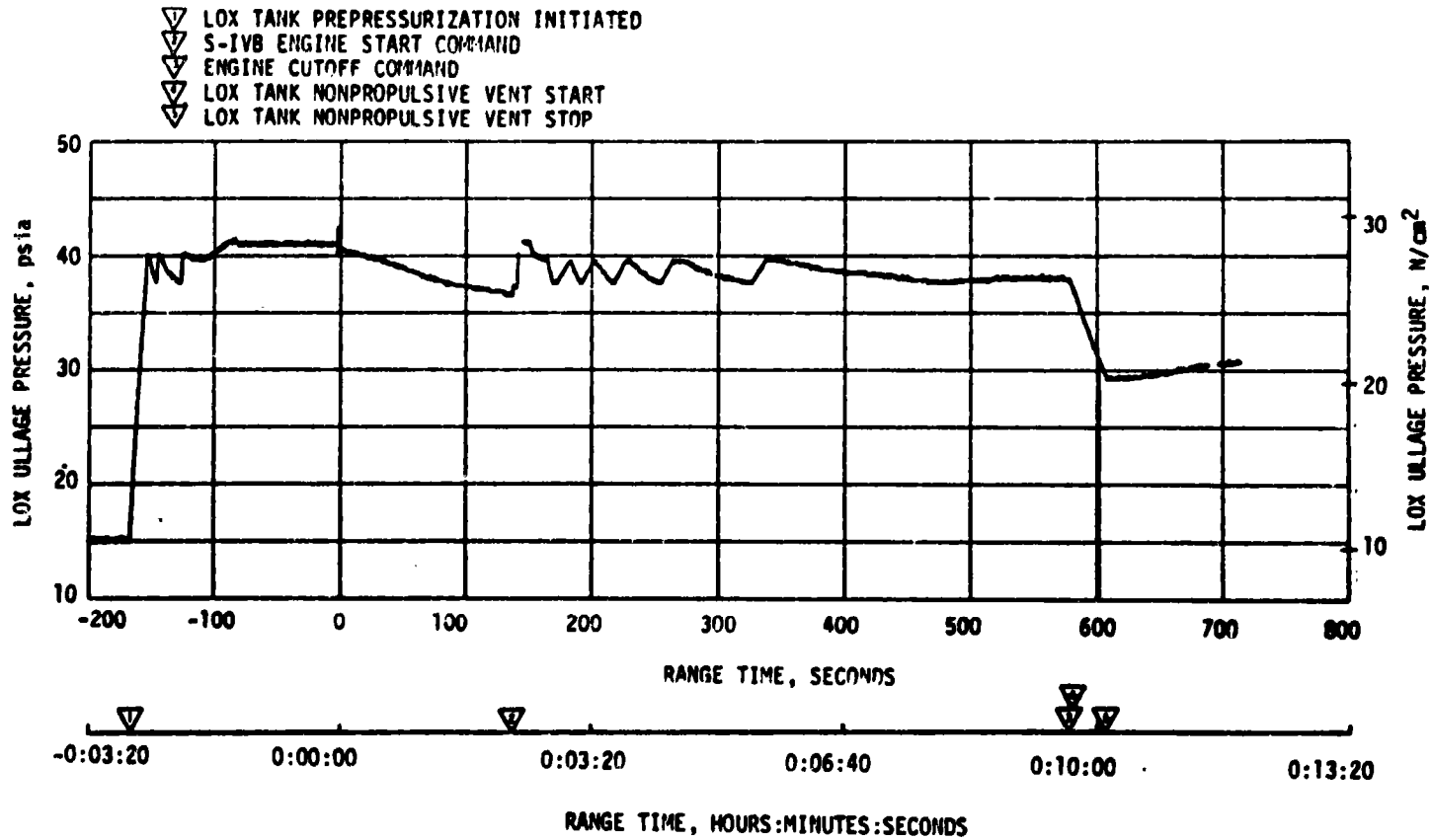


Figure 7-10. S-IVB LOX Tank Ullage Pressure - Boost Phase

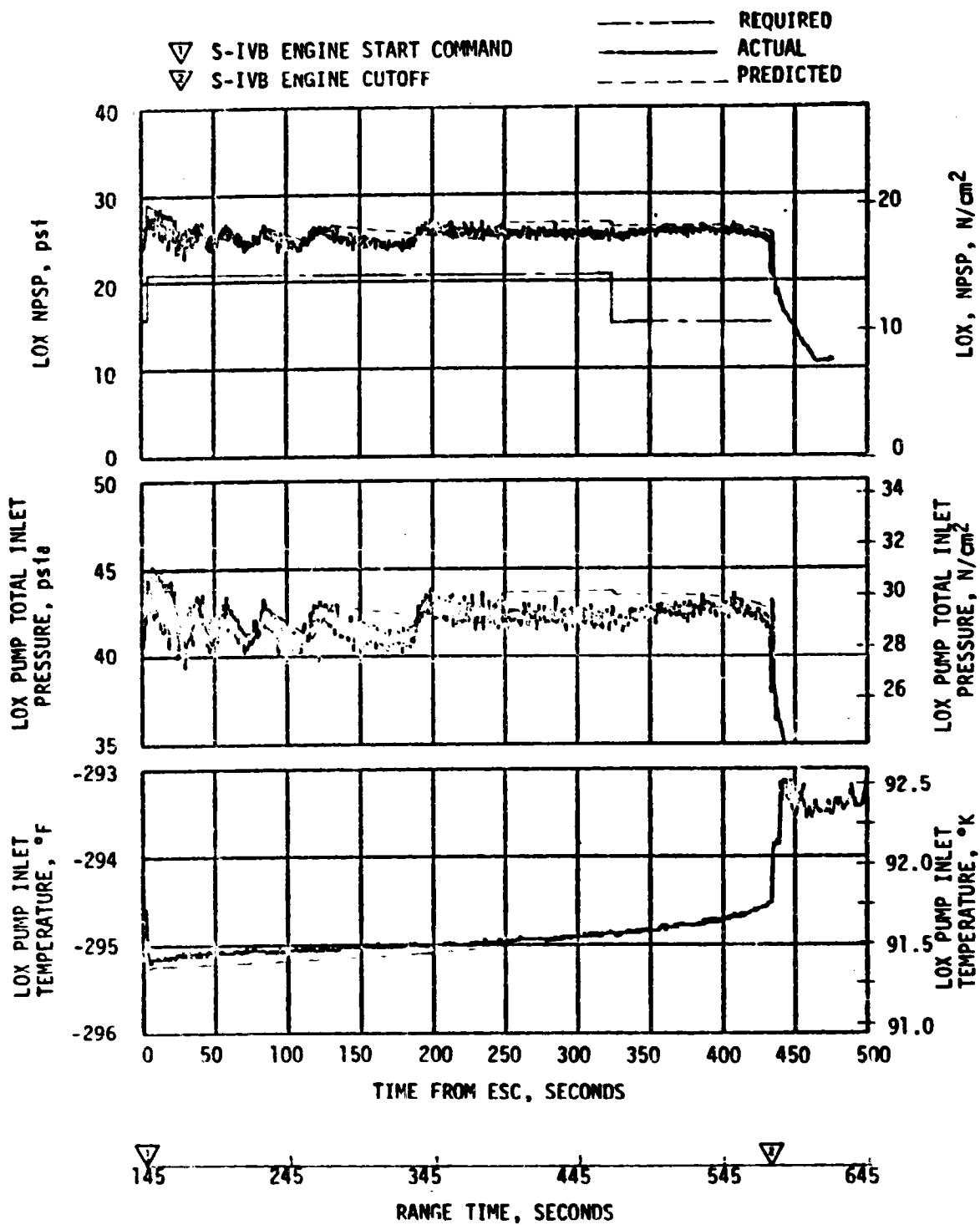


Figure 7-11. S-IVB LOX Pump Inlet Conditions - Burn

- ▽ S-IVB ESC
- ▽ S-IVB ECO
- ▽ START COLD HELIUM DUMP
- ▽ END COLD HELIUM DUMP

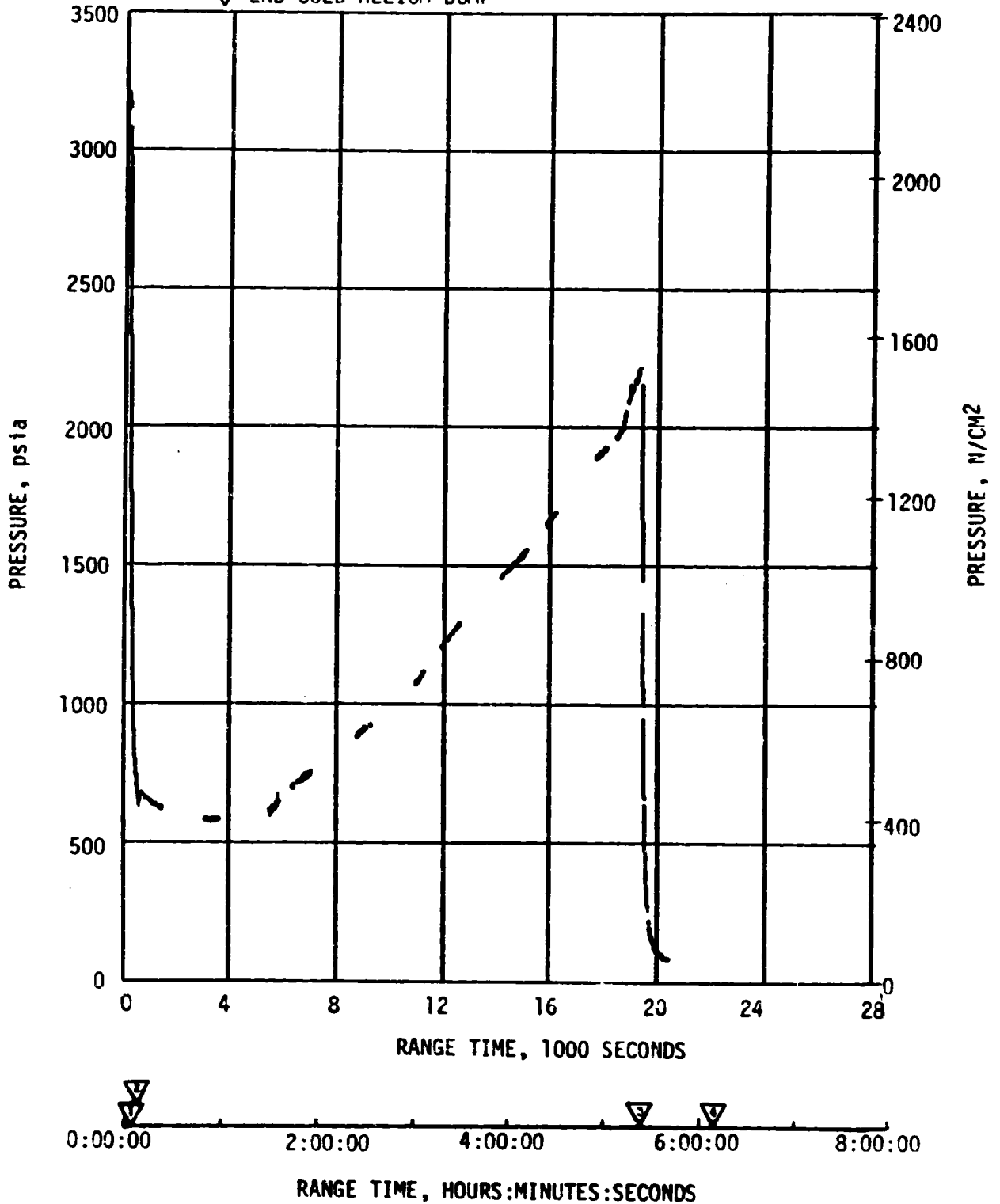


Figure 7-12. S-IVB Cold Helium Supply History

7.7 S-IVB PNEUMATIC CONTROL PRESSURE SYSTEM

The stage pneumatic system performed satisfactorily during all phases of the mission. During orbital coast, the pressure decreased from 2685 psia after the precheck valves were open to 2550 psia at initiation of propellant dump for deorbit. This decrease was due to the continuous LOX chilldown motor container purge.

The stage pneumatic regulator performance was nominal with a near constant discharge pressure of 478 psia.

This was the third flight with a tie-in of the stage pneumatic sphere and the engine control sphere. The tie-in provides additional helium to hold the engine propellant valves open during dump. System performance was satisfactory with helium being transferred to the engine system during engine burn and propellant dump. The pneumatic sphere pressure at the end of propellant dump was 910 psia.

7.8 S-IVB AUXILIARY PROPULSION SYSTEM

The APS met control system demands as required throughout S-IVB burn, orbital coast and through the deorbit sequence.

All Module No. 1 systems, i.e., pneumatic, propellant supply and thrusters, performed nominally during the flight. Oxidizer and fuel propellant temperatures ranged from 542 to 554°F. The pneumatic regulator outlet pressure ranged from 193 to 197 psia, and thruster chamber pressures ranged from 94 to 100 psia.

Propellant usage rate from APS modules 1 and 2 was higher than predicted from about 4200 seconds (01:10:00) to 6000 seconds (01:40:00) as seen in Figures 7-13, 7-14 and Table 7-3. During this same time period LH₂ venting was occurring and the NPV valves were oscillating in a manner similar to that observed on SA-206. For a discussion of the control and disturbance aspects of this activity see paragraph 10.3.2. It is believed that a vent disturbance is responsible for exciting the observed activity and the increased APS propellant usage. This disturbance effect will be included in APS propellant predictions for SA-209.

Module No. 2 pneumatic system performance was nominal. The pneumatic regulator outlet pressure ranged from 197 to 198 psia. Thrusters No. 1 and 3 functioned nominally, but the pitch thruster experienced off nominal performance. The pitch engine chamber pressure and, therefore, thrust level was approximately 30% of nominal (see Figure 7-15). This lower thrust level

- ▽ ESC
- ▽ ECC
- ▽ CSM/S-IVB SEPARATION
- ▽ MANEUVER TO RLH
- ▽ DEORBIT DUMP (TB5)
- ▽ END OF DUMP

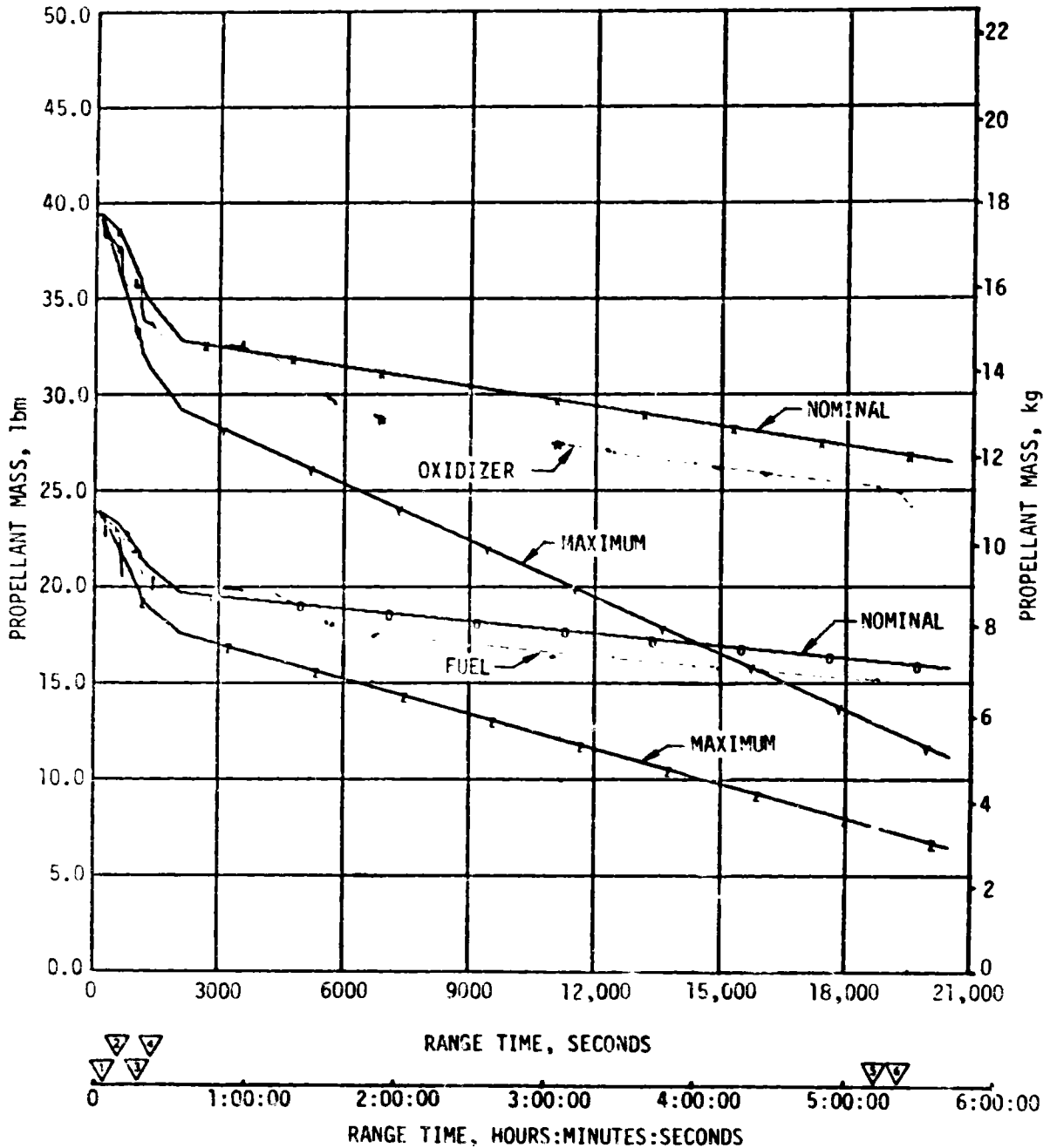


Figure 7-13. S-IVB APS Module No. 1 Propellant Usage

C-2

- ▽ ESC
- ▽ ECC
- ▽ CSM/S-IVB SEPARATION
- ▽ MANEUVER TO RLH
- ▽ DEORBIT DUMP (TB5)
- ▽ END OF DUMP

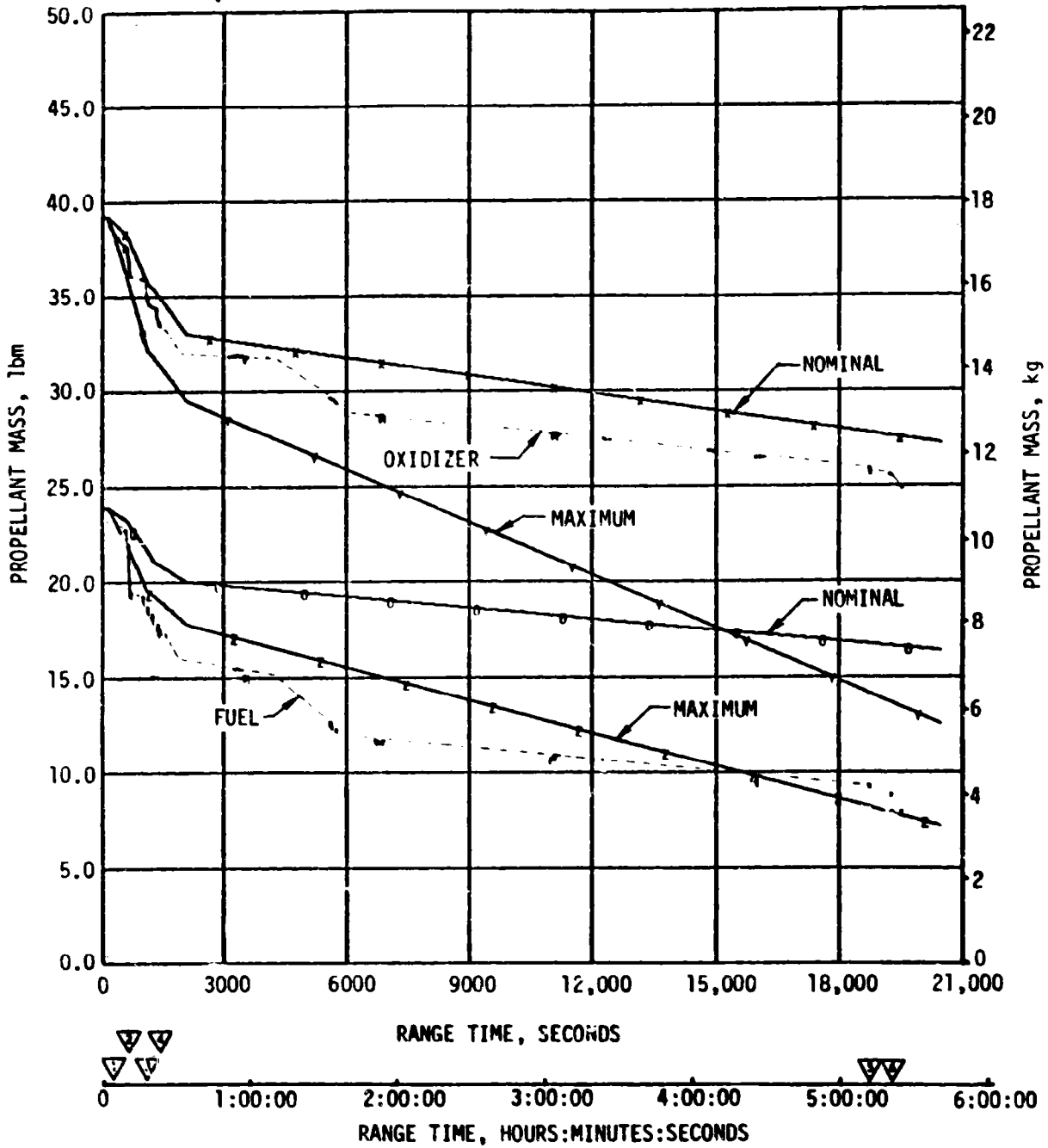
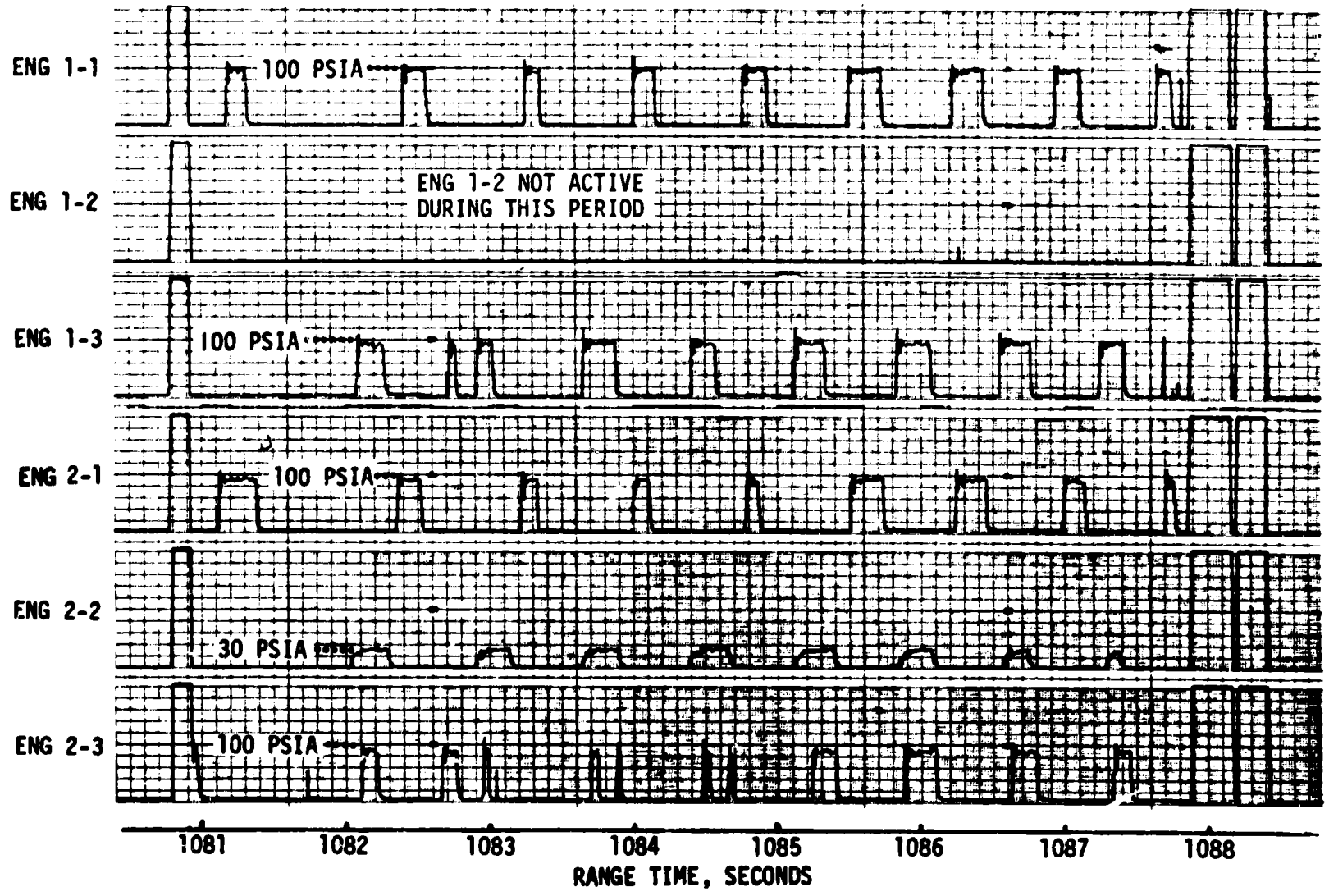


Figure 7-14. S-IVB APS Module No. 2 Propellant Usage

Table 7-3. S-IVB APS Propellant Consumption

	MODULE NO. 1				MODULE NO. 2			
	OXIDIZER		FUEL		OXIDIZER		FUEL	
	LBM	PERCENT	LBM	PERCENT	LBM	PERCENT	LBM	PERCENT
Initial Load	39.4	100	23.9	100	39.2	100	23.9	100
Burn (Roll Control)	1.5	3.8	0.9	3.8	1.5	3.8	0.9	3.8
ECO to Spacecraft Separation	2.1	5.3	1.2	5.0	1.8	4.6	3.6	15.0
Spacecraft Separation to Maneuver to Retrograde Local Horizontal	1.9	4.8	1.3	5.4	1.4	3.6	1.5	6.3
Maneuver to Retrograde Local Horizontal (RLH)	0.7	1.8	0.4	1.7	2.5	6.4	1.8	7.5
From End of Man. to RLH to Start of Stage Disturbance (LH ₂ NPV Oscillatory Operation)	0.9	2.3	0.3	1.3	0.2	0.5	0.8	3.3
LH ₂ NPV Oscillatory Operation	2.8	7.1	1.9	7.9	2.8	7.1	3.2	13.4
From End of Stage Disturbance to Start of Deorbit Dump	4.1	10.5	2.7	11.3	3.1	7.9	2.7	11.3
Deorbit Dump (Roll Control)	0.3	0.7	0.2	0.8	0.5	1.3	0.4	1.7
Total Propellant Usage	14.3	36.3	8.9	37.2	13.8	35.2	14.9	62.3

7-24



REPRODUCIBILITY OF THE ORIGINAL PAGE IS POOR

Figure 7-15. S-IVB APS Chamber Pressure (Spacecraft Separation Disturbance)

resulted in longer pitch engine on-time to provide the required attitude control system total impulse. It has been concluded that this condition resulted from a partial blockage of the pitch engine oxidizer feed system. This oxidizer blockage plus longer engine on-time resulted in approximately nominal oxidizer usage, but about twice the predicted Module No. 2 fuel usage (see Figure 7-14 and Table 7-3).

Blockage could develop in three areas of the oxidizer feed system: Upstream of the engine quad valves, in the quad valves, or in the engine downstream of the quad valves. Blockage upstream of the engine quad valves is improbable since the supply to the quad valves is redundant; i.e., propellant can be supplied through either the recirculation port or main propellant inlet port. Furthermore, the oxidizer manifold pressure transients were normal, indicating an open system down to the valves. Blockage within the quad valves could result from contamination or a combination of contamination and valve failure. As previously mentioned, the oxidizer manifold pressure transients were normal; therefore, this failure is unlikely. It should be noted that the failure of one valve leg would result in less than a 5 psi reduction in chamber pressure as indicated by the engine manufacturer's test data.

The most probable location of the blockage is downstream of the quad valves. This blockage could have been caused by external contamination but the presence of a common filter for all three thrusters combined with the fact that only one thruster was affected, tends to minimize this possibility. A more likely cause was oxidizer seepage through the quad valve combining with atmospheric moisture to produce corrosion somewhere from the oxidizer orifice plate to the injector face. This corrosion would have occurred between hypergol loading and launch. Figure 7-16 shows the most probable location for blockage to occur. Because of limited data, it will be difficult to identify the specific contamination source. The investigation is continuing in this area. A special flow test is planned on the S-IVB-209 APS modules before propellant is loaded, to verify that there is no flow restriction in the fuel or oxidizer injectors. In addition, subsequent to propellant loading, daily visual and toxic vapor checks will be made of the thruster injector areas. The criteria for acceptance if propellant vapor is detected is under investigation.

7.9 S-IVB/IU STAGE DEORBIT PROPELLANT DUMP

All aspects of the S-IVB/IU deorbit were accomplished successfully. The impulse derived from the LOX and fuel dumps was sufficient to satisfactorily deorbit the S-IVB/IU. The total impulse provided, 66,975 lbf-sec, was in good agreement with the real time nominal predicted value of 70,500 lbf-sec. The sequence in which the propellant dumps were accomplished is presented in Figure 7-17.

The LOX dump was initiated at approximately 18,671 seconds (05:11:11) and was satisfactorily accomplished. Reconstructed and real-time predicted nominal LOX dump performance (total impulse, mass flowrate, LOX tank mass

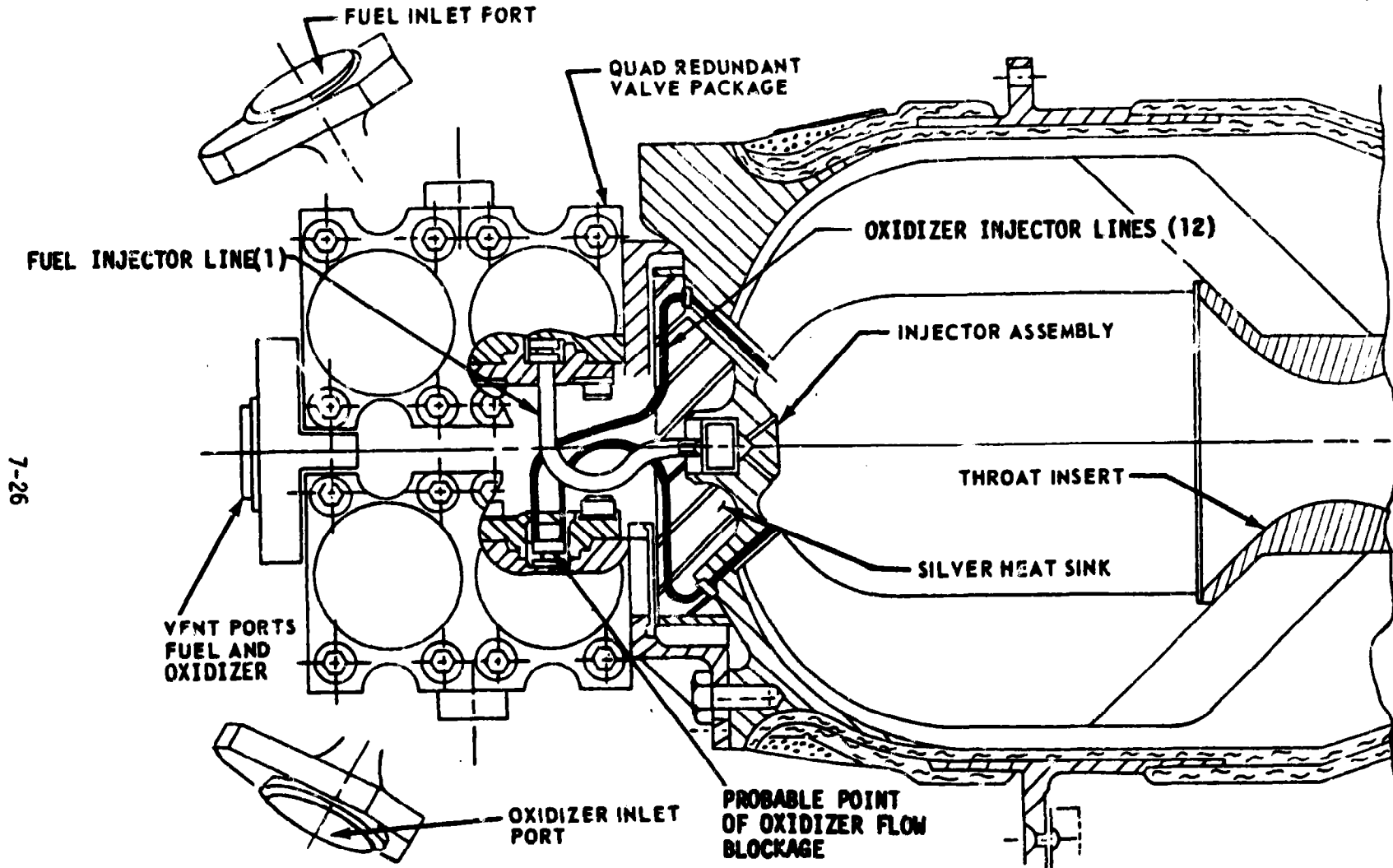


Figure 7-16. S-IVB APS Valve, Injector, Thrust Chamber Assembly

▽ END OF S-IVB TELEMETERED DATA, 20,460

▽ S-IVB BREAKUP (ESTIMATED), 21,214

7-27

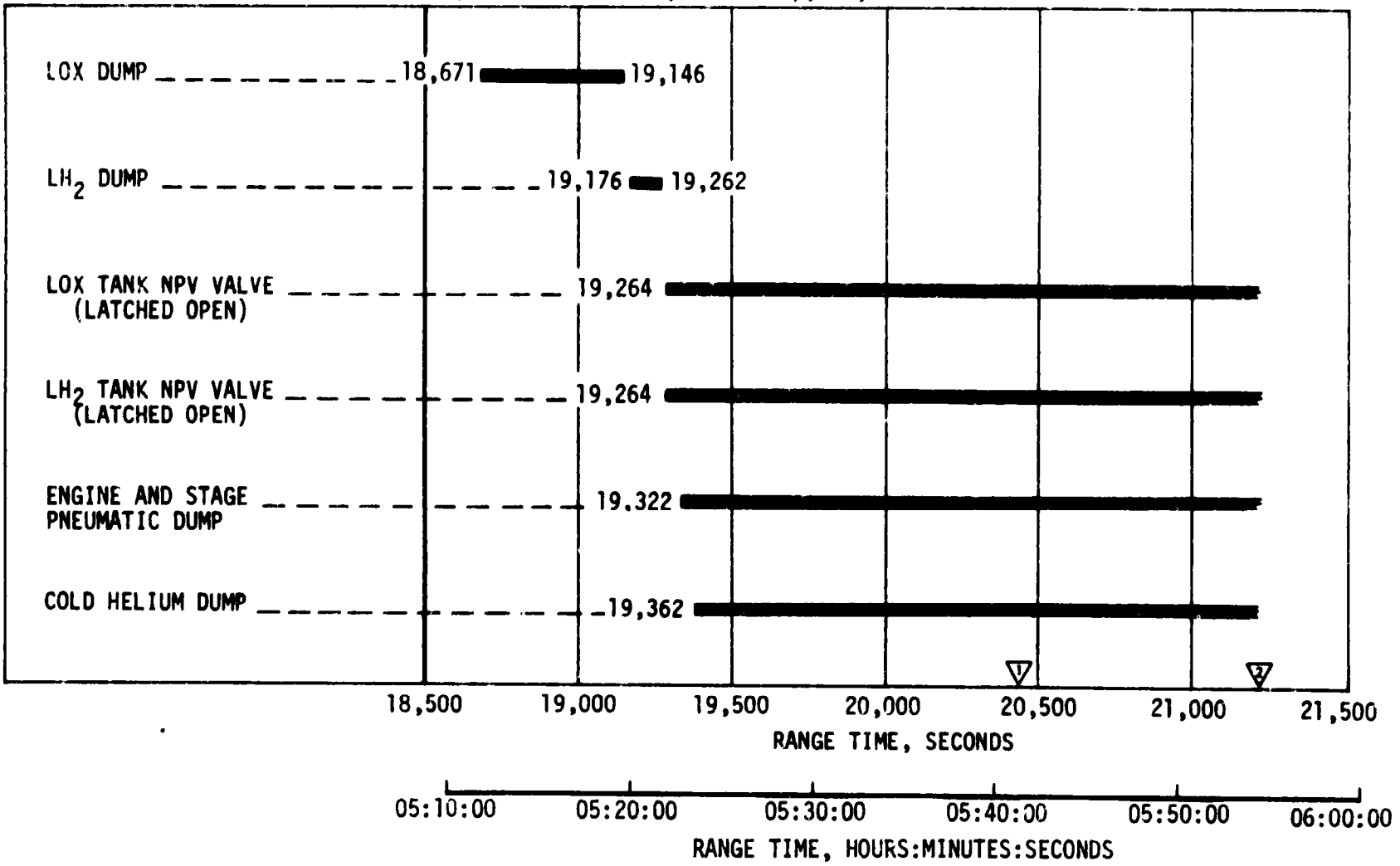


Figure 7-17. S-IVB Deorbit Propellant Dump and Safing Sequence

and actual and real-time predicted LOX ullage pressure) are shown in Figure 7-18. The reconstruction corresponds to the best fit on available LOX ullage pressure flight data and the calculated velocity change (determined from LVDC accelerometer data) for LOX dump.

The LOX tank ullage pressure decreased from approximately 41.4 to 7.2 psia during the 475 second dump. The maximum negative bulkhead differential pressure following LOX dump was 24.8 psi which was within the allowable 26 psi limit. Ullage gas ingestion, based on the reconstruction, occurred at 18,696 seconds (05:11:36). Due to the low LOX residual at dump initiation, early ullage ingestion prevented the attainment of steady state LOX dump thrust. LOX dump was ended at approximately 19,146 seconds (05:19:06) by closing the MOV. The reconstructed total impulse before MOV closure was 57,800 lbf-sec, as compared to real time predicted total impulse of 62,000 lbf-sec.

Ullage gas ingestion occurred early in the LOX dump due to low LOX residual mass. Real time predicted LOX mass at LOX dump was approximately 750 lbm greater than the mass derived from the reconstruction. Of the 750 lbm total discrepancy, 436 lbm was due to lower than predicted LOX residual at the end of engine thrust decay and the remainder was due to higher than predicted orbital boiloff.

Fuel dump was initiated at 19,176 seconds (05:19:36) and was satisfactorily accomplished. Fuel dump impulse, flowrate, mass remaining in fuel tank, and ullage pressure are shown in Figure 7-19. Only GH₂ remained in the tank at dump start. The LH₂ completely boiled off during orbital coast. A reconstruction of dump indicates a dump impulse of 9,175 lbf-sec. Considering a 465 lbf-sec contribution from the pneumatics system, this value is in good agreement with the real time nominal predicted value of 8,500 lbf-sec. The ullage mass at the start of the dump was 302 lbm. Approximately 45 lbm of gaseous hydrogen were dumped through the J-2 engine. The ullage pressure decreased from 32.4 to 26.2 psia during the dump. The dump terminated at 19,262 seconds (05:21:02) when the Main Fuel Valve (MFV) was closed.

7.10 S-IVB ORBITAL COAST AND SAFING

7.10.1 Fuel Tank Orbital Coast and Safing

The fuel tank nonpropulsive vent system satisfactorily controlled the ullage pressure during earth orbit, as shown in Figure 7-20. A 670-second fuel tank vent, initiated at ECO +10 seconds, lowered the ullage pressure from 31.8 to 19.9 psia. NPV system data indicate that liquid hydrogen was vented, as expected, during 90 seconds of the programmed vent. Liquid venting, beginning about 10 seconds after spacecraft separation, results from the momentarily higher deceleration experienced after separation which forces the LH₂ residual to the top of the tank near the vent inlet. The liquid venting did not significantly affect fuel dump impulse capability or mission accomplishment.

REPRODUCIBILITY OF THE ORIGINAL PAGE IS POOR

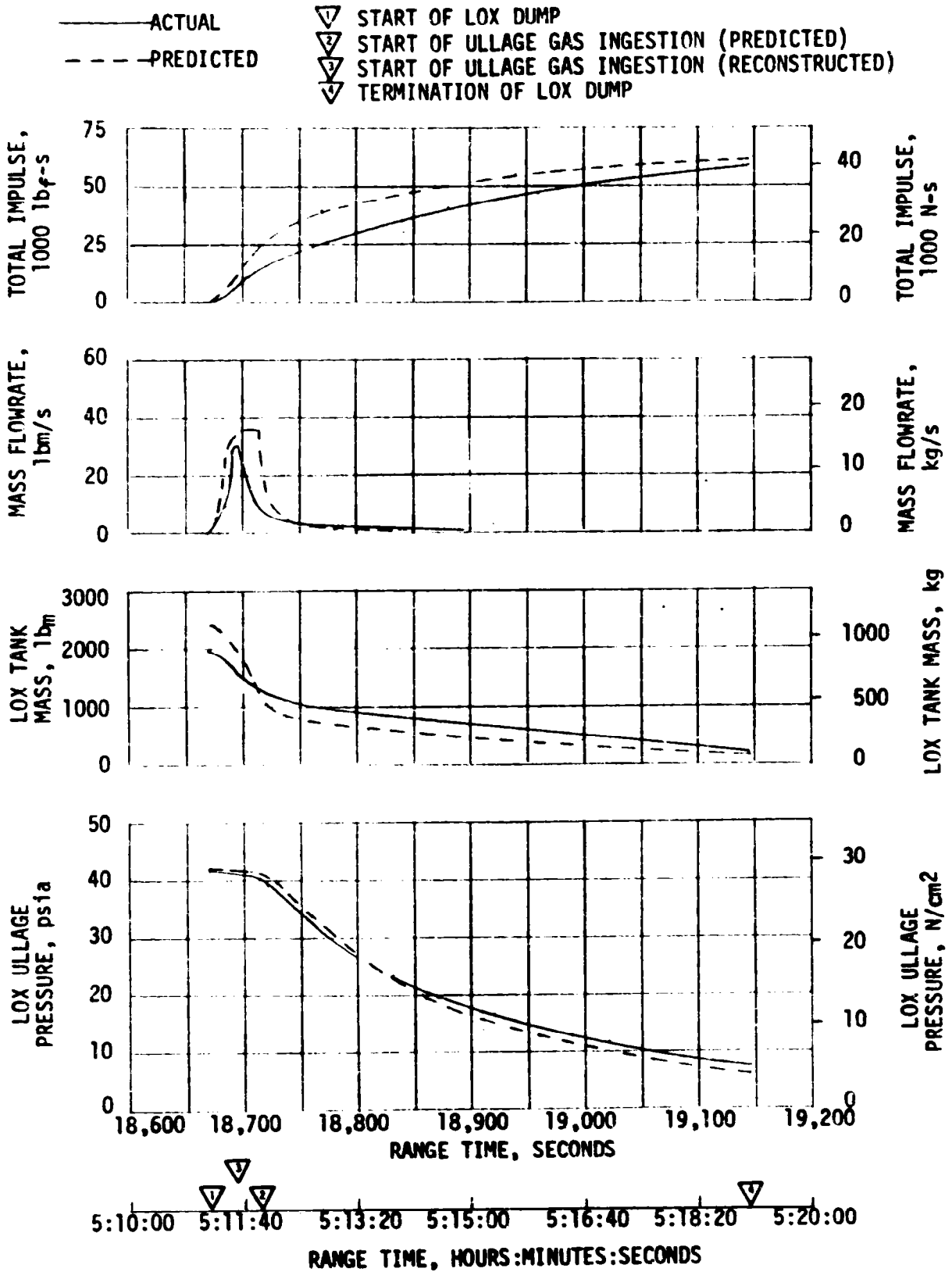


Figure 7-18. S-IVB LOX Dump Parameter Histories

——— ACTUAL
 - - - - - PREDICTED BAND
 ▽ LH₂ DUMP INITIATED
 ▽ LH₂ DUMP TERMINATED

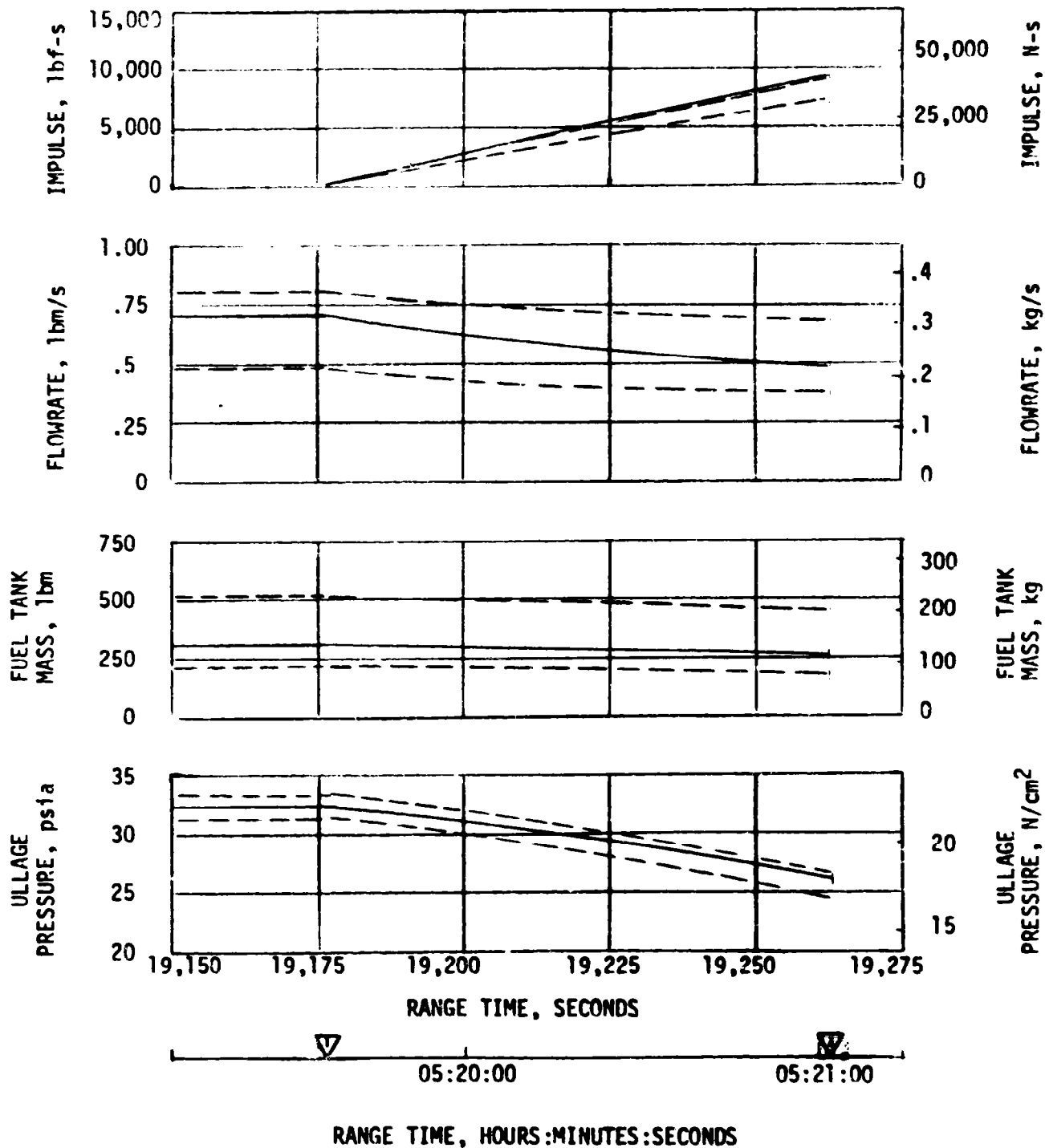


Figure 7-19. S-IVB LH₂ Dump

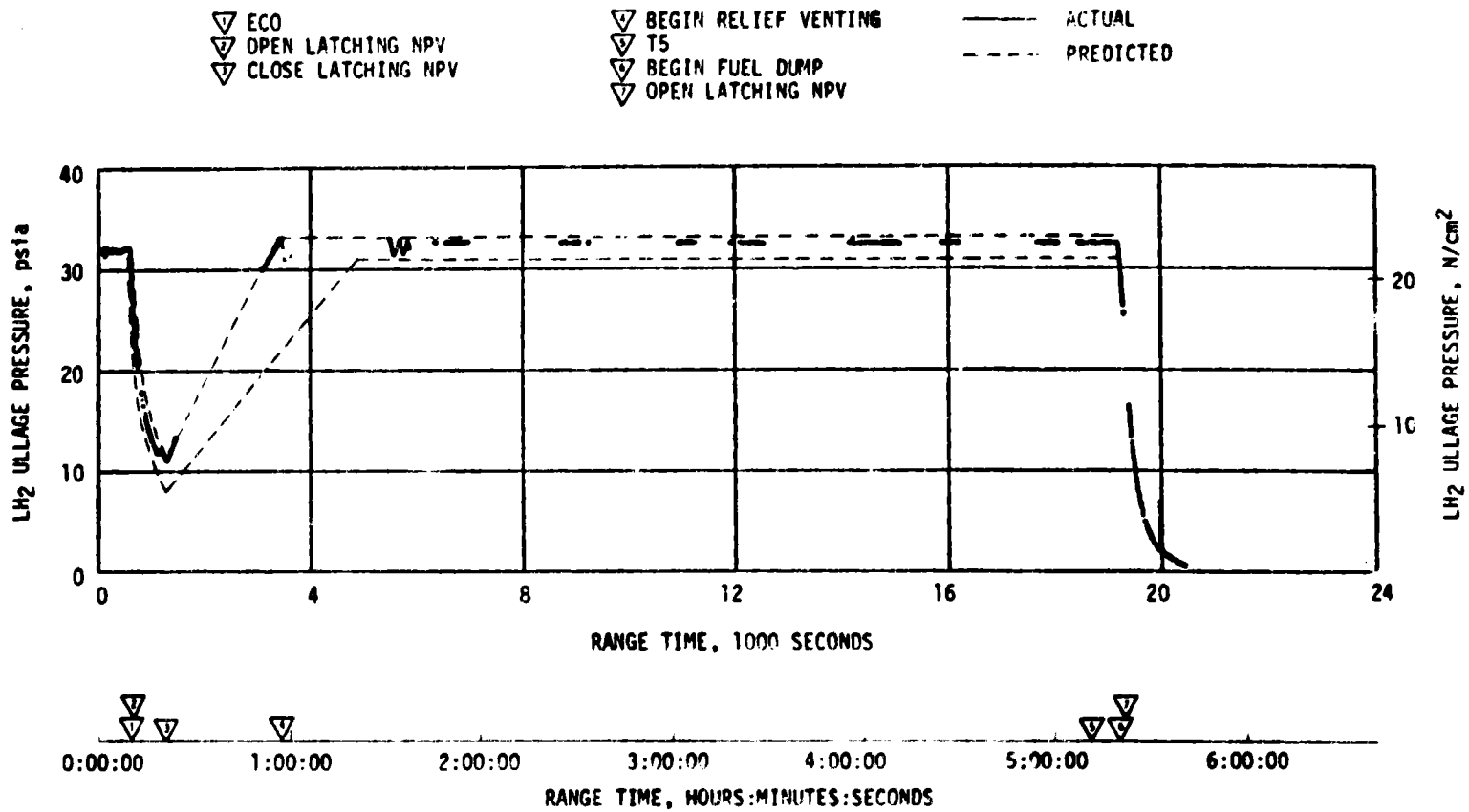


Figure 7-20. S-IVB LH2 Ullage Pressure - Orbital Coast

After the programmed vent, the LH₂ tank reached relief at approximately 3440 seconds (00:57:20). Simultaneous chattering of the LH₂ vent and relief valve and the LH₂ latching vent valve was observed during the early part of orbital coast (3440 seconds (00:57:20) to 5870 seconds (01:37:50)). The valve chattering was evidenced by NPV nozzle pressure oscillations of about +3 psia as shown in Figure 7-21 and valve position microswitch talk-back. The LH₂ tank ullage pressure cycled between 32.6 and 31.1 psia. The chattering occurred on the vent portion of the cycle, approximately a 60-second interval. Both valves were closed during the self-pressurization portion of the cycle, which was about 100 seconds long. Similar oscillations were noted during SA-206 orbital operations and during SA-505 J-2 engine operation. Simulated altitude testing at Arnold Engineering Development Center (AEDC) has shown that such oscillations can be induced in the vent system if the flowrate and temperature are in the appropriate regime. Either one or both valves could be made to chatter at AEDC. Since the flowrates are considerably different from the SA-206-208 situation to the SA-505, it is obvious that a rather large regime of flowrate and temperature can cause chatter.

Extrapolation of the SA-208 data suggests that the oscillatory mode of vent system operation is associated with the presence of liquid hydrogen in the tank. It may be concluded that the vent flowrates and temperatures caused by vaporization of liquid at saturation conditions within the tank provide an appropriate combination to cause chatter of the valves. Also, since the SA-505 chatter and the AEDC data were obtained at accelerations 1 g or greater, mixed phase flow was not present in these cases. The conclusion from the AEDC testing was that the chatter is induced by an "organ pipe" resonance of the LH₂ NPV inlet duct. Based on AEDC data, the resonant frequency of the inlet duct at the measured nozzle gas temperatures on SA-208 is 30 Hz. This is in agreement with the noted frequency in the IU evaluation.

It should be noted that the SA-208 attitude control system data indicates well balanced venting during steady state flow. The oscillatory mode of operation has no detrimental effect on the vent valve, and does not exceed its component qualification testing requirement.

During the period of NPV oscillatory operation, attitude and APS firing data indicate the existence of a disturbing moment acting on the stage. In addition to the disturbing force acting at the NPV, a small translational velocity is also indicated. The attitude data indicate that the magnitude of the disturbance is largest at the initiation and termination of the relief portion of the vent cycle. This disturbance appears to be approximately equal in magnitude and opposite in direction by comparing the initial and terminal effects. The overall effect on attitude indicates that NPV thrust misalignment and/or unbalance combined with propellant slosh activity existed (see Section 10.3.2); however, the physical alignment of the NPV nozzles was very good as verified by the very low level of attitude disturbance noted during NPV operation after engine cutoff, following fuel dump, and when the vent valves were operating in the "feathering" mode (01:45:25 to 05:19:36).

- ▽ NPV OPEN
- ▽ NPV CLOSED
- ▽ NPV OPEN
- ▽ NPV CLOSED

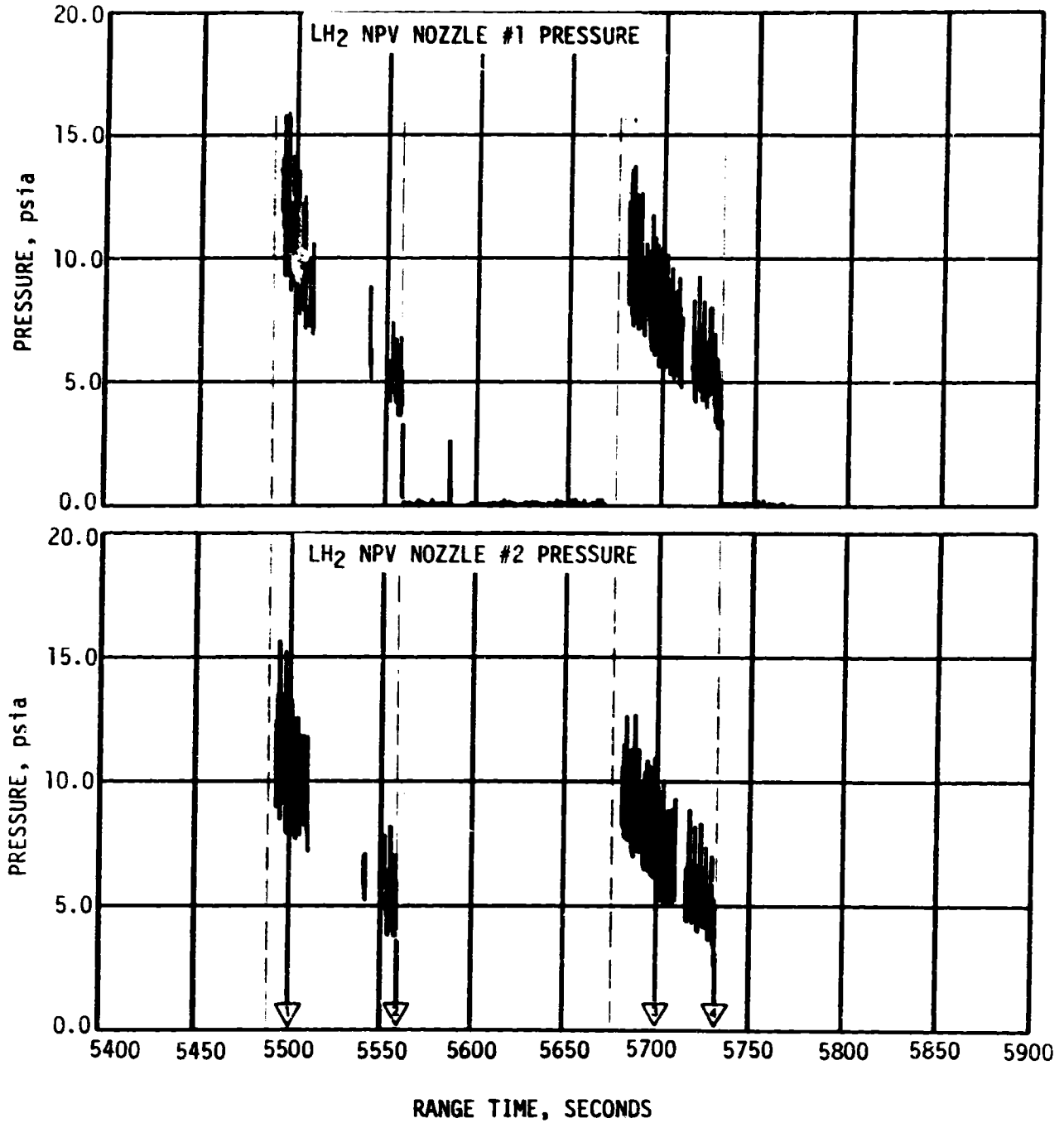


Figure 7-21. S-IVB LH₂ NPV Nozzle Pressure Oscillations

During the period of NPV oscillatory operation, the IU platform accelerometer data indicated a change in the vehicle velocity vector. The force required to produce the indicated change in velocity is much greater than that derived using the attitude and APS firing data which assumed the force acting at the NPV. Although the force appears to have been initiated by the NPV, the net resultant force vector (derived from APS, attitude, and IU data) indicates that the LH₂ NPV thrust could not be the total source of the disturbance (ref. Section 10.3.2).

In order to achieve a moment balance and the indicated velocity change, the location of the resultant force must be near the vehicle center of gravity. An investigation of disturbance sources on the S-IVB Stage has yielded no satisfactory explanation of the translational disturbance.

Based on the time correlation of NPV oscillatory behavior and the attitude and translational data, it has been concluded that the NPV system operation in some manner initiated, but did not necessarily provide the total force, for the observed disturbances. The precise origin of the disturbing forces has not been determined. In particular, the force existing near the termination of the vent appears not to be associated with the vent nozzles only, since the energy contained downstream of the valves is not sufficient to provide such a force when if all the mass was vented through one nozzle. Noting that the primary disturbing forces coincide with the initiation and termination of vent oscillations, other stage systems which could have been indirectly affected were investigated as possible sources of disturbances which could be triggered by NPV operation. The hydraulic system, ambient helium system, cold helium system, APS, and LOX system did not lose sufficient mass to account for the disturbing forces. IU evaluation indicates normal operation (see Section 10.4). The position indicators on the LOX and LH₂ fill and drain valves and the LH₂ directional control valve indicate that the valves were closed throughout the flight. Based on the above findings, the LH₂ NPV system and propellant dynamics (see Section 10.3.2) are left as the only identified sources of disturbance. However, these sources as presently defined do not permit a satisfactory explanation of all of the observed disturbances. Although the precise nature of the mechanism has not been established, the observed disturbances are considered to be benign for future missions, because of the passivity of the systems involved and the repeatability of the phenomena as observed between SA-206 and SA-208. Furthermore, the forces are so small as to have perhaps gone unnoticed had it not been for the abnormal performance of one of the APS thrusters (see Section 7.8).

The LH₂ latching vent valve was opened and latched at the end of fuel dump, 19,264 seconds (05:21:04). The ullage pressure, initially 26.2 psia, decayed to 0.5 psia at end of data, 20,355 seconds (05:39:15).

7.10.2 LOX Tank Orbital Coast and Safing

Following engine cutoff at 577 seconds (00:09:37) a programmed 30-second NPV cycle was satisfactorily accomplished. During the vent, LOX tank

pressure decreased from 38.0 psia to 29.2 psia (Figure 7-22). Reconstruction of the pressure history during the vent indicates that approximately 30 lbm of gas was vented including 25 lbm of helium and 5 lbm of GOX. At the termination of venting, the ullage consisted of approximately 197 lbm of GOX and 138 lbm of helium.

During orbital coast, the LOX tank pressure increased more rapidly than predicted and went above the predicted band at approximately 10,000 seconds (02:46:40) (Figure 7-22). This was probably due to greater than expected LOX boiloff. Analytical reconstruction of the orbital coast phase and the LOX dump both indicate a high LOX boiloff mass. The increased LOX boiloff is due to the increase in tank wetted area resulting from propellant motion. LOX slosh could have been induced by APS engine firing activity during LH₂ tank cyclic relief venting (Section 10.3.2).

At LOX dump termination, the LOX NPV valve was opened and latched. The LOX tank ullage pressure decayed from 7.2 psia at 19,263 seconds (05:21:03) to 5.7 psia at 19,362 seconds (05:22:42). The pressure then increased to 10.4 psia at 19,450 seconds (05:24:10) as a result of cold helium dump, then decayed to 1.4 psia at loss of data. Approximately 100 lbm of helium and 110 lbm of GOX were vented overboard. The LOX tank pressure during safing is shown on Figure 7-22.

7.10.3 Cold Helium Dump

The cold helium supply was safed by dumping the helium through the LOX nonpropulsive vent system (see Section 7.10.2). The dump was initiated at 19,360 seconds (05:22:40) and was programmed to continue for 2800 seconds. At loss of data, 1070 seconds into dump, the cold helium pressure was approximately 90 psia.

7.10.4 Stage Pneumatic Control and Engine Control Sphere Safing

The interconnection between the stage pneumatic and engine control spheres permitted simultaneous safing of both spheres through the engine purge system. Safing was accomplished by energizing the engine helium control solenoid. Safing was initiated at 19,320 seconds (05:22:00) with a stage sphere pressure of 980 psia. At loss of stage sphere data, 1110 seconds into safing, the stage sphere pressure was 80 psia. The engine sphere pressure decreased from approximately 940 psia at initiation of safing to approximately 50 psia at the last available engine sphere data (20,430 seconds, 05:40:30).

7.11 S-IVB HYDRAULIC SYSTEM

The S-IVB Hydraulic System performed within the predicted limits after lift-off with no overboard venting of system fluid as a result of hydraulic fluid expansion. Prior to start of propellant loading, the accumulator was precharged to 2490 psia at 90°F. Reservoir oil level (auxiliary pump off) was 86 percent at 90°F.

7-36

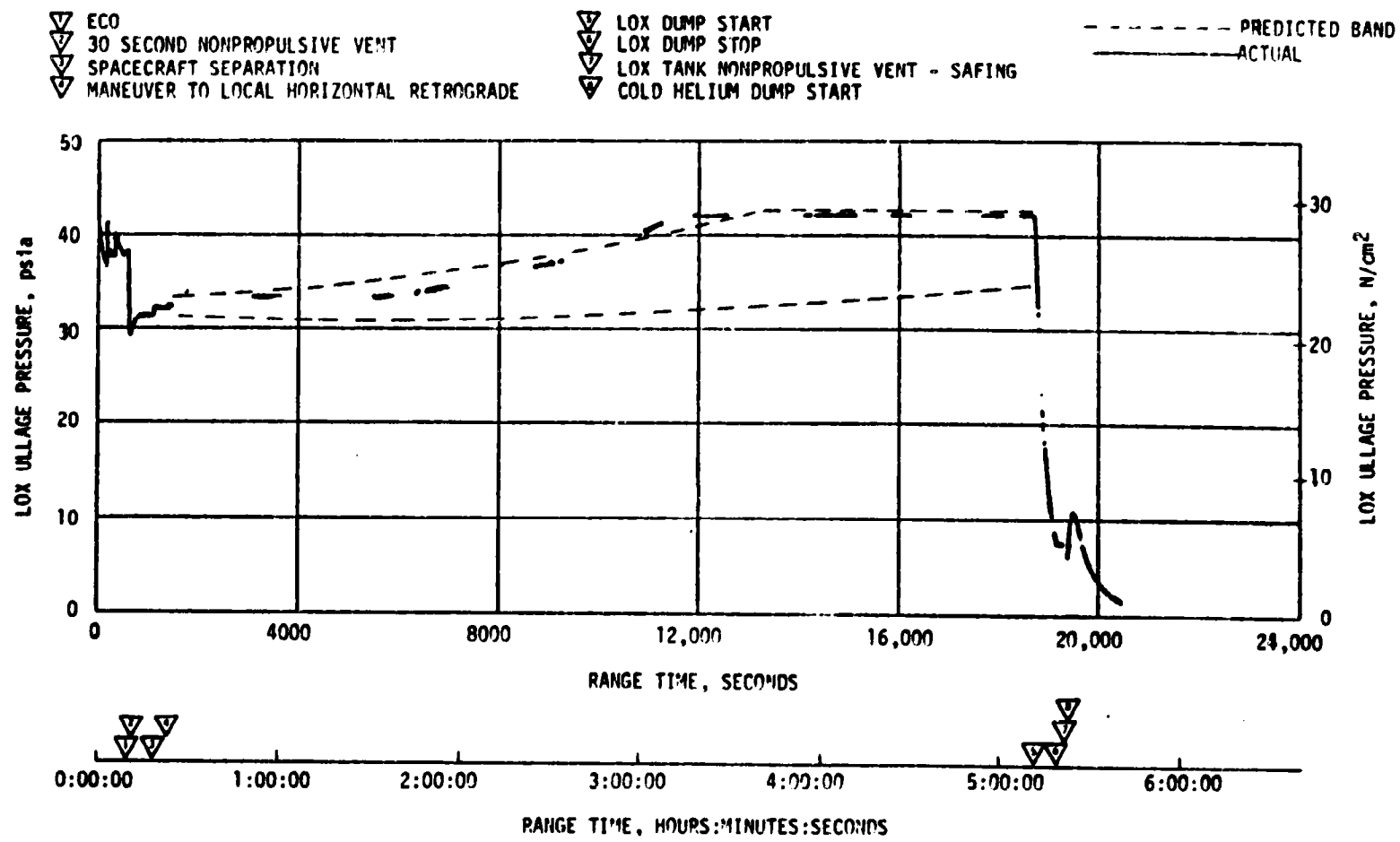


Figure 7-22. S-IVB LOX Tank Ullage Pressure - Orbit, Dump, and Safing

The auxiliary hydraulic pump was programmed to flight mode "ON" at T-11 minutes for lift-off. System pressure stabilized at 3550 psia and remained steady. During boost, all system fluid temperatures rose steadily when the auxiliary pump was operating and convection cooling was decreasing. At S-IVB engine start, system pressure increased to 3620 psia and remained steady through the burn period.

System internal leakage rate, 0.75 gpm (0.4 to 0.8 gpm allowable), was provided primarily by the engine driven pump during burn as characterized by the auxiliary pump current draw of 32 amperes. At engine start, system pressure and reservoir pressure increased indicating the engine pump was providing the internal leakage flow requirement. However, later in the burn the current increased approximately six amperes indicating the auxiliary pump was sharing a portion of the leakage flow.

Engine deflections were nominal throughout the boost phase. Actuator positions were offset from null during powered flight due to the displacement of the vehicle's center of gravity off the vehicle's vertical axis, the J-2 engine installation tolerances, thrust misalignment, uncompensated gimbal clearances, and thrust structure compression effects.

During the orbital coast period, seven programmed auxiliary hydraulic pump thermal cycles were utilized to maintain system readiness for the deorbit phase. Available data during orbital coast indicated nominal system performance. The maximum reservoir oil temperature noted during orbital coast was 110°F.

System operation during the deorbit phase was normal. System pressure stabilized at 3600 psia and remained steady. The maximum pump inlet oil temperature noted during this period was 125°F.

SECTION 8

STRUCTURES

8.1 SUMMARY

The structural loads experienced during the SA-208 flight were well below design values. The maximum bending moment was 10.3×10^6 in-lbf (approximately 18.5 percent of design) at vehicle station 942. The S-IB thrust cutoff transients experienced by SA-208 were comparable to those of the SA-207. The S-IVB engine cutoff transients did not produce the 55 Hz oscillations noted on the SA-207 flight. All vibration and pressure oscillations were nominal during the entire launch and there was no indication of any POGO instability.

The maximum ground wind experienced by the Saturn IB SA-208 during the prelaunch period was 21 knots and during launch was 7 knots. Both values are well below the allowable limits.

There was no evidence during flight of any compromise of structural integrity due to the prelaunch RP-1 tank bulkhead reversal or stress corrosion (E-Beam, fin rear spar fitting and interstage reaction beam).

8.2 TOTAL VEHICLE STRUCTURES

8.2.1 Longitudinal Loads

The SA-208 vehicle liftoff steady-state acceleration was 1.25 g. Maximum longitudinal dynamic response measured during thrust buildup and release was $+0.10$ g at the Instrument Unit (IU) and $+0.75$ g at the Command Module (CM), Figure 8-1. The SA-207 recorded $+0.20$ g and $+0.80$ g at the IU and CM, respectively, for the thrust buildup dynamic responses.

The total longitudinal load at station 942, based on strain data is shown in Figure 8-2 as a function of range time. The envelope of previous flights (S-IB vehicles SA-202 through SA-207) is shown for comparison. The maximum longitudinal load of 1.35×10^6 lbf occurred at Inboard Engine Cutoff, (IECO) and was well within design limit capability. The longitudinal load distribution at the time of maximum bending moment (73.1 seconds) and IECO (137.8 seconds) are shown in Figure 8-3. The steady state longitudinal accelerations at these time slices were 2.05 g and 4.25 g, respectively.

The SA-208 (IECO) and Outboard Engine Cutoff (OECO) transient responses were equal to or less than those of previous flights. The maximum longitudinal dynamics resulting from IECO were $+0.10$ g at the IU and $+0.25$ g at the CM, Figure 8-4.

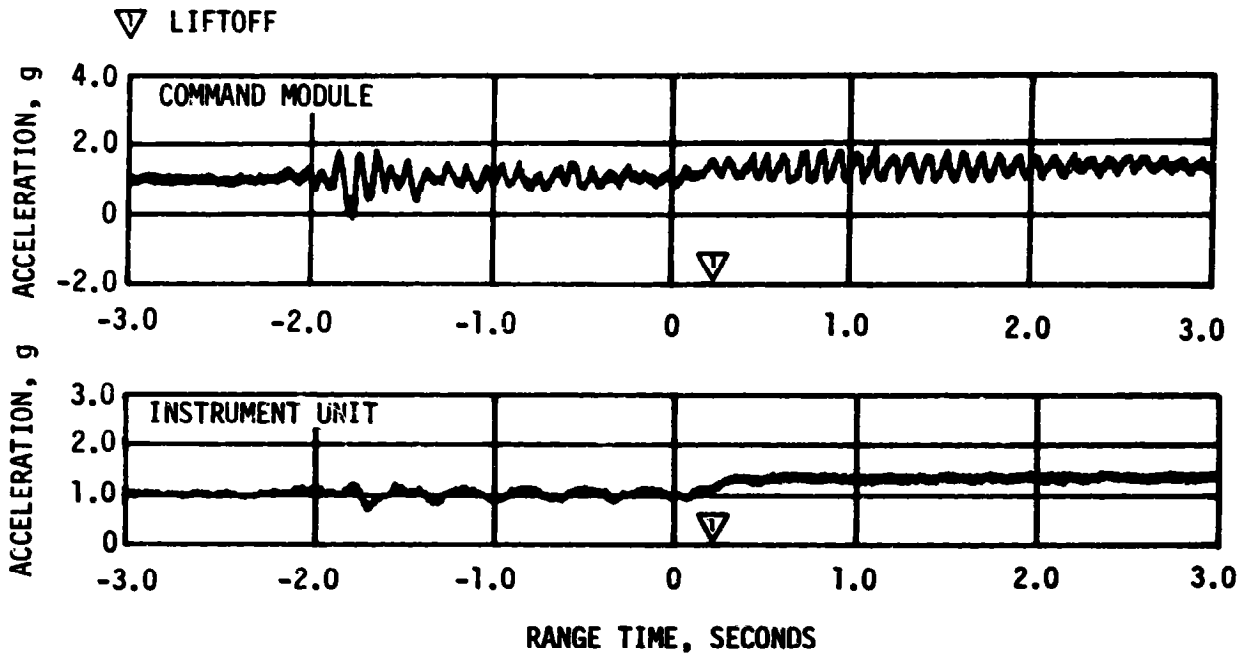


Figure 8-1. Longitudinal Acceleration During Thrust Buildup and Launch

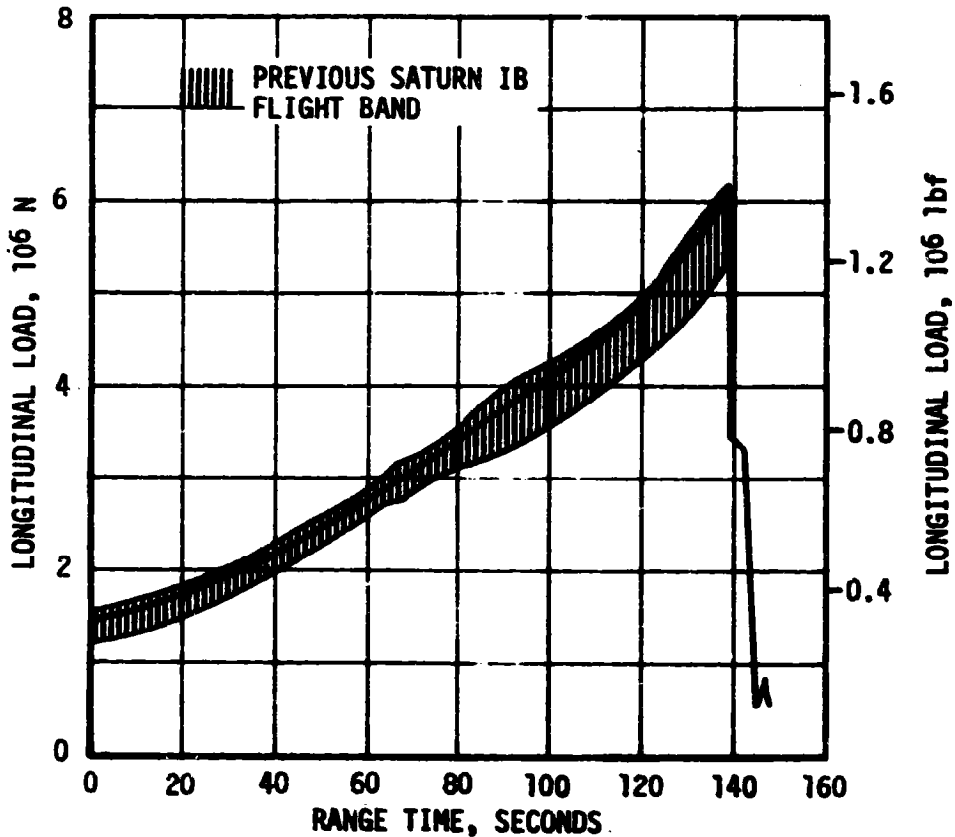


Figure 8-2. Longitudinal Load from Strain Data at Station 942

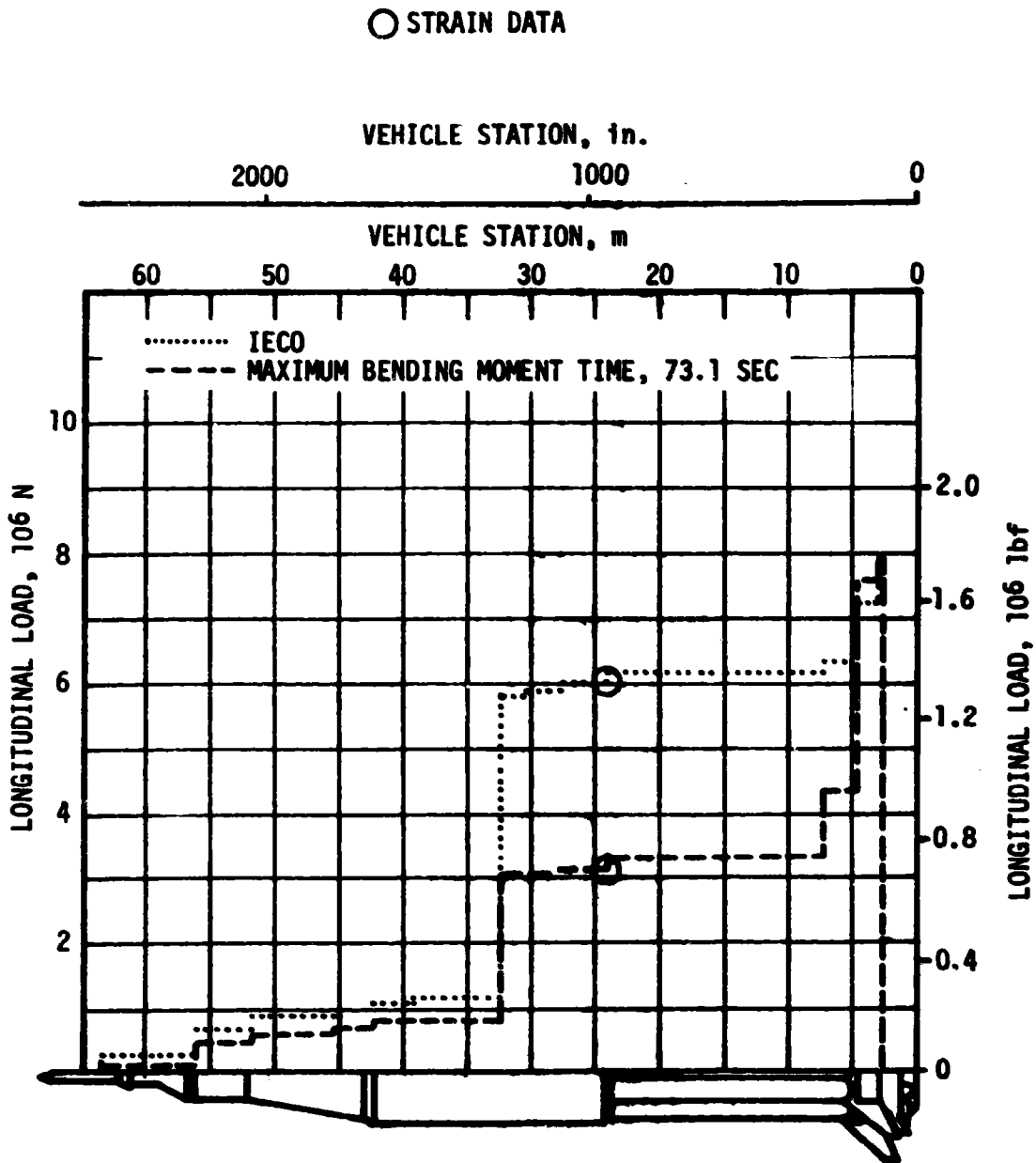


Figure 8-3. Longitudinal Load Distribution at Time of Maximum Bending Moment and IECO

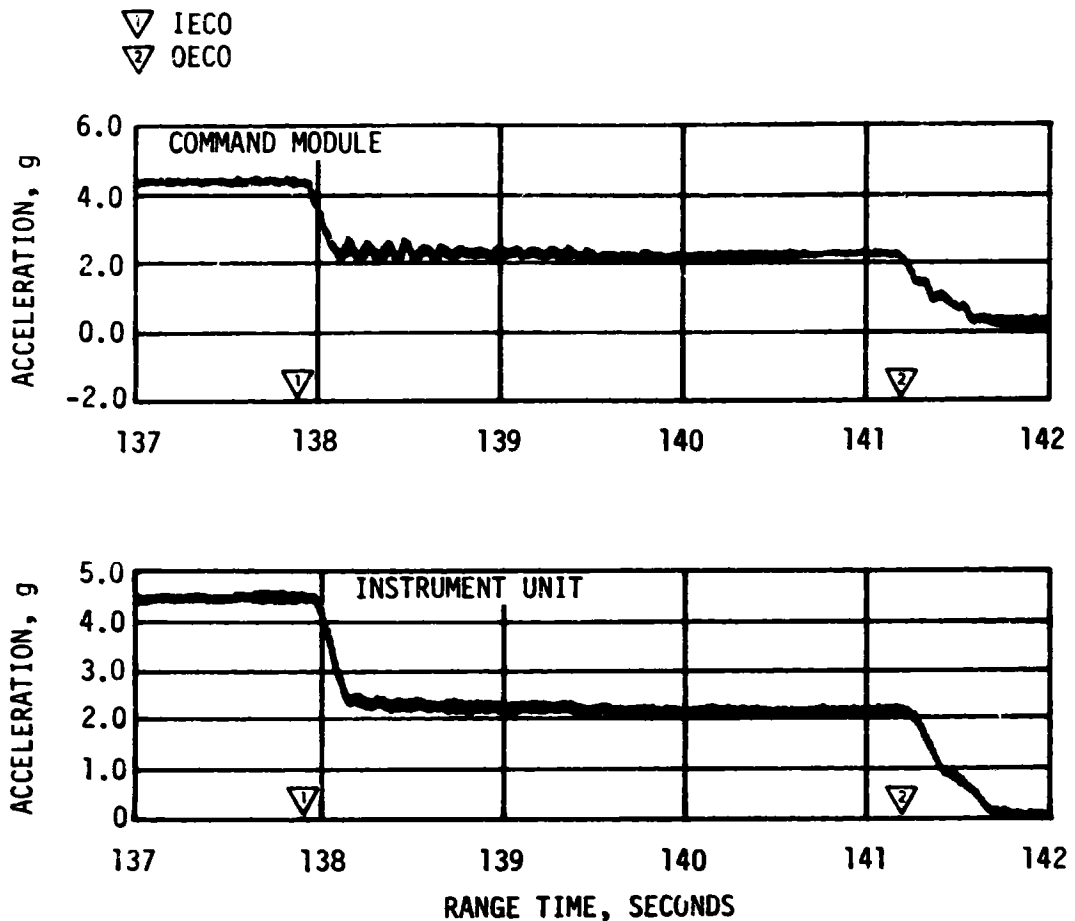


Figure 8-4. Longitudinal Acceleration During Cutoffs

8.2.2 Bending Moments

The maximum measured flight bending moment of 10.3×10^6 in-lbf occurred at 73.1 seconds. This value was derived from eight LOX stud strain gage measurements (at station 942) corrected to include the bending moment carried by the center LOX tank which was not instrumented. The measured flight bending moment, the bending moment distribution (calculated from postflight vehicle mass data and flight trajectory configuration), and the lateral acceleration distribution (normal load factors) are displayed in Figures 8-5 through 8-7. There were no significant lateral modal dynamics contributing to the vehicle bending moment.

CONDITIONS:

T = 73.1 SECONDS
 M = 1.48
 q = 4.652 PSI
 $\alpha_p = 1.80$ deg
 $\beta_p = 0.90$ deg

LEGEND:

- ⊙ BENDING MOMENT DERIVED FROM STRAIN DATA
- ▽ A4-601 ACCELEROMETER DATA
- ⊕ CENTER OF GRAVITY
- ⊙ DESIGN CRITERIA BENDING MOMENT

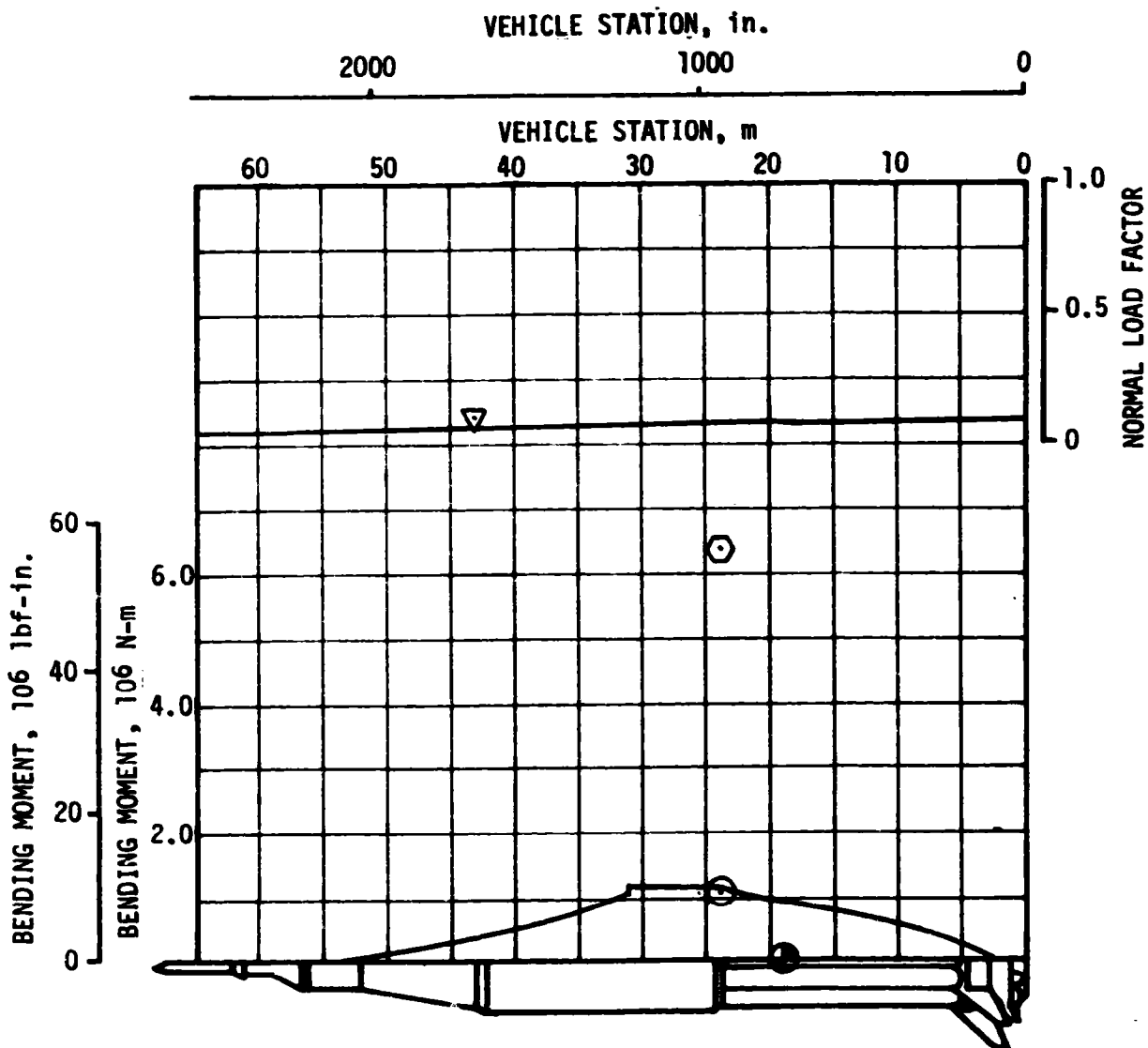


Figure 8-5. Pitch Bending Moment Distributions at Time of Maximum Resultant Moment

CONDITIONS:

T = 73.7 SECONDS
M = 1.48
q = 4.652 PSI
 $\alpha Y = 0.60$ deg
 $\beta Y = 0.50$ deg

LEGEND:

- BENDING MOMENT DERIVED FROM STRAIN DATA
- ▽ A5-603 ACCELEROMETER DATA
- CENTER OF GRAVITY

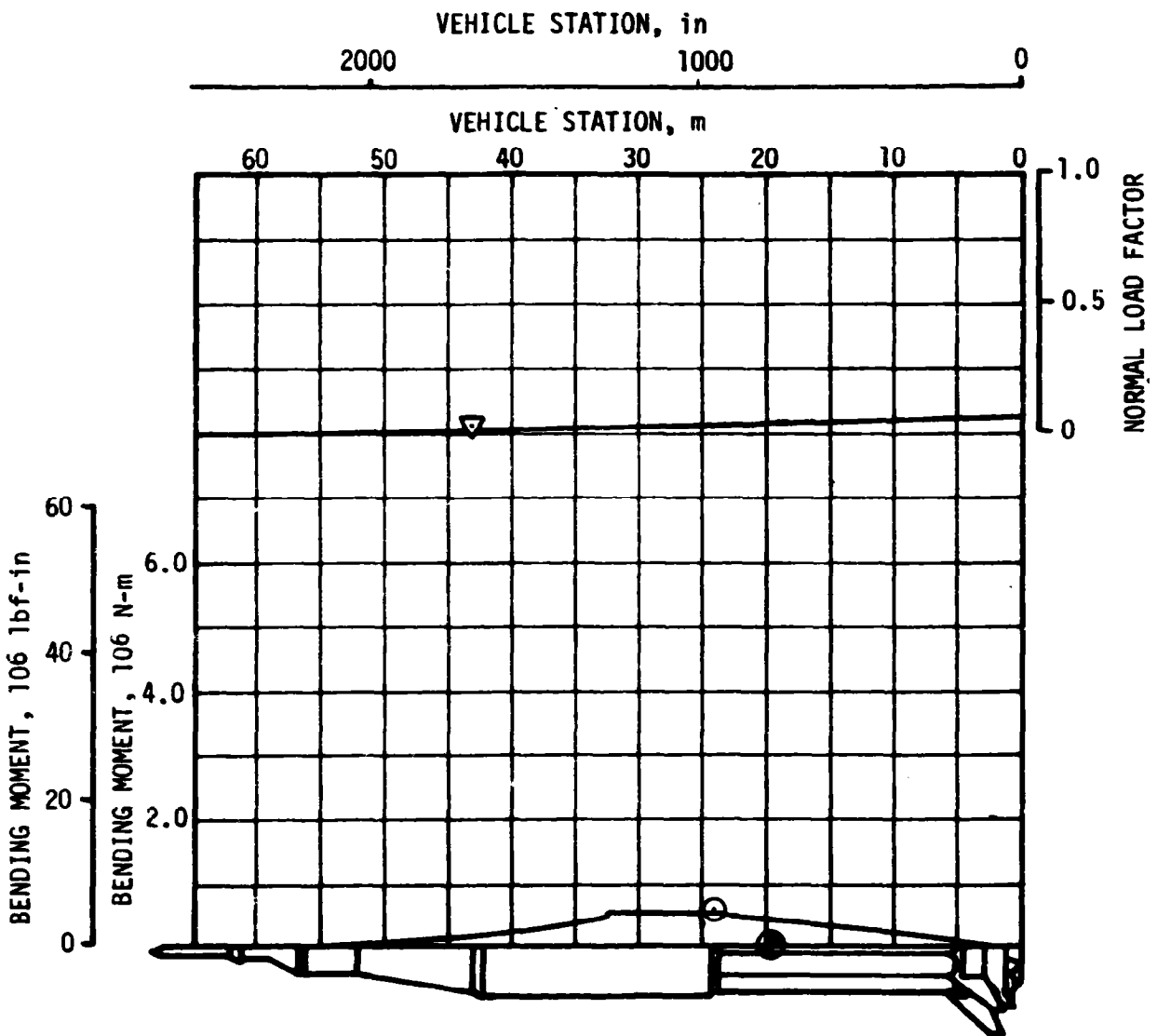


Figure 8-6. Yaw Bending Moment Distributions at Time of Maximum Resultant Moment

CONDITIONS:

T = 73.1 SECONDS
M = 1.48
q = 4.652 PSI
 α = 1.90 deg
 β = 1.03 deg

LEGEND:

⊙ BENDING MOMENT DERIVED FROM STRAIN DATA
⊙ DESIGN CRITERION BENDING MOMENT

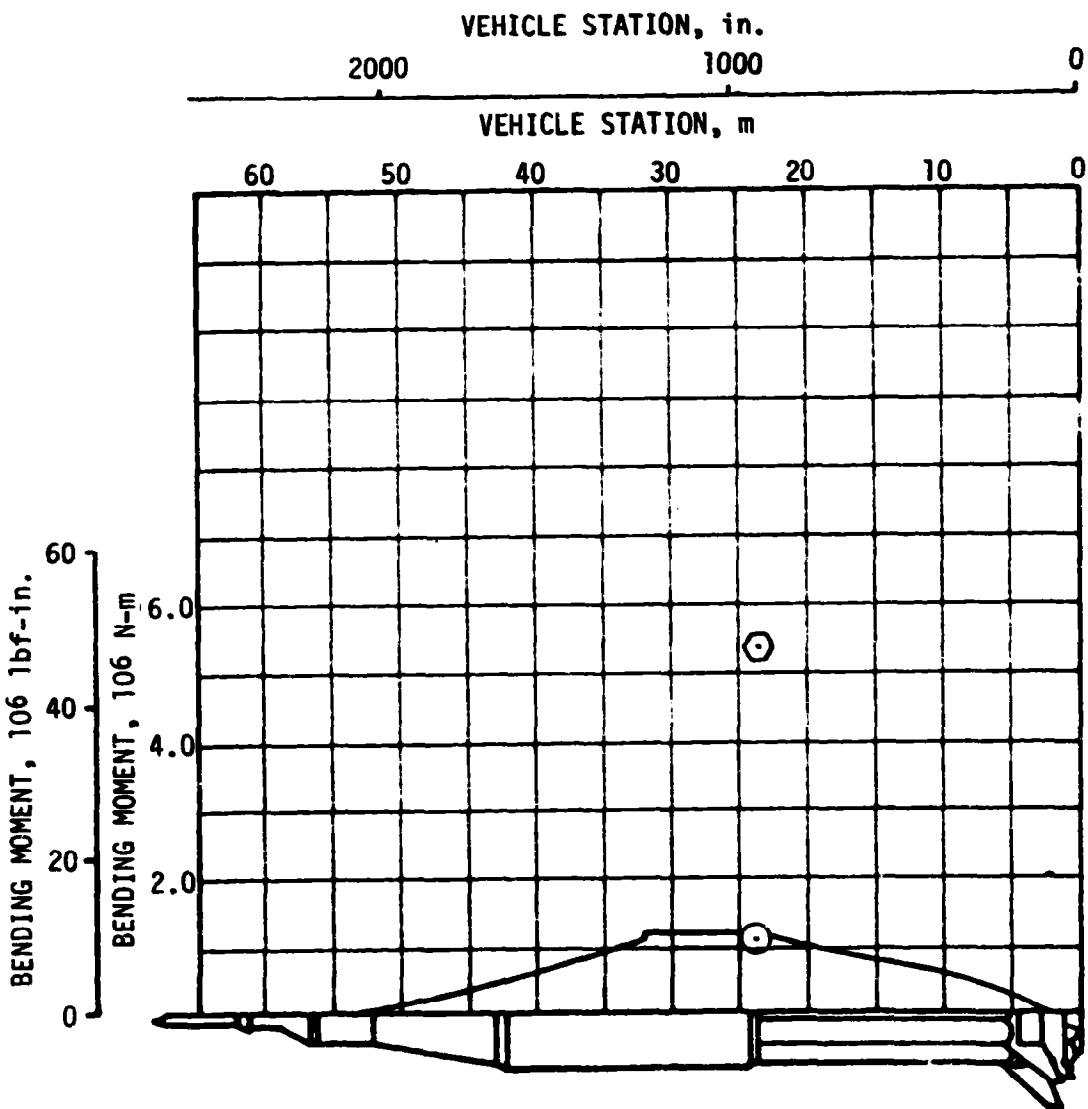


Figure 8-7. Resultant Bending Moment Distributions at Time of Maximum Resultant Moment

8.2.3 Combined Loads

Combined compression and tension loads were computed for maximum bending moment (73.1 seconds) and engine cutoff (137.8 seconds) using measured S-IVB hydrogen ullage pressure (32.0 psig). These results plus an envelope of the allowable combined loads are presented in Figure 8-8. The S-IB is not included because the clustered stage does not lend itself to this format.

The minimum safety factors are plotted versus vehicle station in Figure 8-9. The minimum factor of safety of 1.54 at station 1186 was experienced at IECO. The minimum design safety factor is 1.40.

8.2.4 Vehicle Dynamic Characteristics

The longitudinal stability analysis of SA-208 showed all vibration and pressure fluctuations to be smooth and low with no POGO instability. The vibration levels during S-IB burn were similar to those experienced by SA-207 with peak vibration levels occurring at liftoff, maximum dynamic pressure and first stage cutoff. Comparison of the data from this flight with those from SA-206 and 207 flights is shown in Figure 8-10.

The first, second and third bending mode frequencies are compared to the modes predicted by analysis in Figure 8-11. Amplitudes (Figure 8-12) at these frequencies were low and similar to previous Saturn IB flights.

Low frequency longitudinal vibration and pressure oscillations during S-IVB Stage burn are shown in Figure 8-13. The higher overall vibration and pressure amplitudes on SA-208 correlate with the higher engine thrust. The engine thrust levels at 5.5 Engine Mixture Ratio (EMR) were approximately as follows:

SA-208	236,000 lbf
SA-207	227,000 lbf
SA-206	229,000 lbf

The typical 17 Hz oscillation which occurs immediately after engine ignition damped out in approximately 3 seconds. The maximum level was ± 0.12 g's which is less than that measured on previous flights and well below design values.

Spectral density plots at selected time periods are shown in Figure 8-14. These plots show the same characteristics noted on all previous flights. The 17-19 Hz structural vibration is predominant near engine ignition (147 seconds) and 15-17 Hz near engine cutoff (555 seconds). The "buzz" phenomenon at a frequency of 71 Hz is apparent at 472 seconds.

The S-IVB engine cutoff transient did not produce a 55 Hz oscillation as was noted on the SA-207 flight. Cutoff transients for gimbal block acceleration are shown for SA-206, SA-207 and SA-208 in Figure 8-15.

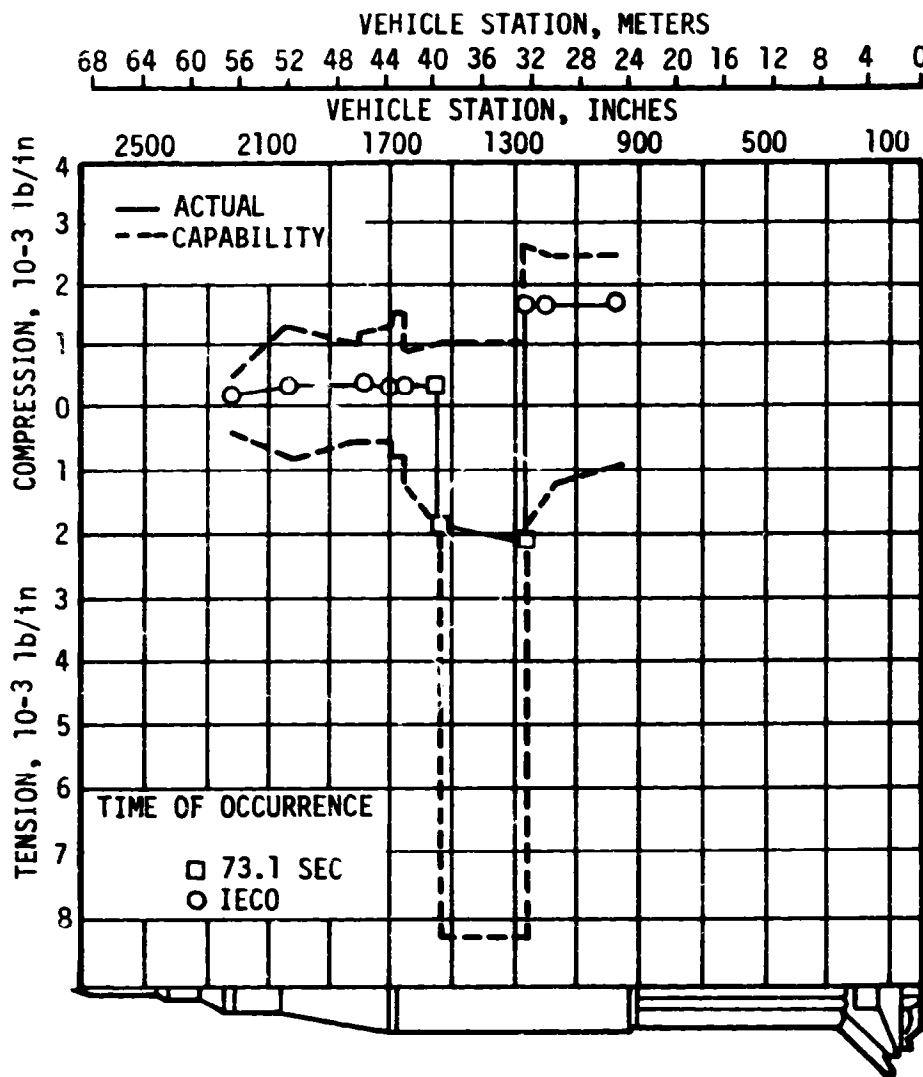


Figure 8-8. Combined Loads Producing Minimum Safety Margin During SA-208 Flight

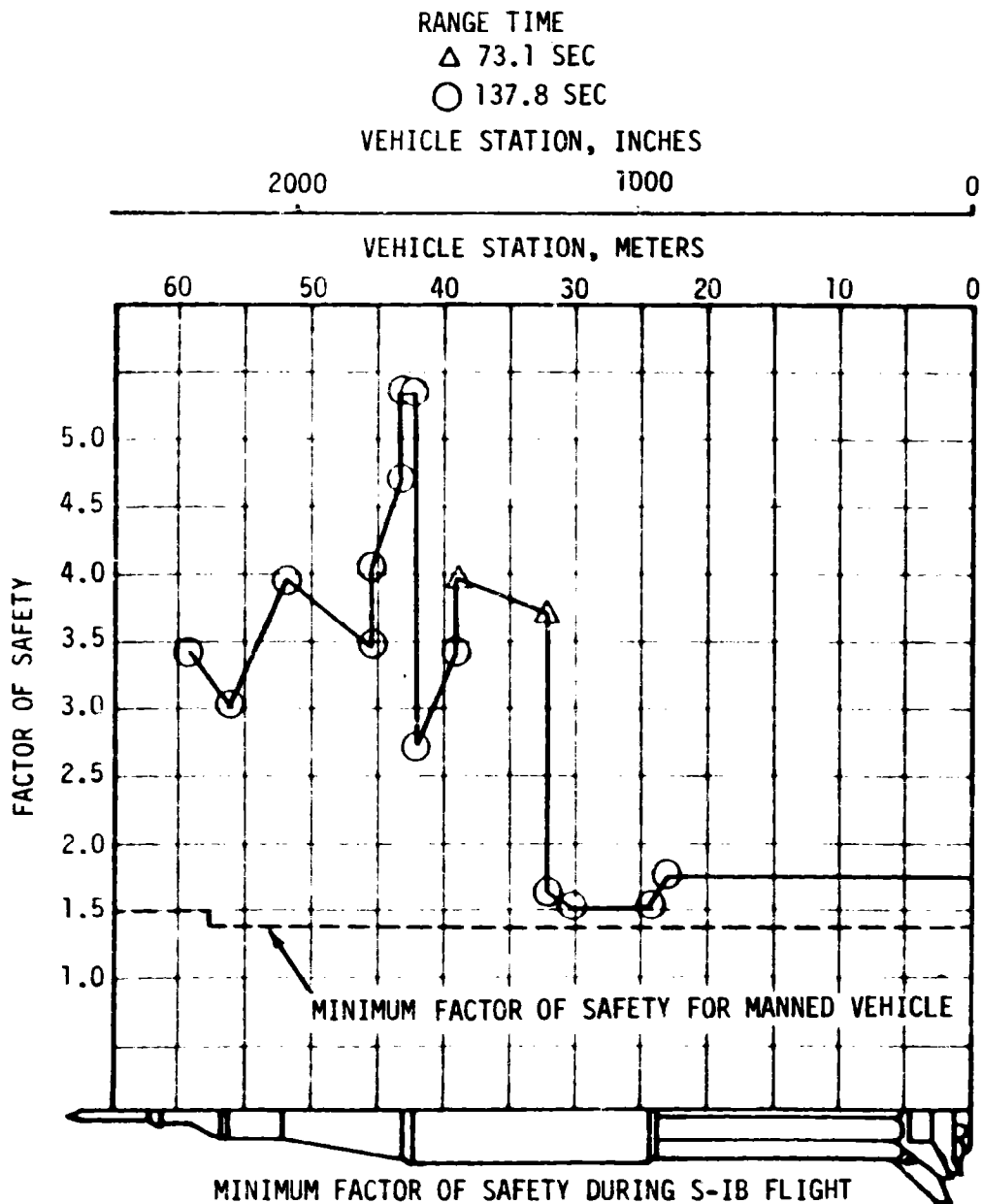


Figure 8-9. Minimum Factor of Safety During SA-208 S-IB Flight

REPRODUCIBILITY OF THE ORIGINAL PAGE IS POOR

A0012-403 GIMBAL BLOCK ACCELERATION, LONGITUDINAL DIRECTION (2-25 HZ)

▽ S-IB/S-IVB SEPARATION

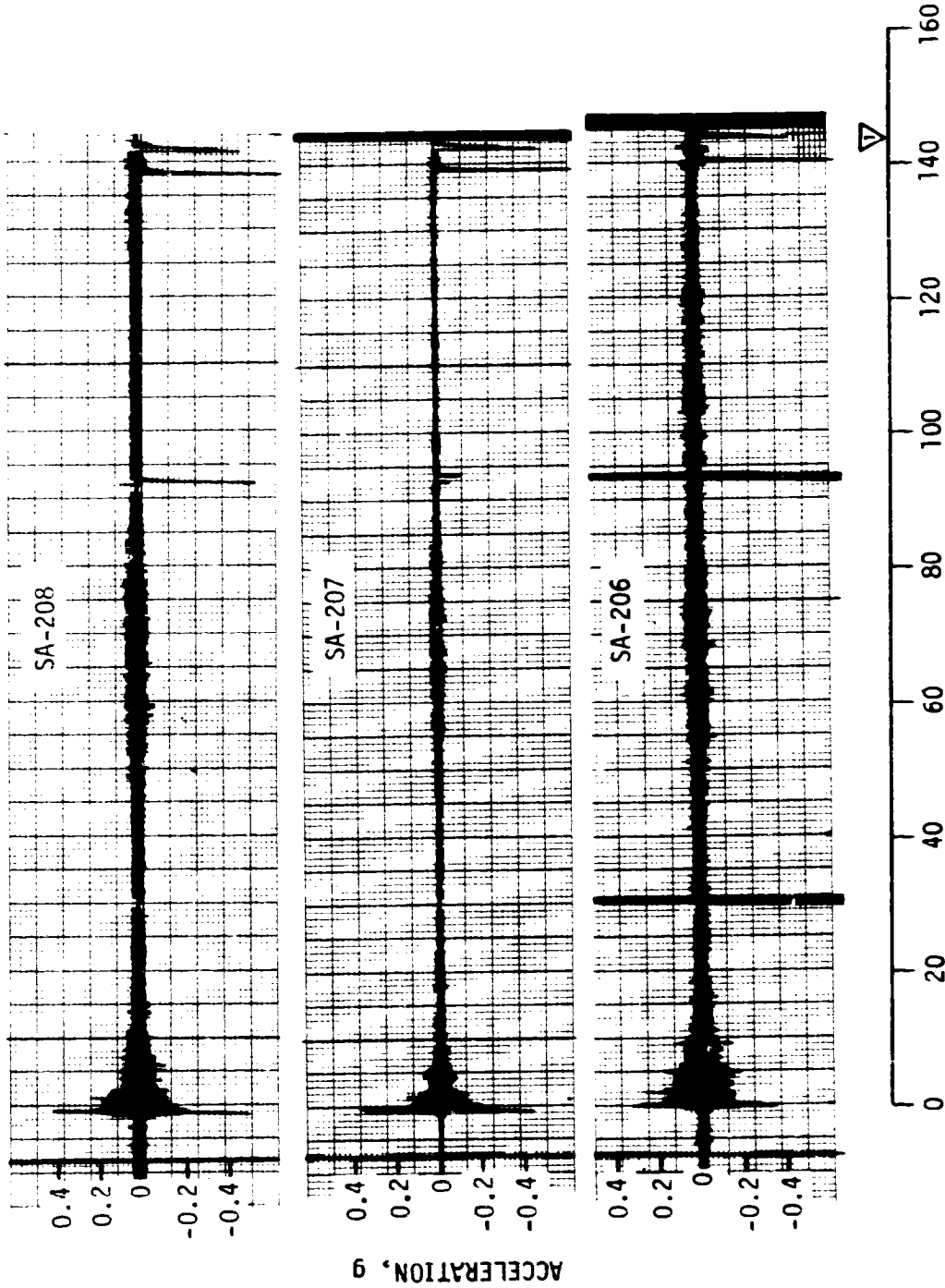


Figure 8-10. Vibration Measured During First Stage Burn

1ST BENDING (FLIGHT DATA)
 Δ 2ND BENDING (FLIGHT DATA)

3RD BENDING (FLIGHT DATA)
 — DYNAMIC ANALYSIS

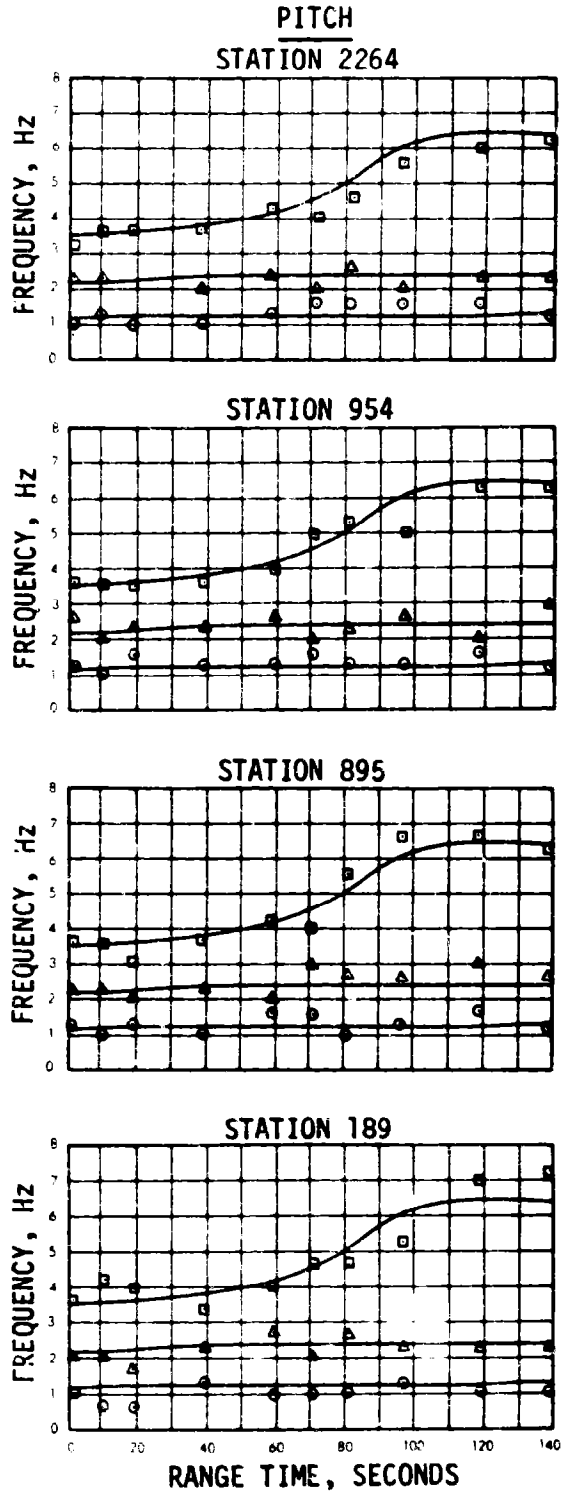
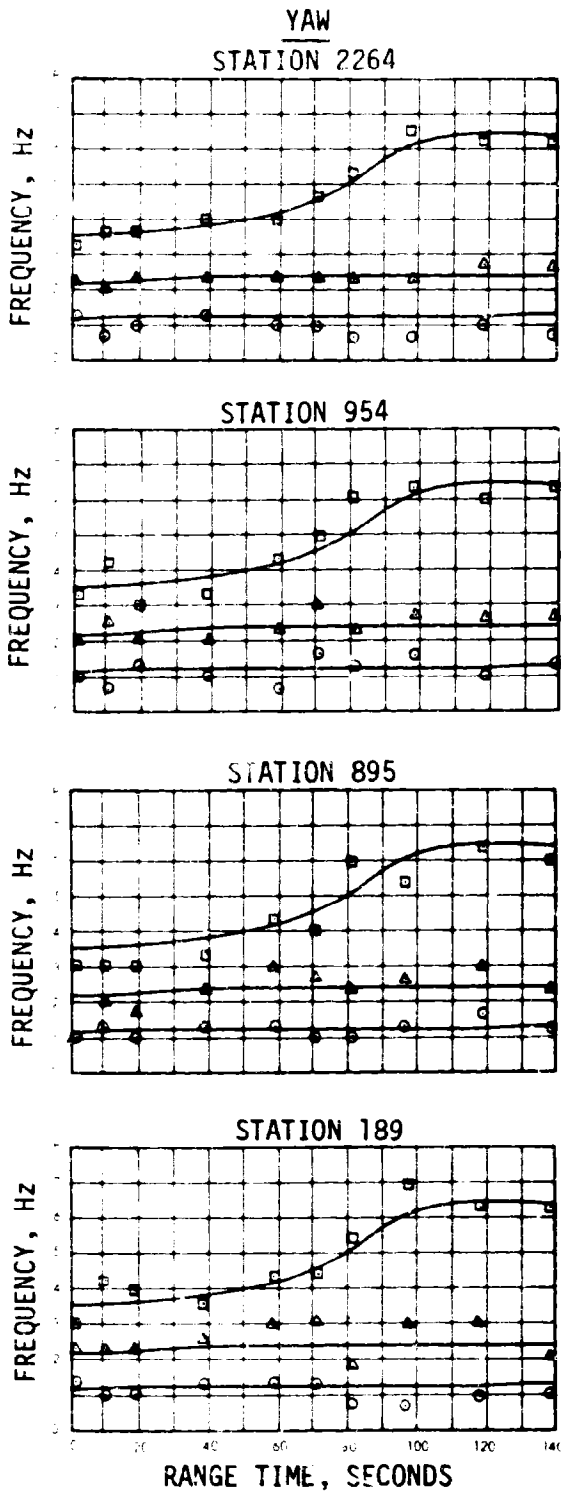


Figure 8-11. Vehicle Bending Frequencies

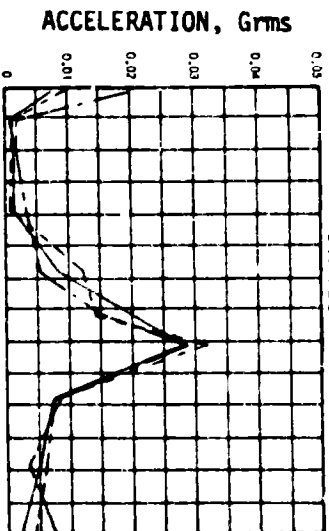
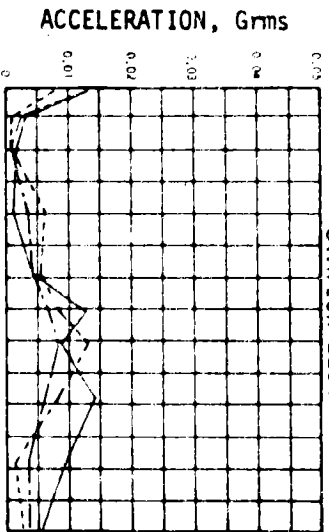
——— 1ST BENDING
 - - - 2ND BENDING
 - - - 3RD BENDING

YAW

PITCH

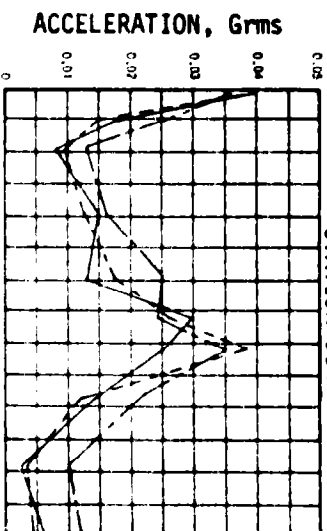
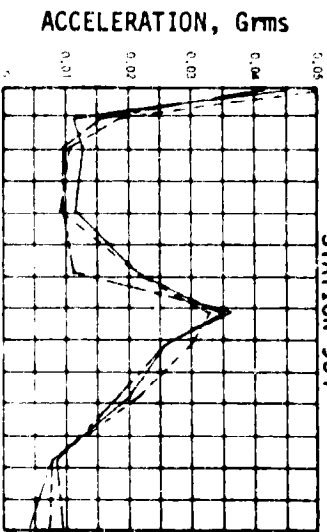
STATION 2264

STATION 2264



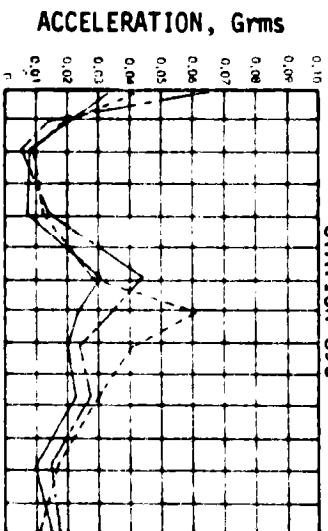
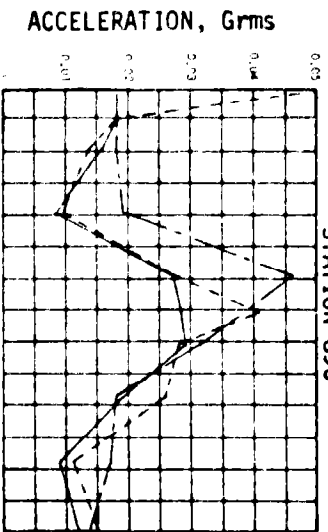
STATION 954

STATION 954



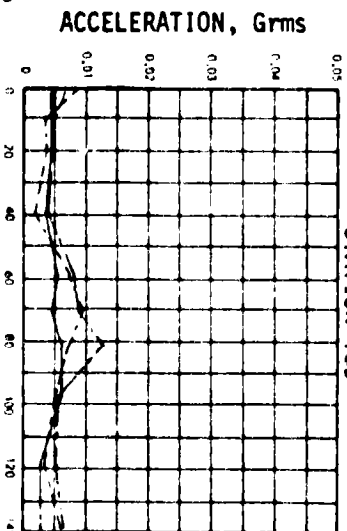
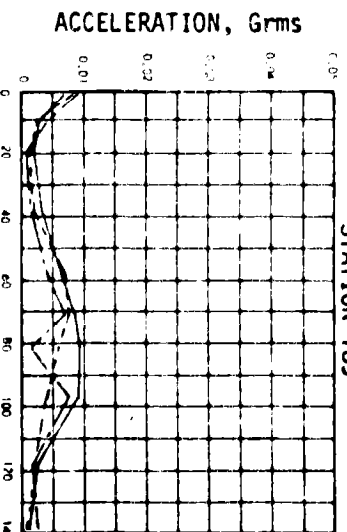
STATION 895

STATION 895



STATION 189

STATION 189



RANGE TIME, SECONDS

RANGE TIME, SECONDS

Figure 8-12. Vehicle Bending Amplitudes

REPRODUCIBILITY OF THE ORIGINAL PAGE IS POOR

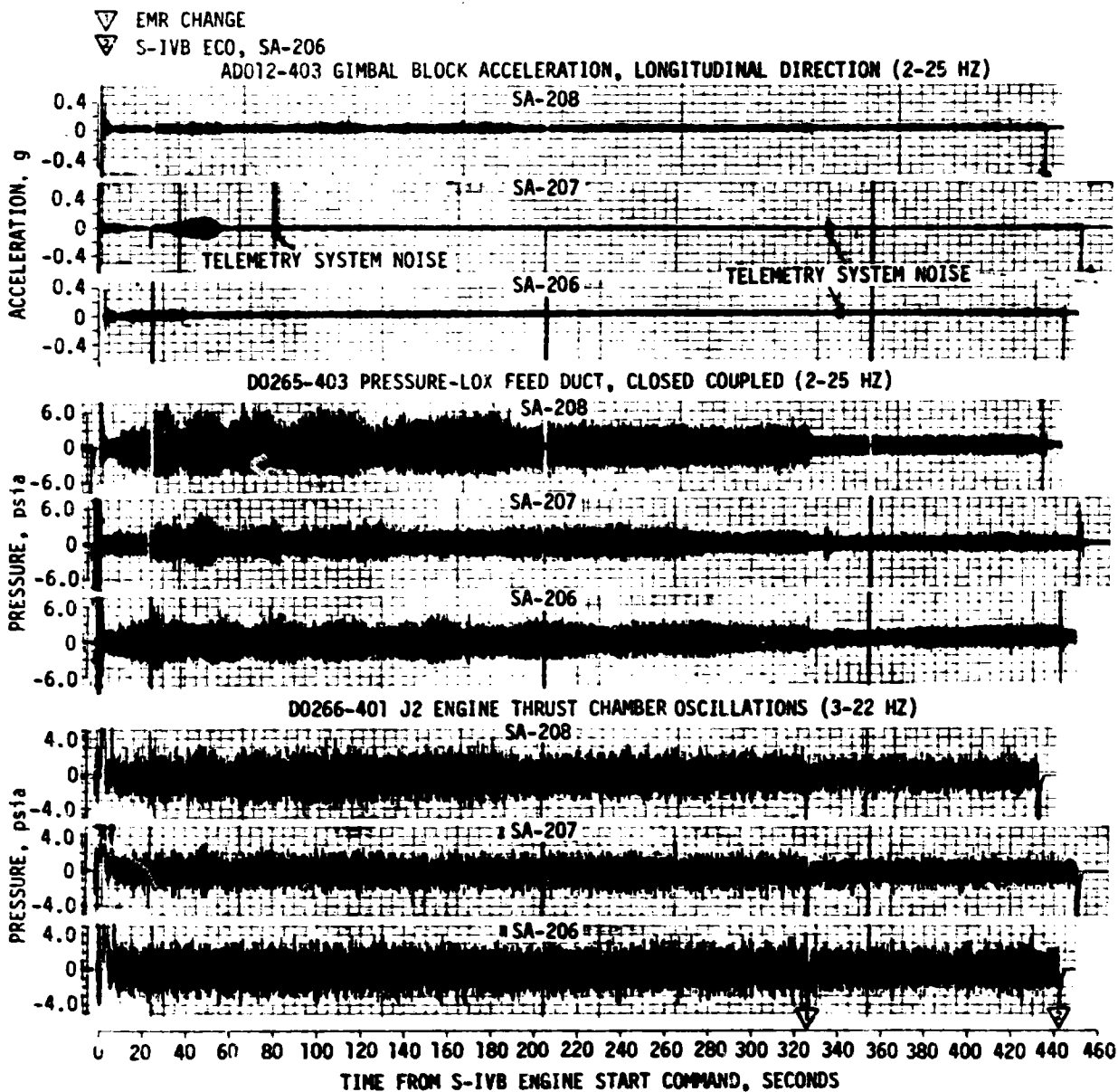
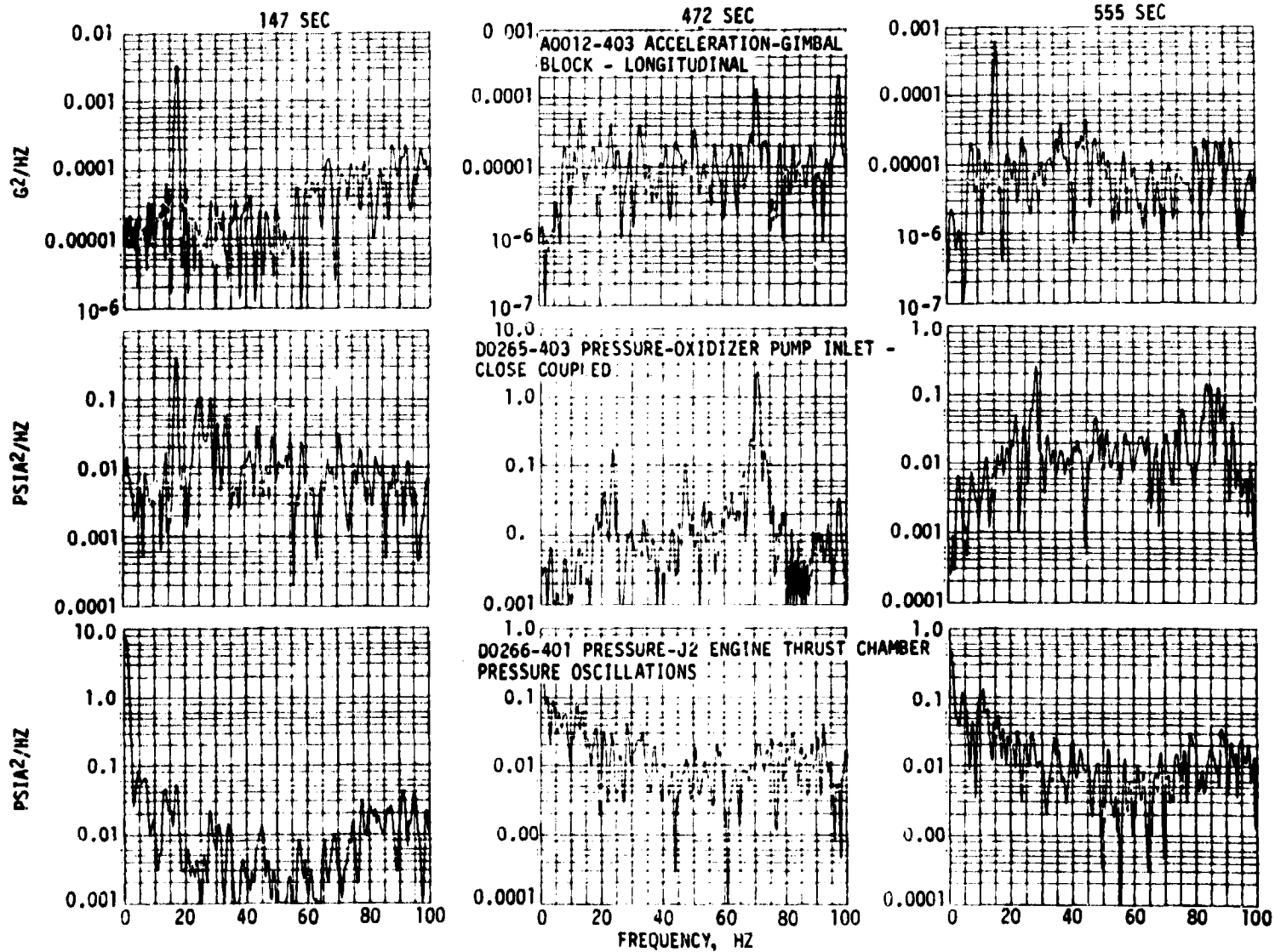


Figure 8-13. Low Frequency Vibration and Pressure Oscillations Measured During S-IVB Stage Burn



REPRODUCIBILITY OF THE
ORIGINAL PAGE IS POOR

Figure 8-14. Low Frequency Analysis of Vibration and Engine Pressures

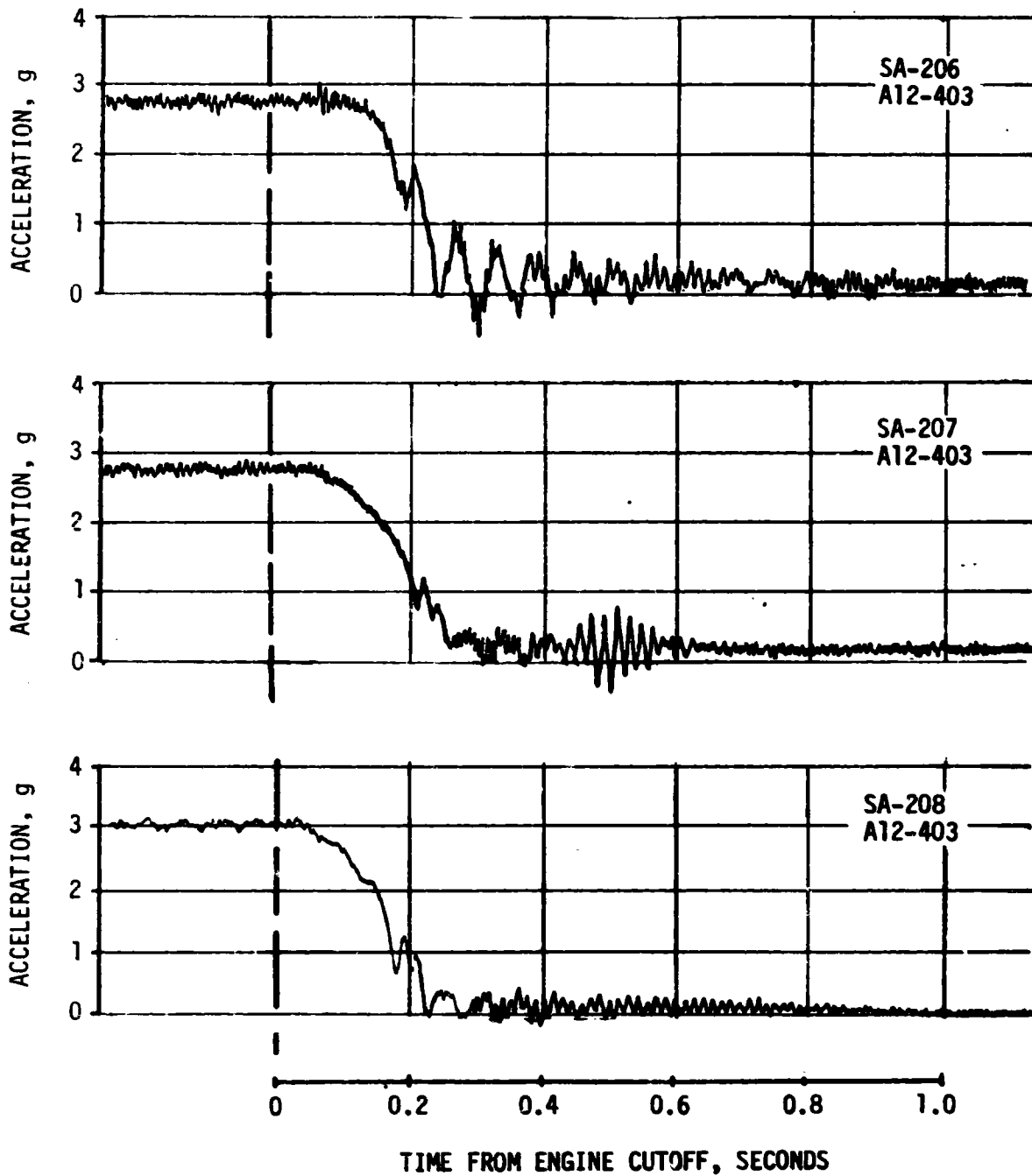


Figure 8-15. S-IVB Engine Cutoff Transients

8.3 STRUCTURAL ASSESSMENT

Prelaunch structural assessments of SA-208 confirmed the vehicle qualified for the SL-4 mission. As a conservative approach, the ground wind limits and the flight envelope were restricted, presupposing recurrence of problems resulting from stress corrosion following the last preflight inspection. The ground wind limit restriction, assuming ineffective tension tie from cracked E-beam, was 30 knots for damper transition for both Countdown Demonstration Test (CDDT) and launch. The maximum wind was 13.3 knots for this condition. The flight envelope angle of attack restriction, assuming cracked fins, was 5.2° as compared to 1.9° actual.

8.3.1 Fuel Tank Forward Bulkhead Damage

Localized curvature reversal of the forward bulkheads of fuel tanks 3 and 4 occurred during the pre-CDDT RP-1 loading operation. Reversal occurred because tank vent covers were not removed during a level adjust drain, causing a negative pressure (2.7 psi), for which the bulkheads were not designed. The system was pressurized to restore the bulkheads to contour and then proof-pressure tested to 21.0 psig. No cracks or structural anomalies were found. Two new vent valves were installed to lower the maximum flight pressure to 19.1 psig; normal setting is 21 to 21.5 psig.

8.3.2 Stress Corrosion Cracking

During pre-CDDT inspection at Kennedy Space Center (KSC), a crack was discovered in the lower web of the upper E-beam of the outrigger assembly, fin position 4. The beam was a forging of 7178-T6 aluminum alloy which is susceptible to stress corrosion. A 1 x 3 x 3/4-inch coupon of cracked material was removed from the lower web and a spacer and splice plate was installed to restore the structure to the full capability of the undamaged hardware. (Figure 8-16).

After the CDDT, stress-corrosion cracks were found in all eight fin assemblies, at the rear-spar to thrust structure E-beam attachment fittings. Seven fins had cracks in both left and right fitting mounting bolt holes, one in only one fitting. All cracked fins were replaced and reinforcing blocks installed about the mounting bolts at each fitting to provide an alternate load path (a "fail-safe" feature) in the event that cracks occurred after the last preflight inspection. (Figure 8-17).

Stress corrosion cracks were also found in seven of the eight S-IB/S-IVB interstage reaction beams (Figure 8-18). The cracks existed at the forged flash line (die parting plane) of the 7079-T652 aluminum alloy forgings from which the beams were machined. A dye penetrant inspection was performed on the inboard and outboard surface of the aft end of the inboard cap of the reaction beams. A one inch wide strip centered on the inboard cap of the beam was also dye-penetrant inspected (all eight beams entire length). No additional cracks were found. A stress analysis of

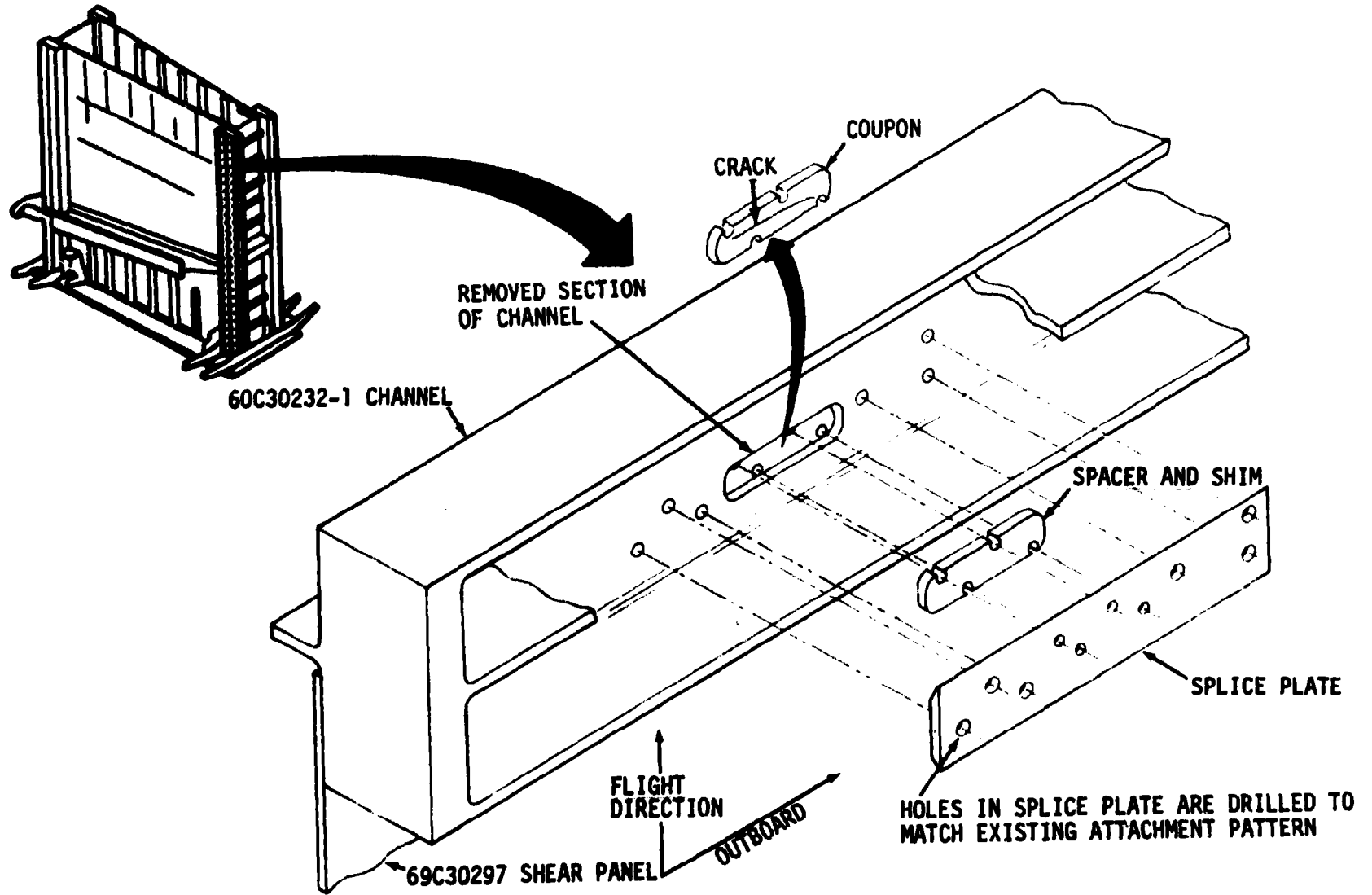


Figure 8-16. S-1B Outrigger Assembly Channel Repair

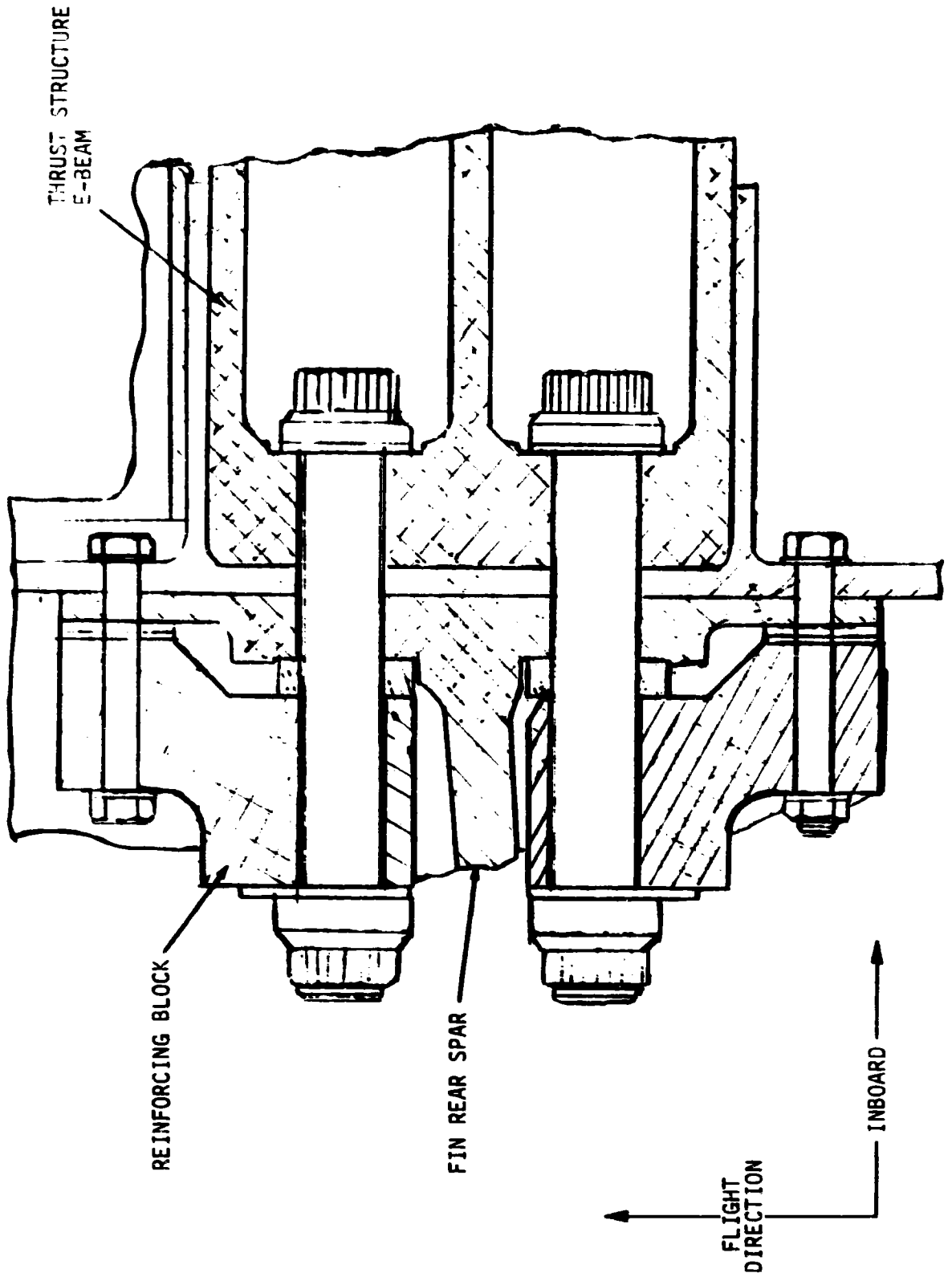


Figure 8-17. S-1B Fin Reinforcing Block Installation

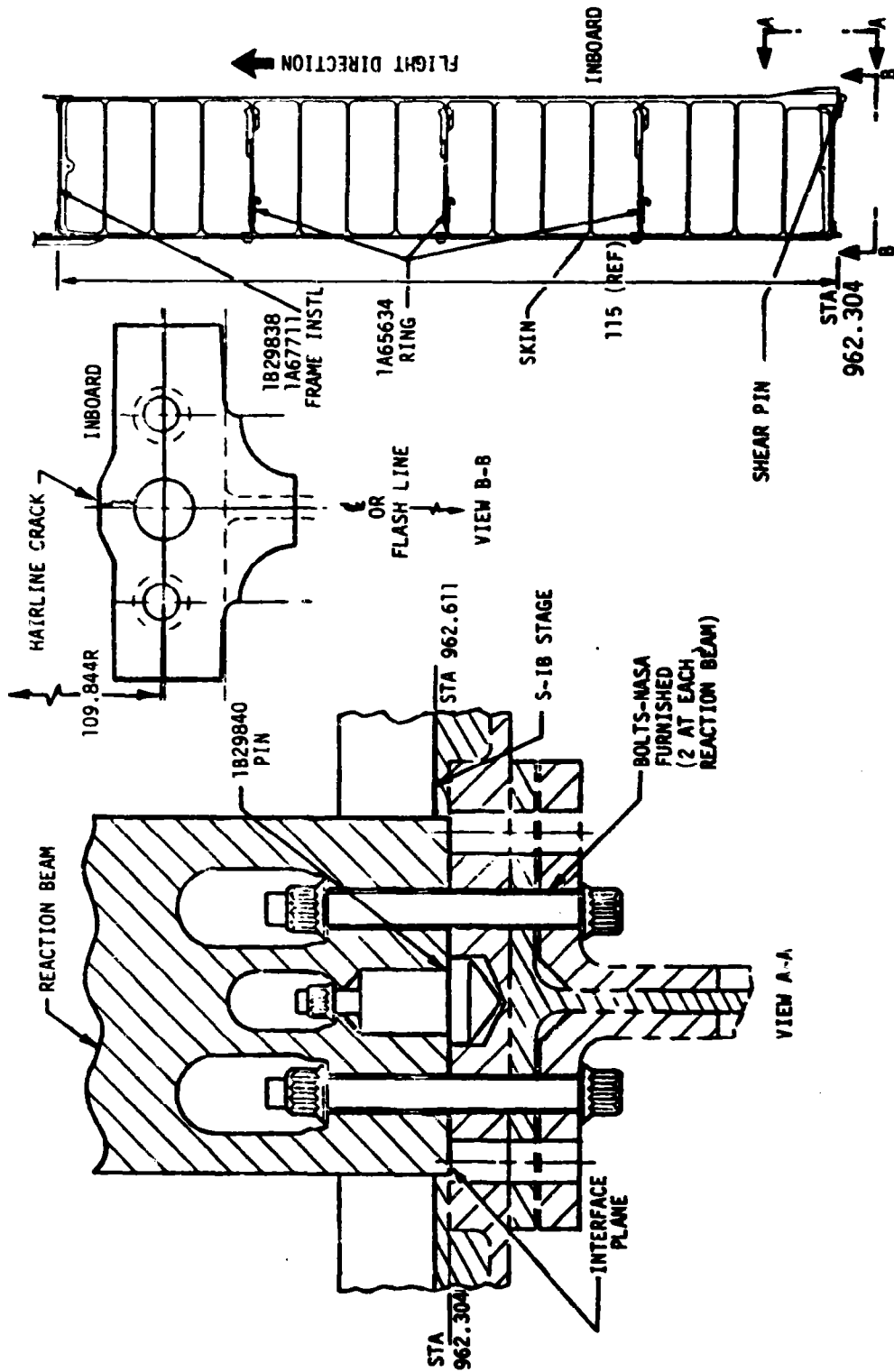


Figure 8-18. S-IB/S-IVB Interstage Reaction Beam

the cracked beams indicated a factor of safety in excess of 1.5 as compared to a minimum required factor of safety of 1.4; and, therefore, the decision was made to fly "as is".

SECTION 9

GUIDANCE AND NAVIGATION

9.1 SUMMARY

The stabilized platform and the guidance computer successfully supported the accomplishment of the SA-208 Launch Vehicle mission objective. Targeted conditions at orbit insertion were attained with insignificant error. No anomalies nor deviations from nominal performance were noted.

The stabilized platform indicated unplanned velocity changes between 3440 and 5735 seconds.

9.2 GUIDANCE COMPARISONS

The postflight guidance error analysis was based on comparisons of position and velocity data from the onboard guidance computer with corresponding data taken from the final Observed Mass Point Trajectory (OMPT) which was established from external tracking and telemetered velocity data (see Section 4). Comparisons of the inertial platform measured velocities with the OMPT data are shown in Figure 9-1 for boost to orbit insertion. The velocity differences are small and well within the accuracies of the onboard measuring system and the OMPT. The differences in vertical and downrange velocities are very small and reflect some combination of small hardware errors and adjustments to telemetered velocities to give the best composite fit of data from several radars tracking the SA-208 vehicle during boost. The crossrange velocity differences indicate platform misalignment due to some combination of small initial orientation error and gyro drifts. At orbit insertion the telemetered crossrange velocity was 2.24 m/s (7.35 ft/s) less negative than the OMPT value.

The inertial platform velocity measurements at significant event times are shown in Table 9-1 along with corresponding data from the OMPT. The differences in velocity components at S-1B inboard (IECO) and outboard (OECO) engine cutoffs are consistent with the plots shown in Figure 9-1 which indicates a good thrust decay simulation used in constructing the OMPT. At orbit insertion, the velocity differences were 0.18 m/s (0.59 ft/s), -2.24 m/s (-7.35 ft/s), and 0.02 m/s (0.07 ft/s) for vertical, crossrange, and downrange velocities, respectively.

Velocity gain due to thrust decay after S-IVB Guidance Cutoff Signal (GCS) was 7.43 m/s (24.37 ft/s) compared to 7.21 m/s (23.66 ft/s) predicted by the Operational Trajectory (OT).

Comparisons of navigation (PACSS-13) positions, velocities, and flight path angle at significant event times are presented in Table 9-2. Dif-

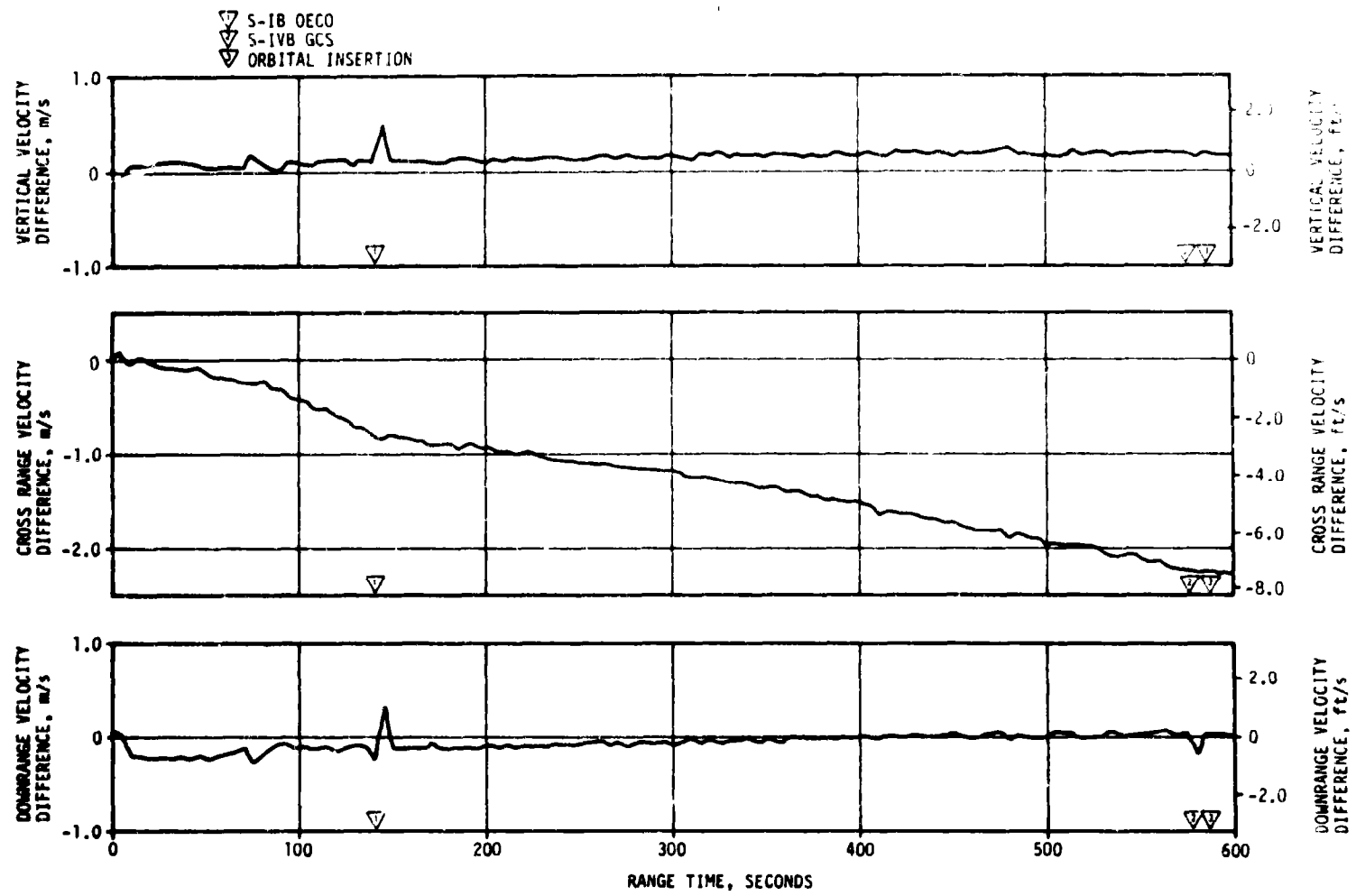


Figure 9-1. SA-208 Trajectory and ST-124M Platform Velocity Comparisons (OMPT Minus LVDC)

Table 9-1. SA-208 Inertial Platform Velocity Comparisons

EVENT	DATA SOURCE	VELOCITY (PACSS-12)*		
		METERS/SECOND (FEET/SECOND)		
		X	Y	Z
S-IB IECO	LVDC	2414.10 (7920.28)	-15.75 (-51.67)	1760.25 (5775.10)
	OMPT	2414.23 (7920.70)	-16.51 (-54.17)	1760.20 (5774.93)
S-IB OECO	LVDC	2450.45 (8039.53)	-18.30 (-60.04)	1831.60 (6009.19)
	OMPT	2450.45 (8039.55)	-18.98 (-62.27)	1831.58 (6009.11)
S-IVB GCS	LVDC	3286.00 (10780.84)	-1429.75 (-4690.78)	7586.45 (24889.93)
	OMPT	3286.19 (10781.47)	-1432.02 (-4698.21)	7586.49 (24890.04)
ORBITAL INSERTION	LVDC	3285.05 (10777.72)	-1432.70 (-4700.46)	7593.20 (24912.07)
	OMPT	3285.23 (10778.30)	-1434.94 (-4707.82)	7593.22 (24912.13)

*Project Apollo Coordinate System Standard, non-rotating vehicle referenced.

Table 9-2. Navigation Position and Velocity Comparisons (PACSS-12)

EVENT	DATA SOURCE	POSITIONS METERS (FEET)				VELOCITIES METERS/SECOND (FEET/SECOND)				FLIGHT PATH ANGLE (DEGREES)
		X _s	Y _s	Z _s	R	X _s	Y _s	Z _s	V _s	
S-1B TECO	LVDC	6,426,249.6 (21,083,496.1)	52,433.4 (172,025.6)	101,003.6 (331,376.6)	6,427,257.1 (21,086,801.5)	901.35 (2,957.19)	219.38 (719.75)	2,082.6 (6,832.74)	2,279.88 (7,479.92)	24.2317
	OMPT	6,426,260.7 (21,083,532.5)	52,397.7 (171,908.6)	100,975.8 (331,285.4)	6,427,267.7 (21,086,836.0)	901.51 (2,957.70)	218.64 (717.31)	2,082.57 (6,832.58)	2,279.83 (7,479.75)	24.2362
	Operational Trajectory	6,426,646. (21,084,795.)	52,559. (172,439.)	101,071. (331,596.)	6,427,655. (21,088,108.)	906.70 (2,974.74)	220.54 (723.57)	2,088.14 (6,850.84)	2,287.15 (7,503.78)	24.300
S-1B OECO	LVDC	6,429,385.9 (21,093,785.8)	53,189.9 (174,507.5)	108,362.0 (355,518.4)	6,430,519.0 (21,097,503.3)	904.21 (2,966.57)	216.61 (710.66)	2,153.40 (7,064.96)	2,345.56 (7,695.41)	23.6811
	OMPT	6,429,401.1 (21,093,835.5)	53,151.7 (174,382.3)	108,340.3 (355,447.2)	6,430,533.5 (21,097,550.7)	904.22 (2,966.62)	215.93 (708.42)	2,153.38 (7,064.88)	2,345.48 (7,695.14)	23.6832
	Operational Trajectory	6,429,374. (21,093,746.)	53,217. (174,596.)	107,435. (352,479.)	6,430,491. (21,097,413.)	909.41 (2,983.63)	217.92 (714.95)	2,150.10 (7,054.13)	2,344.66 (7,692.46)	23.821
S-1VB GCS	LVDC	6,232,144.2 (20,446,667.3)	-16,187.7 (- 53,115.8)	1,943,479.6 (6,376,244.4)	6,528,169.5 (21,417,878.9)	-2,305.97 (-7,565.58)	-1,230.85 (-4,038.22)	7,380.26 (24,213.55)	7,829.48 (25,687.40)	-0.00887
	OMPT	6,232,257.4 (20,447,038.5)	-16,826.0 (- 55,203.4)	1,943,449.9 (6,376,148.1)	6,528,270.0 (21,418,209.5)	-2,305.68 (-7,564.56)	-1,232.93 (-4,045.03)	7,380.37 (24,213.80)	7,829.82 (25,688.38)	-0.00613
	Operational Trajectory	6,228,837. (20,435,816.)	-18,029. (- 59,149.)	1,953,971. (6,410,667.)	6,528,150. (21,417,813.)	-2,318.59 (-7,606.93)	-1,231.48 (-4,040.29)	7,376.18 (24,200.06)	7,829.46 (25,687.20)	-0.008
ORBITAL INSERTION	LVDC	6,208,630.2 (20,369,521.7)	-28,520.9 (- 93,572.5)	2,017,198.6 (6,618,105.6)	6,528,169.2 (21,417,878.0)	-2,396.03 (-7,860.99)	-1,233.35 (-4,046.42)	7,358.62 (24,142.45)	7,836.54 (25,710.43)	0.00324
	OMPT	6,208,744.5 (20,369,896.5)	-29,183.0 (- 95,744.8)	2,017,179.7 (6,618,043.6)	6,528,275.0 (21,418,225.0)	-2,395.73 (-7,859.99)	-1,235.40 (-4,053.15)	7,358.68 (24,142.63)	7,836.82 (25,711.36)	0.00602
	Operational Trajectory	6,205,195. (20,358,251.)	-30,367. (- 99,628.)	2,027,653. (6,652,404.)	6,528,150. (21,417,815.)	-2,408.70 (-7,902.55)	-1,233.64 (-4,047.36)	7,353.95 (24,127.14)	7,836.09 (25,708.96)	0.003

ferences between the Launch Vehicle Digital Computer (LVDC) and OT data reflect differences in actual and nominal vehicle performance and flight environment. Guidance cutoff signal was issued with a total velocity 0.02 m/s (0.07 ft/s) and radius vector 19.5 meters (64 feet) greater than the OT values. At orbit insertion the LVDC velocity was 0.45 m/s (1.48 ft/s) greater than the OT value.

The LVDC and OMPT data were in very good agreement for the total boost phase except for crossrange. The crossrange velocity difference (OMPT minus LVDC) built up to -2.05 m/s (-6.73 ft/s) with a position difference of -662.1 meters (-2172.2 feet) at orbit insertion. If all the crossrange differences are assumed to be guidance measurement errors, the result would be orbit inclination and decending node errors of 0.015 degrees and 0.013 degrees, respectively. These differences are well within three-sigma envelopes, although they are larger than noted on the two previous Saturn IB flights. Crossrange differences for the past three flights are shown below.

		<u>SA-206</u>	<u>SA-207</u>	<u>SA-208</u>
ΔY_s	m/s (ft/sec)	0.78 (2.56)	0.66 (2.17)	-2.05 (-6.73)
ΔY_s	Meters (feet)	94.9 (311.4)	159.1 (522.0)	-662.1 (-2172.2)

The boost terminal conditions are shown in Table 9-3. The guidance system was highly successful in guiding the SA-208 launch vehicle to targeted end conditions.

Table 9-3. SA-208 Boost Terminal Conditions

CONDITIONS	DESIRED	ACHIEVED	ERROR (ACHIEVED - DESIRED)
Velocity, V_T (m/sec)	7836.10303	7836.12041	0.01738
Radius, R_T (km)	6528.1995	6528.1723	-0.0272
Path Angle, θ_T (deg)	0.0	-.001485	-0.001485
Inclination, I (deg)	50.031282	50.0348561	0.0035741
Descending Node, λ (deg)	156.961798	156.9673428	0.0055448

9.3 GUIDANCE AND NAVIGATION SCHEME EVALUATION

The flight program performed all functions properly. Targeted guidance cutoff conditions were achieved with a high degree of accuracy. All events scheduled at preset times occurred within acceptable tolerances. Times of occurrence of major guidance and navigation events are included in Table 2-2, Section 2. Observed and predicted vehicle rate-limited commanded attitude angles are shown for comparison in Figures 9-2 through 9-4. The second stage boost plane-change was the largest ever performed by a Saturn Launch Vehicle, and was accomplished satisfactorily as indicated by the commanded yaw steering during second stage boost (Figure 9-4).

9.3.1 First Stage Boost

Timebase 1 was initiated at 0.471 seconds, 17.425 seconds after Guidance Reference Release (GRR). The roll and time-tilt maneuver, starting at 10.330 seconds aligned the vehicle to a flight azimuth of 53.781 degrees east of north. The roll maneuver was terminated at 48.449 seconds. The vehicle followed a preset attitude time-history during the atmospheric boost phase. Tilt-arrest, signifying completion of the atmospheric boost phase, was commanded at 130.938 seconds with a pitch attitude command of -62.8599 degrees. First stage guidance and navigation was normal.

9.3.2 Second Stage Boost

Second stage guidance was normal with no undue occurrences noted. The desired and achieved guidance terminal conditions for boost are compared in Table 9-3.

9.3.3 Orbital Phase

At the start of Timebase 4 an attitude hold (Chi-freeze) was initiated, followed by a maneuver to local horizontal. The commanded attitudes are shown in Table 9-4. Initiation of orbital navigation (implemented at T4 +15.544 seconds) and all orbital events were within the tolerance of one computation cycle. Unexpected velocity changes were indicated by the stable platform during the period between 3440 and 5735 seconds (Figure 9-5). The times coincide, respectively, with the initial relief venting of the S-IVB fuel tank via the Non-Propulsive Vent (NPV) system and with the depletion of liquid hydrogen fuel. NPV activity during this period is discussed in Section 7. The velocity change had no detrimental effect on mission accomplishment.

- ▽ MACH 1
- ▽ S-IB OECS
- ▽ IGM PHASE 1
- ▽ IGM PHASE 2 (EMR)
- ▽ TERMINAL GUIDANCE
- ▽ S-IVB G.C.S.
- ▽ ORBIT INSERTION

ACTUAL ———
 PREDICTED - - - -

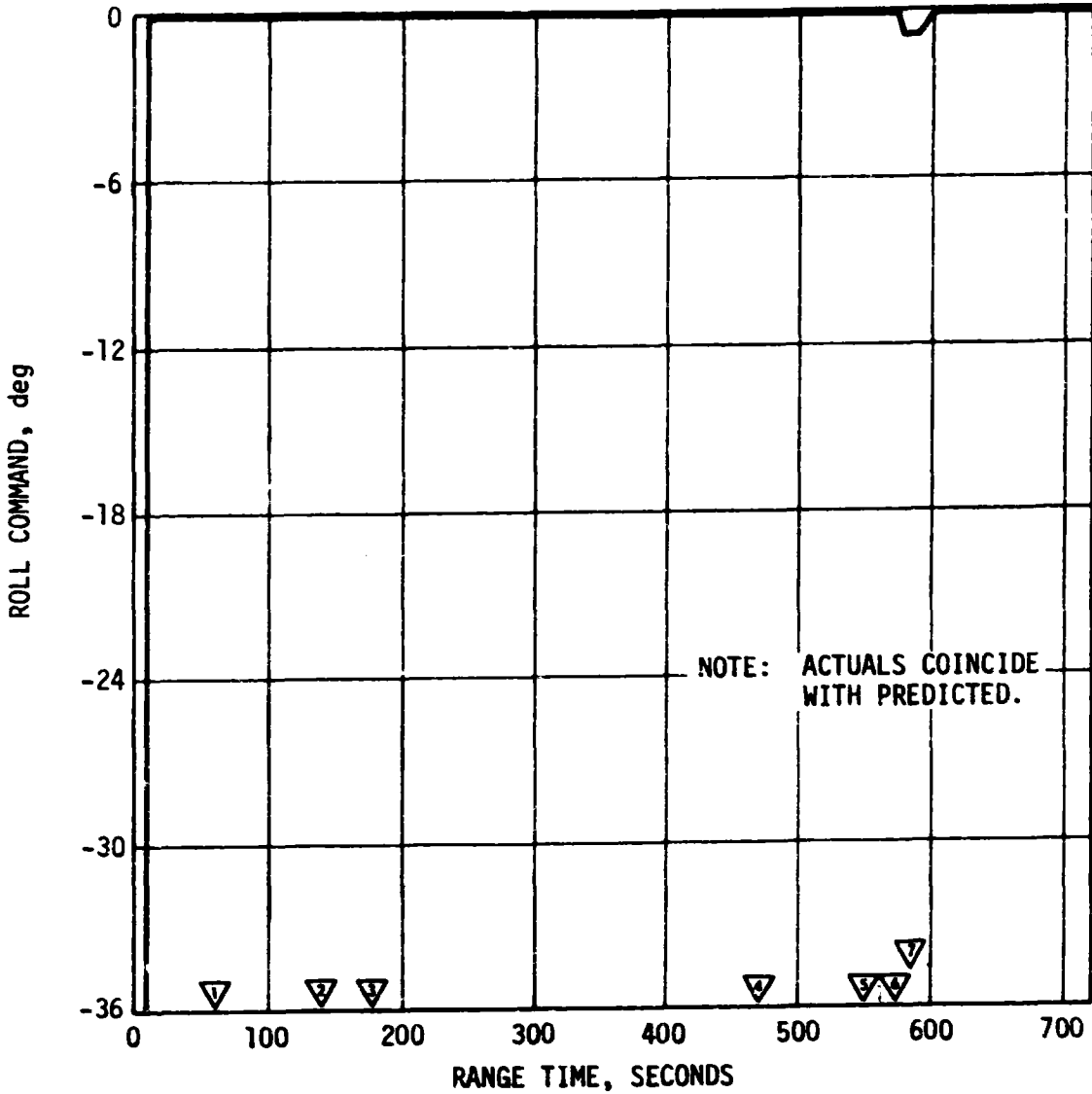


Figure 9-2. Roll Command During Boost

- ▽ MACH 1
- ▽ S-IB OECS
- ▽ IGM PHASE 1
- ▽ IGM PHASE 2 (EMR)
- ▽ TERMINAL GUIDANCE
- ▽ S-IVB G.C.S.
- ▽ ORBIT INSERTION

ACTUAL ———
 PREDICTED - - - - -

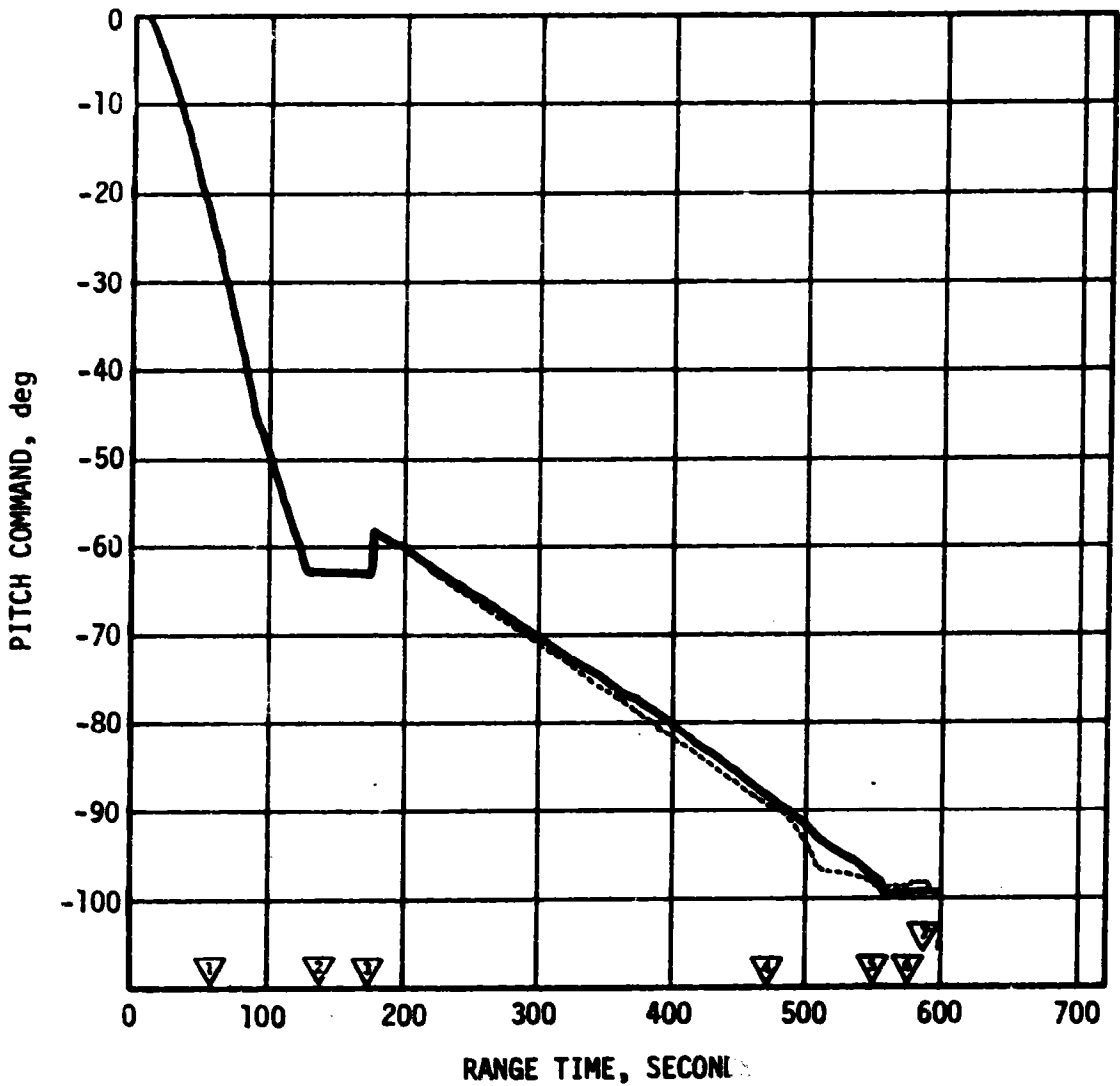


Figure 9-3. Pitch Command During Boost

- ▽ MACH 1
- ▽ S-IB OECO
- ▽ IGM PHASE 1
- ▽ IGM PHASE 2 (EMR)
- ▽ TERMINAL GUIDANCE
- ▽ S-IVB G.C.S.
- ▽ ORBIT INSERTION

ACTUAL ———
 PREDICTED - - - -

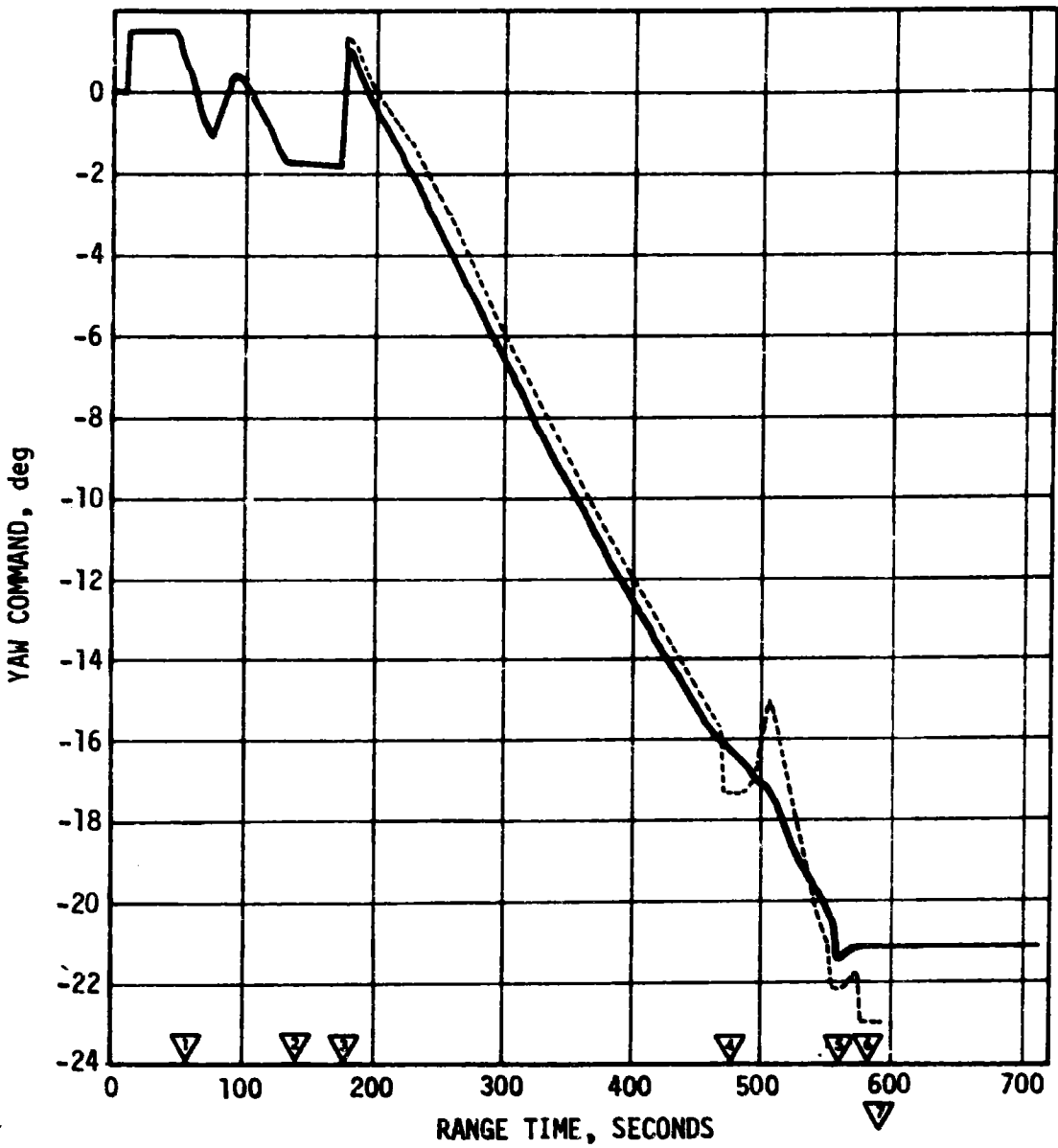


Figure 9-4. Yaw Command During Boost

Table 9-4. SA-208 Orbital Phase Flight Program Attitude Commands

EVENT	COMMANDED ATTITUDE (DEGREES)		
	ROLL	PITCH	YAW
Time Base 4	-0.8845	-98.2562	-22.9799
Time Base 4 + 20 sec. (Local Reference, implemented at TB 4 +21.089 sec)	0.0000	-108.8101	-9.0453

9.3.4 Deorbit Phase

The ground command to initiate the S-IVB/IU deorbit sequence was issued at T4 +15,320.1 seconds. The deorbit parameters commanded were as follows:

Start Timebase 5 at T4 +18,060 seconds (LOX dump initiated at T5 +34 seconds)

Start sequence for stop LOX dump, start LH₂ dump at T5 +508.5 seconds.

Start sequence for stop LH₂ dump, safe vehicle at T5 +624.5 seconds.

These sequences were implemented within the specified tolerances and resulted in deorbit of the S-IVB/IU as planned (see Section 5).

9.4 GUIDANCE AND NAVIGATION SYSTEM COMPONENTS

The guidance and navigation hardware satisfactorily supported the accomplishment of mission objectives.

9.4.1 ST-124M Stabilized Platform System

The three gyro servo loops responded properly to all vehicle motions. The pickoff deflections remained below 0.1 degree peak throughout the mission except possibly at CSM separation. Deflection amplitudes at CSM separation are uncertain due to a momentary loss of synchronization of the telemetry link.

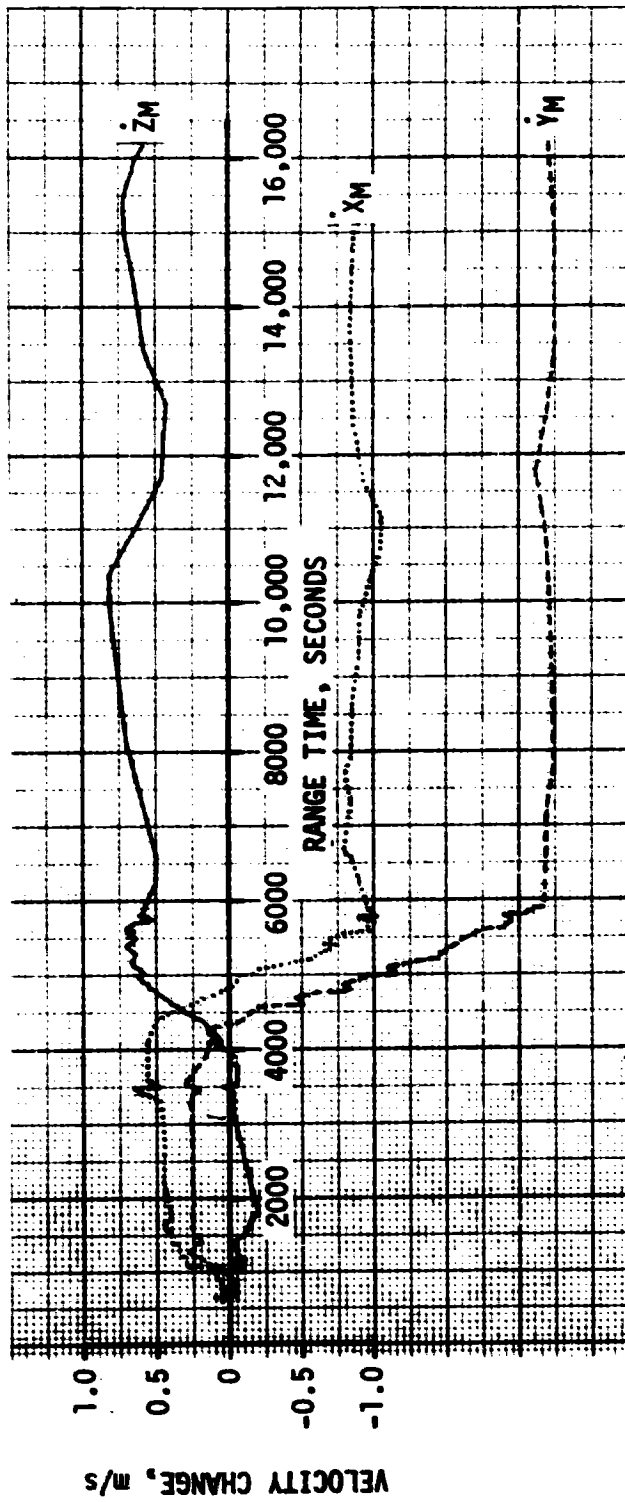


Figure 9-5. SA-208 Inertially-Referenced Velocity Changes in Earth Orbit

The three accelerometer servo loops operated as expected. Maximum deflection probably occurred during Command and Service Module (CSM) separation. As previously mentioned, the telemetry link problem precluded determination of the deflection amplitudes. Some barely discernible pickoff activity was noted during S-IVB LH₂ venting beginning at 3440 seconds and continuing beyond 5867 seconds. The accelerometer encoder outputs reflected this activity as a 30-Hz oscillation with a maximum amplitude of four pulses (0.2 meter/second) peak-to-peak. The phenomena may be due to S-IVB NPV activity.

Deflections at liftoff and during the Mach 1/max Q period were comparable to those of SA-206 and SA-207. They were as follows:

	<u>Z</u>	<u>X</u>	<u>Y</u>
Liftoff	+0.4° -0.4°	+0.6° -0.4°	+0.9° -0.7°
Mach 1/max Q	+1.5° -1.7°	+0.9° -0.8	+1.3° -0.9°

All platform temperature and pressure values were well within expected limits. ST-124M power supplies functioned satisfactorily as evidenced by voltages monitored during the flight.

9.4.2 Guidance Computer

The LVDC and Launch Vehicle Data Adapter (LVDA) performed satisfactorily. No hardware anomalies were observed during any phase of the SA-208 mission.

SECTION 10
CONTROL AND SEPARATION

10.1 SUMMARY

The control and separation systems functioned correctly throughout the powered and coast flight of SA-208. Engine gimbal deflections were nominal, but Auxiliary Propulsion System (APS) propellant usage was higher than predicted due to degraded module 2 pitch thruster operation and stage disturbances which occurred during a period of oscillatory LH₂ relief venting. Rotary slosh motion was identified as a possible contributor to the stage disturbance during relief venting. Bending and slosh dynamics were adequately stabilized during boost flight. Separation dynamics were normal.

10.2 S-IB CONTROL SYSTEM EVALUATION

Liftoff dynamics from the pedestal were as expected. Tower clearance was adequate. Table 10-1 summarizes liftoff misalignments. Effective roll misalignment of the inboard engines exceeded the predicted 3 σ range, but resulted in a roll error of less than 0.3 degree.

Table 10-1. Liftoff Misalignment Summary

	PREDICTED 3 σ RANGE			LAUNCH		
	PITCH	YAW	ROLL	PITCH	YAW	ROLL
Thrust Misalignment, deg	+0.46	+0.46	+0.19	0.0	0.0	-0.02
Inboard Engine Misalignment, deg	+0.25	+0.25	+0.25	0.0	0.0	+0.30
Vehicle Stacking and Pad Misalignment, deg	+0.39	+0.39	0.0	0.0	0.0	0.0

The SA-208 control system performed as expected during S-IB boost. Jimsphere measurements indicate scalar wind velocities near the 84th percentile levels for November. The wind peak was 43.5 meters per second at 12.35 kilometers altitude from an azimuth of 254 degrees. In the high dynamic pressure region, the maximum total angle of attack of 1.9 degrees occurred predominately in the pitch plane in response to a wind peak. The control system adequately stabilized the vehicle response to all winds.

Maximums of about 14 percent of the available pitch and yaw gimbal angles were used. Both peak deflections were due to wind speed peaks and associated shears. Bending and sloshing dynamics were properly stabilized with neither response exhibiting any divergent trend.

The angle of attack and gimbal angle were well within the allowable response (approximately 50%) for the reduced structural limits uniquely imposed on the SA-208 launch vehicle, see paragraph 8.3.

Time histories of pitch, yaw and roll dynamics and average control deflections are shown in Figures 10-1 through 10-3. The maximums are summarized in Table 10-2. Vehicle dynamics in the region between liftoff and 50 seconds resulted primarily from steering commands. Between 50 and 100 seconds, the vehicle responded normally to the pitch and yaw steering programs and the wind. Dynamics from 100 seconds to S-IB outboard engine cutoff were caused by Inboard Engine Cutoff (IECO), tilt arrest, air-flow separation dynamics, and high altitude winds. Pitch and yaw plane control accelerometers were deactivated at 120 seconds.

The effects of thrust unbalance, offset center of gravity (cg), thrust vector misalignment and control system misalignments resulted in attitude errors which were within predicted envelopes. The effective thrust vector misalignments were negligible in both pitch and yaw. Only roll plane thrust misalignments could be detected during first stage burn and they averaged -0.02 degree for all eight engines, 0.30 degree for the four inboard engines and -0.13 degree for the four outboard engines, see Table 10-1.

The peak angles of attack in the high dynamic pressure region were small, -1.8 degrees in pitch and -1.2 degrees in yaw, and did not occur simultaneously. Time histories of the free-stream angles of attack are presented in Figure 10-4. The peak average engine deflections required to trim out the aerodynamic moments in this region were -1.08 degrees in pitch and -1.09 degrees in yaw. The peak engine deflection for roll control occurred just prior to this region and was 0.28 degrees.

10.3 S-IVB CONTROL SYSTEM EVALUATION

The S-IVB thrust vector control system provided satisfactory pitch and yaw control during boost and during the deorbit propellant dumps. The

- ▽ BEGIN PITCH/ROLL MANEUVER
- ▽ BEGIN ACCELEROMETER CONTROL
- ▽ END ROLL MANEUVER
- ▽ MACH 1
- ▽ MAX q
- ▽ 1ST GAIN SWITCH
- ▽ END ACCELEROMETER CONTROL
- ▽ 2ND GAIN SWITCH
- ▽ TILT ARREST
- ▽ INBOARD ENGINE CUTOFF
- ▽ OUTBOARD ENGINE CUTOFF
- ▽ STAGING

————— MEASURED - - - - - SIMULATED

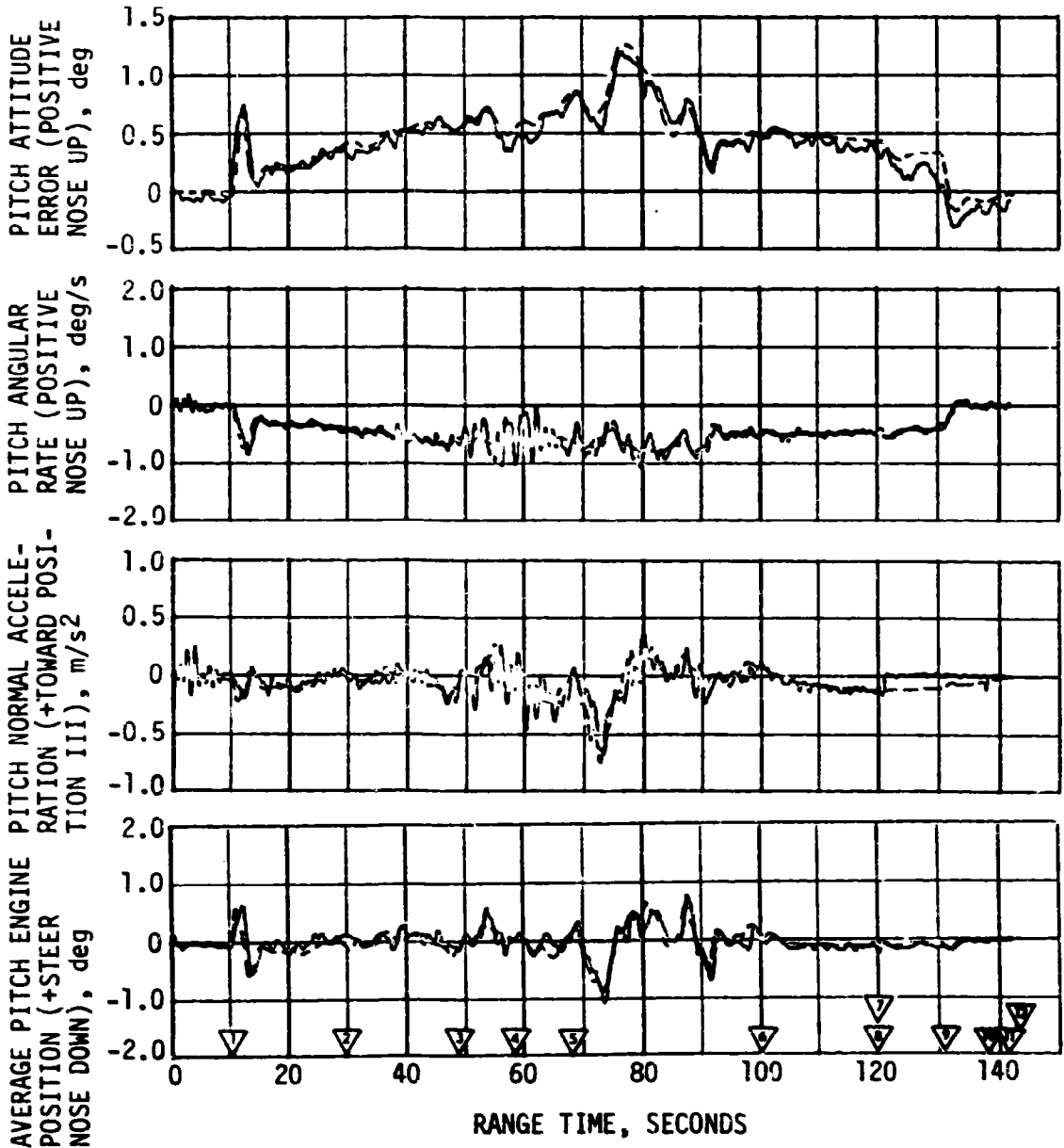


Figure 10-1. Pitch Plane Dynamics During S-IB Burn

- ▽ BEGIN PITCH/ROLL MANEUVER
- ▽ BEGIN ACCELEROMETER CONTROL
- ▽ END ROLL MANEUVER
- ▽ MACH 1
- ▽ MAX q
- ▽ 1ST GAIN SWITCH
- ▽ END ACCELEROMETER CONTROL
- ▽ 2ND GAIN SWITCH
- ▽ TILT ARREST
- ▽ INBOARD ENGINE CUTOFF
- ▽ OUTBOARD ENGINE CUTOFF
- ▽ STAGING

—— MEASURED - - - - SIMULATED

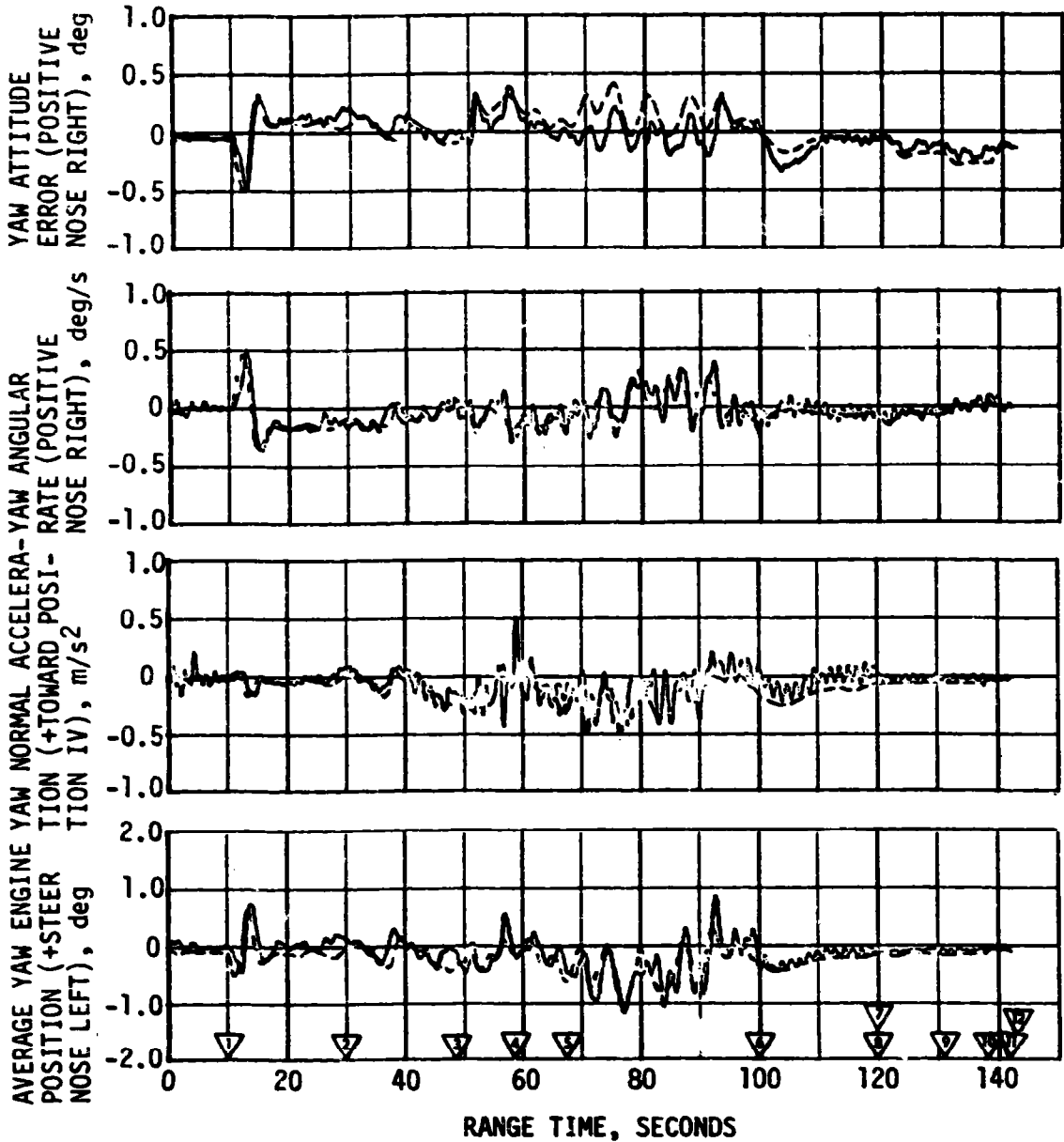


Figure 10-2. Yaw Plane Dynamics During S-IB Burn

REPRODUCIBILITY OF THE
ORIGINAL PAGE IS POOR

- | | |
|-------------------------------|-----------------------------|
| ▽ BEGIN PITCH/ROLL MANEUVER | ▽ END ACCELEROMETER CONTROL |
| ▽ BEGIN ACCELEROMETER CONTROL | ▽ 2ND GAIN SWITCH |
| ▽ END ROLL MANEUVER | ▽ TILT ARREST |
| ▽ MACH 1 | ▽ INBOARD ENGINE CUTOFF |
| ▽ MAX q | ▽ OUTBOARD ENGINE CUTOFF |
| ▽ 1ST GAIN SWITCH | ▽ STAGING |
- MEASURED - - - - SIMULATED

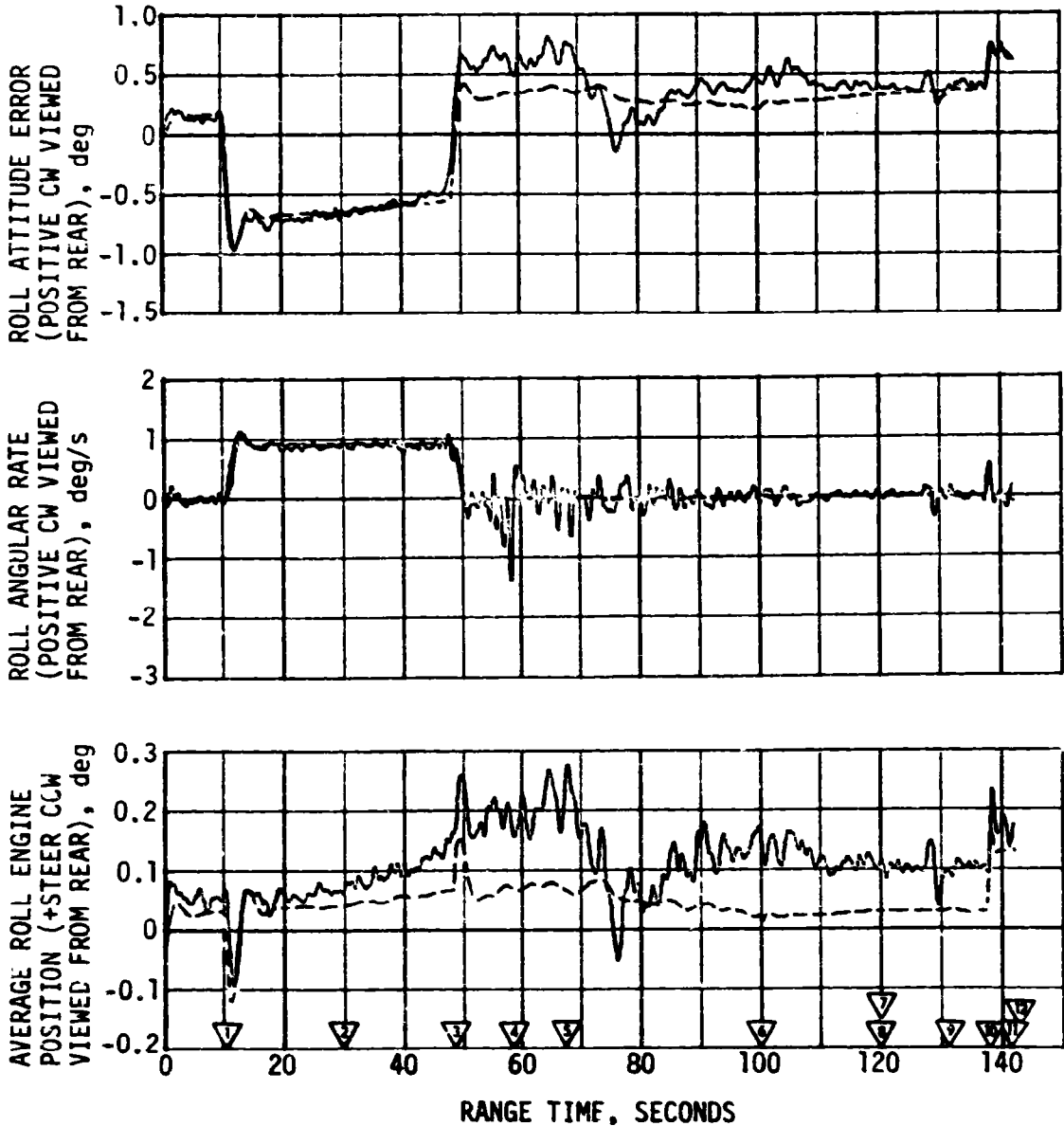


Figure 10-3. Roll Plane Dynamics During S-1B Burn

Table 10-2. Maximum Control Variables During S-IB Burn

VARIABLES	PITCH PLANE		YAW PLANE		ROLL PLANE	
	AMPLITUDE	RANGE TIME (SEC)	AMPLITUDE	RANGE TIME (SEC)	AMPLITUDE	RANGE TIME (SEC)
Attitude Error, deg	1.20	76.7	-0.49	12.4	-0.94	12.4
Angular Rate, deg/s	-1.07	79.7	0.48	13.0	1.09	47.8
Average Gimbal Angle, deg	-1.08	73.5	-1.09	77.5	0.28	67.8
Angle of Attack*, deg	-1.80	72.7	-1.20	76.7	--	--
Angle of Attack Dynamic Pressure Product*, deg-N/cm ² (deg-lbf/ft ²)	-5.73 (-1200)	72.6	-3.83 (-800)	76.7	--	--
Normal Acceleration, m/s ² (ft/s ²)	-0.65 (-2.1)	73.0	0.52 (1.7)	58.9	--	--

NOTE: All data biases and high frequency content removed.

* Simulation results.

REPRODUCIBILITY OF THE
ORIGINAL PAGE IS POOR

- | | | | |
|---|-----------------------------|----|---------------------------|
| 1 | BEGIN PITCH/ROLL MANEUVER | 7 | END ACCELEROMETER CONTROL |
| 2 | BEGIN ACCELEROMETER CONTROL | 8 | 2ND GAIN SWITCH |
| 3 | END ROLL MANEUVER | 9 | TILT ARREST |
| 4 | MACH 1 | 10 | INBOARD ENGINE CUTOFF |
| 5 | MAX q | 11 | OUTBOARD ENGINE CUTOFF |
| 6 | 1ST GAIN SWITCH | 12 | STAGING |
- SIMULATED

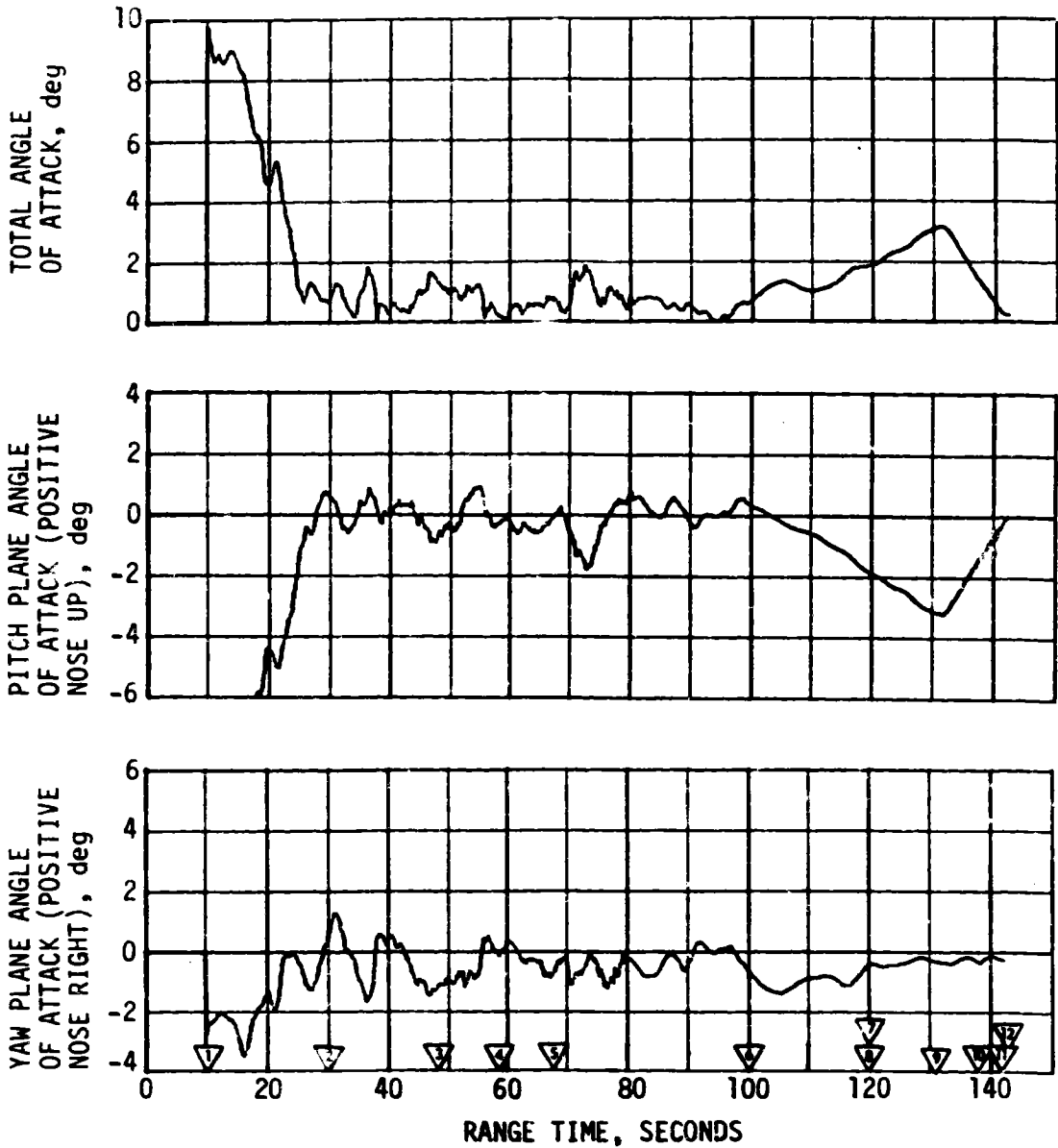


Figure 10-4. Pitch and Yaw Plane Free Stream Angle of Attack During S-IB Burn

APS provided satisfactory roll control while the vehicle was under thrust vector control. The APS also provided satisfactory pitch, yaw, and roll control during orbital coast. APS propellant usage was larger than predicted due to degraded module 2 pitch thruster operation and stage disturbances which occurred during a period of oscillatory LH₂ Non-Propulsive relief venting.

10.3.1 S-IVB Control System Evaluation During Burn

During S-IVB burn, control system transients were experienced at S-IB/S-IVB separation, guidance initiation, Engine Mixture Ratio (MR) shift, terminal guidance mode (chi tilde), and S-IVB Engine Cutoff (ECO). These transients were expected and were well within the capabilities of the control system.

The S-IVB burn pitch attitude error, angular rate, and actuator position are presented in Figure 10-5. The yaw plane burn dynamics are presented in Figure 10-6. The maximum attitude error and rate occurs in the pitch axis at Iterative Guidance Mode (IGM) initiation. A summary of the maximum values of critical flight control parameters is presented in Table 10-3.

The pitch and yaw effective thrust vector misalignments during the first part of burn (prior to MR shift) were +0.45 and -0.28 degree, respectively. Following the MR shift, the misalignments were +0.37 and -0.17 degree for pitch and yaw, respectively. A steady state roll torque prior to MR shift of 32.8 N-m (24.2 lbf-ft) counterclockwise looking forward required roll APS firings. The steady state roll torque following MR shift was 25.2 N-m (18.6 lbf-ft) counterclockwise looking forward and required roll APS firings. The steady state roll torque experienced on previous flights has ranged between 61.4 N-m (45.3 lbf-ft) counterclockwise and 54.2 N-m (40.0 lbf-ft) clockwise.

Propellant sloshing during burn was observed on data obtained from the Propellant Utilization (PU) mass sensors and on the pitch and yaw actuator position and actuator valve current data. The propellant slosh had a negligible effect on the operation of the attitude control system.

10.3.2 S-IVB Control System Evaluation During Orbit

The APS provided satisfactory orientation and stabilization during orbit. Data received following the deorbit propellant dumps and prior to re-entry indicated that the vehicle was stabilized. Higher than predicted APS propellant usage resulted from degraded module 2 pitch thruster operation (refer to Section 7.8 for discussion) and due to a stage disturbance which started with LH₂ relief venting and stopped at the end of venting.

- ▽ S-IVB BURN MODE ON "B"
- ▽ GUIDANCE INITIATION
- ▽ MIXTURE RATIO SHIFT
- ▽ TERMINAL GUIDANCE
- ▽ CHI FREEZE
- ▽ S-IVB ENGINE CUTOFF

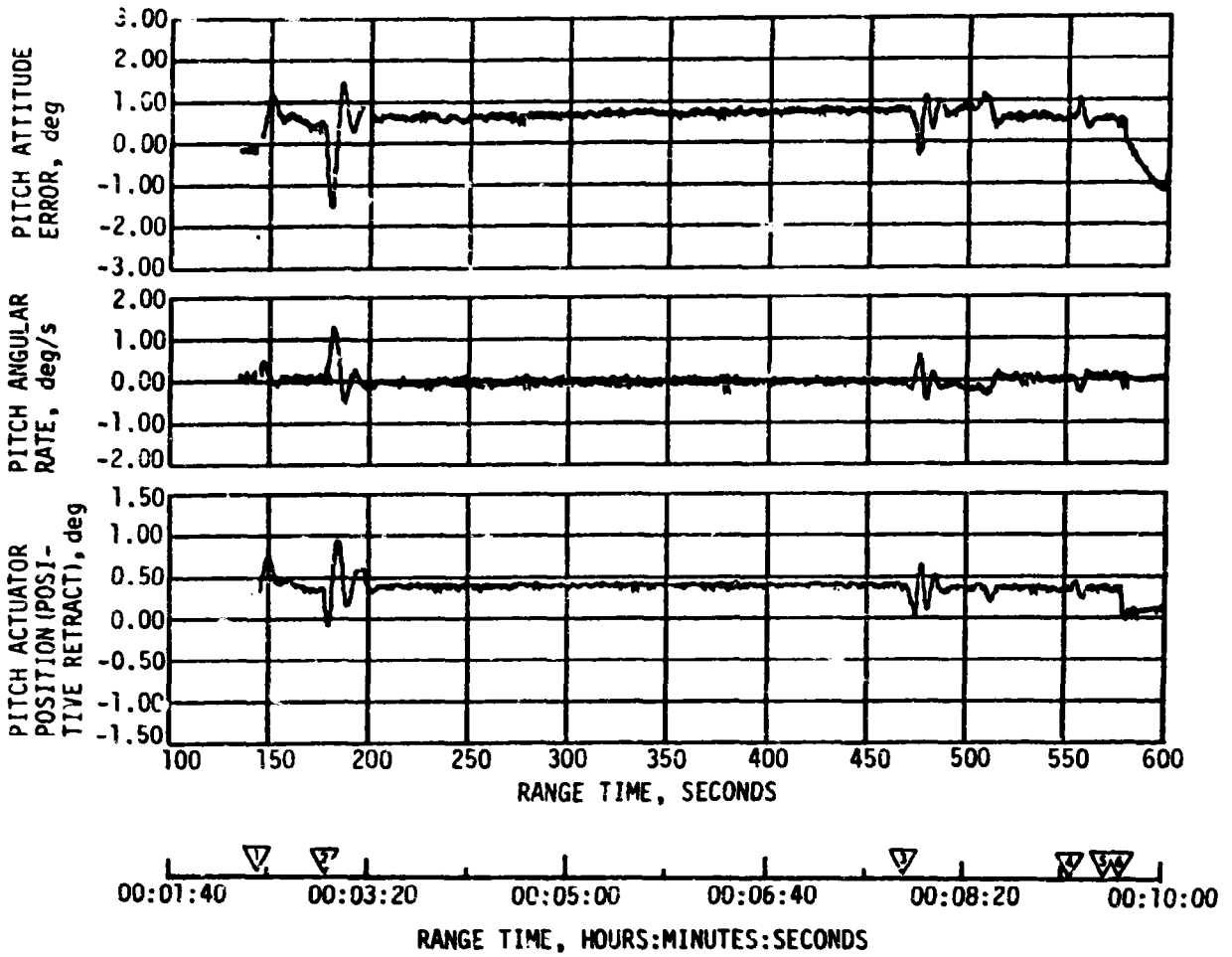


Figure 10-5. Pitch Plane Dynamics - S-IVB Burn

- ▽ S-IVB BURN MODE ON "B"
- ▽ GUIDANCE INITIATION
- ▽ MIXTURE RATIO SHIFT
- ▽ TERMINAL GUIDANCE
- ▽ CHI FREEZE
- ▽ S-IVB ENGINE CUTOFF

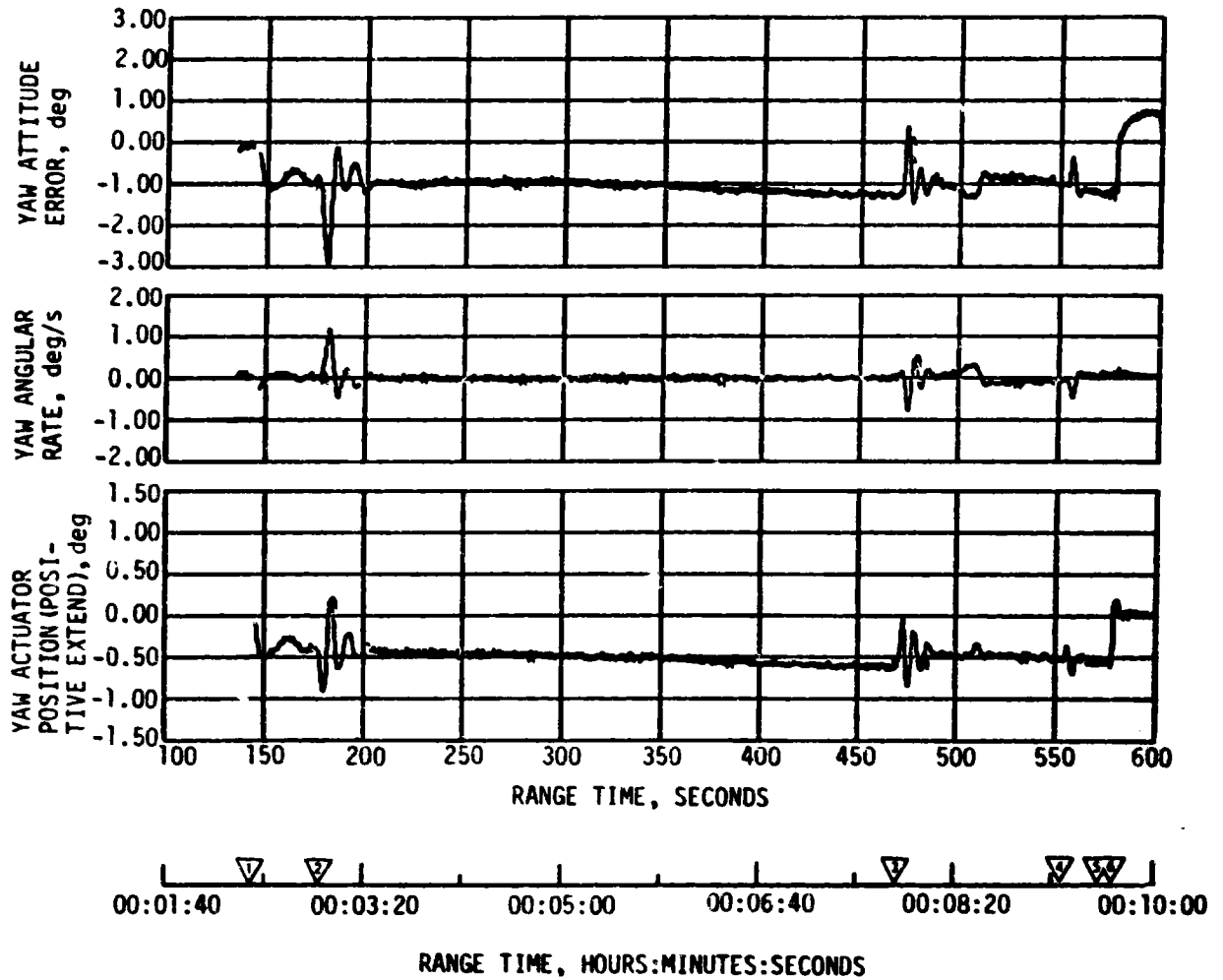


Figure 10-6. Yaw Plane Dynamics - S-IVB Burn

Table 10-3. Maximum Control Variables During S-IVB First Burn

VARIABLES	PITCH PLANE		YAW PLANE		ROLL RATE	
	AMPLITUDE	RANGE TIME (SEC)	AMPLITUDE	RANGE TIME (SEC)	AMPLITUDE	RANGE TIME (SEC)
Attitude Error ^a , deg	-1.6	130.5	-2.9	180.0	-1.4	508.5
Angular Rate, deg/s	1.2	181.5	1.2	182.0	0.3	185.5
Maximum Gimbal Angle, deg	1.0	185.0	-0.95	180.0	--	--
*Biases removed						

Significant events related to orbital coast attitude control were the maneuver to the in-plane local horizontal following S-IVB cutoff, spacecraft separation, and the maneuver to in-plane retrograde local horizontal. The pitch attitude error and angular rate for events during which on-board data were available are shown in Figure 10-7.

Following S-IVB cutoff and switching to the orbital coast control mode, the vehicle was maneuvered to the in-plane posigrade local horizontal (Position plane I down), and the orbital pitch rate was established. This maneuver began at 598 seconds (00:09:58) and consisted of approximately -13 degrees in pitch, 14 degrees in yaw, 0.9 degree in roll.

Spacecraft separation, which occurred at approximately 1080 seconds (00:18:00), produced vehicle disturbances similar to SA-206 and SA-207. See Section 10.5.2 for a discussion of vehicle motion during Command and Service Module (CSM) separation.

At 1334 seconds (00:22:14) the maneuver to in-plane retrograde local horizontal was begun. This maneuver consisted of pitching 180 degrees referenced to the local horizontal and rolling -180 degrees. The pitch maneuver was both begun and terminated by the degraded module 2 pitch thruster. Because of the low thrust from the module 2 thruster, additional firings were necessary to acquire the pitch rate in the desired time.

A review of pitch and yaw actuator position data during thermal conditioning periods revealed that the low frequency small amplitude oscillation observed on SA-207 did not occur on SA-208. In addition, the engine position null offset during these cycles was much smaller than observed

▽ INITIATE MANEUVER TO LOCAL HORIZONTAL
 ▽ SPACECRAFT SEPARATION

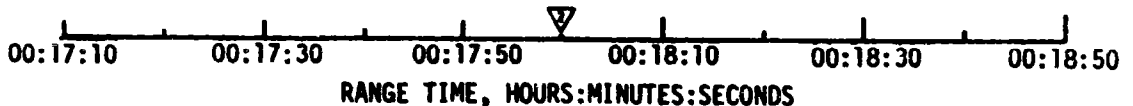
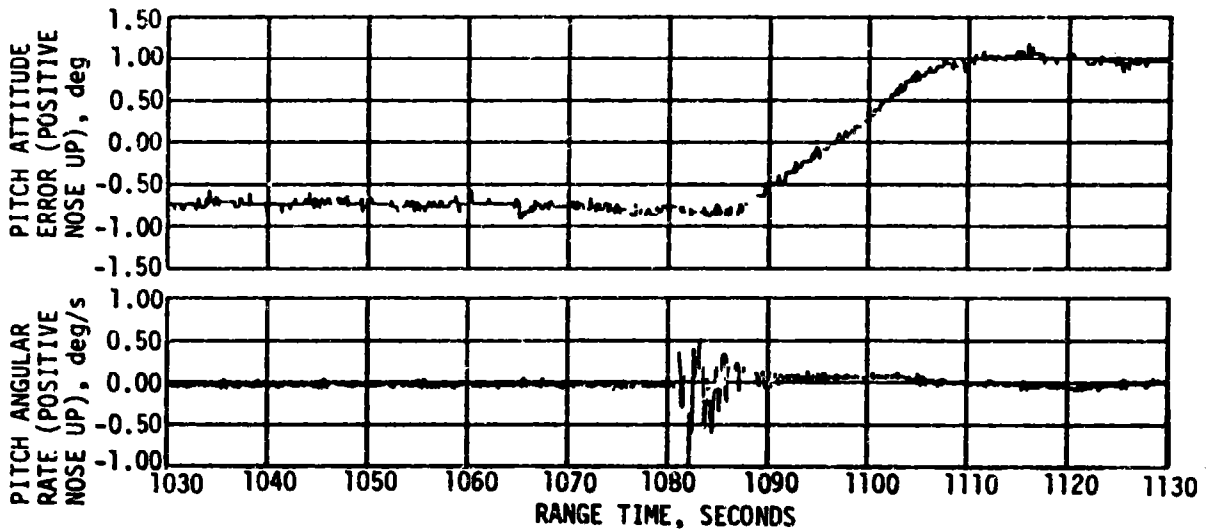
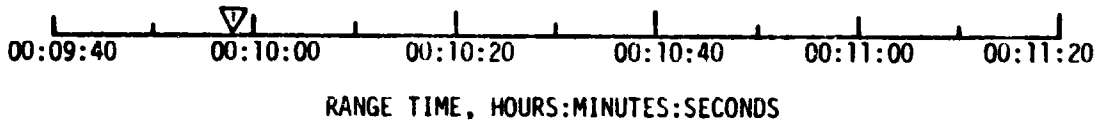
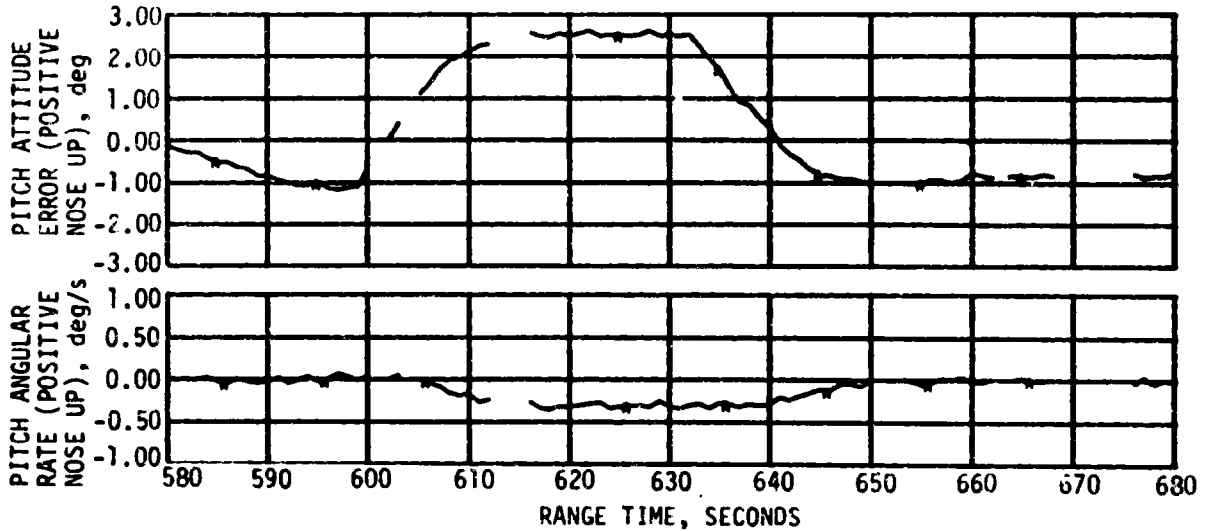


Figure 10-7. Pitch Plane Dynamics During Orbit (Sheet 1 of 2)

▽ INITIATE MANEUVER TO RETROGRADE
 LOCAL HORIZONTAL

TERMINATE MANEUVER TO RETROGRADE
 LOCAL HORIZONTAL (≈1820 SECONDS)

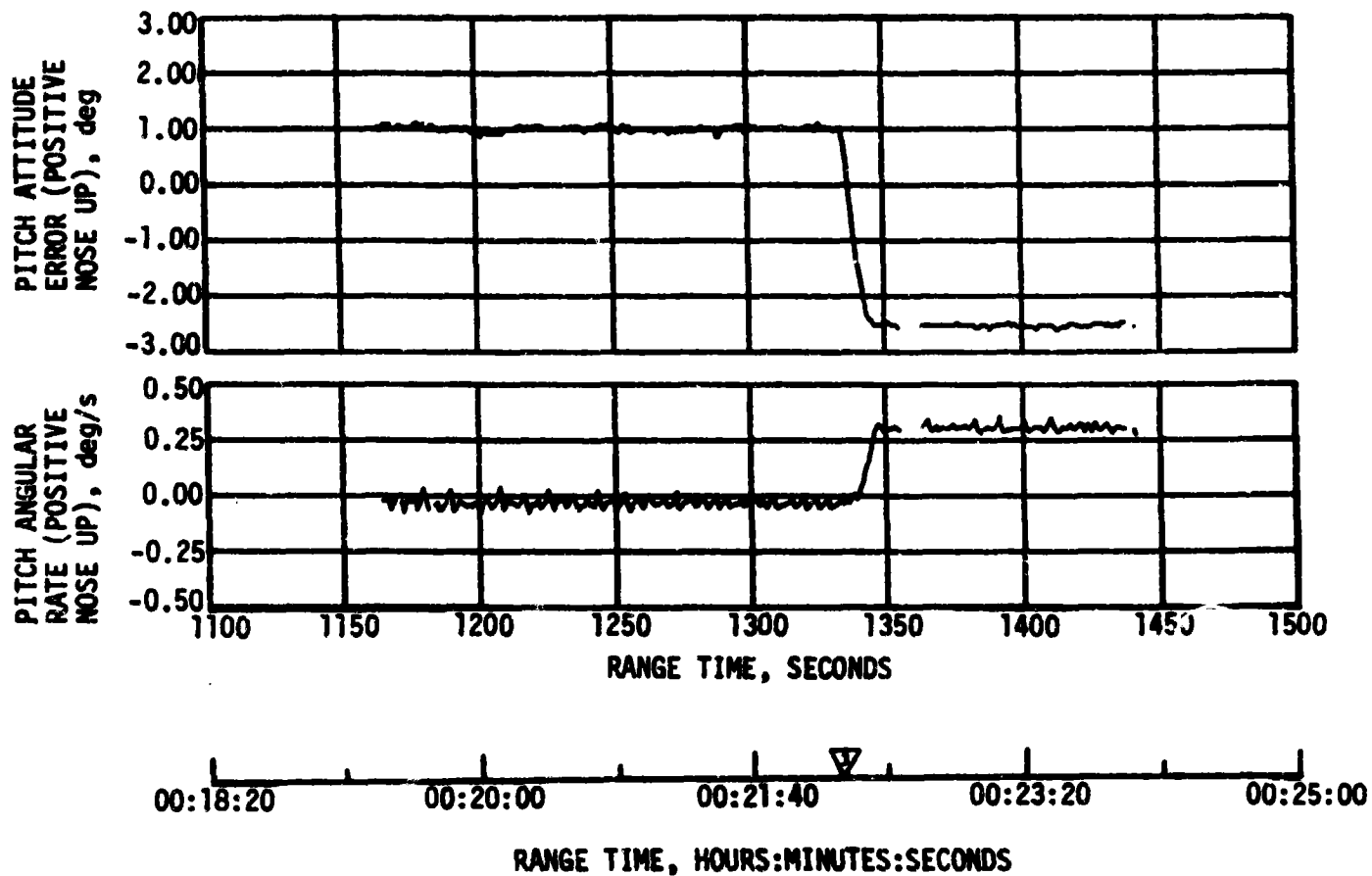


Figure 10-7. Pitch Plane Dynamics During Orbit (Sheet 2 of 2)

on SA-207. Pitch and yaw actuator position null offset on SA-208 was $+0.2^\circ$ in pitch and 0.0° in yaw, while the SA-207 data showed -0.3° in pitch and 0.4° in yaw.

During the period from about 4200 seconds (01:10:00) to 6000 seconds (01:40:00) the APS usage in each module was higher than predicted by approximately 3.8 lbm (800 lbf-sec). During this same time period LH₂ venting was occurring and the Non-Propulsive Vent (NPV) valves were oscillating in a manner similar to that observed on SA-206. A discussion of vent valve oscillation is contained in Section 7.10.1 and Section 7.8 (Figures 7-13 and 7-14) presents the APS usage data.

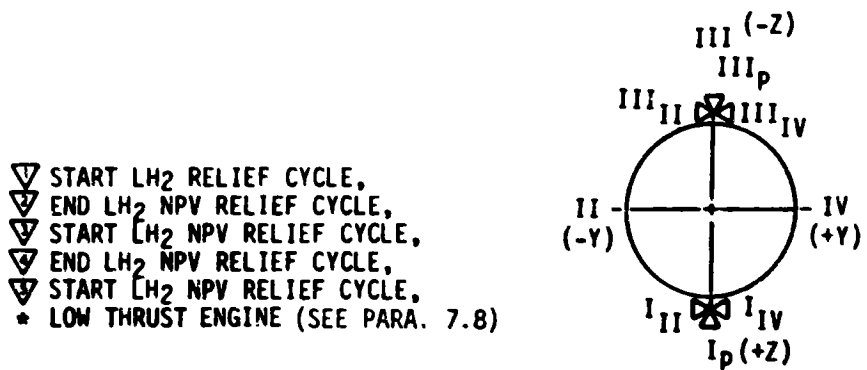
Figure 10-8 shows the attitude errors and APS firings during a period where two LH₂ vent cycles occurred. Disturbance moments in pitch, yaw and roll were seen both during and following the vent "on" periods resulting in a cyclic response with the attitude error and APS firing sequence appearing nearly the same during the two vent cycles shown. It is believed that a vent disturbance is responsible for exciting the observed activity and the increased APS propellant usage. Re-evaluation of SA-206 data shows a similar characteristic was excited on this earlier flight except that the directions were different. This disturbance effect will be included in the APS propellant predictions for SA-209.

Preliminary analyses have shown that a swirling slosh condition, excited by the NPV disturbance and sustained by the APS firings, could have contributed to the observed response. Figure 10-8 shows that the sequence of APS firings follows a rotary pattern. Firings begin in the +Z direction and proceed in a counterclockwise (looking forward) manner around the stage. This sequence would, in turn, result in the propellant swirling in a counterclockwise direction. Computing the net APS roll impulse during the time period of 5524 to 5810 seconds revealed that an average of -1.5 ft-lbs (counterclockwise) of roll disturbance existed during this time. This also correlates with the propellant swirl direction.

Data from the IU stable platform accelerometers have also been correlated with attitude control and S-IVB vent system data to better understand the exact nature of the vent disturbance. The results of this comparison indicate translational as well as rotational disturbances. Although a specific mechanism for producing the observed translational disturbances has not been identified, time correlation substantiates that the oscillatory operation of the NPV relief valve is a contributor to this phenomenon. These translational disturbances did not significantly effect either APS usage or the orbital trajectory.

10.3.3 S-IVB Control System Evaluation During Deorbit

Satisfactory vehicle stability and control characteristics were observed during the deorbit propellant dump. Thrust Vector Control (TVC) was used for pitch and yaw, while the APS was used for roll control. Attitude error and attitude rate data for the pitch, yaw and roll axes, along with pitch and yaw actuator position data and roll APS firing data, are presented in Figure 10-9. These data cover the 475 second LOX dump and the 86 second LH₂ dump periods. The figure also shows the 30 second period between LOX and LH₂ dump, during which time no TVC control is provided.



- ▽ START LH₂ RELIEF CYCLE,
- ▽ END LH₂ NPV RELIEF CYCLE,
- ▽ START LH₂ NPV RELIEF CYCLE,
- ▽ END LH₂ NPV RELIEF CYCLE,
- ▽ START LH₂ NPV RELIEF CYCLE,
- * LOW THRUST ENGINE (SEE PARA. 7.8)

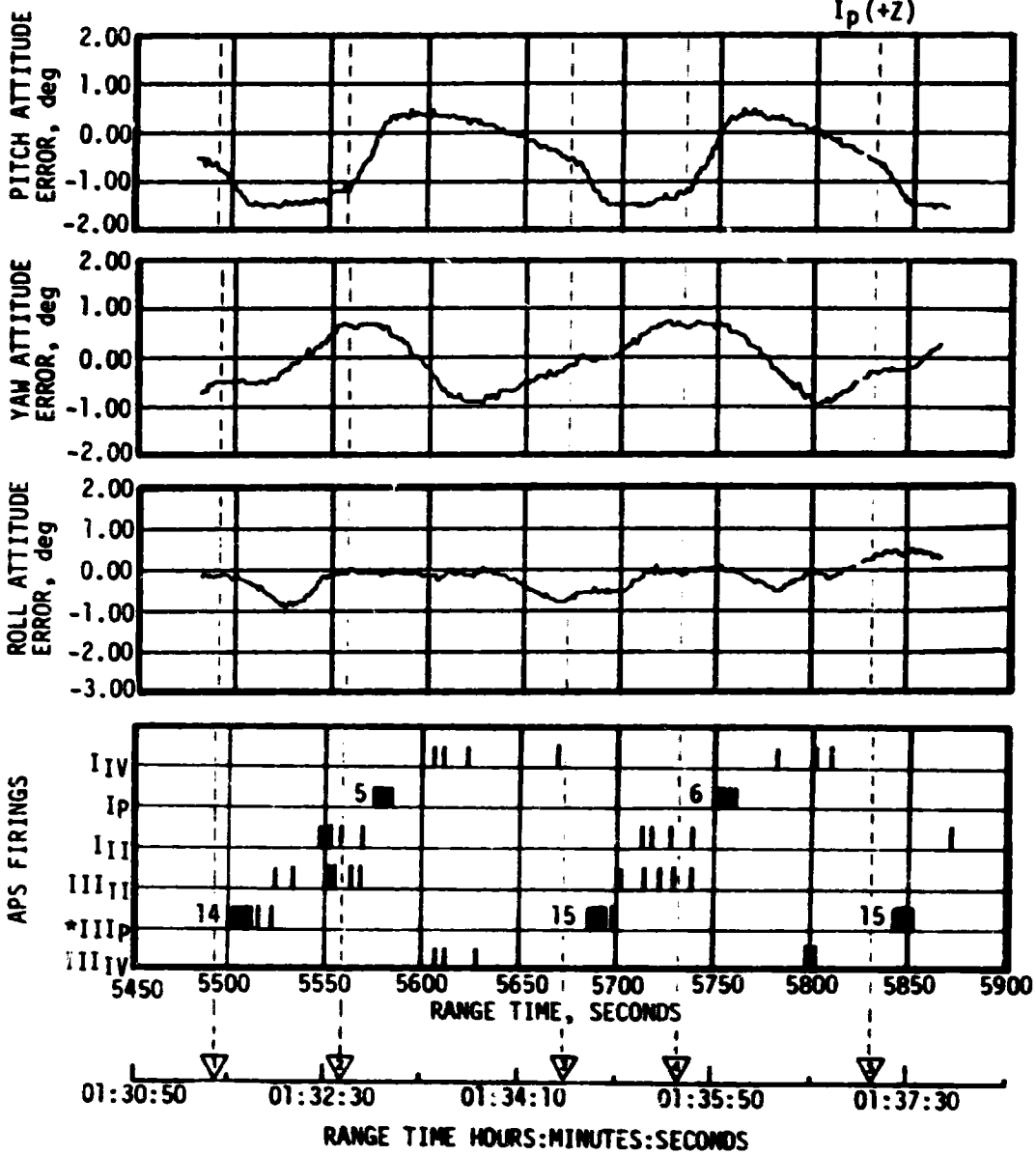


Figure 10-8. SA-208 Vehicle Dynamics During LH₂ NPV Relief Venting

- ▽ START OF TIMEBASE 5
- ▽ START LOX DUMP
- ▽ END LOX DUMP
- ▽ START FUEL DUMP
- ▽ END FUEL DUMP
- ▽ FCC BURN MODE OFF "B"
- * LOW THRUST ENGINE (SEE PARA. 7.8)

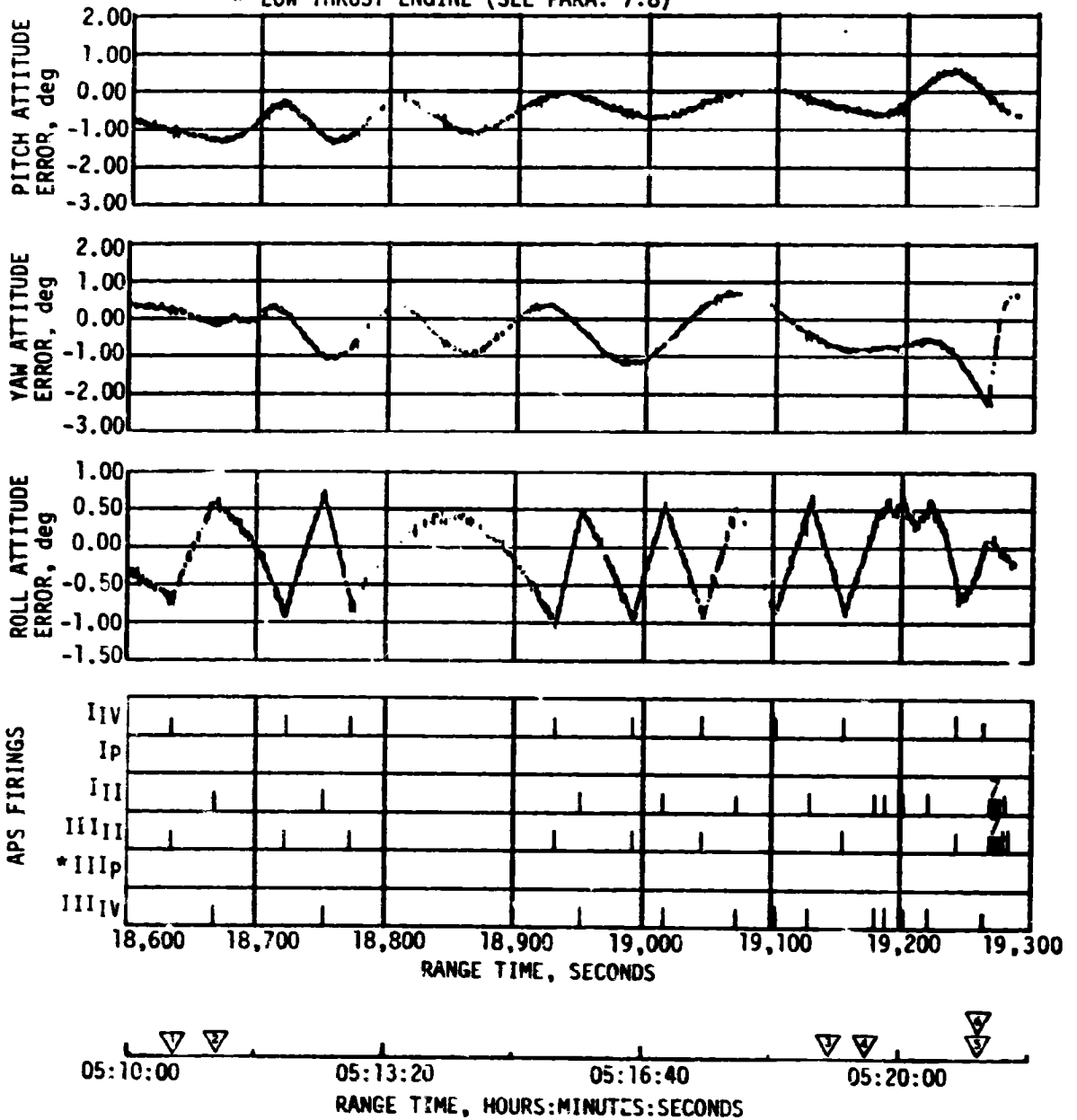


Figure 10-9. Vehicle Dynamics During Deorbit (Sheet 1 of 2)

- ▽ FCC BURN MODE OFF "B"
- ▽ LOX NPV OPEN
- ▽ LH₂ NPV OPEN
- ▽ START ENGINE PNEUMATIC DUMP
- ▽ START COLD HELIUM DUMP
- * LOW THRUST ENGINE (SEE PARA. 7.8)

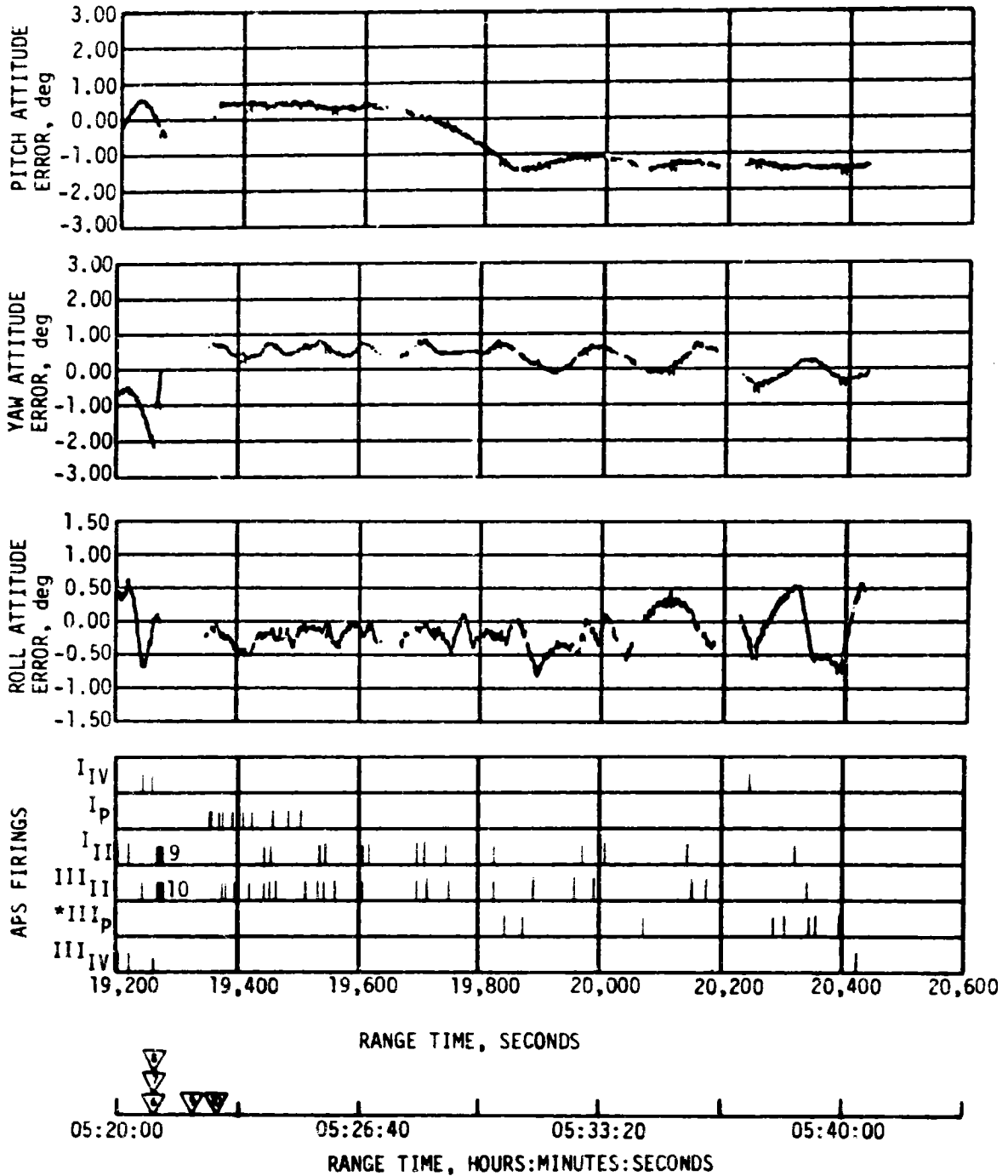


Figure 10-9. Vehicle Dynamics During Deorbit (Sheet 2 of 2)

A comparison of the steady state value of the attitude error data in the figure with predicted maximum values shows that, in general, performance was better than predicted. For example, during the initial 100 seconds of LOX dump the steady state pitch attitude error was predicted to be approximately -3.12 degrees maximum, while the actual is observed to be approximately -0.76 degree. A comparison of the steady state yaw attitude error over the same period shows a similar improvement over the predicted values. The predicted maximum steady state yaw attitude error is approximately -3.94 degrees, while the actual is only -0.38 degree. Both predicted values were based upon known cg offsets and the worst case thrust vector misalignments within the engine.

Analysis of the observed data shows that, in addition to attitude errors due to cg offset and thrust vector misalignment, a small contribution to the total attitude error is the result of an actuator null bias. The SA-208 actuator null bias was only observed on the pitch actuator and contributed 0.14° in pitch actuator position. In general, actuator null bias has been negligible on flights prior to SA-207. For example, SA-206 actuator null bias during deorbit was not measurable and during powered flight amounted to approximately -0.06 degree and 0.07 degree in pitch and yaw actuator position, respectively. On the other hand, the SA-207 average null bias amounted to -0.1 and 0.27 degree in pitch and yaw, respectively, during powered flight and -0.26 and -0.40 degrees during deorbit. Including the actuator null bias in the analysis of the SA-208, the average pitch attitude error during deorbit shows that the observed value of -0.76 degree is composed of (a) -1.12 degrees of attitude error due to known cg offset, (b) -0.28 degree of attitude error due to null bias, and (c) 0.64 degree of attitude error due to the effective thrust vector misalignment. Since no yaw actuator null bias was observed, the average yaw attitude error of -0.38 degree is composed of (a) -1.94 degrees of attitude error due to the known cg offset, and (b) 1.56 degrees of attitude error due to thrust vector misalignment.

Following the end of LOX dump and prior to LH₂ dump initiation there is a 30 second period, during which, there is no thrust for control. On previous flights, residual rates at the start of this "no thrust" period were such that a relatively large increase in vehicle attitude occurred before the start of LH₂ dump. However, SA-208 attitude rates during the dump were significantly smaller than observed on either SA-206 or SA-207 and consequently only a slight variation in attitude occurred during the no thrust period. The smaller attitude rates occurred because the thrust vector misalignment in both pitch and yaw was of the right magnitude and direction to partially nullify the disturbance moment due to cg offset. For example, on SA-207 the thrust vector misalignment in yaw was 0.20 degree while on SA-208 the thrust vector misalignment was 0.78 degree. Yaw engine deflection needed for cg trim was -0.85 degree on SA-207 and -0.97 degree for SA-208. This condition was also reflected in smaller attitude errors on SA-206 and SA-207. Maximum attitude errors reported previously for SA-206 and SA-207 occurred in yaw and were 4.6 degrees and 2.7 degrees, respectively. SA-208 attitude errors were within +1.0

degree for most of the dump with the maximum of -2.1 degrees occurring in yaw at the end of LH₂ dump. The increase in attitude error during the 86 second LH₂ dump is a direct result of a change in the thrust vector misalignment in both magnitude and direction. Variation in the thrust vector misalignments is to be expected due to the different physical properties and states of the propellants being dumped. The transient nature of the thrust vector was also observed in roll APS firing data, indicating that a roll torque existed during the LH₂ dump.

The programmed command for transferring pitch and yaw attitude control from the thrust vector control system to coast attitude control system (S-IVB burn mode off "B") was commanded at approximately 19,262 seconds (05:21:12).

Initial conditions for coast attitude control were as follows:

Pitch Attitude Error	-0.2 deg	Pitch Angular Rate	-0.04 deg/sec
Yaw Attitude Error	-2.2 deg	Yaw Angular Rate	-0.05 deg/sec
Roll Attitude Error	-0.0 deg	Roll Angular Rate	0.05 deg/sec

These attitude errors and angular rates were easily nulled out by the coast attitude control system (see Figure 10-9, sheet 2 of 2). Following termination of the LH₂ dump, the LOX and LH₂ NPV's were opened. NPV disturbances were less than expected during this phase of flight.

10.4 INSTRUMENT UNIT CONTROL COMPONENTS EVALUATION

The IU control subsystem functioned properly throughout the SA-208 mission. All planned maneuvers occurred at or near the anticipated time of flight.

10.5 SEPARATION

10.5.1 S-IB/S-IVB Separation

A detailed reconstruction of the separation dynamics was not possible, since S-IVB data dropped out for approximately 3.0 seconds following separation. The separation analysis was done by comparing SA-205 data with the available SA-208 data. Comparison of S-IB and S-IVB longitudinal acceleration and body rates with SA-205 data showed essentially nominal separation.

Figure 10-10 shows the S-IB/S-IVB longitudinal acceleration, and Figure 10-11 shows pitch, yaw, and roll angular rates during S-IB/S-IVB separation. Vehicle dynamics were nominal and well within staging limits.

10.5.2 S-IVB/CSM Separation

S-IVB/CSM separation was accomplished on SA-208 with the vehicle in the in-plane local horizontal attitude with an orbital pitch rate of approximately -0.068 degree/second. S-IVB disturbances due to spacecraft separation were first observed at 1081.0 seconds (00:18:01) on APS engine firing

10-20

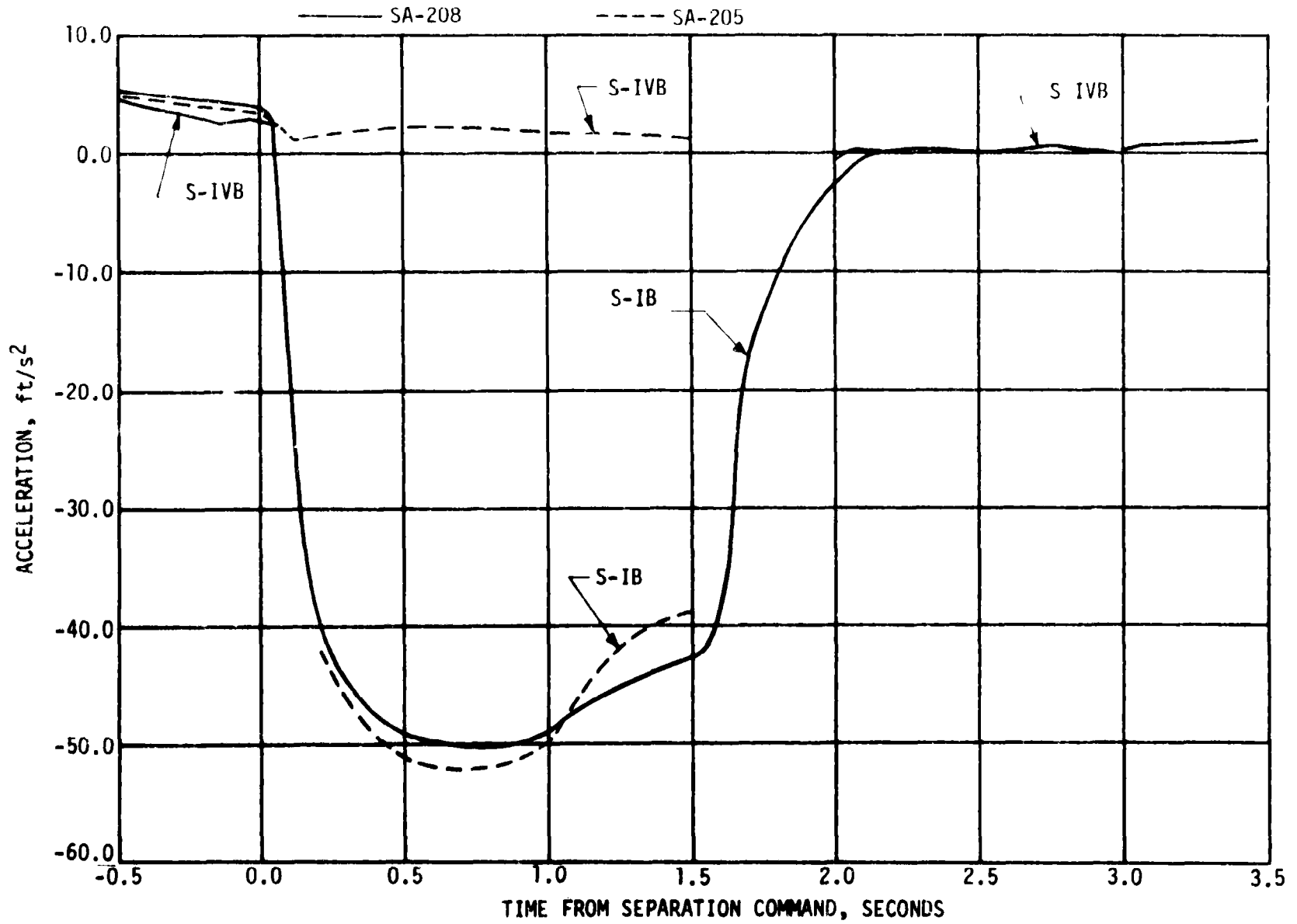


Figure 10-10. S-IB/S-IVB Longitudinal Acceleration

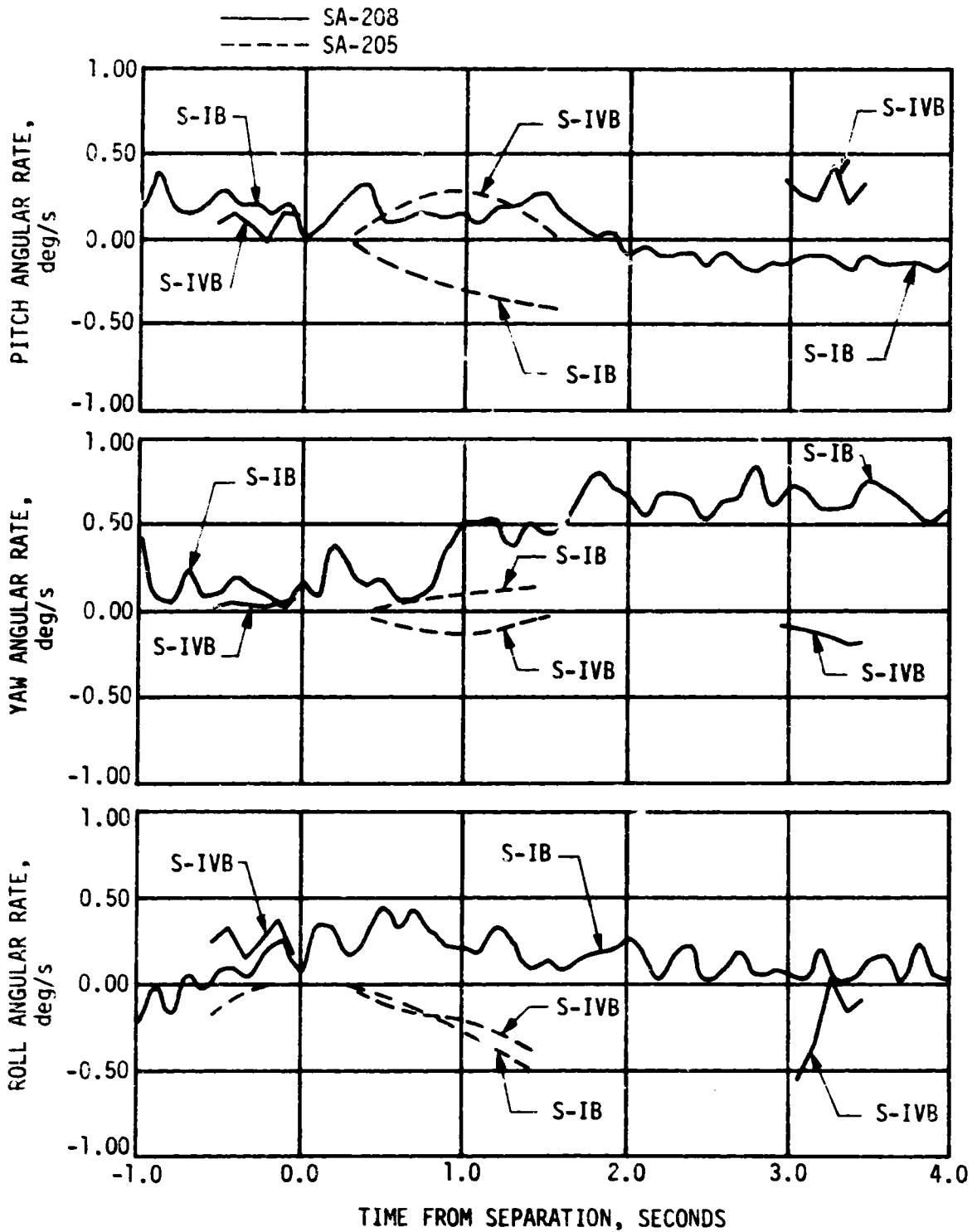


Figure 10-11. Angular Velocities During S-IB/S-IVB Separation

data. However, disturbances may have occurred earlier but gone undetected due to data dropouts during separation. Maximum vehicle rates following separation were 0.08 degree/second pitch, 0.03 degree/second yaw, and 0.15 degree/second roll. Typical and expected firings occurred for approximately 30 seconds following separation in response to separation induced disturbances.

SECTION 11

ELECTRICAL NETWORKS AND EMERGENCY DETECTION SYSTEM

11.1 SUMMARY

The electrical systems and Emergency Detection System (EDS) of the SA-208 launch vehicle performed satisfactorily during the flight. Battery performance (including voltages, currents, and temperatures) was satisfactory and remained within acceptable limits. Operation of all power supplies, inverters, Exploding Bridge Wire (EBW) firing units, and switch selectors were nominal. During the countdown at T minus 75 minutes, an out-of-tolerance indication terminated the Instrument Unit (IU) internal power test by switching power to external. This anomaly is discussed in paragraph 11.4.1.

11.2 S-IB STAGE ELECTRICAL SYSTEM

The S-IB-8 stage electrical system was modified to incorporate two minor changes to the electrical networks. The fire detection system was simplified by substituting a cable for two plug-in type J-boxes used for interconnection of the four groups of temperature sensors, and all 1N2150A diodes in the Propulsion System Distributor were replaced by 1N1204A diodes. The S-IB stage electrical system operated satisfactorily. Battery voltage and current excursions during flight coincided with significant vehicle events as predicted. Voltages for the 1D10 and 1D20 batteries averaged 28.8 V and 28.2 V, respectively, from power transfer to S-IB/S-IVB separation. The current from batteries 1D10 and 1D20 averaged 9.6 amperes and 19.7 amperes, respectively, throughout the boost phase. The most pronounced power drains were caused by the H-1 engines conax valve firings and prevalue operations during S-IB stage engine cutoff. The voltage and current profiles for the batteries are presented in figures 11-1 and 11-2. Battery power consumption was within the rated capacity of each battery, as shown in Table 11-1.

The three master measuring voltage supplies performed satisfactorily and remained within the allowable range of 5.000 ± 0.0125 V.

All switch selector channels functioned as commanded by the IU and were within the required time limits.

The separation and retro motor EBW firing units were armed and triggered as programmed. Charging time and voltage characteristics were within performance limits.

The range safety command system EBW firing units were in a state-of-readiness for vehicle destruct had it been necessary.

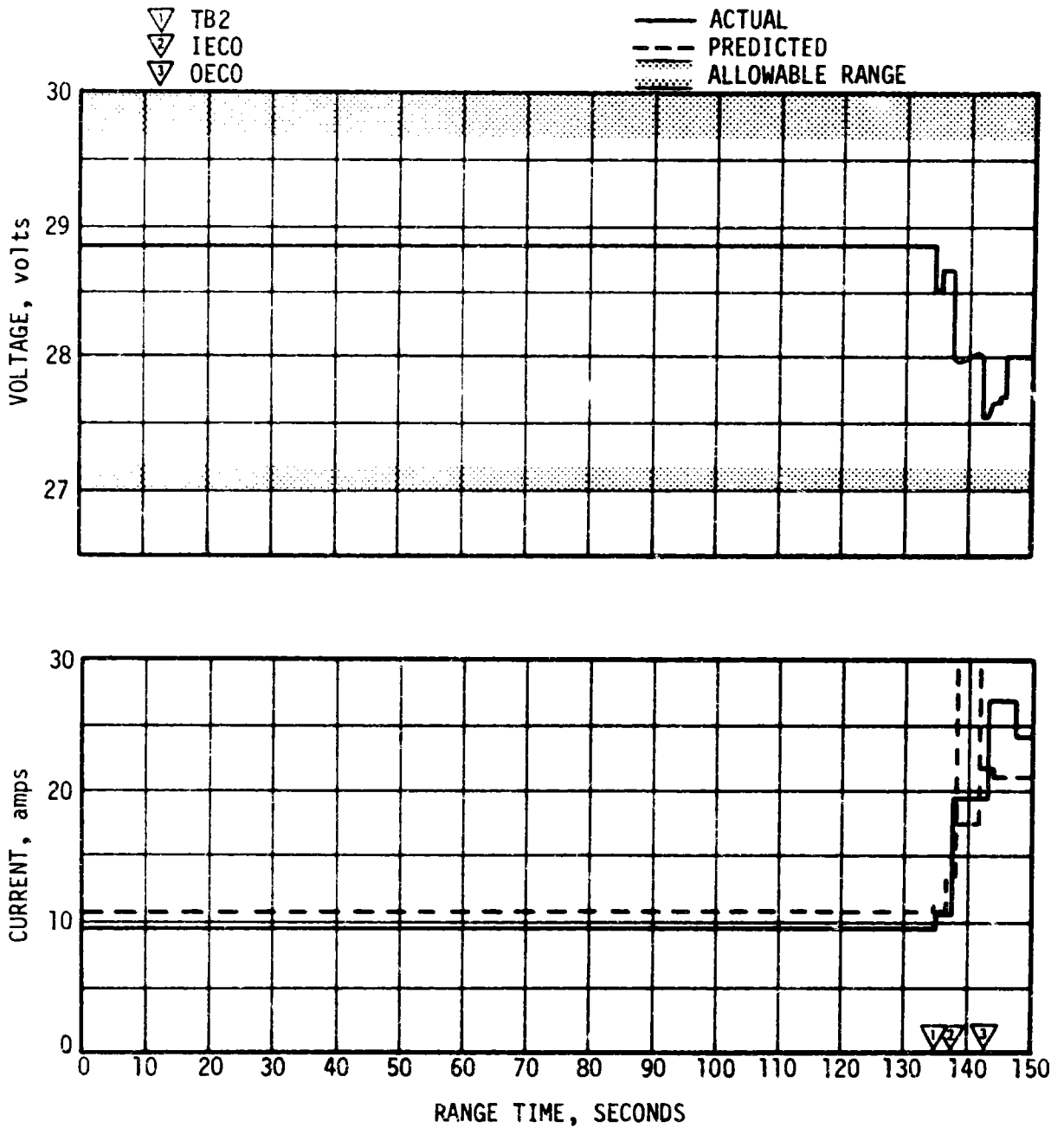


Figure 11-1. S-1B 1D10 Battery Voltage and Current

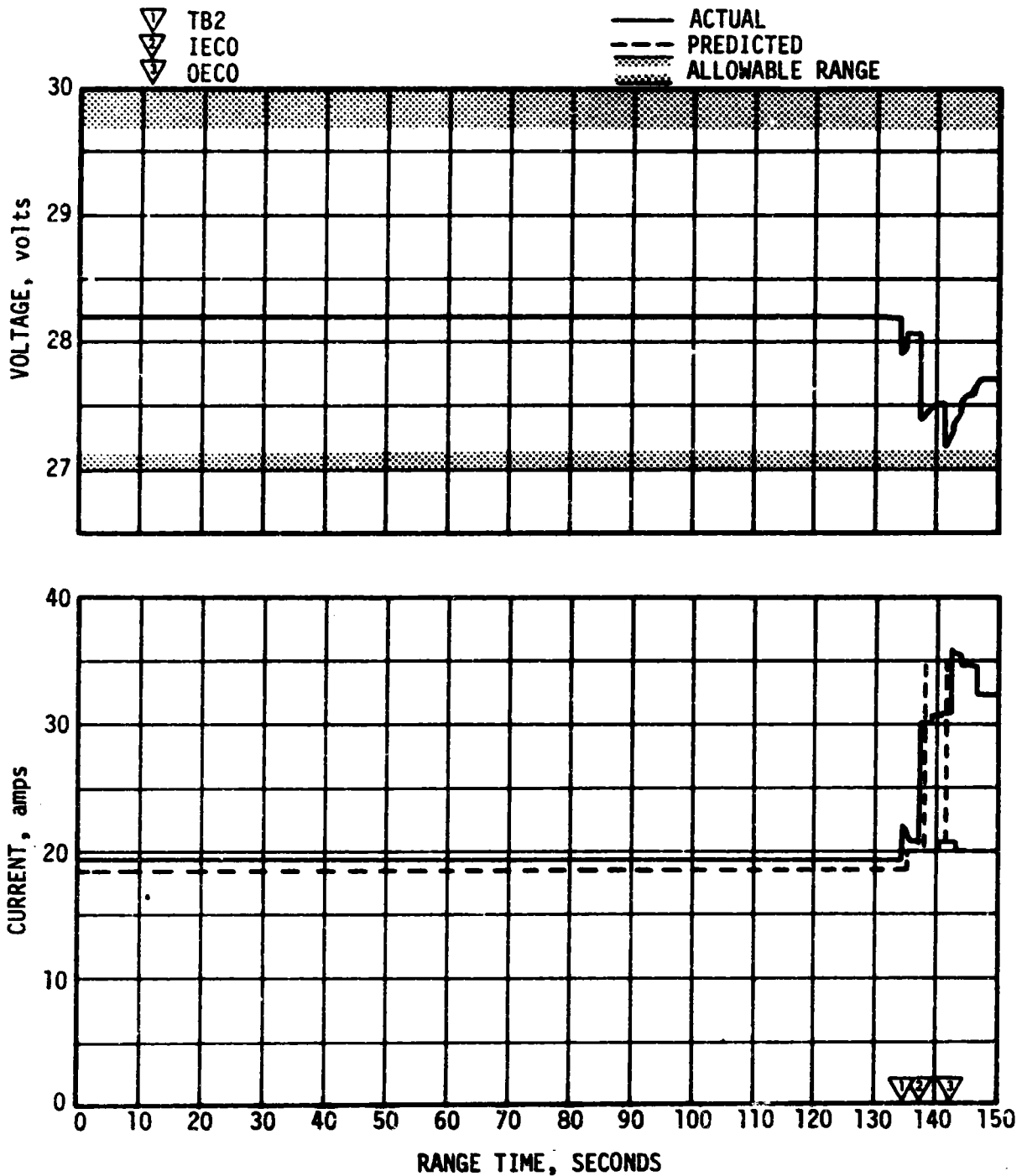


Figure 11-2. S-IB 1D20 Battery Voltage And Current

Table 11-1. S-IB Stage Battery Power Consumption

BATTERY	RATED CAPACITY (amp-hr)	POWER CONSUMPTION*	
		amp-hr	PERCENT OF CAPACITY
1D10	33.3	4.3	12.9
1D20	33.3	5.1	15.3

*Battery Power Consumptions were calculated from activation until end of telemetry (at 397 seconds).

11.3 S-IVB ELECTRICAL SYSTEM

The S-IVB Stage electrical system performed satisfactorily. The battery voltages, currents, and temperatures remained within the normal range.

Battery voltage, current, and temperature plots are shown in Figures 11-3 through 11-6 and battery power consumption and capacity for each battery are shown in Table 11-2. The three 5-VDC and five 20-VDC excitation modules all performed within acceptable limits. The LOX and LH₂ chilldown inverters performed satisfactorily and fulfilled load requirements.

All switch selector channels functioned properly, and all sequencer outputs were issued within required time limits.

Performance of the EBW circuitry for the separation system was satisfactory. Firing unit charge and discharge responses were within predicted time and voltage limits. The command destruct firing units were in the required state of readiness had vehicle destruct been necessary.

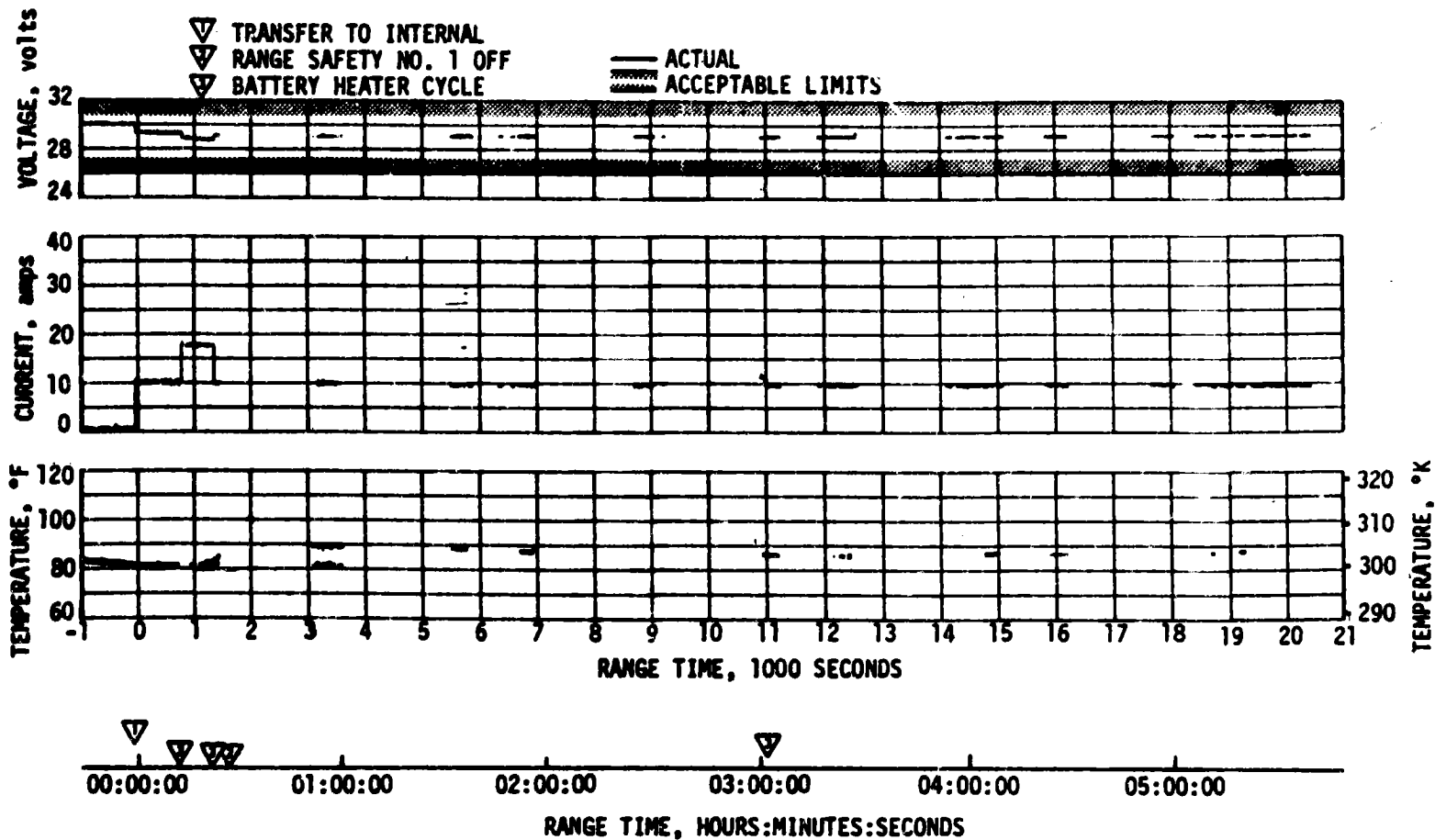


Figure 11-3. S-IVB Stage Forward No. 1 Battery Voltage, Current, and Temperature

REPRODUCIBILITY OF THE ORIGINAL PACE IS POOR

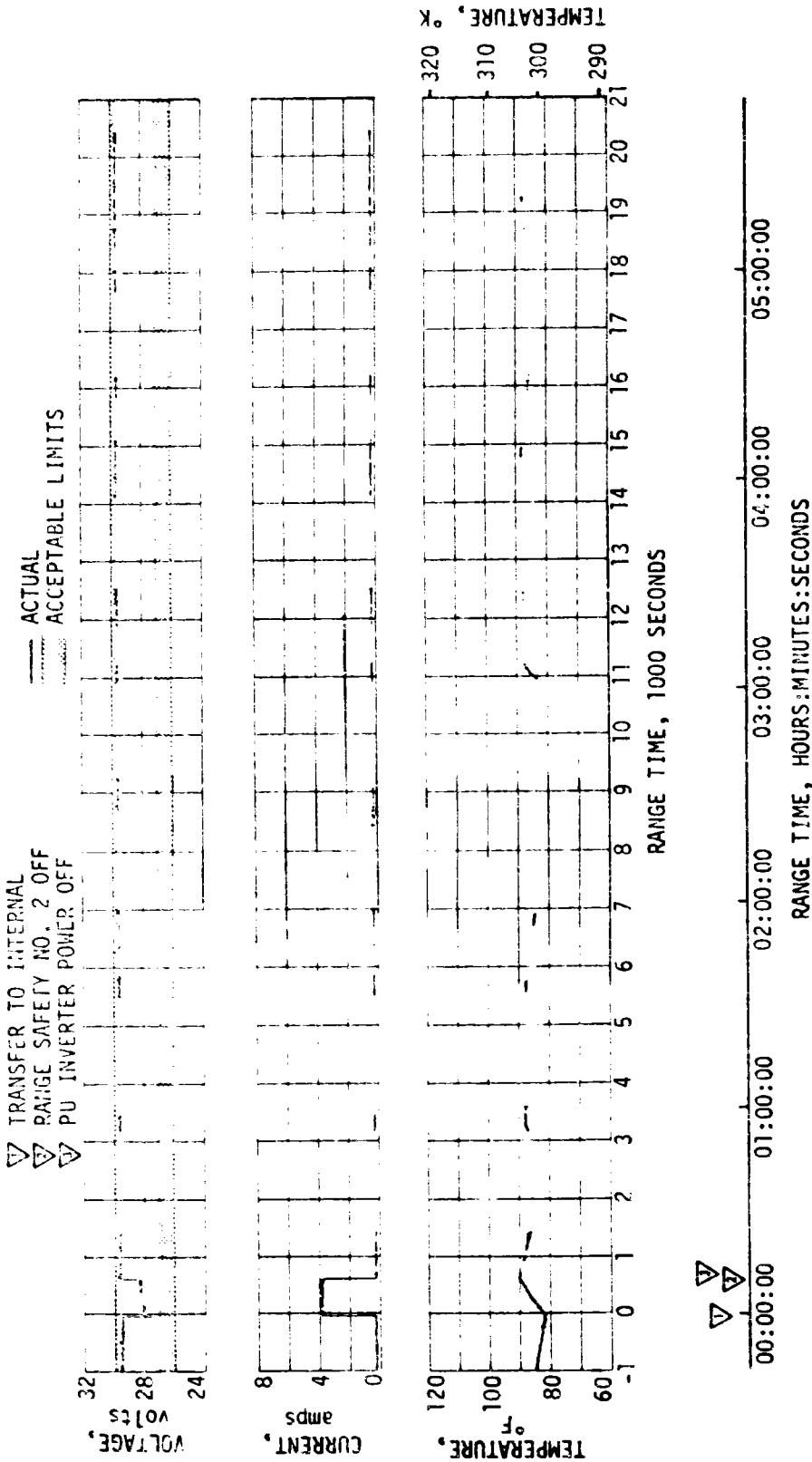


Figure 11-4. S-IVB Stage Forward No. 2 Battery Voltage, Current, and Temperature

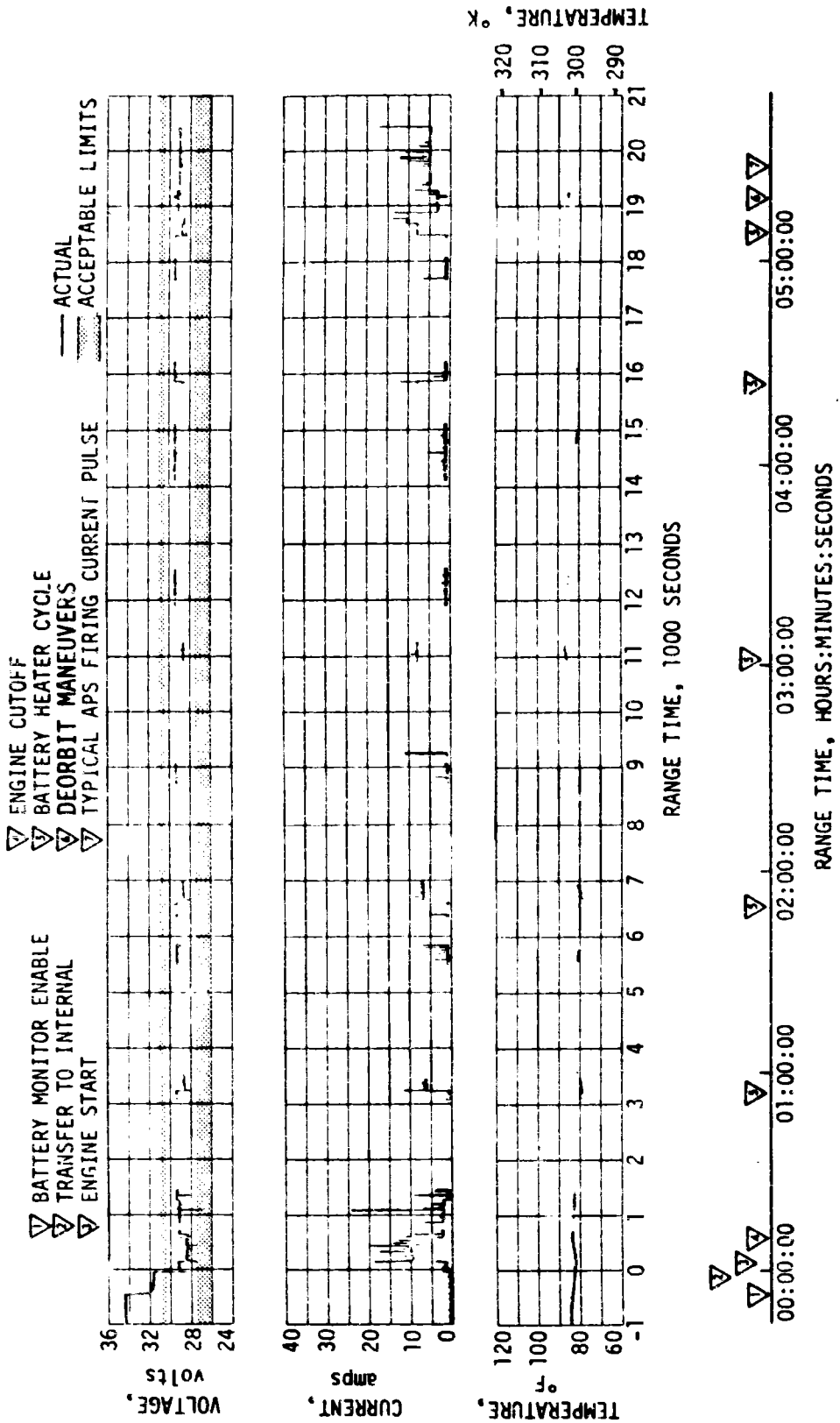


Figure 11-5. S-IVB Stage Aft No. 1 Battery Voltage, Current and Temperature

REPRODUCIBILITY OF THE ORIGINAL PAGE IS POOR

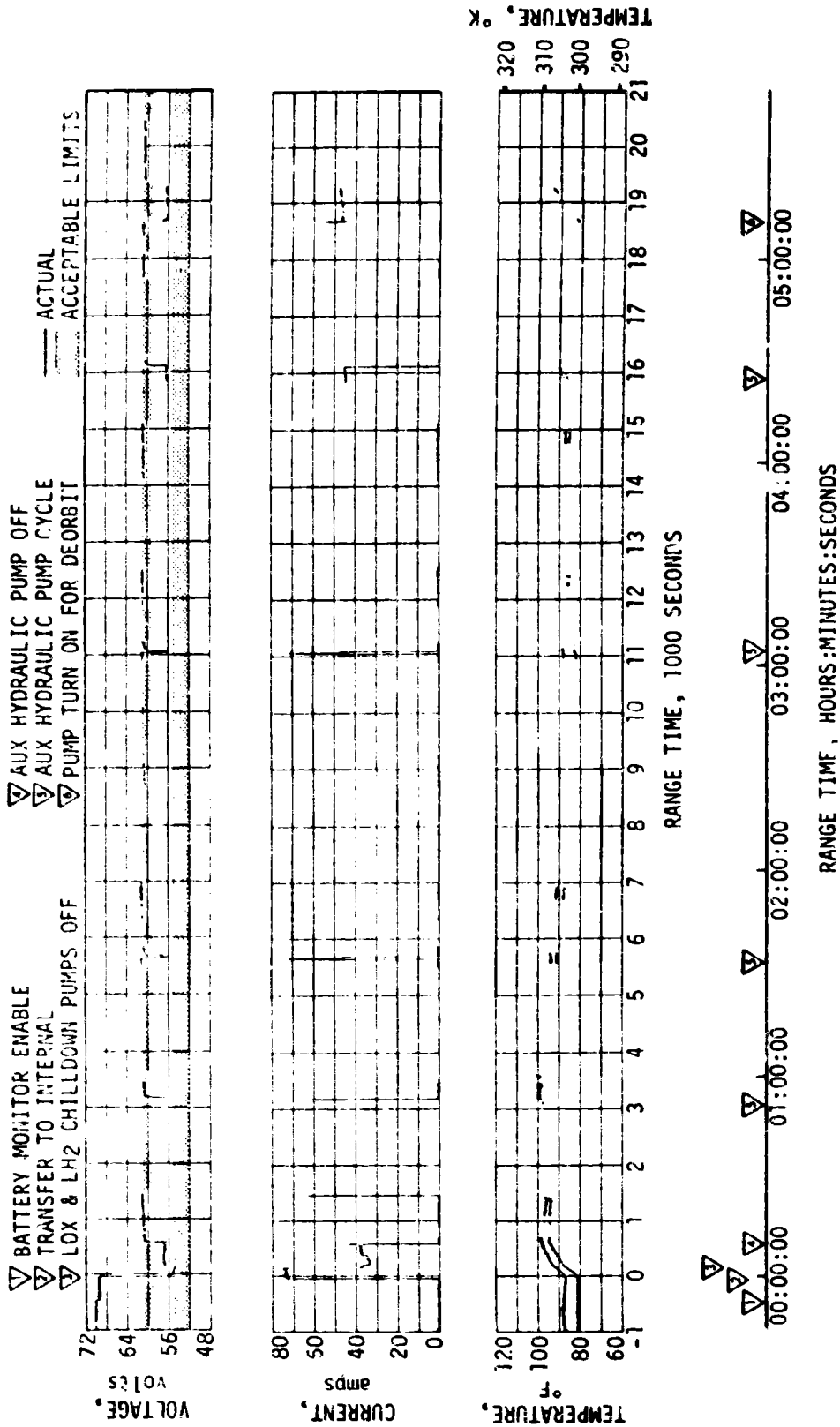


Figure 11-6. S-IVB Stage Aft No. 2 Battery Voltage, Current, and Temperature

Table 11-2. S-IVB Stage Battery Power Consumption

BATTERY	RATED CAPACITY (amp-hr)	POWER CONSUMPTION*	
		amp-hr	PERCENT OF CAPACITY
Forward No. 1 (4D30)	227.5	79.32	34.9
Forward No. 2 (4D20)	3.5	3.26	93.1
Aft No. 1 (4D10)	59.8	19.18	32.1
Aft No. 2 (4D40)	66.5	56.07	84.3

*From Battery activation until end of telemetry (at 20,460 seconds)

11.4 INSTRUMENT UNIT ELECTRICAL SYSTEM

The IU electrical system functioned satisfactorily. All battery voltages remained within performance limits of 26 to 30 V. The battery temperature and current were nominal. Battery voltages, currents and temperatures are shown in Figures 11-7 through 11-9.

Battery power consumption and capacity for each battery are shown in Table 11-3.

The current sharing of the 6D10 and 6D30 batteries, to provide redundant power to the ST-124M-3 platform was satisfactory throughout the flight. During the S-IB burn, current sharing reached a maximum of 24 amperes and 23 amperes from the 6D10 and 6D30 battery, respectively, with an average of 20.5 amperes and 20 amperes (see Figures 11-7 and 11-8).

The 56 volt power supply maintained an output voltage of 55.5 to 56.5 V which is well within the required range of 56 ± 2.5 V.

The 5 volt measuring power supply performed nominally, maintaining a constant voltage within specified tolerances.

The switch selector, electrical distributors and network cabling performed nominally.

REPRODUCIBILITY OF THE ORIGINAL PAGE IS POOR

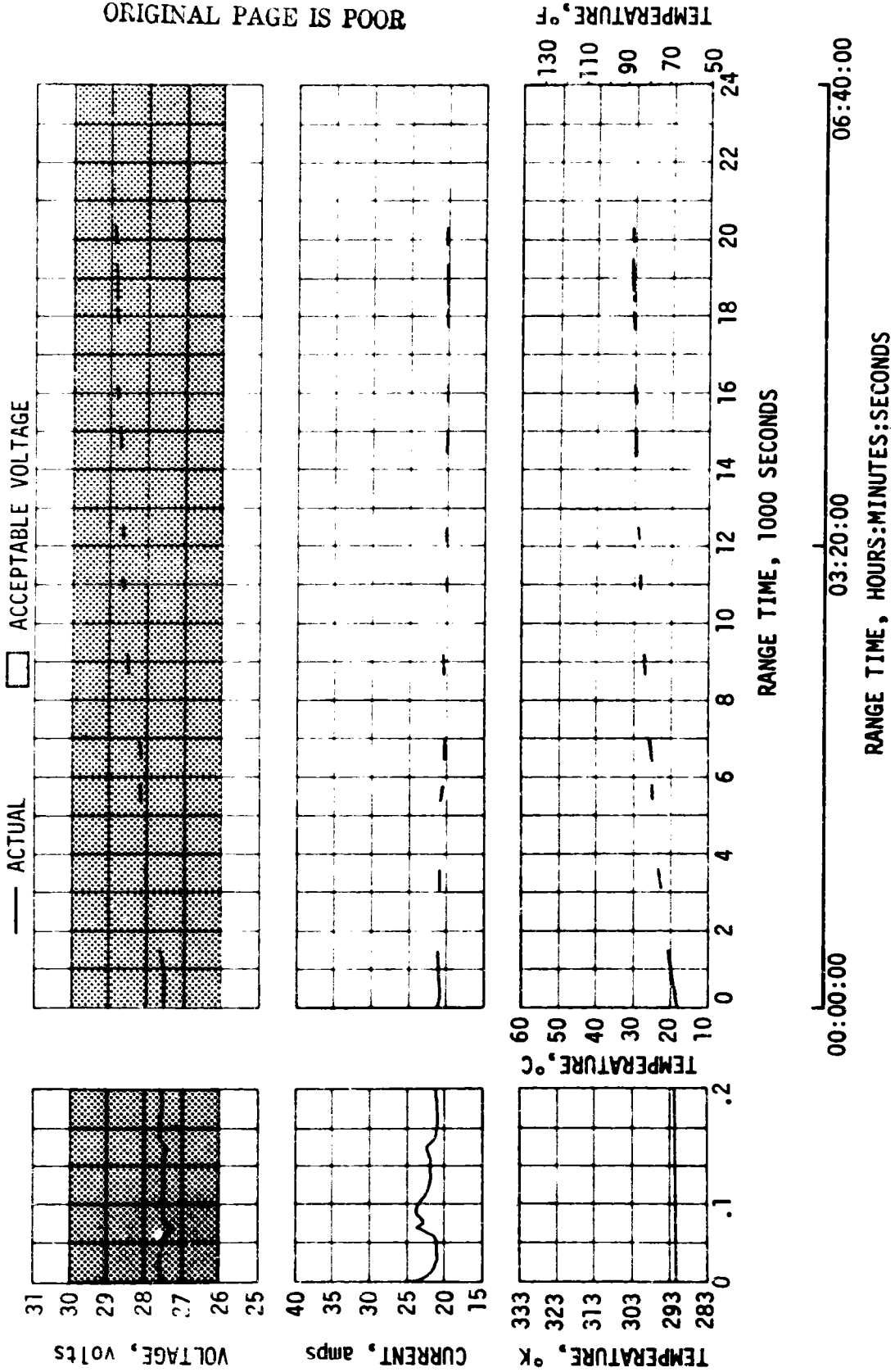


Figure 11-7. IU 6D10 Battery Parameters

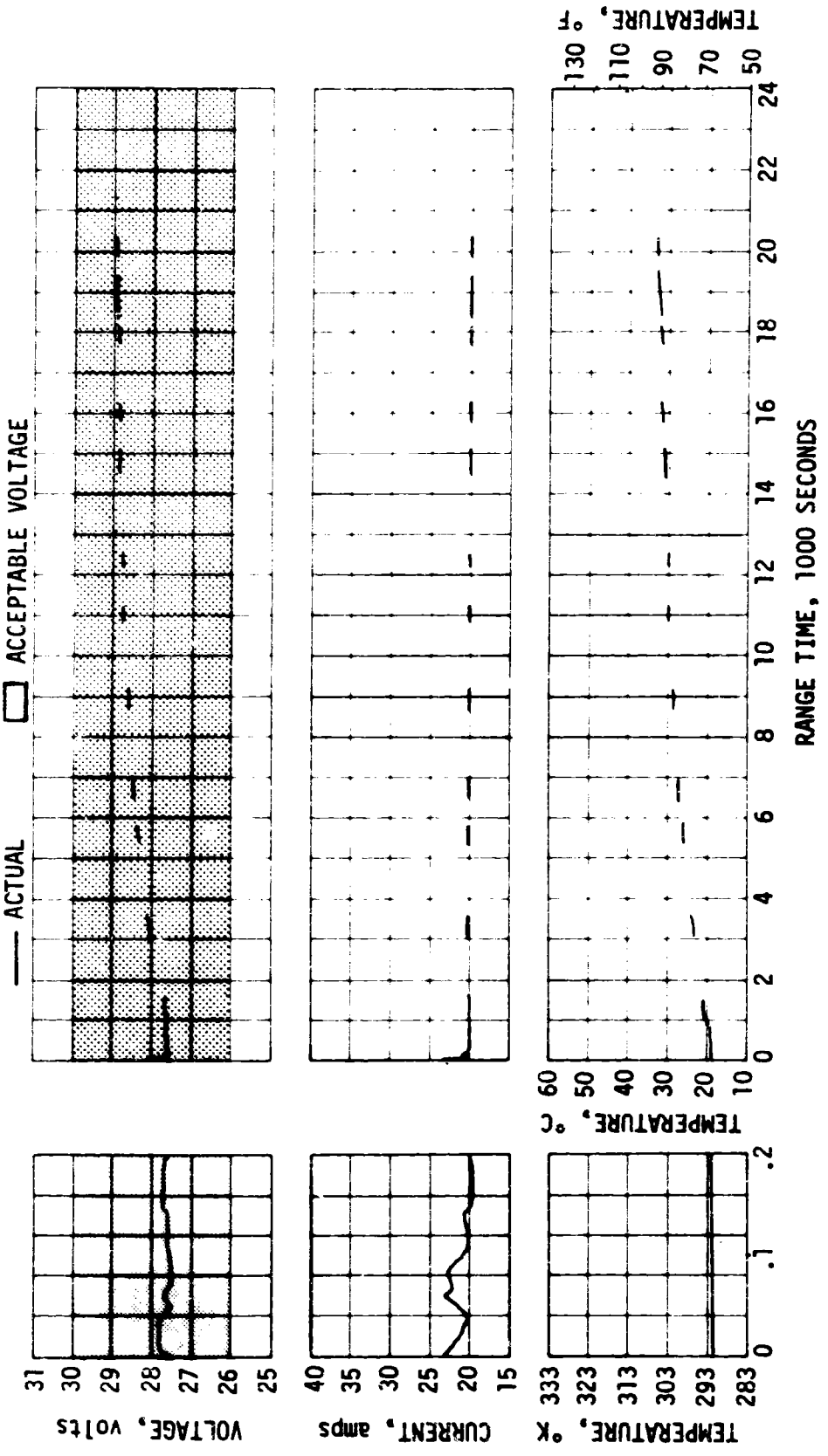
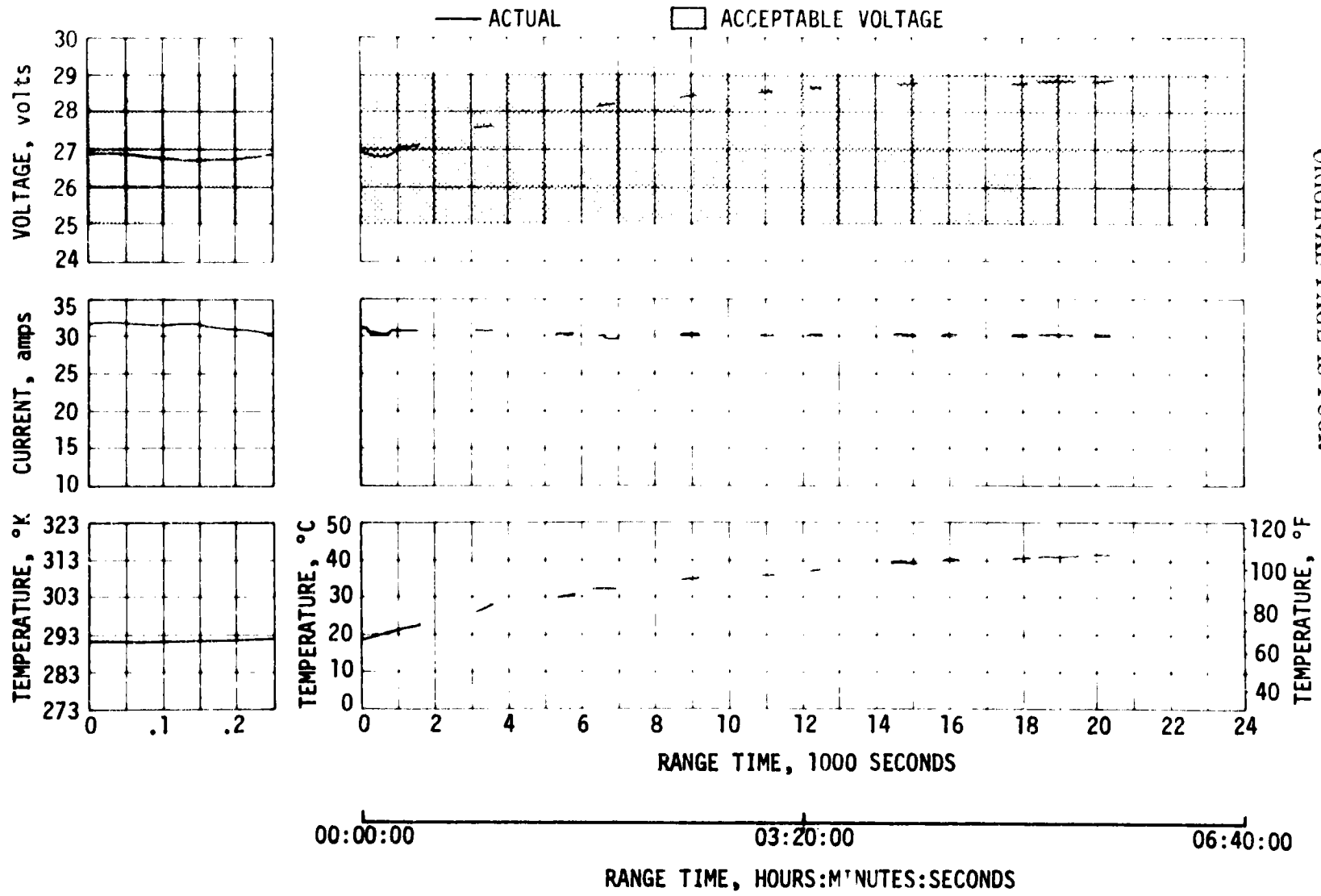


Figure 11-8. IU 6030 Battery Parameters

11-12



REPRODUCIBILITY OF THE ORIGINAL PAGE IS POOR

Figure 11-9. IU 6D40 Battery Parameters

Table 11-3. IU Battery Power Consumption

BATTERY	RATED CAPACITY (amp-hr)	POWER CONSUMPTION*	
		amp-hr	PERCENT OF CAPACITY
6D10	350	127.7	36.5
6D30	350	124.7	35.6
6D40	350	184.5	52.7

* From battery activation until end of telemetry (at 20,460 seconds).

11.4.1 Prelaunch Power Transfer Test Anomaly

During the countdown Power Transfer Test (IAPX) at approximately 75 minutes before launch, the IU internal power was returned to external because of an out-of-tolerance IU current measurement. The 6D10 battery current was 29.2 amperes at the time of transfer to internal power and reduced to 25.1 amperes in about 1.5 seconds. The 6D10 current was tested for 25 amperes maximum by the IAPX software and the out-of-tolerance indication terminated the IU internal power test by switching power to external.

The IU console engineers verified acceptable IU internal power conditions by manual tests immediately after the IAPX test was completed. The power transfer by terminal countdown sequencer at T-50 seconds was accomplished smoothly and no countdown delay was experienced. All IU batteries performed satisfactorily during flight.

It is not unusual for batteries of the type used on the Saturn vehicles to momentarily exceed the steady state current level when first placed under load after an extended period of inactivity. For SA-209 the software limits for the IAPX have been revised to provide a test which ensures short circuit detection but allows for the higher initial current conditions apparent after a period of battery inactivity. The manual power transfer test at T-7:40:00 in the countdown has been moved to the T-3:30:00 hold, thus shortening the time of battery inactivity and precluding the loss of battery plate seasoning.

The performance of the vehicle systems was nominal, but the combination of stringent test limits and extended battery inactivity caused test failure. These conditions have been corrected, and this anomaly is considered closed.

11.5 EMERGENCY DETECTION SYSTEM

The performance of the SA-208 EDS was normal and no abort limits were exceeded. All switch selector events associated with EDS for which data are available, were issued at the scheduled times. The discrete indications for EDS events also functioned normally. The performance of all thrust OK pressure switches and associated voting logic, which monitors engine status, was nominal insofar as EDS operation was concerned. S-IVB tank ullage pressures remained below the abort limits. EDS displays to the crew were normal.

As shown in Section 10, none of the rate gyros gave an indication of angular overrate about the pitch, yaw, or roll axis. The maximum angular rates were well below the abort limits.

The operation of the EDS Cutoff Inhibit Timer was nominal. The timer ran for 41.1 seconds which is within the specified limits of 40 to 42 seconds.

SECTION 12

VEHICLE PRESSURE ENVIRONMENT

12.1 S-IB BASE PRESSURE

Base pressure data obtained from SA-208 have been compared with preflight predictions and/or previous flight data and show good agreement. Base drag coefficients were also calculated using the measured pressures and actual flight trajectory parameters. There were three base pressure measurements made in the S-IB base region; two on the heat shield and one on the flame shield. One measurement on the heat shield was a differential pressure across the shield, whereas the other two measurements were of absolute pressures.

Results of the heat shield and flame shield absolute pressure measurements are shown in Figures 12-1 and 12-2, respectively. These data are presented as the difference between measured base pressures and ambient pressure. Values are compared with the band of data obtained from previous S-IB flights of similar vehicle base configuration and show good agreement. Both the heat shield and flame shield pressure measurements were almost identical to the data from SA-206 and SA-207 flights. The data indicate that during the first 70 seconds of flight (6 n mi. altitude) the H-1 engine exhausts were aspirating the heat shield region, resulting in base pressures below ambient pressures. In the flame shield area, the aspirating effect was terminated at an altitude of 4 nautical miles. Above these altitudes the reversal of engine exhaust products, due to plume expansion, resulted in base pressures above ambient.

Pressure loading measured near the outer perimeter of the SA-208 heat shield is compared with data from previous flights in Figure 12-3. The SA-208 data remained on the lower side of the data band during the first 7 nautical miles of flight altitude. This also occurred on the SA-206 and SA-207 flights and the agreement is very good. Also shown on the figure are the predicted ΔP deviations for the heat shield. The flight values are within these predicted values during the entire flight. Above 15 nautical miles altitude, the SA-208 flight data return to near zero indicating the engine compartment has vented to near base pressure. This is normal and has occurred on all previous flights except SA-205.

Base drag coefficients calculated from the SA-208 data are compared to the data band from previous flights in Figure 12-4. The comparison is very good considering the drag coefficients were determined from measurements taken at only two locations on the base. However, they are representative of average base pressures.

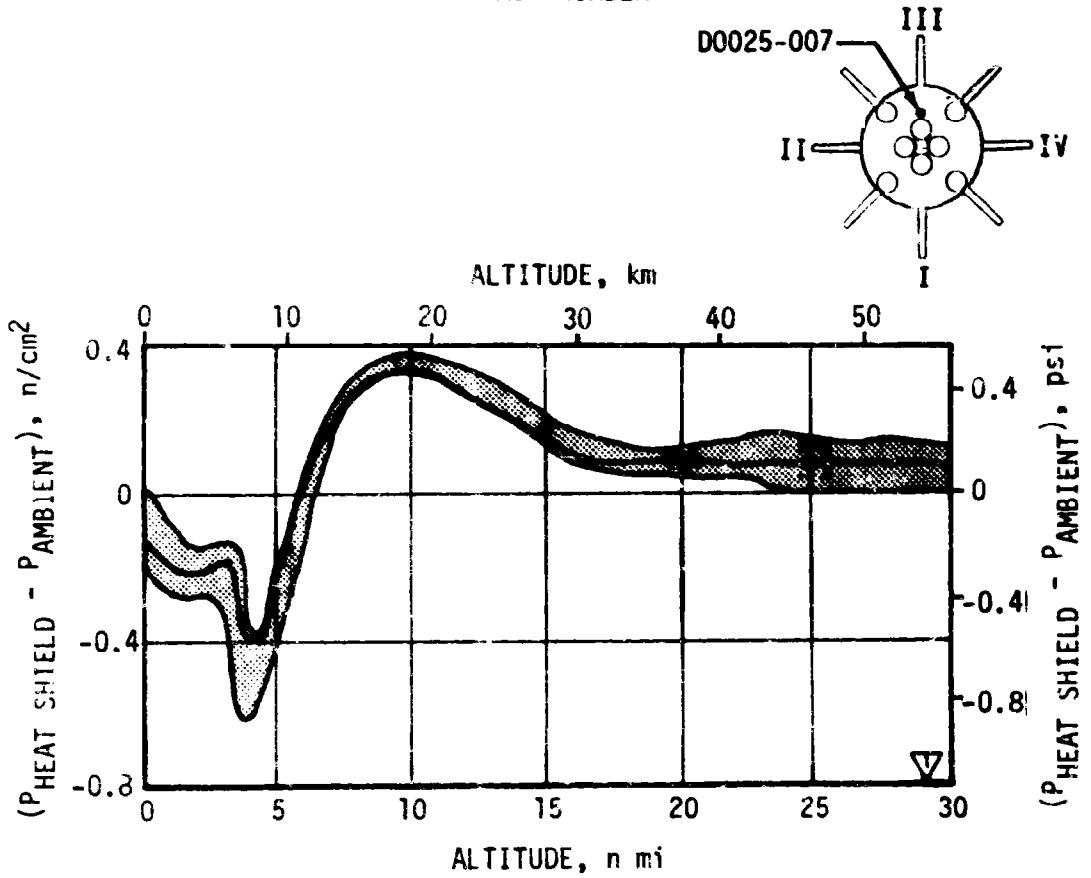
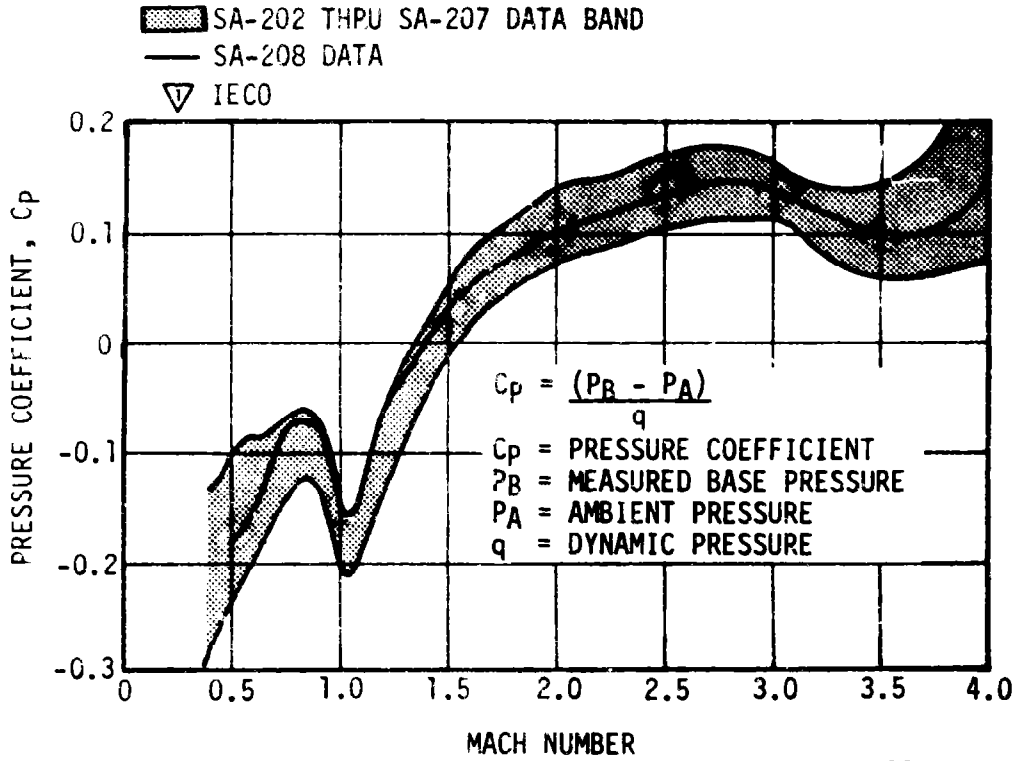


Figure 12-1. S-IB Stage Heat Shield Pressure

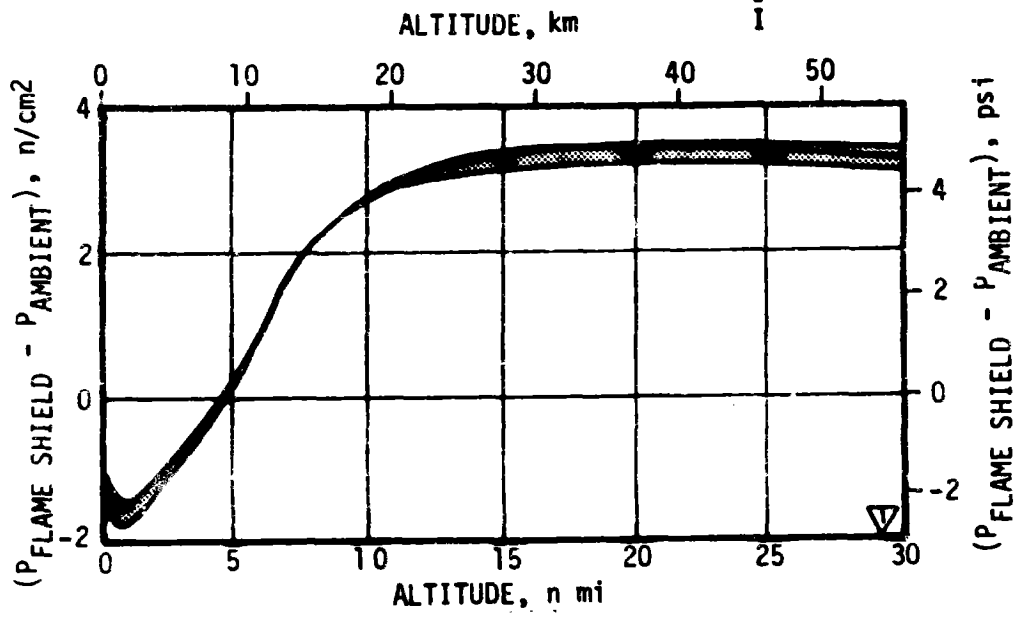
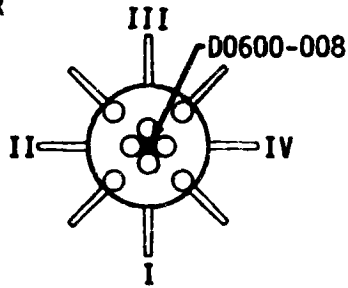
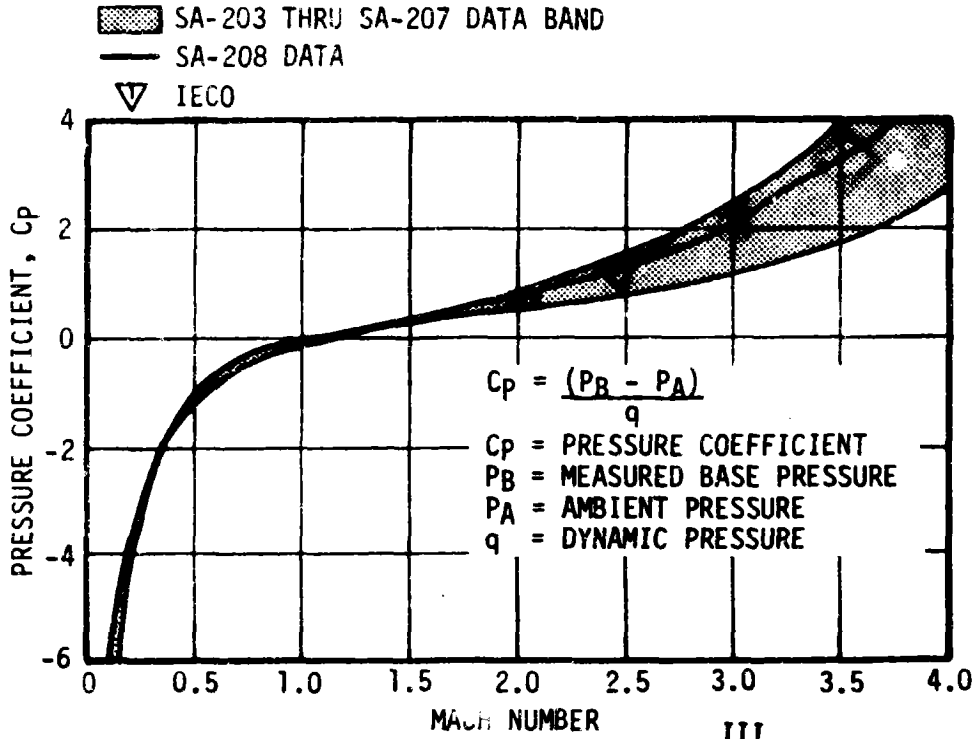


Figure 12-2. S-IB Stage Flame Shield Pressure

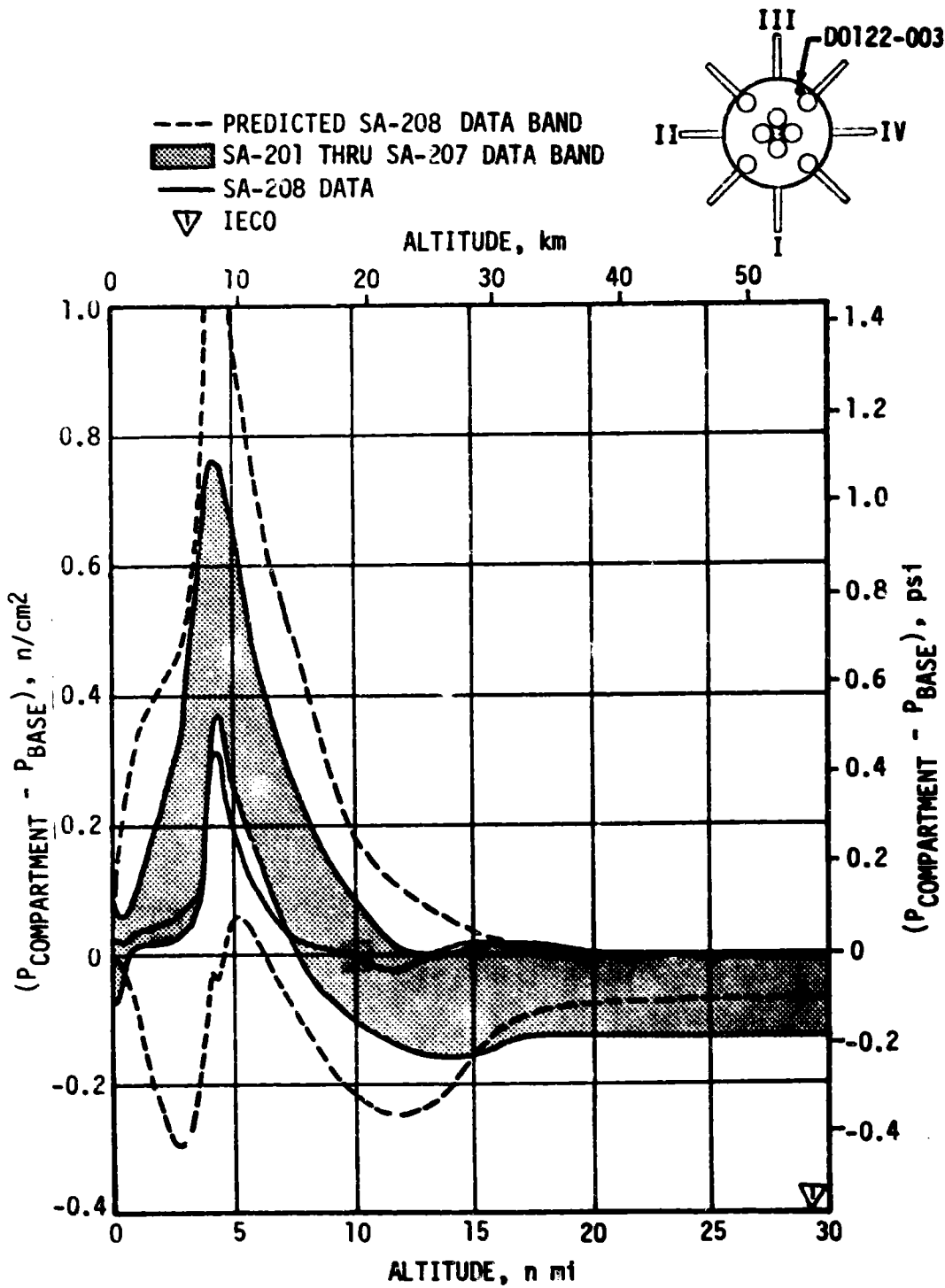


Figure 12-3. S-IB Stage Heat Shield Loading

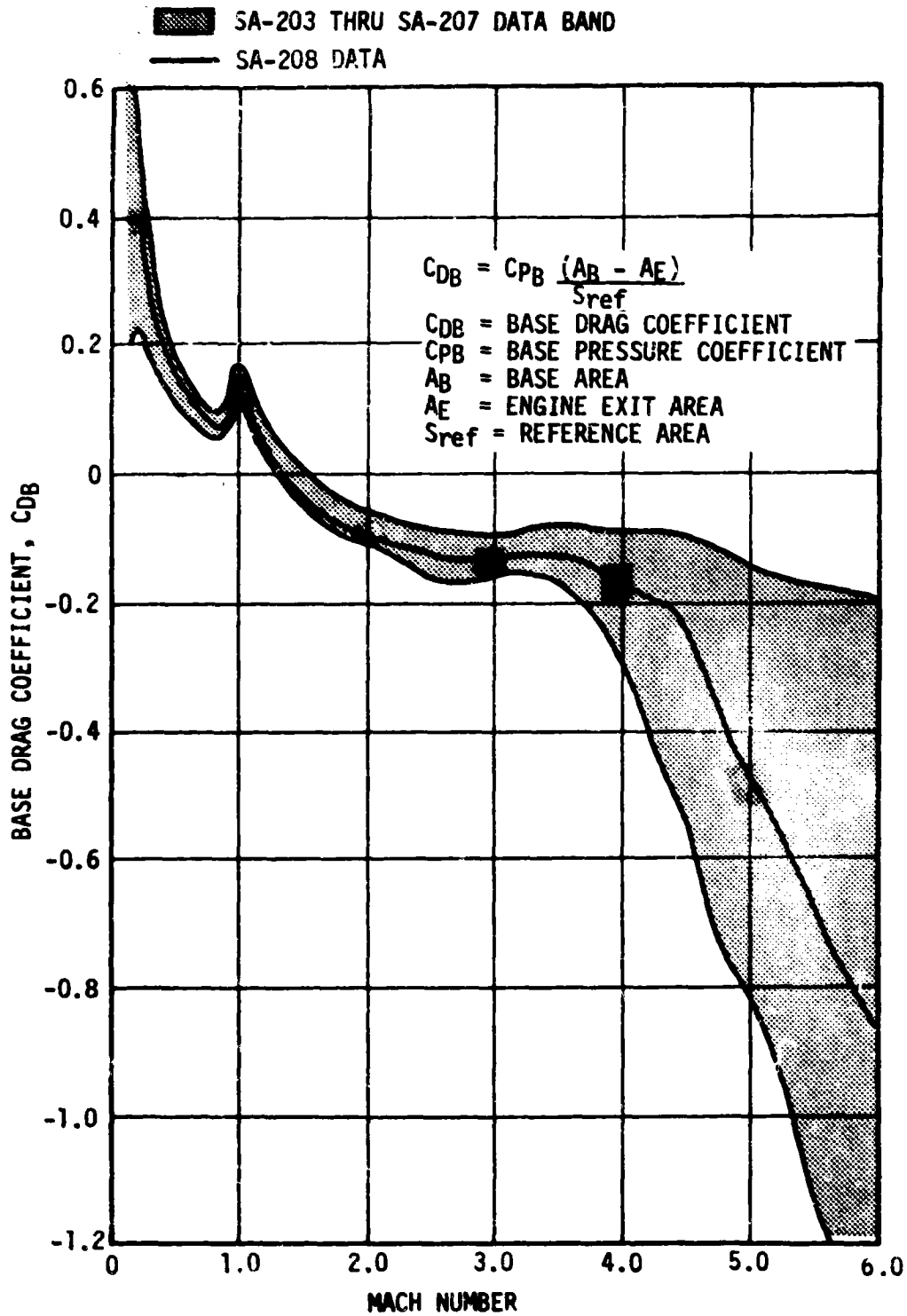


Figure 12-4. S-IB Stage Base Drag Coefficient

SECTION 13

VEHICLE THERMAL ENVIRONMENT

13.1 S-IB BASE HEATING

Data traces from the seven SA-208 S-IB stage base thermal measurements have been compared with corresponding data from the flights of SA-203 through SA-207. These comparisons indicate an SA-208 base region thermal environment of comparable magnitude, with the flame shield radiant data trend being similar to that recorded on SA-207. All measured thermal environment data were well below S-IB stage design levels.

The S-IB stage base region thermal environment of SA-208 was recorded by three gas temperature thermocouples and four heat flux calorimeters. Data from these SA-208 measurements are compared with bands formed by the maximum and minimum data extremes recorded by comparable instrumentation on previous flights.

Heat shield thermal environment data are presented as a function of vehicle altitude in Figures 13-1 through 13-4. As indicated by these comparison plots, the SA-208 heat shield thermal environment was nominal, except for some minor deviations above and below the previous flight data band up to 20 n mi. However, these deviations from the established data bands are not considered significant.

In the flame shield area the recorded SA-208 thermal environment was similar to that experienced on SA-207. Total heating rate and gas temperature data were generally in the upper portion of the previous data bands through the first 55 seconds of flight; i.e., to a vehicle altitude of approximately 3.35 n mi, except for a deviation at 1 n mi which is not considered significant. These data are presented as a function of vehicle altitude in Figures 13-5 and 13-6. During this same period, the SA-208 flame shield radiation data (presented in Figure 13-7) were generally above the data trend established through the flight of SA-206, but slightly below that of SA-207, except for a short period at launch. However, this deviation was still within the previous flight data band. At an altitude of approximately 4.5 n mi, the flame shield thermal environment leveled off to a steady nominal level. At this altitude the inboard engine exhaust plumes had expanded sufficiently to interact and cause a sustained flow reversal of exhaust gases onto the flame shield. This reversal placed the relatively cool (800°K) and opaque inboard engine turbine exhaust gases nearer the flame shield surface, and substantially reduced the magnitude of the flame shield thermal environment.

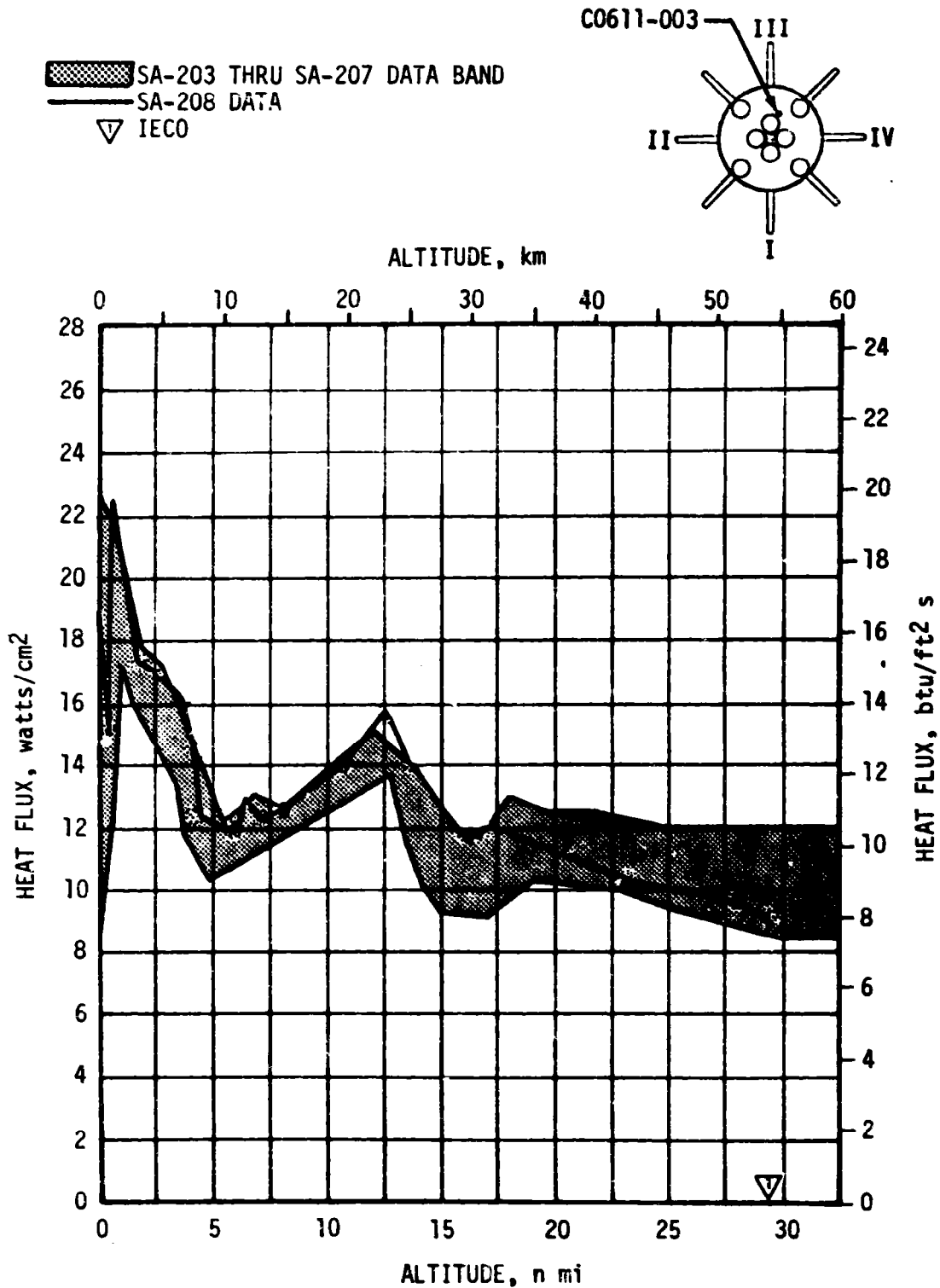


Figure 13-1. S-IB Stage Heat Shield Inner Region Total Heating Rate

 SA-203 THRU SA-207 DATA BAND
 SA-208 DATA
 IECCO

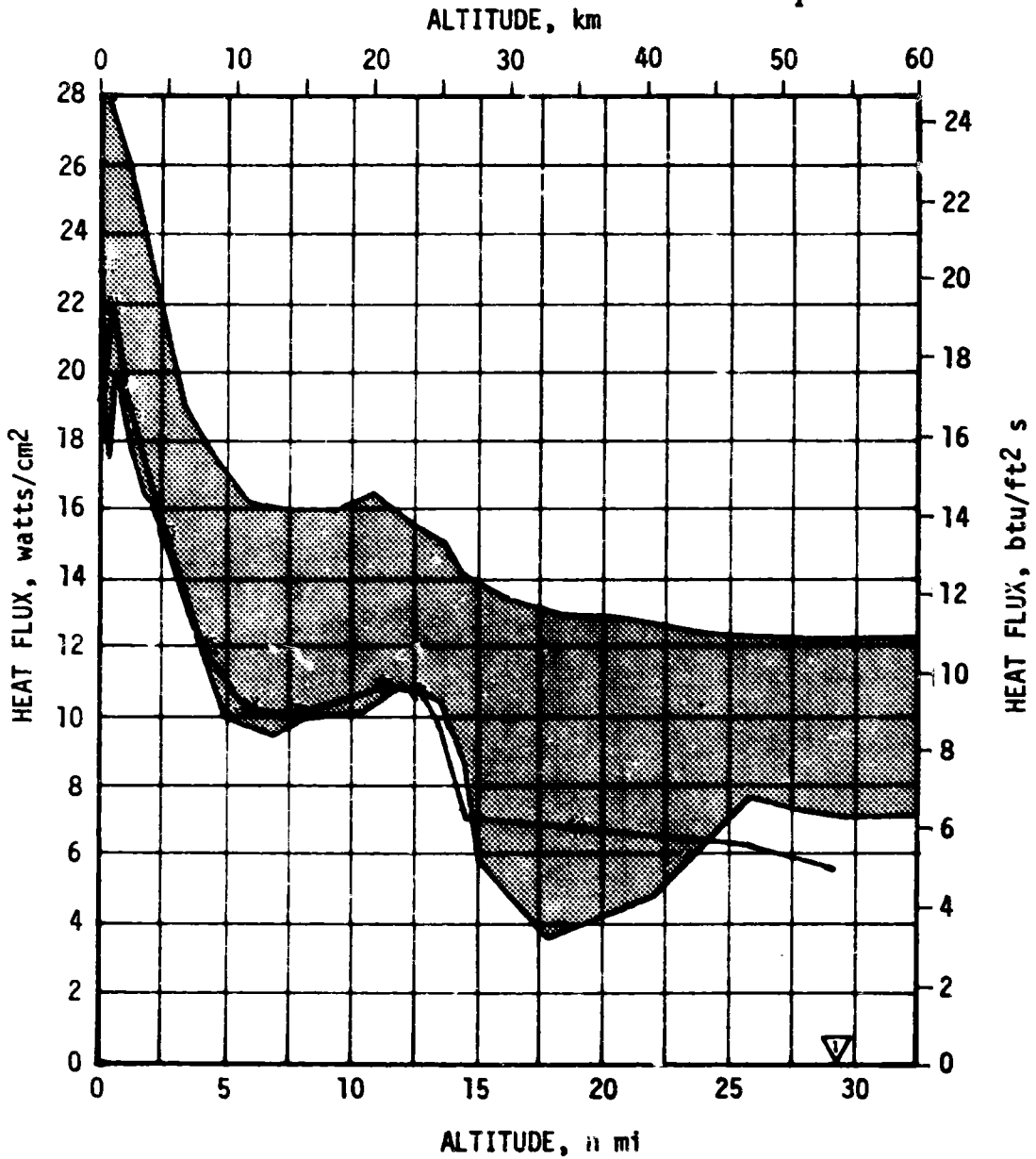
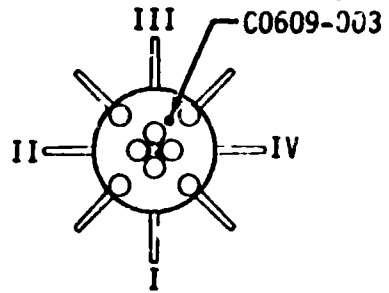


Figure 13-2. S-IB Stage Heat Shield Inner Region Radiation Heating Rate

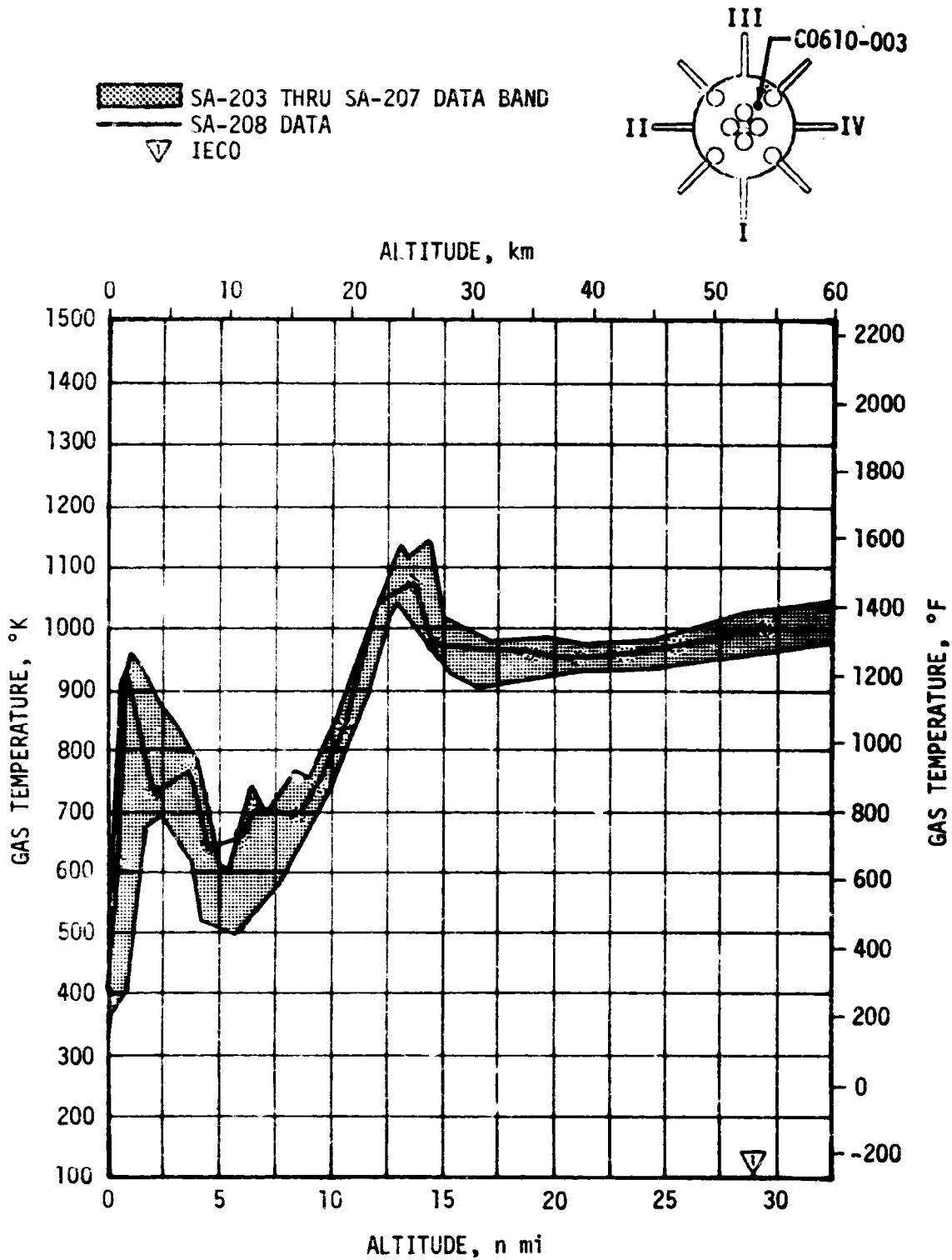


Figure 13-3. S-IB Stage Heat Shield Inner Region Gas Temperature

 SA-203 THRU SA-207 DATA BAND
 SA-208 DATA
 IE CO

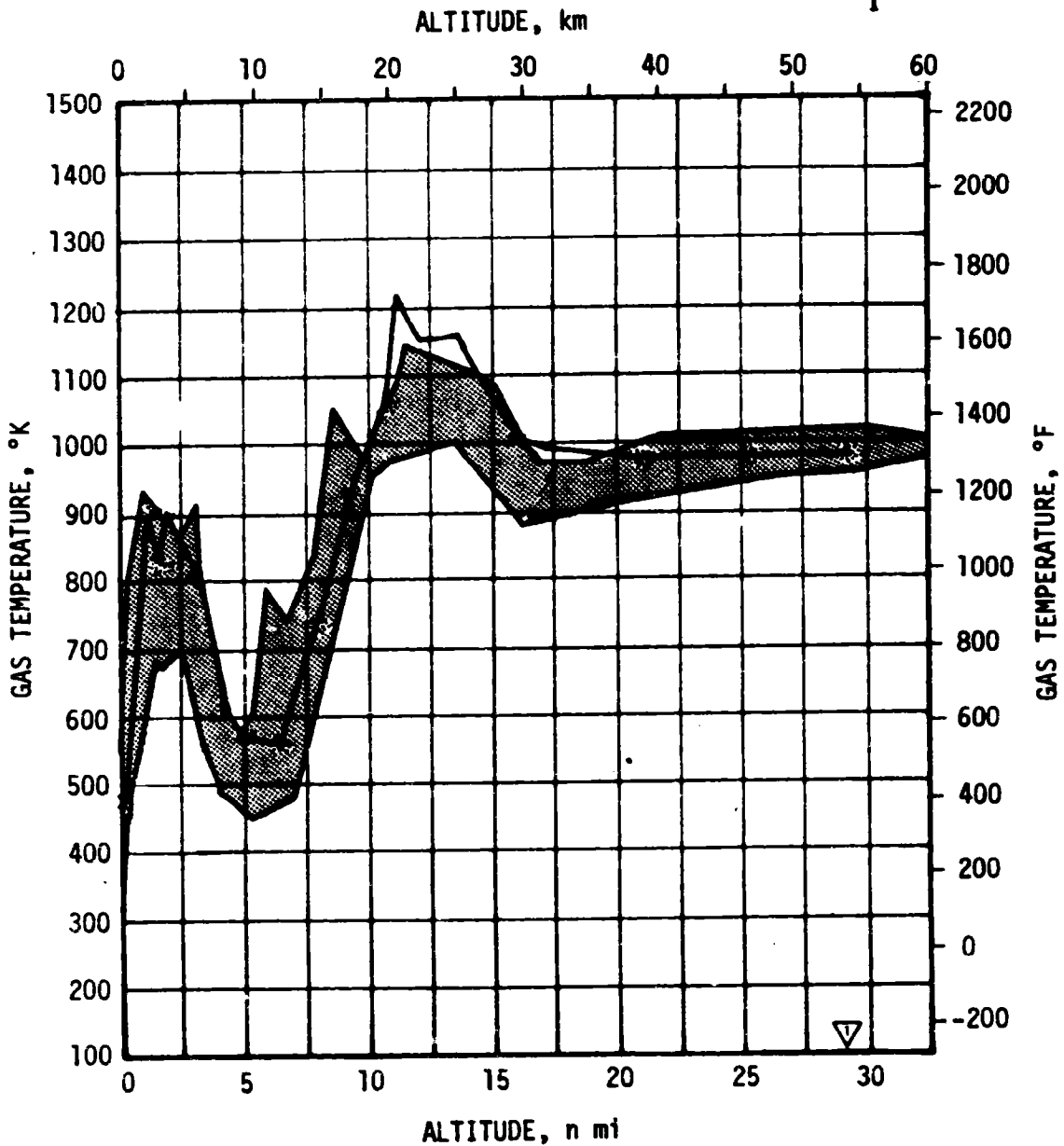
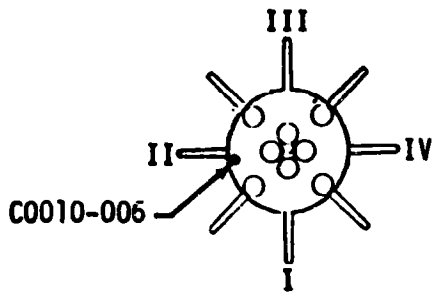


Figure 13-4. S-IB Stage Heat Shield Outer Region Gas Temperature

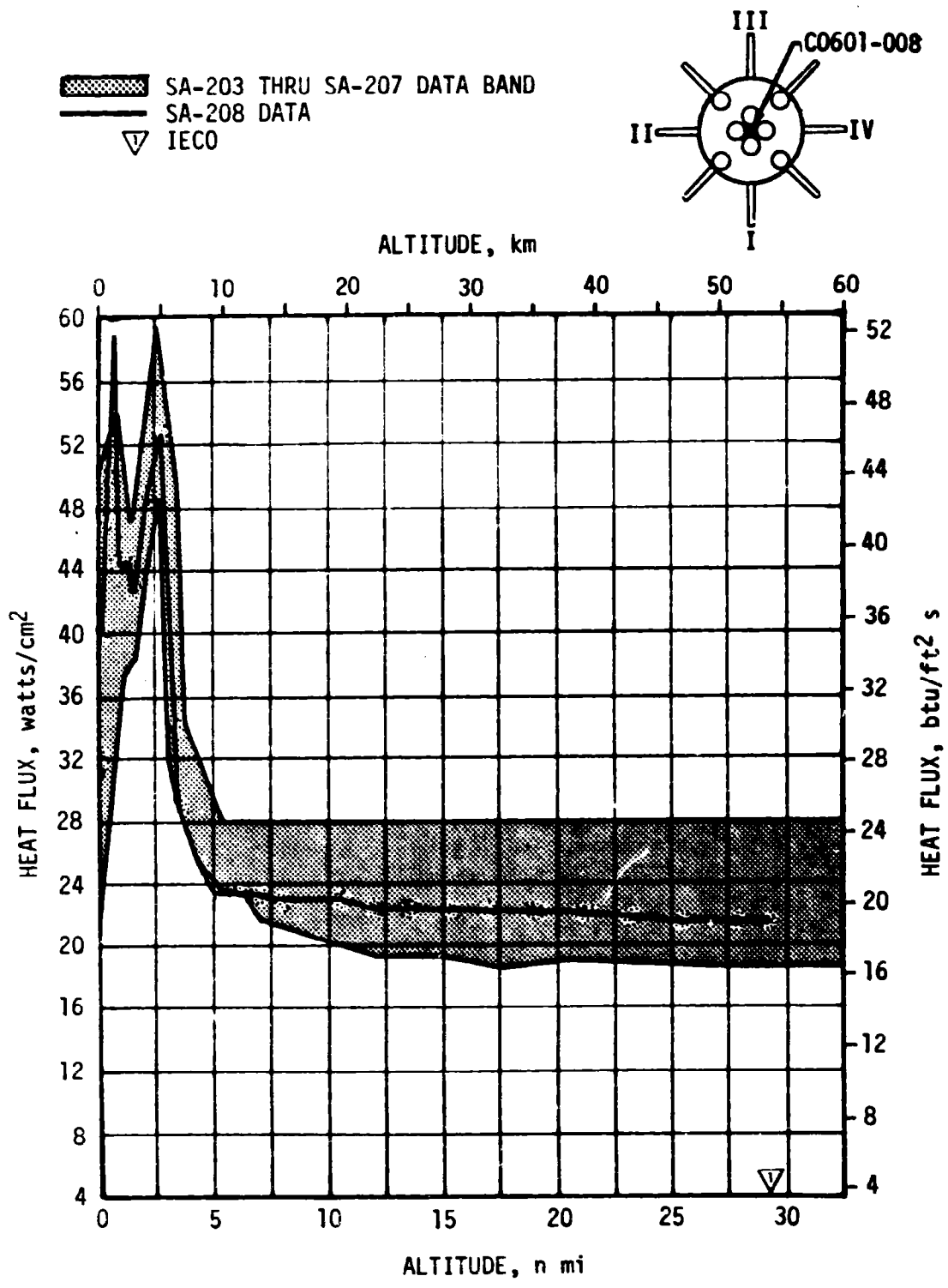


Figure 13-5. S-IB Stage Flame Shield Total Heating Rate

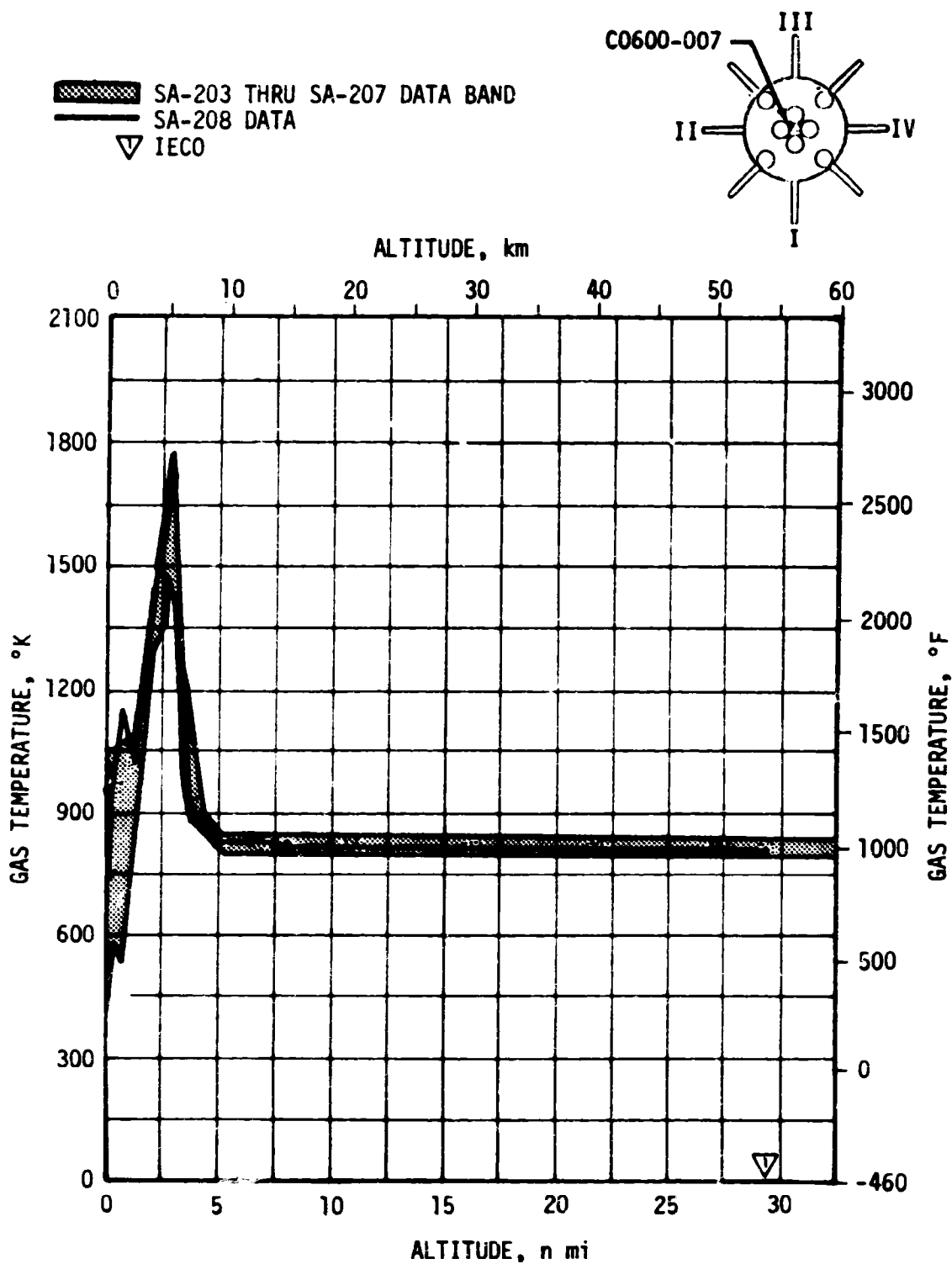


Figure 13-6. S-IB Stage Flame Shield Gas Temperature

C-3

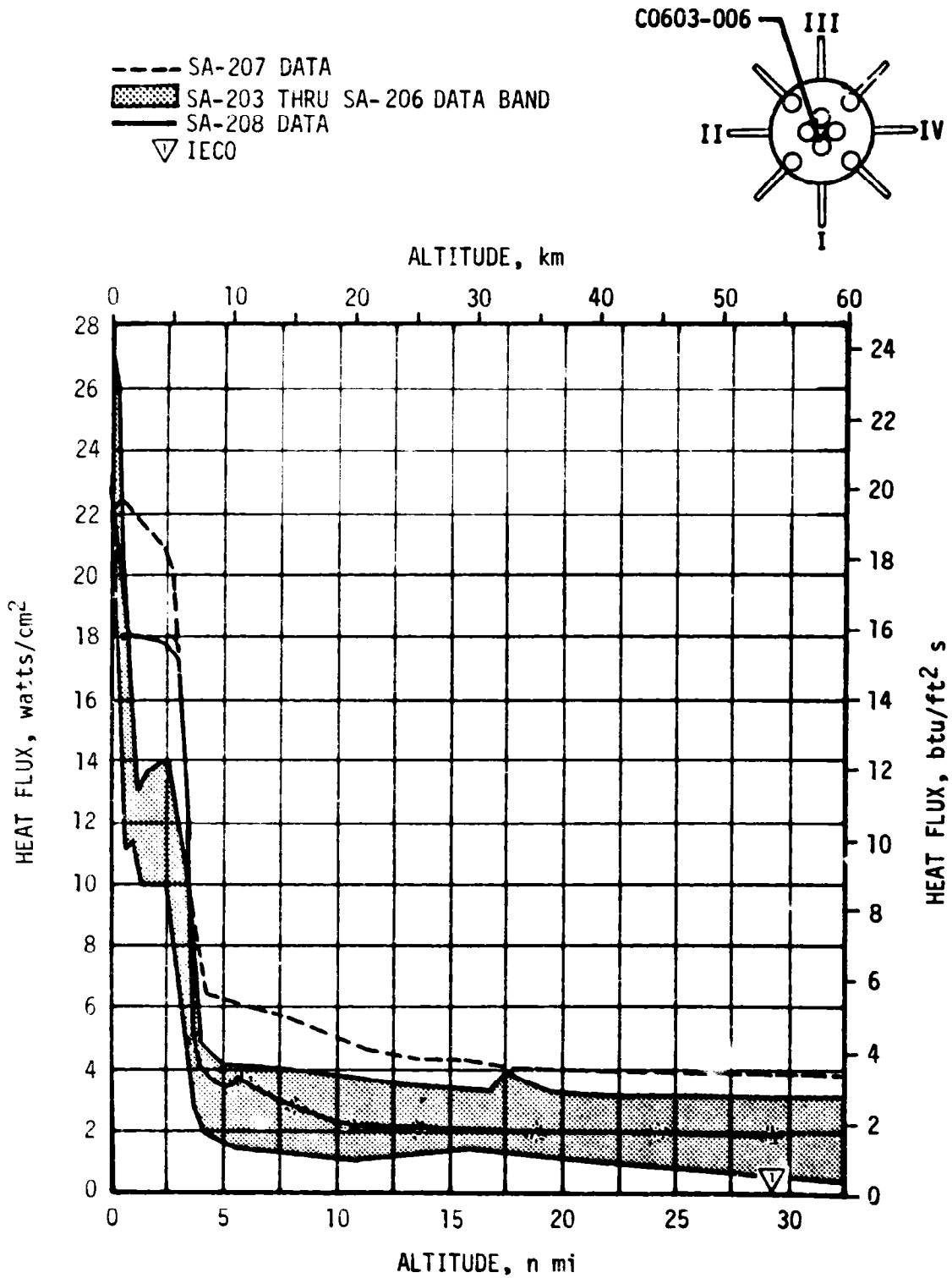


Figure 13-7. S-IB Stage Flame Shield Radiation Heating Rate

Because of the similarity of the SA-208 and SA-207 data, possible causes of the flame shield radiant heating deviations were again investigated, and still no definite conclusion was reached as to why the data differed from the trend established during the previous four flights. The data appears to be valid. The flame shield and turbine exhaust duct configurations were essentially unchanged from SA-203.

Three explanations for more radiation reaching the flame shield radiometer have been offered:

- a. A reduction in opacity of the turbine exhaust gases.
- b. Sustained local afterburning of the turbine exhaust gases.
- c. A variation in incident radiation correlated to the variation in inboard engine thrust level.

The possible relationship between inboard engine thrust and flame shield radiation has been investigated and a comparison of the data for flights SA-203 to SA-208 is shown in Figure 13-8. The apparent correlation suggests a mechanism whereby the increased thrust level of the inboard engine may be responsible for the decreased opacity of the turbine exhaust gases, but analytical confirmation is not possible within the state-of-the-art.

Available data will not support a final conclusion as to the cause of the increased flame shield radiant heat level. Regardless of the cause, the flame shield, because of its high thermal design capability, is not in jeopardy as shown in Figure 13-9. Since the reroute of the inboard engine turbine exhaust duct, effective on SA-203, the recorded flame shield radiant heat load through the first 55 seconds of flight has not exceeded 50 percent of the design level; beyond 60 seconds of flight (above an altitude of 4 n. mi.) recorded data have been below 15 percent of the radiation design level. No further action is contemplated.

○ FLAME SHIELD
 RADIANT HEAT FLUX
 □ TOTAL INBOARD
 ENGINE THRUST

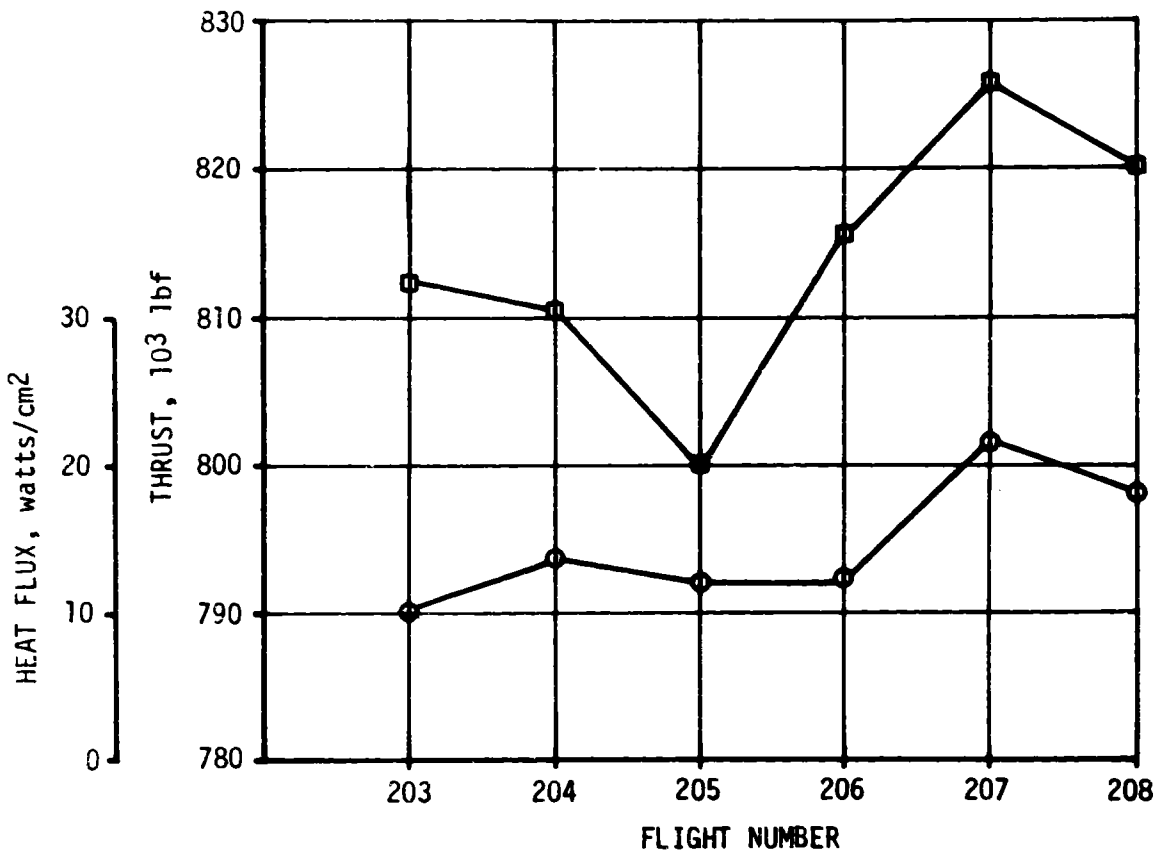
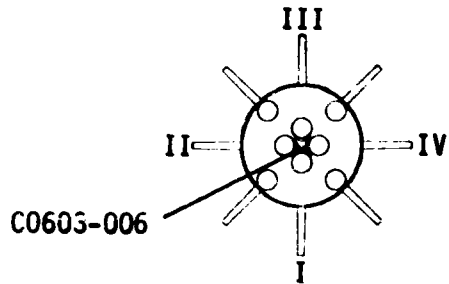


Figure 13-8. Variation of S-IB Flame Shield Radiant Heating with Inboard Engine Thrust

- SA-208 DATA
- - - SA-207 DATA
- · - · SA-206 DATA
- - - S-IB DESIGN LEVEL
- ▨ DATA BAND
SA-203 THROUGH SA-205

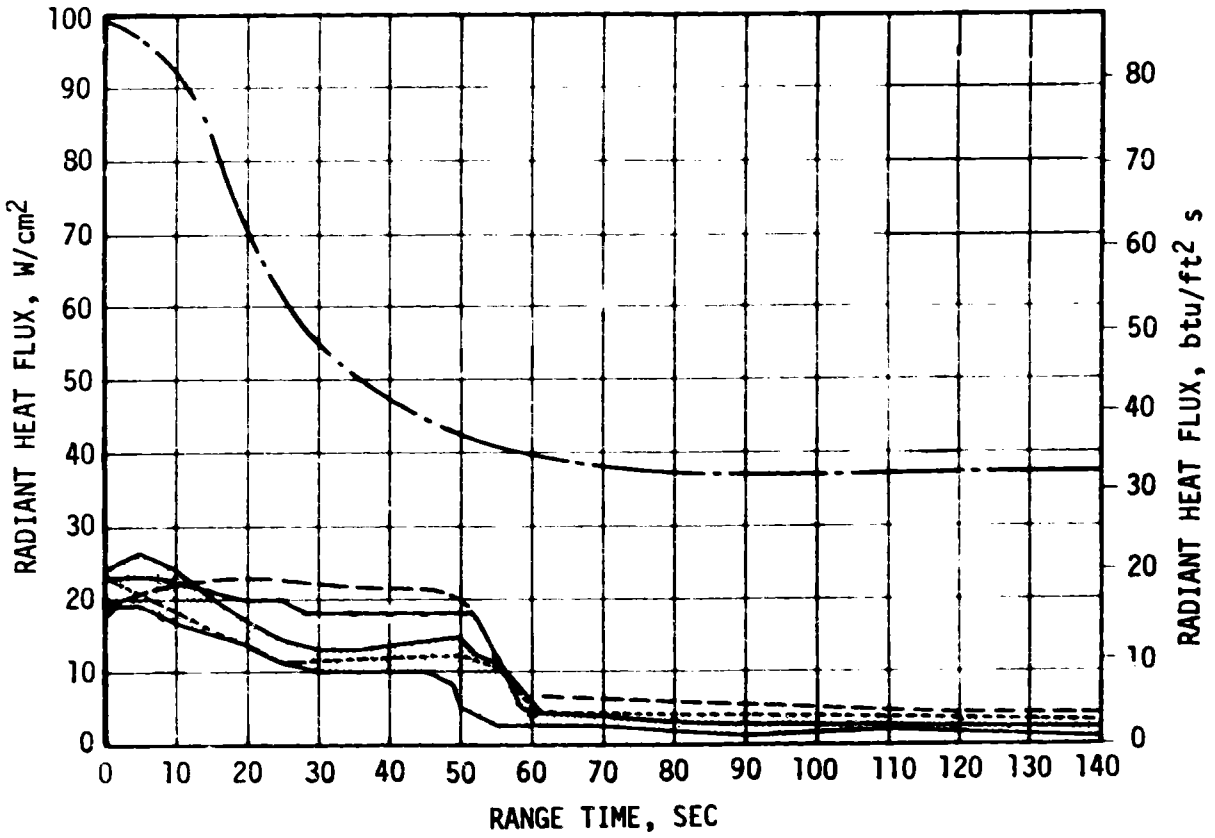


Figure 13-9. Comparison of S-IB Stage Flame Shield Radiant Heating Data

SECTION 14

ENVIRONMENTAL CONTROL SYSTEMS

14.1 SUMMARY

The S-IB stage engine compartment and instrument compartment require environmental control during prelaunch operations, but are not actively controlled during S-IB boost. The desired temperatures were maintained in both compartments during the prelaunch operation.

The Instrument Unit (IU) stage Environmental Control System (ECS) exhibited satisfactory performance for the duration of the IU mission. Coolant temperatures, pressures, and flowrates were continuously maintained within the required ranges and design limits.

14.2 S-IB ENVIRONMENTAL CONTROL

The S-IB engine compartment temperature was maintained at approximately 59°F for 7 hours prior to liftoff. Engine compartment temperature data are monitored during prelaunch activities to assess ECS flow and supply temperature requirements for maintaining engine compartment temperature within the specified limits of 53 and 75°F. In maintaining the 59°F engine compartment temperature, the ECS delivery was nominal.

The S-IB instrument compartment environmental conditioning system also performed satisfactorily during countdown. This was evidenced by the D20 and D10 battery case temperatures. Battery temperatures remained at approximately 73°F throughout the countdown. This temperature range was maintained after LOX load by nominal GN₂ conditioning.

It was concluded that the critical component temperatures in the engine and instrument compartments were well within their qualification limits.

14.3 IU ENVIRONMENTAL CONTROL

The IU ECS exhibited normal performance for the duration of the IU mission including initiation of deorbit. Coolant temperatures, pressures, and flowrates were continuously maintained within the required ranges and design limits.

14.3.1 Thermal Conditioning System (TCS)

The TCS performance was satisfactory throughout the IU mission. The temperature of the coolant supplied to the IU thermal conditioning panels, IU internally cooled components, and the S-IVB was continuously maintained within the required limits of 45 to 68°F for the IU lifetime.

Sublimator performance parameters for the initial cycle are presented in Figure 14-1. The water supply valve opened as programmed at approximately 181 seconds, allowing water to flow to the sublimator. At the first thermal switch sampling (480 seconds), the coolant temperature was above the thermal switch actuation point; hence the water supply valve remained open. Significant cooling by the sublimator was evident at approximately 520 seconds at which time the temperature of the coolant began to decrease rapidly.

Figure 14-2 shows temperature control parameters over the total mission. Sublimator cooling was normal and the coolant control temperature was maintained within the required limits of 45 to 68°F.

Hydraulic performance of the TCS was nominal as indicated by the parameters shown in Figure 14-3. System flowrates and pressures were relatively constant throughout the mission.

The TCS GN₂ supply sphere pressure decay, which is indicative of the GN₂ usage rate, was nominal as reflected by Figure 14-4.

14.3.2 Gas Bearing System (GBS)

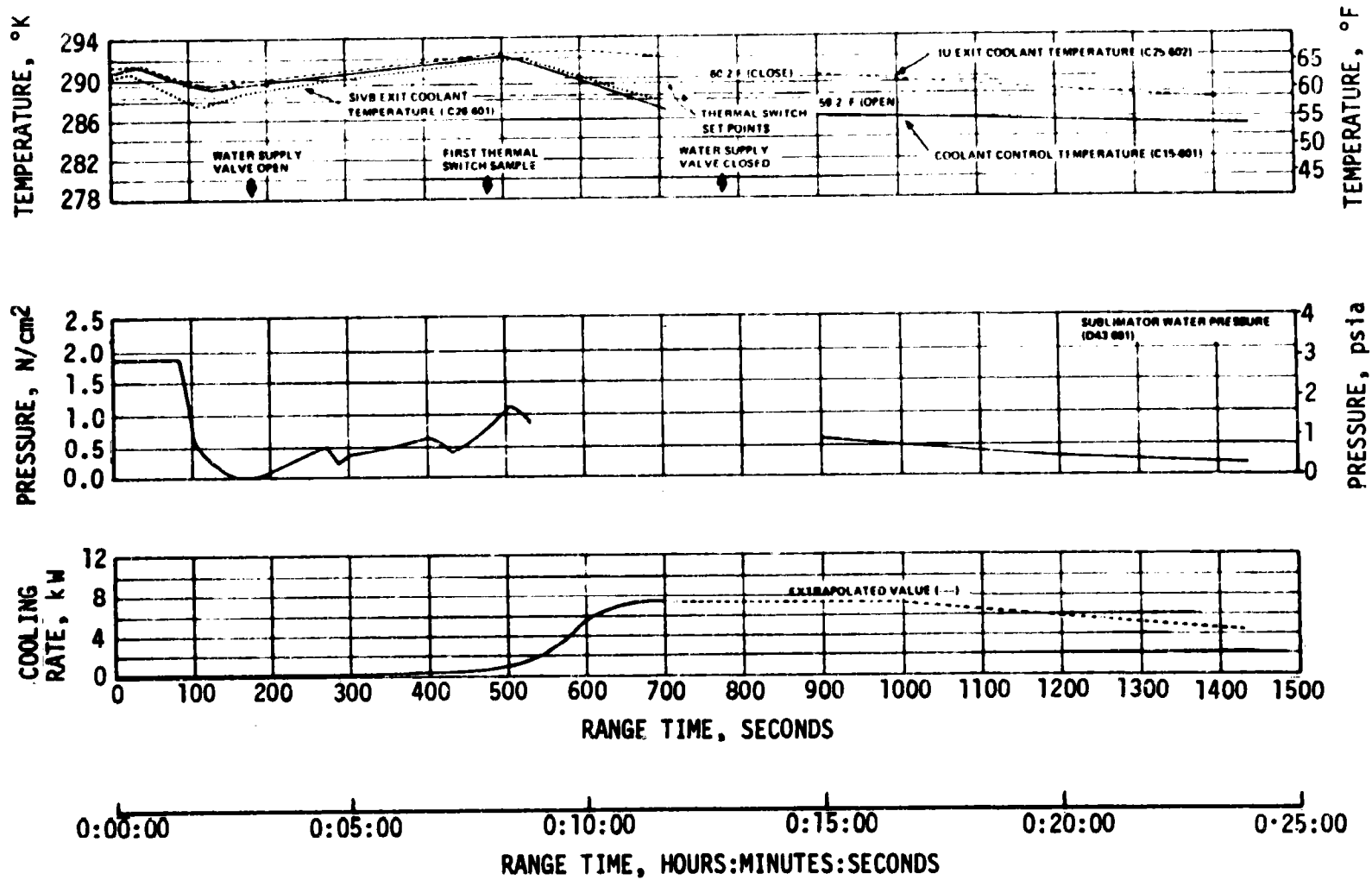
The GBS performance was nominal throughout the IU mission. Figure 14-5 depicts the platform pressure differential and platform internal pressure.

The GBS GN₂ supply sphere pressure decay was nominal as shown in Figure 14-6.

14.3.3 Component Temperatures

All measured component temperatures were normal throughout the mission. Selected component temperatures for major subsystems of most concern are shown in Figures 14-7 and 14-8.

14-3



REPRODUCIBILITY OF THE ORIGINAL PAGE IS POOR

Figure 14-1. IU Sublimator Start Up Parameters for Initial Cycle

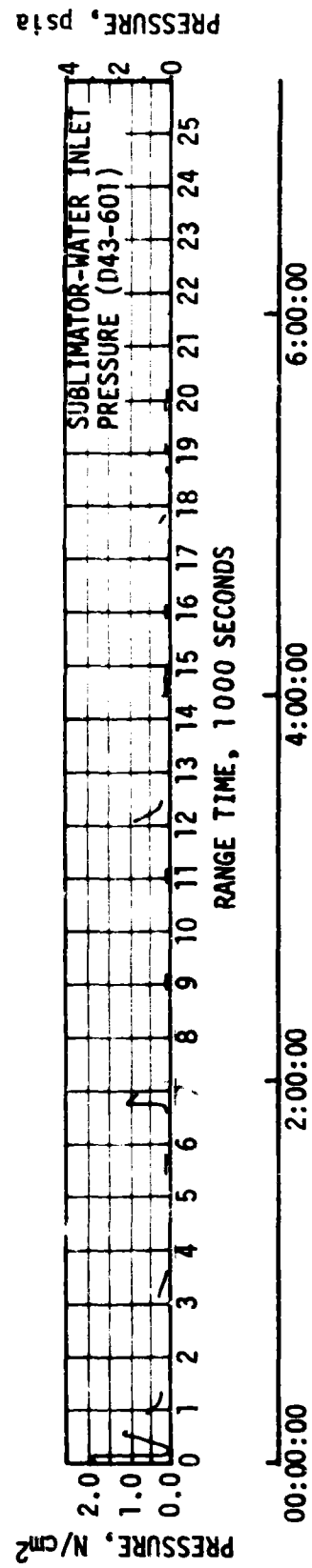
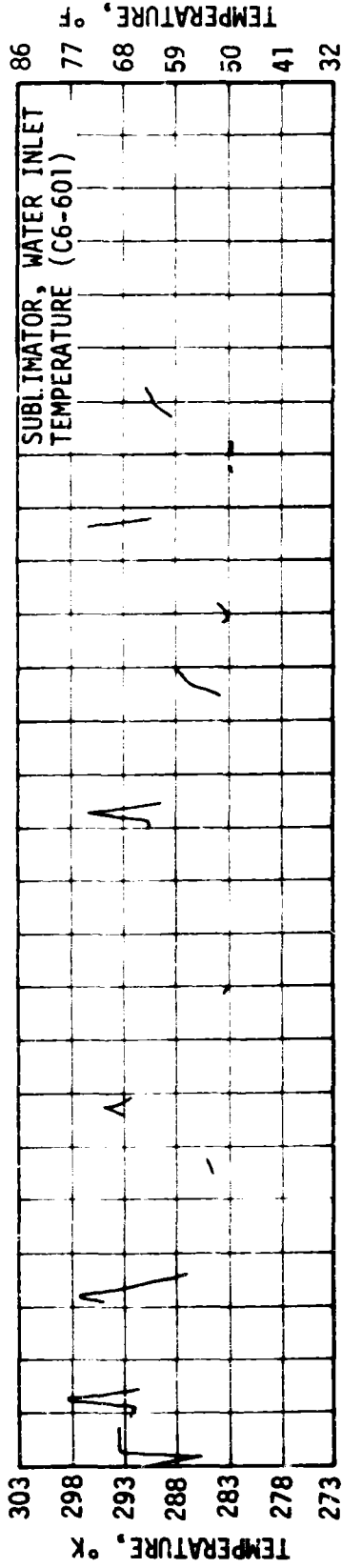
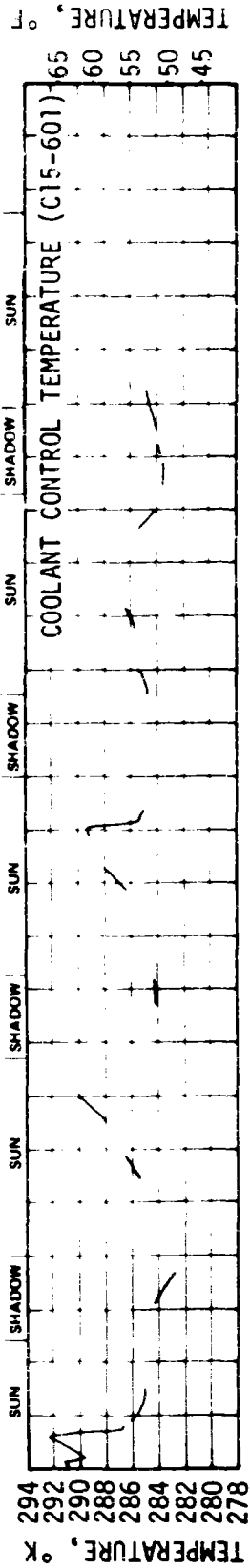


Figure 14-2. IU TCS COOLANT CONTROL PARAMETERS

14-5

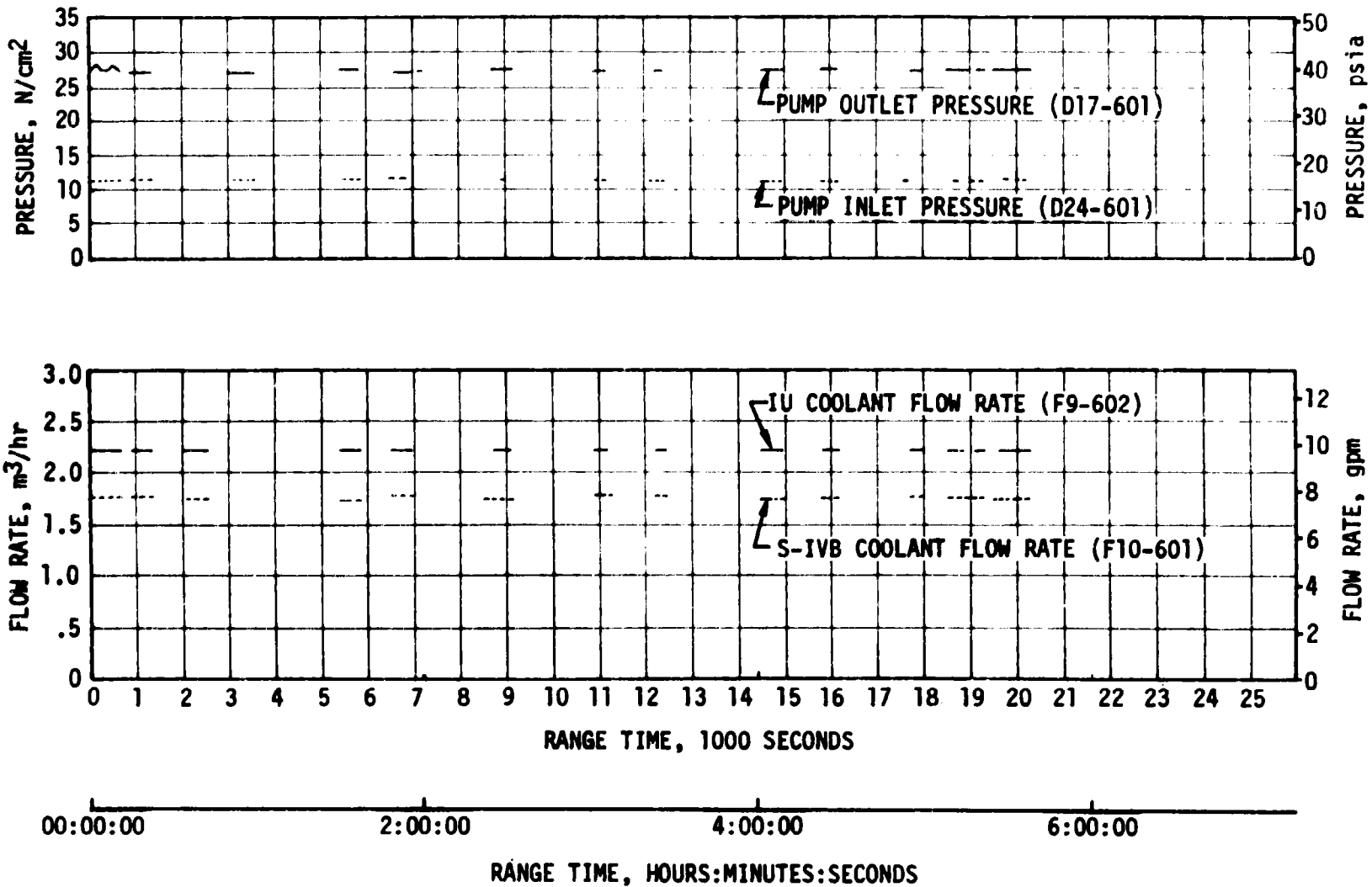


Figure 14-3. IU TCS Hydraulic Performance

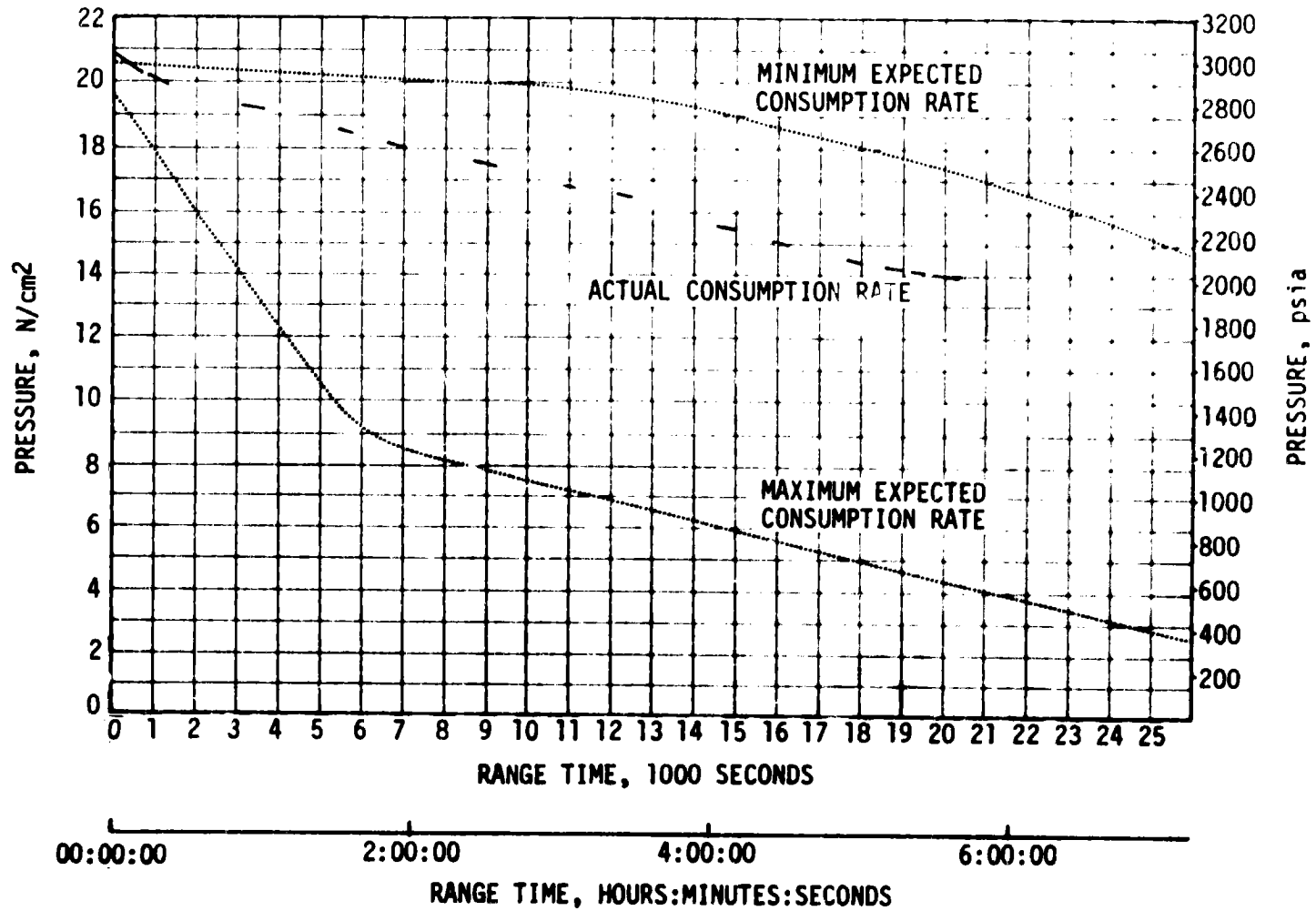


Figure 14-4. IU TCS GN₂ Sphere Pressure (D25-601)

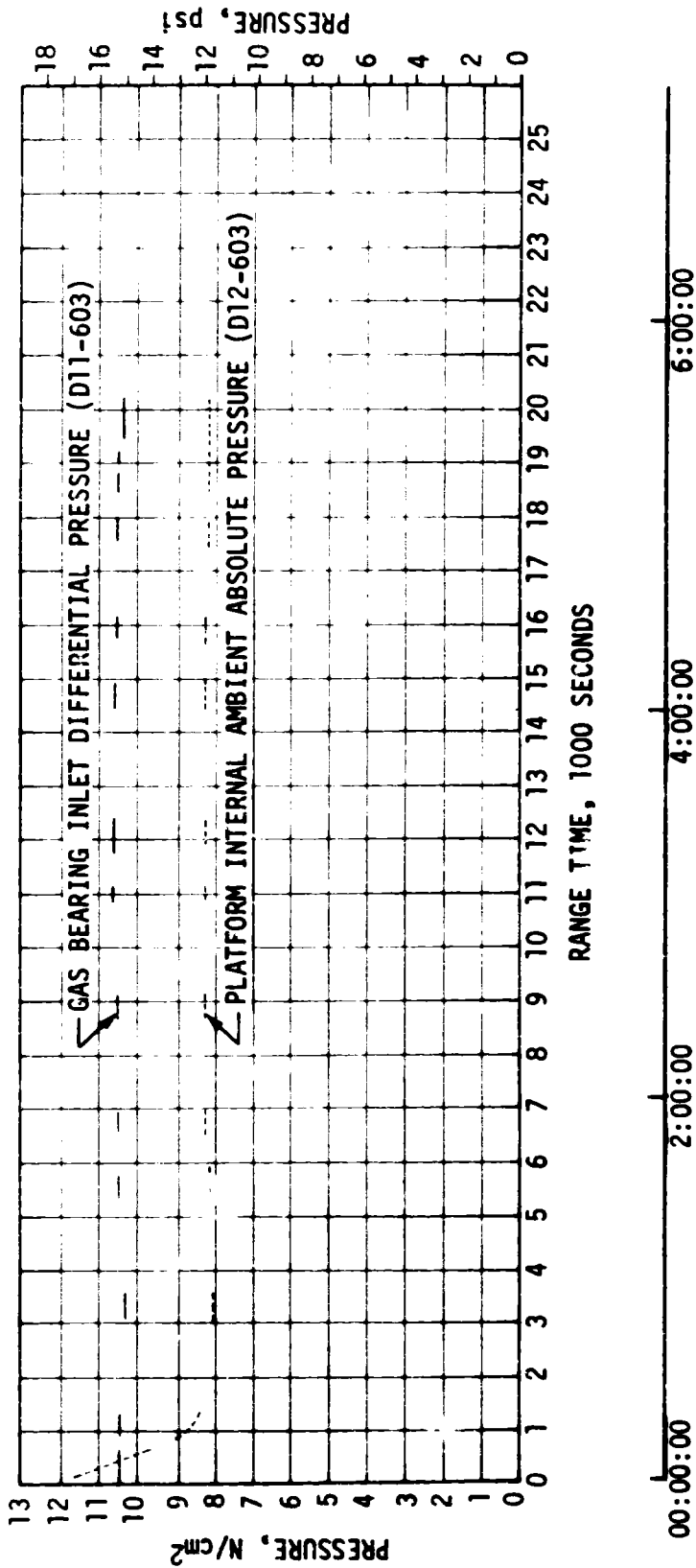
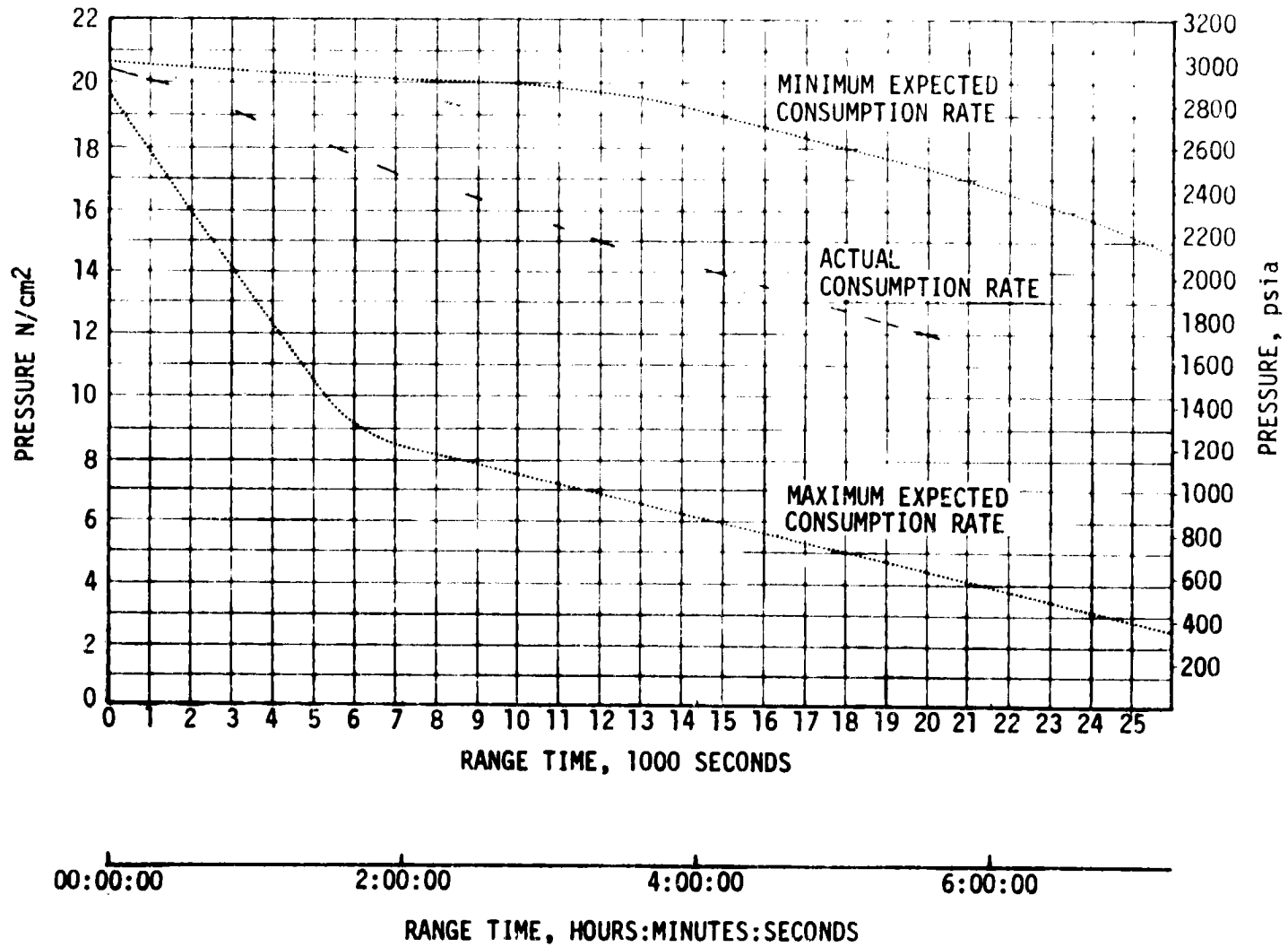


Figure 14-5. IU Inertial Platform Internal Gas Bearing GN₂ Pressure

Figure 14-6. 1U GBS GN₂ Sphere Pressure (D10-603)

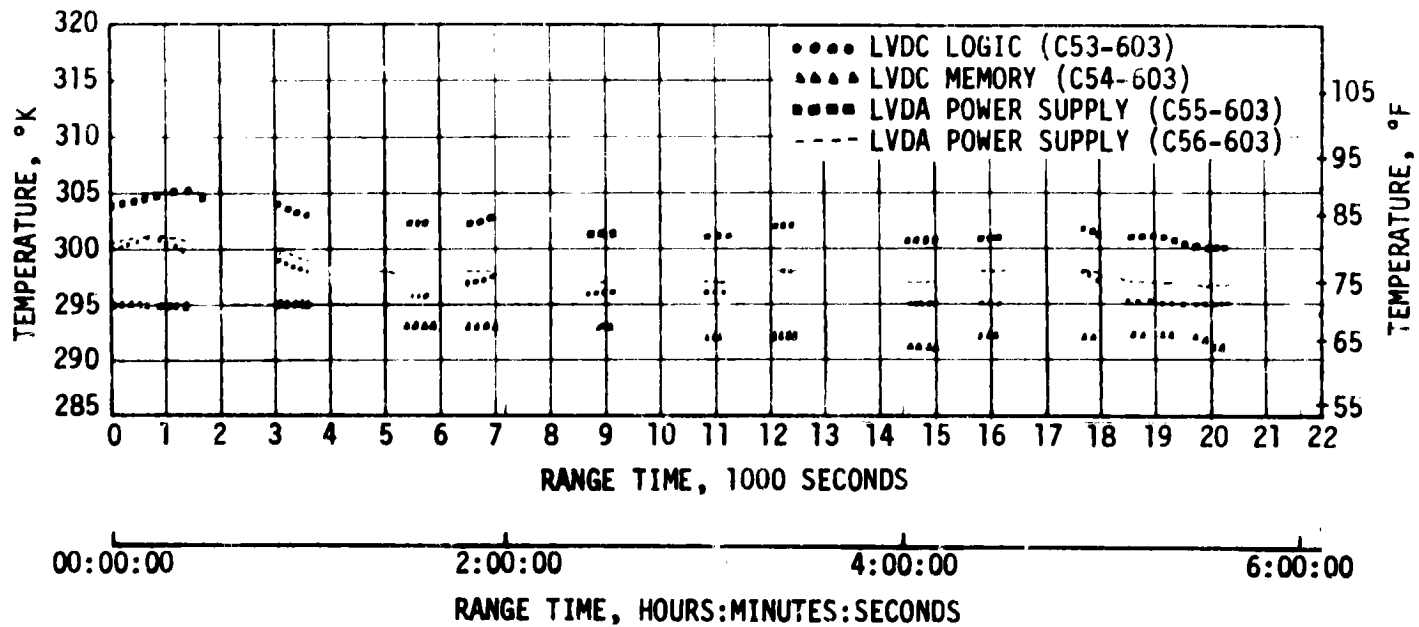


Figure 14-7. Selected IU Component Temperatures

REPRODUCIBILITY OF THE ORIGINAL PAGE IS POOR

- ST-124M (C34-603)
- ACCELEROMETER SIGNAL CONDITIONER (C62-603)
- PLATFORM ELECTRONICS ASSEMBLY (C63-603)
- ▲▲▲▲ 250 VOLT-AMPERE INVERTER (C67-603)
- FLIGHT CONTROL COMPUTER (C69-603)

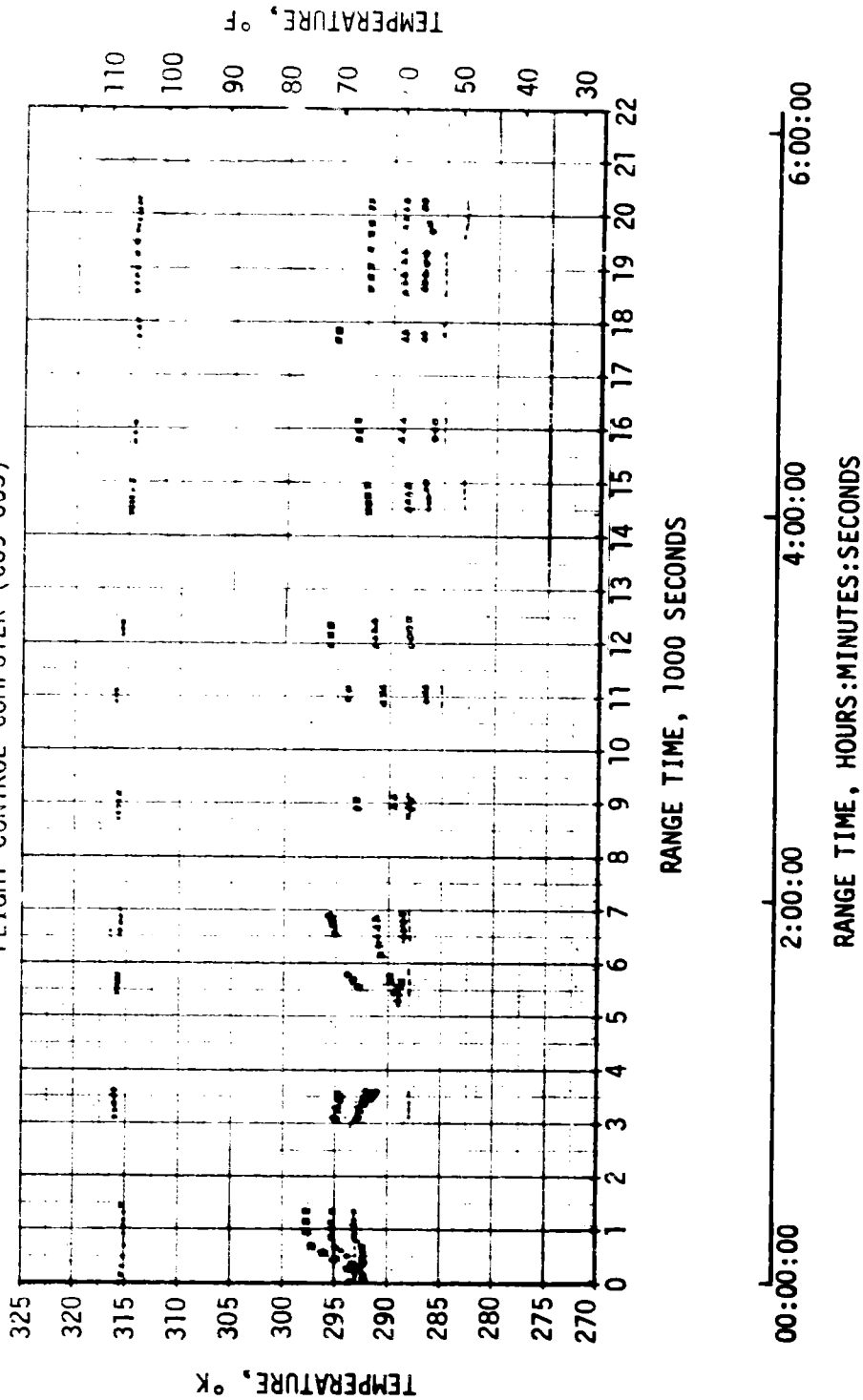


Figure 14-8. Selected IU Component Temperatures

SECTION 15

DATA SYSTEMS

15.1 SUMMARY

The SA-208 vehicle data systems performed satisfactorily except for a problem with the Instrument Unit (IU) DP-1 telemetry link. This problem resulted in the loss of some IU and S-IVB data, but sufficient data were recovered to reconstruct all important flight parameters and to provide real time mission support. The overall measurement system reliability was 100 percent. The usual telemetry interference due to flame effects and staging was experienced. Usable telemetry data were received until 20,460 seconds (5:41:00). Good tracking data were received from the C-Band radar, with Kwajalein (KWJ) indicating final Loss of Signal (LOS) at approximately 21,180 seconds (5:53:00). The Secure Range Safety Command Systems on the S-IB and S-IVB stages were ready to perform their functions properly, on command, if flight conditions during launch phase had required destruct. The Digital Command System (DCS) performed satisfactorily from liftoff through deorbit. In general, ground engineering camera coverage was good.

15.2 VEHICLE MEASUREMENT EVALUATION

The SA-208 launch vehicle had 706 measurements scheduled for flight; five measurements were waived prior to start of the automatic countdown sequence leaving 701 measurements active for flight. All measurements were successful during flight, resulting in an overall measurement system reliability of 100 percent. A summary of measurement reliability is presented in Table 15-1 for the total vehicle and for each stage. The waived measurements and partially failed measurements are listed by stage in Tables 15-2 and 15-3. These measurement problems had no significant impact on post-flight evaluation.

15.3 AIRBORNE TELEMETRY SYSTEM EVALUATION

The S-IB telemetry system provided good data from liftoff until the stage exceeded each subsystem's range limitations. The S-IVB CP-1 link and the IU DF-1 link provided good data throughout the mission. The IU DP-1 link performance was normal until 600 seconds when the Radio Frequency (RF) power output and the ground-received signal strength dropped abruptly. This anomaly is discussed in detail in paragraph 15.3.1. Real time mission support was provided primarily through use of the IU measurements cross-strapped to the S-IVB CP-1 telemetry link. The IU DP-1 link was used when H60-603 (Guidance Computer Operation) data were of critical importance. This support mode proved satisfactory and no significant data were lost. In spite of the very low DP-1 link signal strength, sufficient

Table 15-1. SA-208 Measurement Summary

MEASUREMENT CATEGORY	S-IB STAGE	S-IVB STAGE	INSTRUMENT UNIT	TOTAL VEHICLE
Scheduled	266	239	201	706
Waived	1	4	0	5
Failed	0	0	0	0
Partial Failed	2	1	0	3
Questionable	0	0	0	0
Reliability Percent	100%	100%	100%	100%

data were recovered from the ground station tapes to adequately support postflight analysis and to reconstruct all important flight information. Data dropouts, as shown in Table 15-4, were experienced. These dropouts are similar to those on previous flights and are not indicative of flight hardware problems. No S-IB telemetry dropout occurred even though the usual signal strength variations and electrical noise bursts were present during the first 13 seconds of flight. As on previous flights, S-IB/S-IVB separation caused IU and S-IVB data dropouts at approximately 143 seconds. All inflight calibrations occurred as programmed and were within specifications. The last telemetry signal was received at approximately 20,460 seconds (5:41:00) by the Honeysuckle ground station. A summary of IU and S-IVB telemetry coverage showing Acquisition of Signal (AOS) and LOS for each station is shown in Figure 15-1.

15.3.1 IU DP-1 Telemetry Link RF Power Output Variations

At 600 seconds, during the vehicle pitch maneuver to local horizontal, the Bermuda ground station observed an abrupt drop in the IU DP-1 telemetry link signal strength from -82 dbm to -104 dbm. Measurement J29-602 detected a simultaneous drop in Pulse Code Modulation (PCM) RF power output from 17.9 watts to 0.3 watts. In addition, measurement M18-601 (6D30 Battery Current) registered a slight decrease. Strong signals from the DF-1 and CP-1 telemetry links continued to be received. At 1081 seconds, while physical shocks associated with Command and Service Module (CSM) separation were sensed in the IU, measurement J29-602 detected an abrupt

Table 15-2. SA-208 Flight Measurements Waived Prior to Flight

MEASUREMENT NUMBER	MEASUREMENT TITLE	NATURE OF FAILURE	REMARKS
S-IB STAGE			
L0501-0F1	Fuel Level Discrete	Intermittent output from probe.	Access to probe located inside fuel tank no. 1 was not feasible. Waiver 1-C-208-1. Valid data received during flight.
S-IVB STAGE			
N0037-414	Misc-Qty-Oxid Tank Mod-1 (APS)	Intermittent and erratic response to bellows extension and retraction during APS checkout and loading.	Inflight data was erratic but of sufficient quality to determine measurement trends.
N0038-415	Misc-Qty-Oxid Tank Mod-2 (APS)		
N0039-414	Misc-Qty-Fuel Tank Mod-1 (APS)		
N0040-415	Misc-Qty-Fuel Tank Mod-2 (APS)		

Table 15-3. SA-208 Measurement Malfunctions

MEASUREMENT NUMBER	MEASUREMENT TITLE	NATURE OF FAILURE	TIME OF FAILURE (RANGE TIME)	DURATION OF SATISFACTORY OPERATION	REMARKS
PARTIAL FAILURES, S-IB STAGE					
XCO089-001	Temperature, Gear Case Lubricant	Measurement dropped to zero and remained there.	116 sec.	116 sec.	Probably caused by either transducer, amplifier, or wiring failure.
D0013-002	Pressure, LOX Pump Inlet	Measurement value decreased and became noisy. Returned to normal 80 sec. later.	20 sec.	62 sec.	Failure signature indicative of wiper lifting in pressure sensor potentiometer.
PARTIAL FAILURES, S-IVB STAGE					
D0066-415	Press-Oxid Sup Manf Mod 2 (APS)	Unrealistic measurement increase of 12 to 15 psi.	60 sec.	60 sec.	Data received after the failure was valid for determining measurement trend. Probable cause of failure was transducer potentiometer wiper displacement resulting from max "Q" vibration.

REPRODUCIBILITY OF THE ORIGINAL PAGE IS POOR

Table 15-4. SA-208 Launch Vehicle Telemetry Links Performance Summary

LINK	FREQUENCY (MHz)	MODULATION	STAGE	FLIGHT PERIOD (RANGE TIME, SEC)	DATA DROPOUTS	
					RANGE TIME (SEC)	DURATION (SEC)
GF-1	240.2	FM/FM	S-IB	0 to 397	-	-
GP-1	256.2	PCM/FM	S-IB	0 to 397	-	-
CP-1	258.5	PCM/FM	S-IVB	0 to 20,460	143.2	1.8
DF-1	250.7	FM/FM	IU	0 to 20,460	142.7	2.1
DP-1	255.1	PCM/FM	IU	0 to 20,460	142.7	2.1

PCM RF power output increase to 16.5 watts. Also the ground-received signal strength returned to normal and measurement M18-601 registered a slight increase. By 1237 seconds, the PCM RF power output had increased to 18.0 watts. The DP-1 signal strength continued strong through the Madrid and Apollo Range Instrumented Aircraft (ARIA) 3 passes on revolution one. Between ARIA 3 LOS and Texas AOS, the signal strength dropped again and then continued weak throughout the remainder of the mission. Changes in measurements J29-02 and M18-601 corresponding to the signal strength changes were also present. The last drop in signal strength occurred while the vehicle was experiencing unplanned velocity changes and vibration. The apparent correlation with vehicle movement, shock, and vibration indicates that the anomaly was caused by a mechanical problem. Figure 15-2 shows a history of the DP-1 telemetry link RF power output variations.

A series of tests was conducted in an effort to simulate the flight anomaly signature. The telemetry subsystems flight configuration was breadboarded using lab models of telemetry RF hardware and cables built to IU requirements. Since only the DP-1 link was affected and both the signal strength and the RF power output indicated the malfunction, the problem area was isolated to either the PCM RF Assembly, Directional Coupler, RF Multicoupler, or the interconnecting cables. The tests isolated the anomaly to the PCM RF assembly.

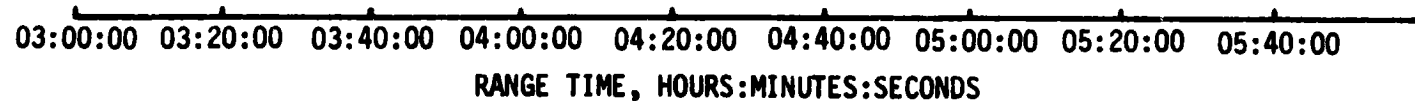
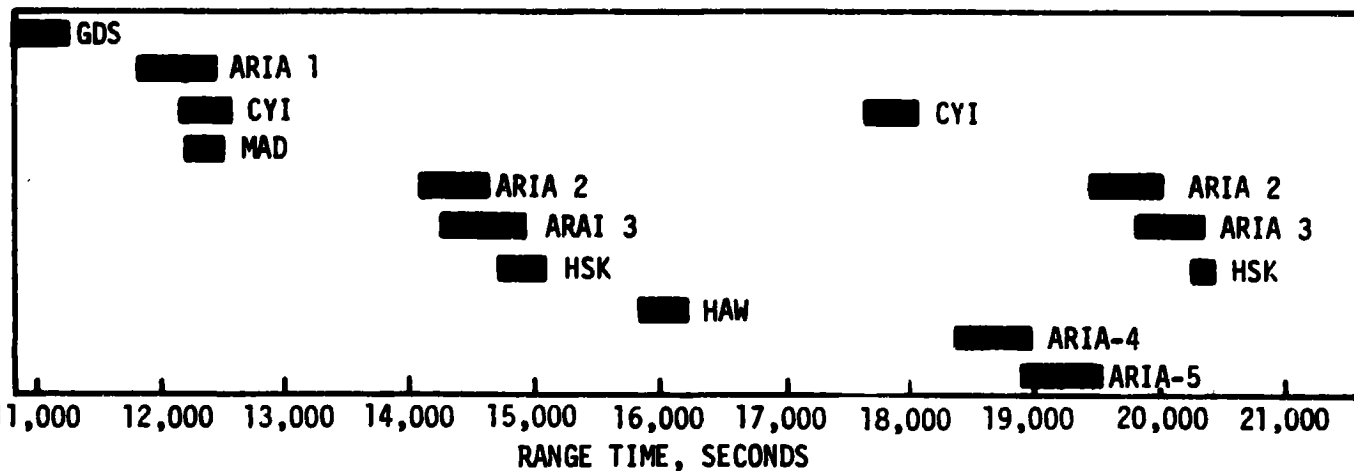
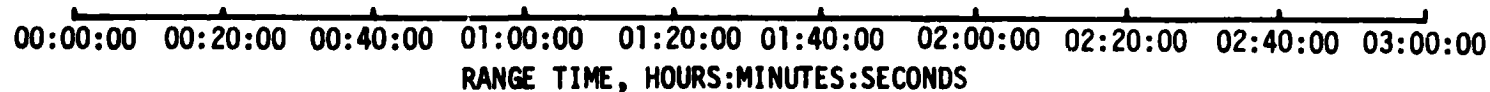
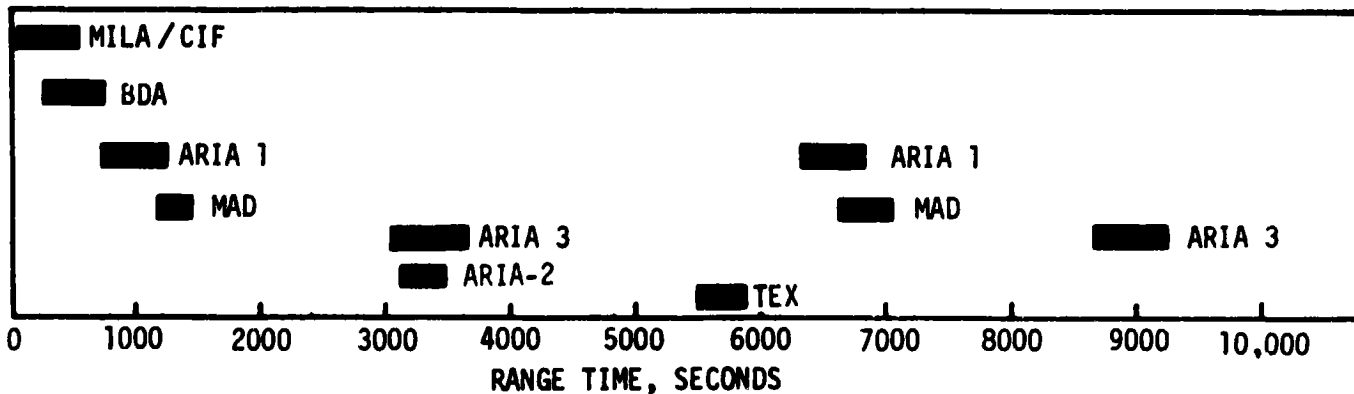


Figure 15-1. SA-208 Telemetry Ground Station Coverage

- ▽ BEGIN MANEUVER TO LOCAL HORIZONTAL
- ▽ CSM SEPARATION
- ▽ UNPLANNED VEHICLE VELOCITY CHANGES AND VIBRATION

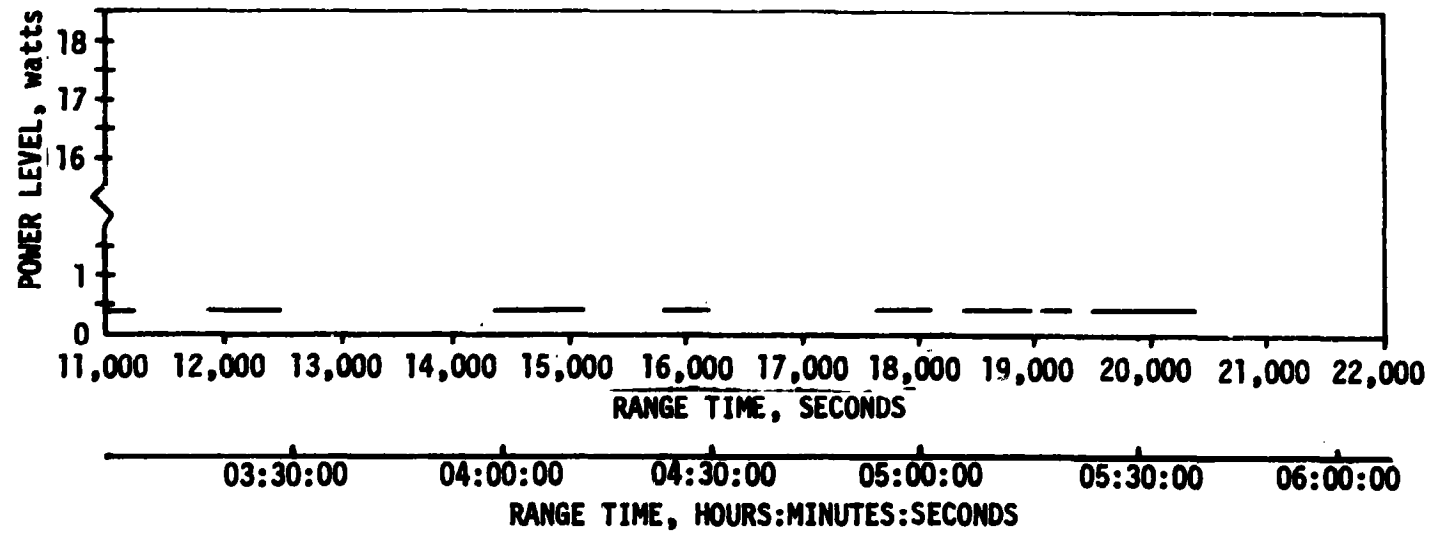
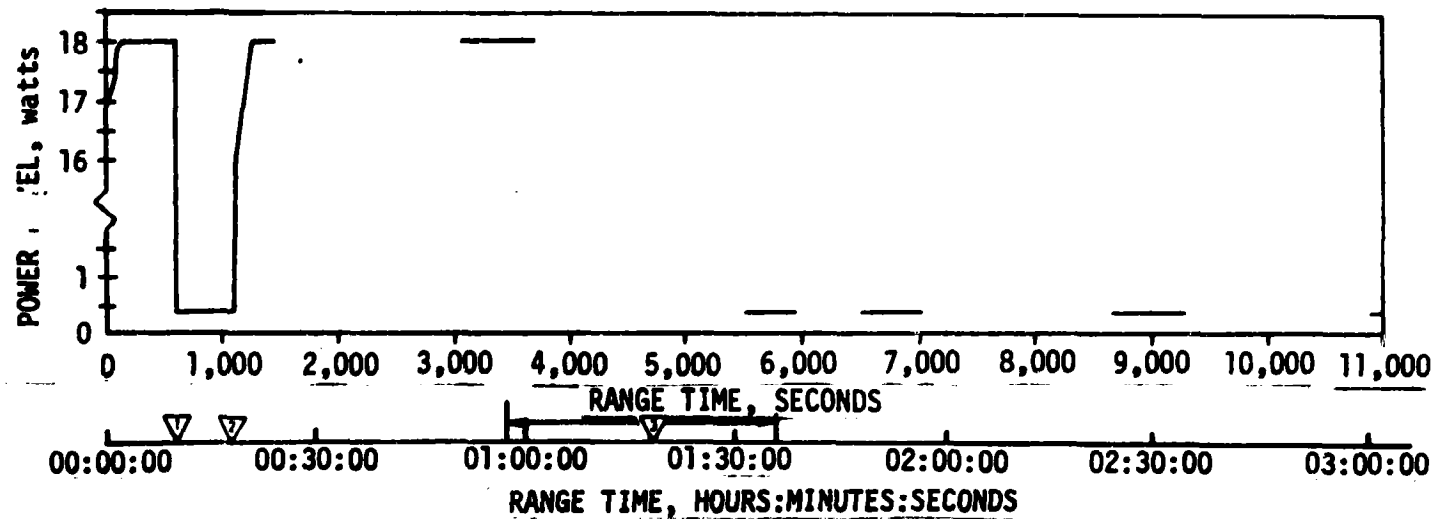


Figure 15-2. SA-208 DP-1 Link RF Power Output

The flight anomaly signature was closely simulated by introducing failures at two points in the PCM RF Assembly: an open circuit at the RF input to the power amplifier subassembly and a short circuit in the antenna filter subassembly. Opening the input to the power amplifier resulted in J29-602 decreasing to 0.3 watts (a 24 db drop in power output) and a 150 mA input current drop. Shorting the antenna filter produced similar results; however, a short in the filter is considered unlikely because of the filter mechanical construction. During these tests, it was discovered that the retaining nut on the power amplifier subassembly RF input connector prevented the mating cable connector from seating properly which resulted in relative motion between the cable connector and the female receptacle.

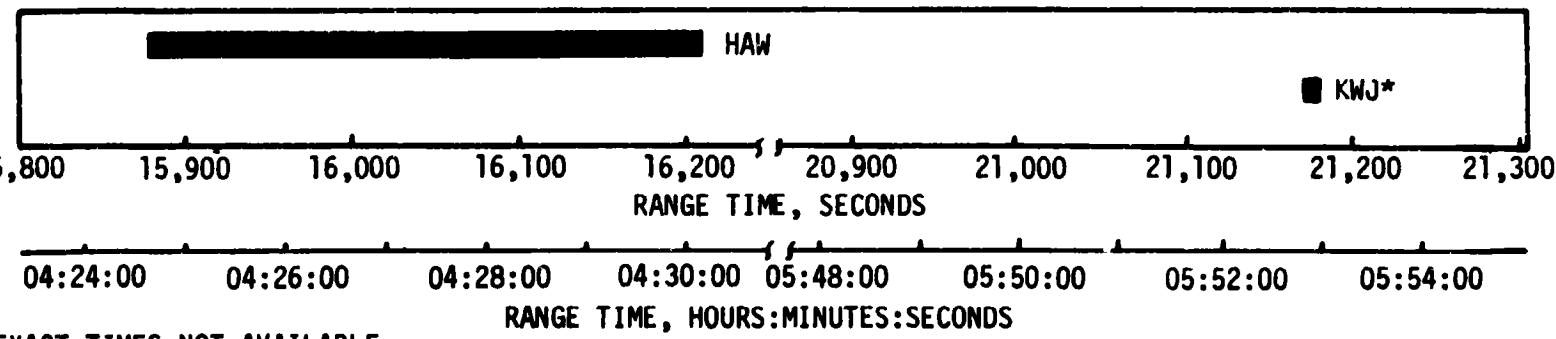
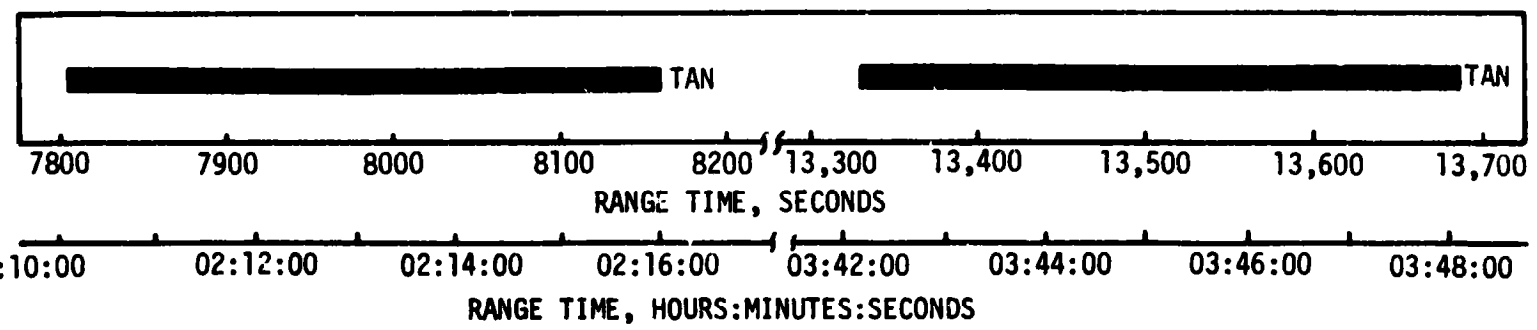
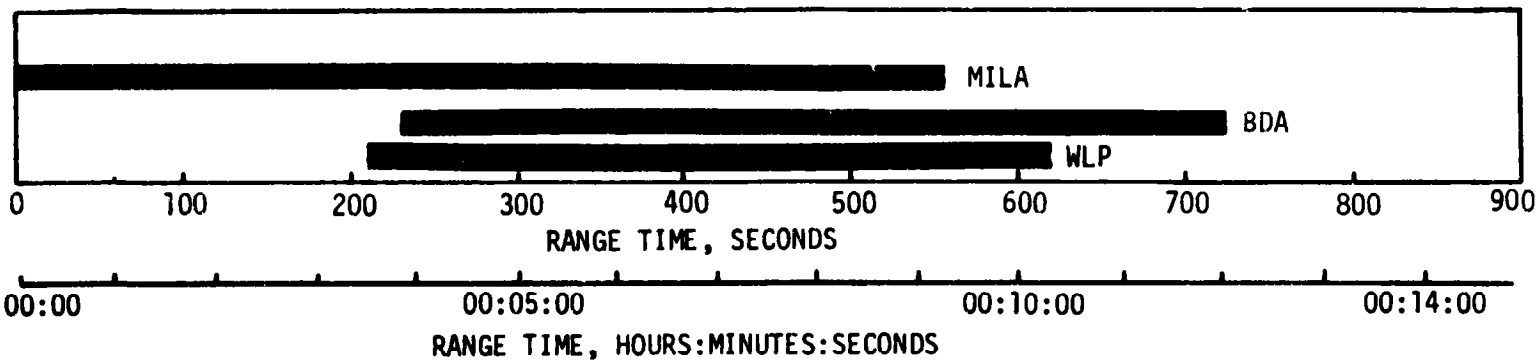
Attempts were made to simulate the flight anomaly signature by inducing failures inside the transmitter subassembly in the RF Assembly. A failure in the transmitter subassembly could result from a defective solder joint or a piece of loose foreign material creating an intermittent short. Accessible suspect circuit areas were shorted but did not reproduce the flight anomaly signature. However, this does not discount the possibility of a problem in the transmitter subassembly since more than half of the suspect circuit areas are not accessible for probing to simulate a failure. Cracked solder joints have been found, through inspection, in similar transmitters.

In summary, the observed anomalous behavior was probably caused by one of the following: 1) Incomplete connector seating at the power amplifier RF input, 2) loose conductive material within the transmitter, or 3) a bad solder joint within the transmitter.

Although the exact cause of the anomaly cannot be determined, corrective action has been taken to eliminate as many of the possible failure modes as can be accomplished without affecting schedules. Corrective action for the rescue mission on SA-209 IU RF assemblies consisted of reworking the power amplifier subassembly RF input connector to obtain proper seating of the mating cable connector and inspection of this cable connector for a broken or bent center pin. The connector rework consisted of removing the lock washer which was beneath the retaining nut and then securing the nut with a locking compound. Corrective action planned for the Apollo Soyuz Test Program (ASTP) mission consists of inspection, solder joint rework in the transmitters, and power amplifier RF input connector rework on all stages.

15.4 C-BAND RADAR SYSTEM EVALUATION

The C-Band radar performed satisfactorily during flight. A summary of C-Band radar coverage time from AOS to LOS for each station is shown in Figure 15-3. As on previous missions, phase front disturbances were observed at Merritt Island Launch Area during boost phase. These phase front disturbances result from severe antenna nulls or distorted beacon returns and cause momentary tracking errors at the ground stations.



*EXACT TIMES NOT AVAILABLE

Figure 15-3. SA-208 C-Band Acquisition and Loss Times

15-8

The only reported problem during orbital operations occurred at Hawaii (HAW). HAW acquired late because the predicted acquisition time and azimuth supplied to them were wrong. No problems with the onboard equipment were reported.

Last contact with the IU was made by KWJ during re-entry. KWJ reportedly beacon tracked for a few seconds around 21,180 (5:53:00) at a very low elevation angle. Exact AOS and LOS times for KWJ are not available.

15.5 SECURE RANGE SAFETY COMMAND SYSTEMS EVALUATION

Telemetered data indicated that the command antennas, receivers/decoders, exploding bridge wire networks, and destruct controllers on each powered stage functioned properly during flight. They were in the required state-of-readiness if flight conditions during the launch had required vehicle destruct. Since no arm/cutoff or destruct commands were required, all data except receiver signal strength remained unchanged during the flight. Power to the S-IVB stage range safety command systems was cut off at 595.1 seconds by ground command, thereby deactivating (safing) the systems.

15.6 DIGITAL COMMAND SYSTEM EVALUATION

The DCS performed satisfactorily throughout this mission. Twelve commands were initiated by Mission Control Center-Houston and all were accepted by the onboard equipment. Table 15-5 lists the commands transmitted to the IU.

The first command was issued to keep the launch vehicle from going through a programmed maneuver to retrograde attitude, because CSM separation had not been verified. When CSM separation was verified, a command was issued at 1332 seconds, returning the computer to its normal program. All other commands were issued as scheduled.

15.7 GROUND ENGINEERING CAMERAS

In general, ground camera coverage was good. Fifty-one items (45 from fixed cameras and 6 from tracking cameras) were received from Kennedy Space Center for evaluation. Data loss was experienced on 14 items: three cameras jammed, two had erratic timing, one had an incorrect field of view, six had their field of view obscured by falling frost and ice, one had severely underexposed film and one tracking camera never acquired the vehicle. As a result of the 14 failures, system efficiency was 72.5%.

Table 15-5. SA-208 IU Commands

RANGE TIME		TRANS. STATION	COMMAND (NO. OF WORDS IN COMMAND)	NO. OF WORDS TRANS.	REMARKS
SECONDS	HRS:MIN:SEC				
1255	0:20:55	MAD	Execute Generalized Maneuver (21)	21	Accepted
1263	0:21:03	MAD	Memory Dump (7)	7	Accepted
1332	0:22:12	MAD	Return to Nominal Timeline (6)	6	Accepted
1334	0:22:14	MAD	Memory Dump (7)	7	Accepted
5600	1:33:20	TEX	Compressed Data Dump (1)	1	Accepted
10,940	3:02:20	GDS	Ladder Magnitude Limit (2)	2	Accepted
10,941	3:02:21	GDS	Memory Dump (7)	7	Accepted
10,954	3:02:34	GDS	Compressed Data Dump (1)	1	Accepted
15,897	4:24:57	HAW	S-IVB/IU Deorbit (8)	8	Accepted
15,914	4:25:14	HAW	Memory Dump (7)	7	Accepted
15,932	4:25:32	HAW	Compressed Data Dump (1)	1	Accepted
17,788	4:56:28	CYI	Compressed Data Dump (1)	1	Accepted

SECTION 16

MASS CHARACTERISTICS

16.1 SUMMARY

Total vehicle mass, determined from post-flight analysis, was within 1.47 percent of predicted from ground ignition through S-IVB/spacecraft separation. Hardware weights, propellant loads and propellant utilization were close to predicted values during flight.

16.2 MASS EVALUATION

Post-flight mass properties are compared with final predicted mass properties (MSFC Memorandum S&E-ASTN-SAE-73-92) and the post launch operational trajectory.

The post-flight mass properties were determined from an analysis of all available actual and reconstructed data from S-IB ignition through S-IVB cutoff. Dry weights of the launch vehicle are based on actual weighings and evaluation of the weight and balance log books (MSFC Form 998). Propellant loading and utilization was evaluated by stage contractors from propulsion system performance reconstructions. Spacecraft data were obtained from the Johnson Space Center.

Differences between predicted and actual dry weights of the inert stages and the loaded spacecraft were all within 0.54 percent of predicted, which is within acceptable limits.

During S-IB burn phase, the total vehicle mass was greater than predicted by 823 kilograms (1815 lbm) (0.06 percent) at ignition, and greater than predicted by 477 kilograms (1051 lbm) (0.26 percent) at physical separation. These small differences may be attributed to a larger than predicted propellant loading and a larger than predicted S-IB stage dry weight.

S-IB burn phase total vehicle mass is shown in Tables 16-1 and 16-2.

During S-IVB burn phase, the total vehicle mass was greater than predicted by 91 kilograms (201 lbm) (0.07 percent) at ignition, and less than predicted by 72 kilograms (160 lbm) (0.23 percent) at S-IVB stage cutoff signal. These differences are due primarily to a greater than predicted spacecraft weight and a less than expected residual. Total vehicle mass for the S-IVB burn phase is shown in Tables 16-3 and 16-4.

A summary of mass utilization and loss, both actual and predicted, from S-IB stage ignition through spacecraft separation is presented in Table 16-5. A comparison of actual and predicted mass, center of gravity, and moment of inertia is shown in Table 16-6.

Table 16-1. Vehicle Masses (Kilograms)

EVENT	GROUND IGNITION		FIRST MOTION		INBOARD ENGINE CUTOFF SIGNAL		OUTBOARD ENGINE CUTOFF SIGNAL		SEPARATION SIGNAL	
	PREU	ACTUAL	PREU	ACTUAL	PREU	ACTUAL	PREU	ACTUAL	PREU	ACTUAL
5-18 SIG DRY	35077	35170	35077	35170	35077	35170	35077	35170	35077	35170
LOX IN TANKS	283156	283801	271761	271761	1091	1271	0	0	0	0
LOX BELOW TANKS	3527	3527	3722	3722	3677	3677	1327	1327	1236	1236
LOX ULLAGE	13	13	35	35	188	188	1202	1202	1202	1202
RPI IN TANKS	124668	125091	122754	123023	2070	2068	331	331	748	367
RPI BELOW TANKS	2154	2157	2571	2594	257	254	2372	2372	2222	2275
RPI ULLAGE	2	2	0	0	26	26	27	27	27	27
HELIUM SUPPLY	35	35	34	34	11	11	10	10	10	10
NITROGEN	6	6	6	6	4	4	4	4	4	4
HYDRAULIC OIL	12	12	12	12	12	12	12	12	12	12
ORONITE	14	14	14	14	2	2	2	2	2	2
FROST	453	453	453	453	453	453	453	453	453	453
TOTAL 5-18 STAGE	452127	452820	445674	445740	48715	49674	43595	43880	42888	43197
5-1R/5-1VR DRY	2606	2606	2606	2606	2606	2606	2606	2606	2606	2606
RETRO PROPELLANT	481	481	481	481	481	481	481	481	481	481
TOTAL FIRST SIG	455215	455902	448762	448823	51304	52750	46644	46963	45846	46274
TOTAL 5-1VR SIG	114242	114602	114602	114602	114237	114237	114237	114237	114237	114237
INSTRUMENT UNIT	1860	1855	1860	1855	1855	1855	1860	1860	1860	1855
SPACECRAFT	20856	20871	20856	20871	20856	20871	20856	20871	20856	20871
TOTAL VEHICLE	594214	595038	587761	587761	587358	587358	58598	58598	58400	58325

REPRODUCIBILITY OF THE ORIGINAL PAGE IS POOR

Table 16-2. Vehicle Masses (Pounds)

EVENT	GROUND IGNITION		FIRST MOTION		INBOARD ENGINE CUTOFF SIGNAL		OUTBOARD ENGINE CUTOFF SIGNAL		SEPARATION SIGNAL	
	PRED	ACTUAL	PRED	ACTUAL	PRED	ACTUAL	PRED	ACTUAL	PRED	ACTUAL
RANGE TIME (SEC)	-3.00	-3.00	0.3	0.3	138.	137.8	140.98	141.29	142.3	142.5
S-IB STG DRY	83969.	84152.	83969.	84152.	83969.	84152.	83969.	84152.	83969.	84152.
LOX IN TANKS	624254.	624572.	612797.	612170.	2339.	2925.	0.	0.	0.	0.
LOX BELOW TANKS	7761.	7843.	8206.	8210.	8098.	8108.	2287.	2925.	2725.	2473.
LOX ULLAGE	30.	30.	79.	81.	2619.	2619.	2652.	2656.	2654.	2658.
RPI IN TANKS	274846.	275779.	270650.	271219.	4565.	5883.	774.	1649.	0.	836.
RPI BELOW TANKS	4748.	4761.	5682.	5697.	5682.	5697.	2215.	2229.	4900.	5017.
RPI ULLAGE	5.	5.	8.	8.	59.	58.	59.	59.	59.	59.
HELIUM SUPPLY	78.	78.	75.	75.	24.	24.	24.	24.	24.	23.
NITROGEN	15.	15.	15.	15.	9.	9.	9.	9.	9.	9.
HYDRAULIC OIL	28.	28.	28.	28.	28.	28.	28.	28.	28.	28.
ORONITE	33.	33.	33.	33.	6.	6.	6.	6.	6.	6.
FROST	1000.	1000.	1000.	1000.						
TOTAL S-IB STAGE	996770.	998298.	982544.	982690.	107400.	109512.	96025.	96740.	96376.	95234.
S-IB/S-IVB DRY	5747.	5734.	5747.	5734.	5747.	5734.	5747.	5734.	5747.	5734.
RETRO PROPELLANT	1062.	1062.	1062.	1062.	1062.	1062.	1062.	1062.	1062.	1062.
TOTAL FIRST STG	1003579.	1005094.	989353.	989486.	114209.	116308.	102834.	103536.	101185.	102030.
TOTAL S-IVB STG	256360.	256623.	256360.	256623.	256250.	256423.	256260.	256423.	256260.	256423.
INSTRUMENT UNIT	4101.	4091.	4101.	4091.	4101.	4091.	4101.	4091.	4101.	4091.
SPACECRAFT	45980.	46028.	45980.	46028.	45980.	46028.	45980.	46028.	45980.	46028.
TOTAL VEHICLE	1310021.	1311836.	1295794.	1296228.	420550.	422850.	409175.	410078.	407526.	408574.

16-3

THE QUALITY OF THIS REPORT IS POOR

REPRODUCIBILITY OF THE
ORIGINAL PAGE IS POOR

Table 16-3. Vehicle Masses (Kilograms)

	S-1B STAGE GROUND IGNITION		J-2 ENGINE START COMMAND		VALVE STAGE		J-2 ENGINE CUTOFF COMMAND		ORBITAL INSERTION	
	PRED	ACTUAL	PRED	ACTUAL	PRED	ACTUAL	PRED	ACTUAL	PRED	ACTUAL
RANGE TIME (SEC)	-3.		14337	14394	14487	14764	57964	57762	58964	58764
S-1VB STAGE DRY	10013.	10013.	9997.	9996.	9997.	9996.	9997.	9996.	9997.	9996.
ULL ROCKET CASES	97.	98.	97.	98.	97.	98.				
ULL ROCKET GRAIN	79.	79.	47.	47.						
LOX IN TANK	88251.	88158.	88251.	88158.	88125.	88049.	8822.	8822.	775.	823.
LOX BELOW TANK	180.	180.	180.	180.	180.	180.	180.	180.	180.	180.
LOX ULLAGE	11.	12.	11.	12.	14.	13.	15.	15.	15.	15.
LM2 IN TANK	17306.	17434.	17306.	17434.	17379.	17379.	764.	920.	794.	920.
LM2 BELOW TANK	26.	25.	26.	25.	26.	25.	26.	25.	21.	19.
M2 ULLAGE	72.	58.	72.	58.	72.	59.	215.	174.	215.	174.
MELIUM-LOX PRESS	114.	116.	114.	116.	114.	116.	41.	42.	41.	42.
APS PROPELLANT	59.	61.	59.	61.	59.	61.	57.	58.	57.	58.
GH2/START TANK	2.	2.	2.	2.	0.	0.	0.	0.	0.	0.
HYDRAULIC OIL	6.	6.	6.	6.	6.	6.	6.	6.	6.	6.
M2-HYD RESERVOIR	1.	1.	1.	1.	1.	1.	1.	1.	1.	1.
ENVIRONMENT FLUID	6.	12.	6.	12.	6.	12.	6.	12.	6.	12.
MELIUM-APS	1.	1.	1.	1.	1.	1.	1.	1.	1.	1.
MELIUM PNEUMATIC	5.	5.	5.	5.	5.	5.	5.	5.	5.	5.
FROST	45.	136.	0.	45.	0.	45.	0.	45.	0.	45.
TOTAL S-1VB STG	116402.	116402.	116188.	116202.	115964.	116034.	12274.	12184.	12219.	12126.
INSTRUMENT UNIT	1860.	1855.	1860.	1855.	1860.	1855.	1860.	1855.	1860.	1855.
SPACECRAFT	20856.	20877.	20856.	20877.	20856.	20877.	18094.	18094.	18094.	18094.
TOTAL VEHICLE	138999.	139155.	138905.	138996.	138680.	138764.	30628.	30759.	30773.	30706.

Table 16-4. Vehicle Masses (Pounds)

	S-1B STAGE GROUND IGNITION		J-2 ENGINE START COMMAND		MAINSTAGE		J-2 ENGINE CUTOFF COMMAND		ORBITAL INSERTION	
	PRED	ACTUAL	PRED	ACTUAL	PRED	ACTUAL	PRED	ACTUAL	PRED	ACTUAL
RANGE TIME (SEC)	-3.	-3.	143.7	143.94	144.7	147.4	579.4	577.2	589.4	587.2
S-1VB STAGE DRY	22077.	22075.	22041.	22039.	22041.	22039.	22041.	22039.	22041.	22039.
ULL ROCKET CASES	214.	217.	214.	217.	214.	217.				
ULL ROCKET GRAIN	176.	176.	105.	105.						
LOX IN TANK	194561.	194356.	194561.	194356.	194282.	15.	1770.	1214.	1710.	1154.
LOX BELOW TANK	397.	397.	397.	397.	397.	397.	397.	397.	367.	367.
LOX ULLAGE	25.	27.	25.	27.	32.	30.	367.	340.	367.	340.
LH2 IN TANK	38155.	38436.	38155.	38436.	38039.	38014.	1685.	2051.	1684.	2029.
LH2 BELOW TANK	58.	52.	58.	52.	58.	52.	58.	52.	48.	42.
LH2 ULLAGE	160.	130.	160.	130.	160.	152.	475.	384.	475.	384.
HELIUM-LOX PRESS	253.	257.	253.	257.	251.	256.	91.	94.	91.	94.
APS PROPELLANT	132.	135.	132.	135.	132.	135.	126.	129.	126.	129.
GH2/START TANK	5.	5.	5.	5.	1.	1.	1.	1.	1.	1.
HYDRAULIC OIL	15.	15.	15.	15.	15.	15.	15.	15.	15.	15.
N2-HYD RESERVOIR	3.	3.	3.	3.	3.	3.	3.	3.	3.	3.
ENV1 CONT FLUID	14.	27.	14.	27.	14.	27.	14.	27.	14.	27.
HELIUM-APS	3.	3.	3.	3.	3.	3.	3.	3.	3.	3.
HELIUM PNEUMATIC	12.	12.	12.	12.	12.	12.	12.	12.	12.	12.
FROST	100.	300.	0.	100.	0.	100.	0.	100.	0.	100.
TOTAL S-1VB STG	256360.	256623.	256153.	256316.	255657.	255348.	27059.	26661.	26938.	26739.
INSTRUMENT UNIT	4101.	4091.	4101.	4091.	4101.	4091.	4101.	4091.	4101.	4091.
SPACECRAFT	45980.	46028.	45980.	46028.	45980.	46028.	36004.	36552.	36804.	36852.
TOTAL VEHICLE	306441.	306742.	306234.	306435.	305738.	305968.	67464.	67804.	67843.	67882.

REPRODUCIBILITY OF THE ORIGINAL FIGURES IS POOR

16-5

REPRODUCIBILITY OF THE
ORIGINAL PAGE IS POOR

Table 16-5. Flight Sequence Mass Summary

	ACTUAL		PREDICTED	
	KG	LBM	KG	LBM
S-IB STAGE AT GROUND IGNITION (G.I.)	452520.	998296.	452127.	996770.
S-IB/S-IVB INTERSTAGE AT G.I.	3082.	6796.	3080.	6809.
S-IVB STAGE AT G.I.	116402.	256623.	116282.	256360.
INSTRUMENT UNIT AT G.I.	1855.	4091.	1860.	4101.
CSM:SLA:LES	20877.	46028.	20856.	45980.
FIRST FLIGHT STAGE AT G.I.	595036.	1311836.	594214.	1310021.
THRUST BUILDUP PROP	-7079.	-15608.	-6453.	-14226.
FIRST FLIGHT STAGE AT FIRST MOTION	587956.	1296226.	587761.	1295794.
MAIN STAGE PROP	-400092.	-882054.	-400337.	-882593.
FROST	-433.	-1000.	-453.	-1000.
SEAL PURGE (N2)	-2.	-6.	-2.	-6.
GEAR BOX CONSUMPTION (RP-1)	-320.	-706.	-320.	-706.
FUEL ADDITIVE (ORONITE)	-12.	-27.	-12.	-27.
I.E.T.D. PROP	-977.	-2136.	-991.	-2183.
S-IVB FROST	-90.	-200.	-45.	-100.
FIRST FLIGHT STAGE AT O.E.C.O.S.	186008.	410078.	185598.	409175.
OETD TO SEP PROP	-696.	-1534.	-763.	-1683.
FIRST FLIGHT STAGE AT SEPARATION (PHYSICAL)	185312.	408543.	184835.	407492.
S-IB STAGE AT SEPARATION	-43184.	-95205.	-42792.	-94342.
S-IB/S-IVB INTERSTAGE	-3332.	-6796.	-3088.	-6809.
S-IVB AFT FRAME	-14.	-31.	-14.	-31.
S-IVB ULLAGE ROCKET PROPELLANT	-32.	-71.	-32.	-71.
S-IVB DETONATION PACKAGE	-2.	-5.	-2.	-5.
SECOND FLIGHT STAGE AT IGNITION (ESC)	138996.	306433.	138903.	306234.
THRUST BUILDUP PROP	-162.	-353.	-173.	-386.
ULLAGE ROCKET PROPELLANT	-47.	-103.	-47.	-103.
GM2 START TANK	-1.	-4.	-1.	-4.
SECOND FLIGHT STAGE AT 90 PERCENT THRUST	138734.	305906.	138606.	305733.

Table 16-5. Flight Sequence Mass Summary (Continued)

	ACTUAL		PREDICTED	
	KG	LBM	KG	LBM
SECOND FLIGHT STAGE AT 90 PERCENT THRUST	138784.	305968.	138680.	305738.
AUX-PROP. POWER ROLL	-2.	-6.	-2.	-6.
MAINSTAGE	-103765.	-228764.	-103590.	-228577.
ULLAGE ROCKET CASES	-98.	-217.	-97.	-214.
LES	-4162.	-9176.	-4162.	-9176.
SECOND FLIGHT STAGE AT ECC	30755.	67804.	30828.	67964.
THRUST DECAY PROP	-36.	-81.	-36.	-81.
PROP BELOW VALVE	-18.	-40.	-18.	-40.
SECOND FLIGHT STAGE AT ETD	30700.	67682.	30773.	67843.
CSM	-14916.	-32885.	-14894.	-32837.
SLA PANELS ROTATED	0.	0.	0.	0.
VENT	-229.	-506.	-90.	-199.
CSM SEPARATED	15554.	34291.	15788.	34806.
S-IVB STAGE	-11899.	-26233.	-12128.	-26738.
V.I.U.	-1355.	-4091.	-1860.	-4101.
SLA	-1799.	-3967.	-1799.	-3967.

REPRODUCIBILITY OF THE
ORIGINAL PAGE IS POOR

Table 16-6. Mass Characteristics Comparison

EVENT	MASS		LONGITUDINAL C.G. (X STA.)		RAJIAL C.G.		ROLL MOMENT OF INERTIA		PITCH MOMENT OF INERTIA		YAW MOMENT OF INERTIA	
	KILO POUNDS	U/U DEV.	METERS INCHES	DELTA INCHES	PETERS INCHES	DELTA INCHES	KG-M ² X10 ⁻⁶	DEV. X10 ⁻⁶	KG-M ² X10 ⁻⁶	DEV. X10 ⁻⁶	KG-M ² X10 ⁻⁶	DEV. X10 ⁻⁶
S-1B STAGE DRY	PRED		30088	8.605	0.6179	0.223	0.223	2.590			2.590	
	ACTUAL		30171	8.620	0.6154	0.0025						
S-1B/S-1VB INTER-STAGE TOTAL	PRED		3089	26.710	0.559	0.223	0.001	2.594	0.16	2.594	0.16	
	ACTUAL		6809	1051.6	0.559	0.0000						
S-1VB STAGE DRY AT G.I.	PRED		10111	33.345	0.6112	0.073	0.073	0.269		0.269		
	ACTUAL		22291	1301.0	0.6112							
INSTRUMENT UNIT TOTAL	PRED		1856	42.788	0.4012	0.074	0.074	0.269	0.10	0.270	0.10	
	ACTUAL		4091	1684.6	0.4012	0.074	0.074	0.007	0.007	0.001	0.008	0.008
SPACECRAFT TOTAL	PRED		20526	55.775	0.6803	0.039	0.039	0.240		0.240		
	ACTUAL		45980	2195.9	0.6152							
1ST FLIGHT STAGE AT IGNITION	PRED		20878	55.778	0.6032	0.0000	0.0000	0.240		0.240		
	ACTUAL		46028	2196.0	0.6162	0.0000	0.0000	0.240	0.000	0.240	0.000	0.000
1ST FLIGHT STAGE AT FIRST MOTION	PRED		594216	19.006	0.0099	2.123	2.123	77.307		77.309		
	ACTUAL		1310021	748.2	0.3905							
1ST FLIGHT STAGE AT FIRST MOTION	PRED		594585	19.008	0.0071	0.0027	0.0027	77.307		77.307		
	ACTUAL		1310836	748.3	0.0071	0.0027	0.0027	77.307	0.16	77.453	0.16	
1ST FLIGHT STAGE AT FIRST MOTION	PRED		587762	18.948	0.0101	2.123	2.123	77.307		77.307		
	ACTUAL		1295794	746.0	0.6004							
1ST FLIGHT STAGE AT FIRST MOTION	PRED		587959	18.949	0.0073	0.0027	0.0027	77.307		77.307		
	ACTUAL		1296228	746.0	0.02906	0.1096	0.01	77.461	0.14	77.483	0.14	

EVENT	MASS		LONGITUDINAL		RADIAL		ROLL MOMENT		PITCH MOMENT		YAW MOMENT	
	KILO	POUNDS	DEV. INCHES	DELTA	METERS	INCHES	DELTA	KG-M2	O/O	KG-M2	O/O	KG-M2
1ST FLIGHT STAGE PRED	18999.0	29.205	0.031	1.006	0.427	39.095	39.095	39.095	39.097	39.097	39.097	39.097
1ST FLIGHT STAGE PRED	40917.0	1149.0	0.000	1.006	0.427	39.095	39.095	39.097	39.097	39.097	39.097	39.097
AT OUTWARD ENGINE												
CUTOFF SIGNAL	18608.0	29.181	-0.023	0.0229	-0.0102	0.427	0.427	0.427	39.097	39.097	39.097	39.097
ACTUAL	41007.0	0.22	1.006	-0.92	0.9035	-0.4029	0.427	0.427	39.097	39.097	39.097	39.097
1ST FLIGHT STAGE PRED	18635.0	29.304	0.0334	1.006	0.423	38.647	38.647	38.649	38.649	38.649	38.649	38.649
1ST FLIGHT STAGE PRED	40749.0	1153.7	1.006	1.006	0.423	38.647	38.647	38.649	38.649	38.649	38.649	38.649
AT SEPARATION (PHYSICAL)												
ACTUAL	40854.0	0.26	1.006	-1.78	0.9135	-0.4029	0.423	38.649	38.649	38.649	38.649	38.649
18905.0	35.905	0.0251	0.9914	0.136	11.264	11.270	11.270	11.270	11.270	11.270	11.270	11.270
2ND FLIGHT STAGE PRED	30623.0	1409.6	0.9914	0.136	11.264	11.270	11.270	11.270	11.270	11.270	11.270	11.270
AT IGNITION (ESC)												
ACTUAL	30643.0	0.07	1.000	0.41	0.9932	0.0018	0.136	11.270	11.270	11.270	11.270	11.270
2ND FLIGHT STAGE PRED	30573.0	1409.7	0.9914	0.135	11.266	11.267	11.267	11.267	11.267	11.267	11.267	11.267
AT 90 PERCENT THRUST												
ACTUAL	30598.0	0.08	1.001	0.36	0.9932	0.0018	0.135	11.270	11.270	11.270	11.270	11.270
3082.0	44.410	0.1086	0.1086	0.132	3.085	3.085	3.085	3.085	3.085	3.085	3.085	3.085
2ND FLIGHT STAGE PRED	6764.0	1748.4	4.2768	0.132	3.085	3.085	3.085	3.085	3.085	3.085	3.085	3.085
AT CUTOFF SIGNAL												
ACTUAL	6750.0	1766.3	4.2768	0.132	3.085	3.085	3.085	3.085	3.085	3.085	3.085	3.085
2ND FLIGHT STAGE PRED	6784.0	1749.5	4.2768	0.132	3.085	3.085	3.085	3.085	3.085	3.085	3.085	3.085
AT ETD												
ACTUAL	6782.0	1767.4	4.2768	0.132	3.085	3.085	3.085	3.085	3.085	3.085	3.085	3.085
2ND FLIGHT STAGE PRED	6783.0	1749.5	4.2768	0.132	3.085	3.085	3.085	3.085	3.085	3.085	3.085	3.085
SPACECRAFT SEP-ARATED												
PRED	1578.0	35.594	0.1492	5.8777	0.128	0.004	0.004	0.004	0.004	0.004	0.004	0.004
ACTUAL	34291.0	-1.47	1.4017	-0.10	6.0108	0.1326	0.0033	0.0033	0.0033	0.0033	0.0033	0.0033

Table 16-6. Mass Characteristics Comparison (Continued)

REPRODUCIBILITY OF THE ORIGINAL PAGE IS POOR

16-916-10

SECTION 17

SPACECRAFT SUMMARY

The SA-208/Skylab-4 space vehicle was launched at 14:01:23 Universal Time (UT) (09:01:23 Eastern Standard Time) on November 16, 1973, (visit day 1) from Launch Complex 39B at the Kennedy Space Center, Florida. This vehicle, for the third visit to the Saturn Work Shop (SWS), was manned by Lieutenant Colonel Gerald P. Carr, Commander; Doctor Edward D. Gibson, Science Pilot; and Lieutenant Colonel William R. Pogue, Pilot.

The launch was originally scheduled for November 11, 1973; however, cracks were found in the first stage fin assemblies (see Section 8.3.2) and the launch was rescheduled to allow time for fin replacement.

The Command and Service Module (CSM) was inserted into earth orbit approximately 9 minutes and 47 seconds after liftoff. The orbit achieved was 227.08 by 150.10 kilometers. Stationkeeping with the SWS began approximately 7.5 hours after liftoff. A hard dock was achieved at approximately 8 hours after liftoff following two unsuccessful docking attempts.

During the initial 4 days of the visit, the Commander and Pilot experienced stomach awareness and the flight plan activities were adjusted accordingly. During all subsequent visit activities, the crew health was good.

Activation of the SWS was accomplished during visit days 2 through 4. Included in the activation was the reservicing of the Airlock Module primary coolant loop. The first extravehicular activity was accomplished on visit day 7 and lasted approximately 6 1/2 hours. During the extravehicular activity, the Apollo Telescope Mount film was installed; the antenna for the failed experiment S-193, Microwave Radiometer/Scatterometer and Altimeter, was pinned; and the experiment D-024, Thermal Control Coating, panels, experiment S-149, Particle Collection impact detectors, experiment S-228, Transuranic Cosmic Rays, detector modules, and the experiment S-230, Magnetosphere Particle Composition, collector assembly were deployed.

The second extravehicular activity occurred on visit day 40 and lasted 7 hours. Work accomplished during the extravehicular activity included observing and documenting the Comet Kohoutek through use of the S-201K, Extreme Ultraviolet Electronographic Camera, and the T-025K, Coronagraph Contamination Measurement, experiments. In addition, the Apollo Telescope Mount film was replaced in all cameras, the experiment S-082A, Extreme Ultraviolet Spectroheliograph, door was pinned open, and the experiment S-054, X-ray Spectrographic Telescope, filter was moved.

The third extravehicular activity, accomplished on visit day 44, was about 3 1/2 hours in duration and included Comet Kohoutek photography utilizing experiments S-201K, Extreme Ultraviolet Electronographic Camera, and the T-025K, Coronagraph Contamination Measurements. Also, the sun was photographed using experiment S-020, X-ray/Ultraviolet Solar Photography.

A fourth extravehicular activity is planned for visit day 79 to retrieve the Apollo Telescope Mount film and to perform the S-020, X-ray Solar Photography, and the S-201K, Extreme Ultraviolet Electronographic Camera, experiments.

Comet Kohoutek observations were made from within the SWS utilizing the S-019K, Kohoutek Emission and Absorption Spectra, the S-201K, Extreme Ultraviolet Electronographic Camera, the S-063, Ultraviolet Airglow Horizon Photography, and the T-025, Coronagraph Contamination Measurements, experiments. Data were obtained from experiments S-149, Particle Collection, S-230, Magnetosphere Particle Composition, and M-509, Astronaut Maneuvering Unit.

Medical experiments were performed to assess the effect of an 85-day duration space visit. Included were a hematology and immunology program, a mineral balance assessment, an evaluation of the changes in hormonal and associated fluid and electrolyte parameters, the extent of bone mineral loss, the cardiovascular effects utilizing the lower body negative pressure and the vectorcardiogram experiments, and an assessment of the metabolic activity.

Earth Resources Experiment Package activities were continued throughout the visit. All experiment coverage was normal with the exception of the experiment S-193, Microwave Radiometer/Scatterometer and Altimeter, which failed during the second visit, consequently the antenna was pinned in the pitch axis during the first extravehicular activity of the third visit. Also, experiment S-190A, Multispectral Camera Facility, data were lost during the first 11 passes of the third visit because of a procedural error.

Undocking, CSM deorbit, and command module landing is planned for visit day 85, February 8 at 20:15:00 UT in the Pacific Ocean, southwest of San Diego, California.

APPENDIX A ATMOSPHERE

A.1 SUMMARY

This appendix presents a summary of the atmospheric environment at launch time of the SA-208/SL-4. The format of these data is similar to that presented on previous launches of Saturn Vehicles to permit comparisons. Surface and upper level winds, and thermodynamic data near launch time are given.

A.2 GENERAL ATMOSPHERIC CONDITIONS AT LAUNCH TIME

During the morning launch of Skylab-4, the Kennedy Space Center (KSC) launch area was experiencing mild temperatures, good visibility conditions, and gentle surface winds. Most of Florida was under the influence of a weakening surface high pressure ridge at launch time. A cold front, extending out of a low pressure area in Connecticut, was located through Tallahassee, oriented northeast-southwest, as shown in the surface synoptic weather map of Figure A-1. Surface winds in the KSC area were light and southwesterly as given in Table A-1. Wind flow aloft is shown in Figure A-2 (500 millibar level). The maximum wind belt was located north of Florida, giving less intense wind flow aloft over the KSC area.

A.3 SURFACE OBSERVATIONS AT LAUNCH TIME

At launch time skies were clear (less than 1/10 altocumulus at 13,000 ft) with visibility 10 miles. Neither precipitation nor lightning were observed at launch time.

Surface ambient temperature was 295°K (72.0°F) with 79% relative humidity. During ascent the vehicle did not pass through any clouds. All surface observations at launch time are summarized in Table A-1. Solar radiation data for the days of November 15 and 16, 1973 are given in Table A-2.

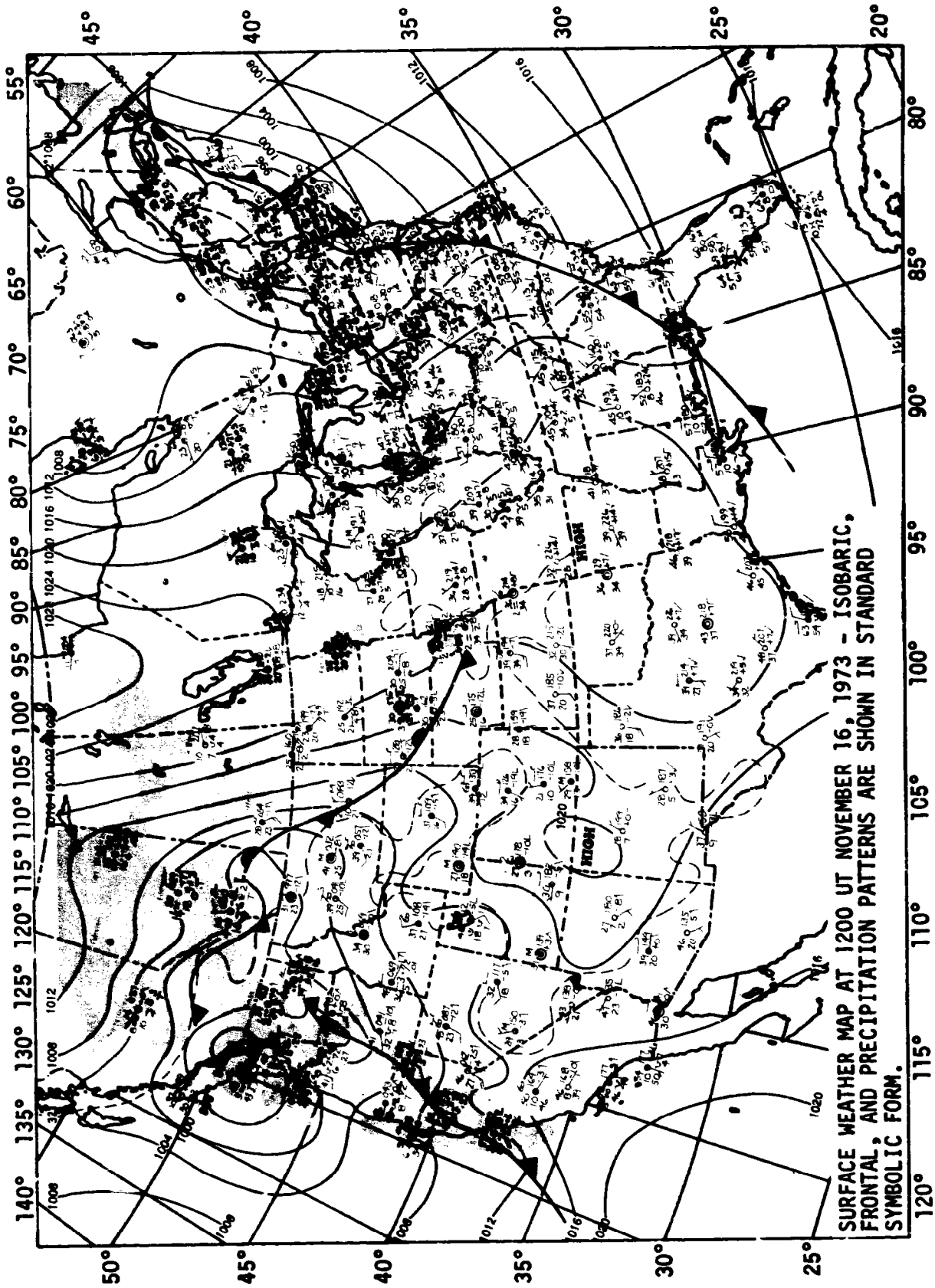


Figure A-1. Surface Weather Map Approximately 2 Hours Before Launch of SA-208/SL-4.

Table A-1. Surface Observations at SA-208 Launch Time

LOCATION**	TIME AFTER T-0 (min)	PRES-SURE N/cm ² (psia)	TEM-PERATURE °K (°F)	DEW POINT °K (°F)	RELATIVE HUMIDITY (%)	VISI-BILITY km (miles)	SKY COVER			WIND*	
							CLOUD AMOUNT	CLOUD TYPE	HEIGHT OF BASE METERS (feet)	SPEED m/s (knots)	DIRECT-ION (deg)
NASA 150 m Ground Wind Tower Winds measured at 16.5 m (54 ft)	0	--	--	--	--	16 (10)	Clear			4.4# (8.5)	250#
MSOB Kennedy Space Center Winds measured at 41.1 m (135 ft)	0	10.186 (14.77)	295.4 (72.0)	291.5 (65.0)	79	--	--	--	--	3.6## (7.0)	220##
KSC AFS*** Surface Measurements 5 m (16.4 ft) level	13	10.169 (14.75)	295.9 (72.9)	290.9 (63.9)	73	--	--	--	--	2.0## (3.9)	240##
Pad 39B Lightpole NW 18.3 m (60.0 ft)	0	--	--	--	--	--	--	--	--	3.6 (7.0)	202
Pad 39B LUT W 161.5 m (530 ft)	0	--	--	--	--	--	--	--	--	3.9 (7.6)	237

* Instantaneous readings at T-0, unless otherwise noted.
 ** Altitudes of wind measurements are above natural grade.
 # 30 minute average about T-0.
 *** Balloon release site.
 ## 1 minute average.

A-3



Figure A-2. 500 Millibar Map Approximately 2 Hours Before Launch of SA-208/SL-4

Table A-2. Solar Radiation at SA-208 Launch Time, Launch Pad 39B

DATE	HOUR ENDING EST	TOTAL HORIZONTAL SURFACE g-cal/cm ² -min	NORMAL INCIDENT g-cal/cm ² -min	DIFFUSE (SKY) g-cal-cm ² -min
November 15, 1973	06.00	0.00	0.00	0.00
	07.00	0.01	0.00	0.01
	08.00	0.11	0.12	0.08
	09.00	0.31	0.29	0.19
	10.00	0.61	0.35	0.42
	11.00	0.67	0.23	0.52
	12.00	0.95	0.88	0.35
	13.00	1.02	0.99	0.37
	14.00	0.95	0.91	0.42
	15.00	0.68	0.59	0.40
	16.00	0.47	0.69	0.27
	17.00	0.23	0.56	0.18
	18.00	0.02	0.03	0.02
19.00	0.00	0.00	0.00	
November 16, 1973	06.00	0.00	0.00	0.00
	07.00	0.01	0.00	0.01
	08.00	0.16	0.12	0.13
	09.00	0.43	0.71	0.13
	10.00	0.70	0.79	0.26

A.4 UPPER AIR MEASUREMENTS

Data were used from three of the upper air wind systems to compile the final meteorological tape. Table A-3 summarizes the wind data systems used. Only the Rawinsonde and the Loki Dart meteorological rocket data were used in the upper level atmospheric thermodynamic analyses. The 1430 UT rocket measured only the wind parameters, with the thermodynamic results failing. Two subsequent rockets were also fired, but they also failed. Therefore, the thermodynamic parameters used, were obtained from the 1300 UT rocket flight of November 15, 1973.

Table A-3. Systems Used to Measure Upper Air Wind Data for SA-208

TYPE OF DATA	RELEASE TIME		PORTION OF DATA USED			
	TIME (UT) (hours:min)	TIME AFTER T+0 (min)	START		END	
			ALTITUDE m (ft)	TIME AFTER T+0 (min)	ALTITUDE m (ft)	TIME AFTER T+0 (min)
FPS-16 Jimsphere	14:15	14	125 (410)	14	15,250 (50,032)	66
Rawinsonde	14:14	13	15,500 (50,852)	64	24,750 (81,200)	94
Loki Dart	14:30	29	59,000 (193,567)	29	25,000 (82,020)	54

A.4.1 Wind Speed

Wind speeds were light, being 2.0 m/s (3.9 knots) at the surface and increasing to a maximum of 43.5 m/s (84.5 knots) at 12.35 kilometers (40,518 ft). The maximum wind speed was near the eighty fourth percentile level for November. The winds decreased above this altitude, and then became stronger again as shown in Figure A-3. The overall maximum speed was 73.0 m/s (141.9 knots) at 52.00 kilometers (170,602 ft) altitude. Maximum dynamic pressure occurred at 10.72 kilometers (35,178 ft); the wind speed and direction was 27.9 m/s (54.2 knots), from 266 degrees. SL-4 pad 39B wind data is available in MSFC memorandum, S&E-AERO-YT-36-73.

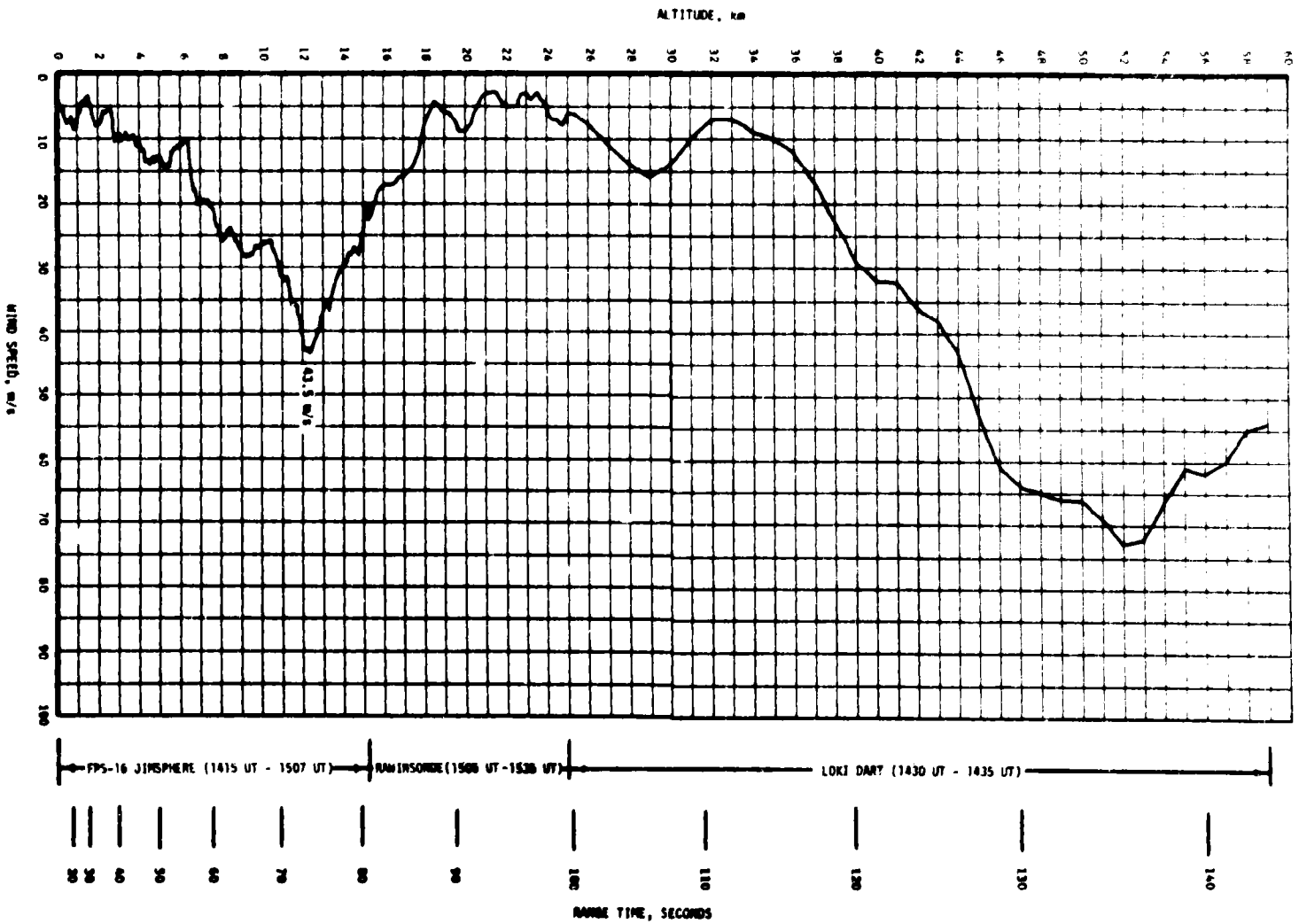


Figure A-3. Scalar Wind Speed at Launch Time of SA-208/SL-4

A.4.2 Wind Direction

At launch time, the surface wind direction was from 240 degrees. The wind directions had a westerly component throughout the troposphere and stratosphere. Figure A-4 shows the complete wind direction versus altitude profile. As shown in Figure A-4, wind directions became variable at altitudes with low wind speeds.

A.4.3 Pitch Wind Component

The pitch wind velocity component (component parallel to the horizontal projection of the flight path) at the surface was a tailwind of 2.0 m/s (3.9 knots). The maximum wind, in the altitude range of 8 to 16 kilometers (26,247 to 52,493 ft), was a tailwind of 41.1 m/s (79.8 knots) observed at 12.20 kilometers (40,026 ft) altitude. See Figure A-5.

A.4.4 Yaw Wind Component

The yaw wind velocity component (cross range wind component) at the surface was a wind from the left of 0.2 m/s (0.4 knots). The peak yaw wind velocity in the high dynamic pressure region was from the left of 17.3 m/s (33.6 knots) at 12.65 kilometers (41,502 ft). See Figure A-6.

A.4.5 Component Wind Shears

The largest component wind shear ($\Delta h = 1000$ m) in the maximum dynamic pressure region (max Q) was a pitch shear of 0.0131 sec^{-1} at 11.50 kilometers (37,729 ft). The largest yaw wind shear, at these lower levels, was 0.0078 sec^{-1} at 13.53 kilometers (44,373 ft). See Figure A-7.

A.4.6 Extreme Wind Data in the High Dynamic Region

A summary of the maximum wind speeds and wind components is given in Table A-4. A summary of the extreme wind shear values ($\Delta h = 1000$ meters) is given in Table A-5.

A.5 THERMODYNAMIC DATA

Comparisons of the thermodynamic data taken at SA-208 launch time with the annual Patrick Reference Atmosphere, 1963 (PRA-63) for temperature, pressure, density, and Optical Index of Refraction are shown in Figures A-8 and A-9, and are discussed in the following paragraphs.

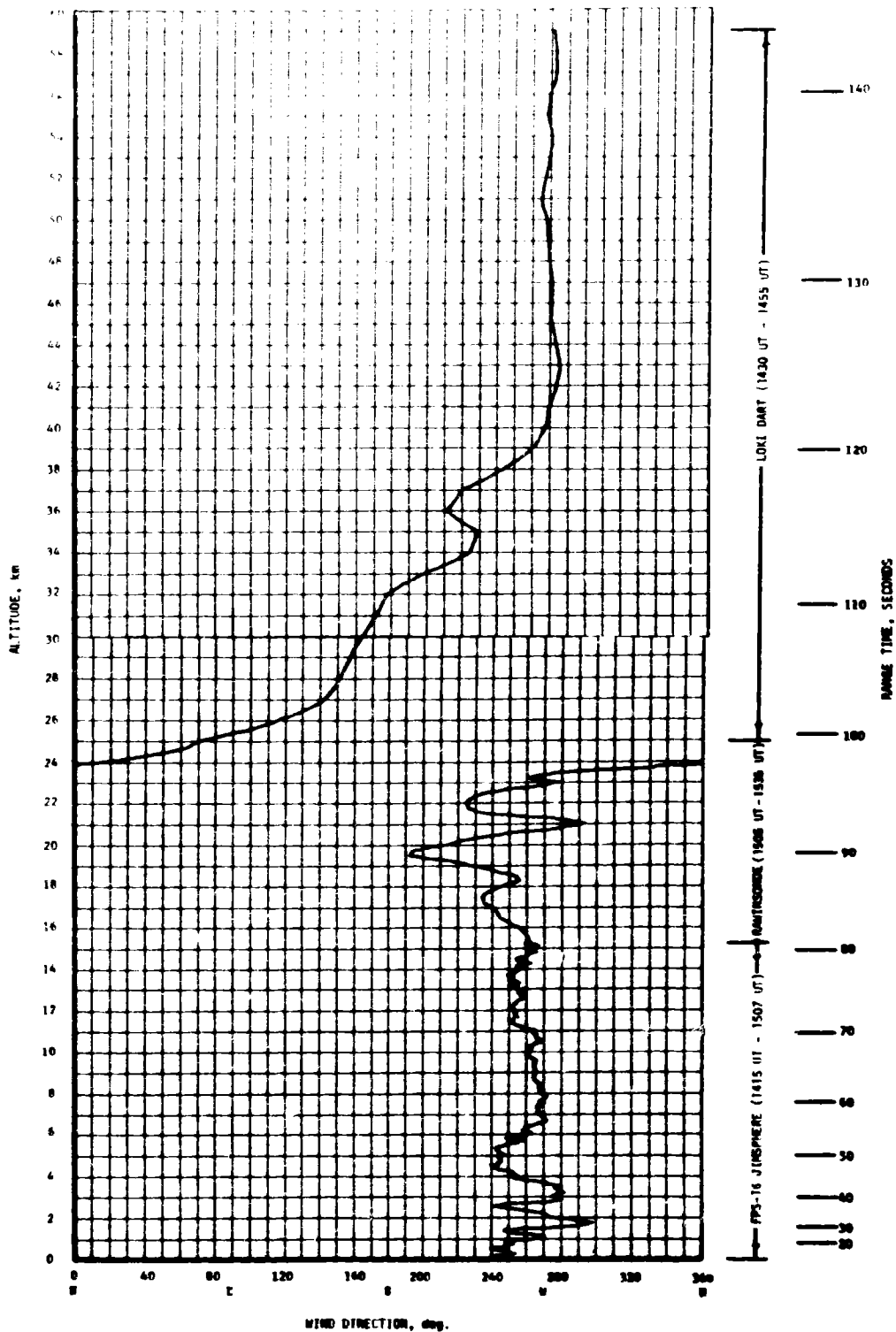


Figure A-4. Wind Direction at Launch Time of SA-208/SL-4

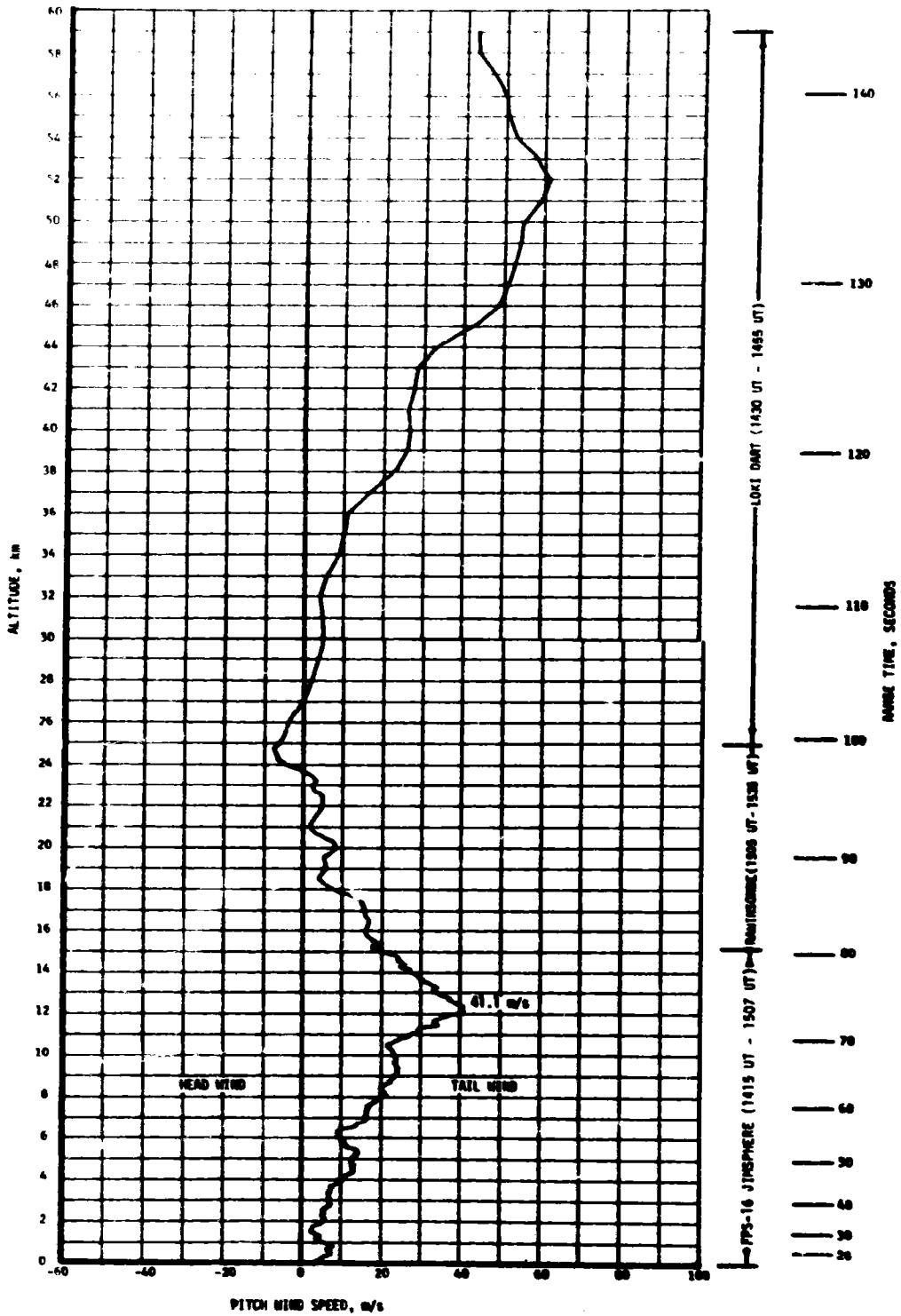


Figure A-5. Pitch Wind Velocity Component (W_x) at Launch Time of SA-208/SL-4

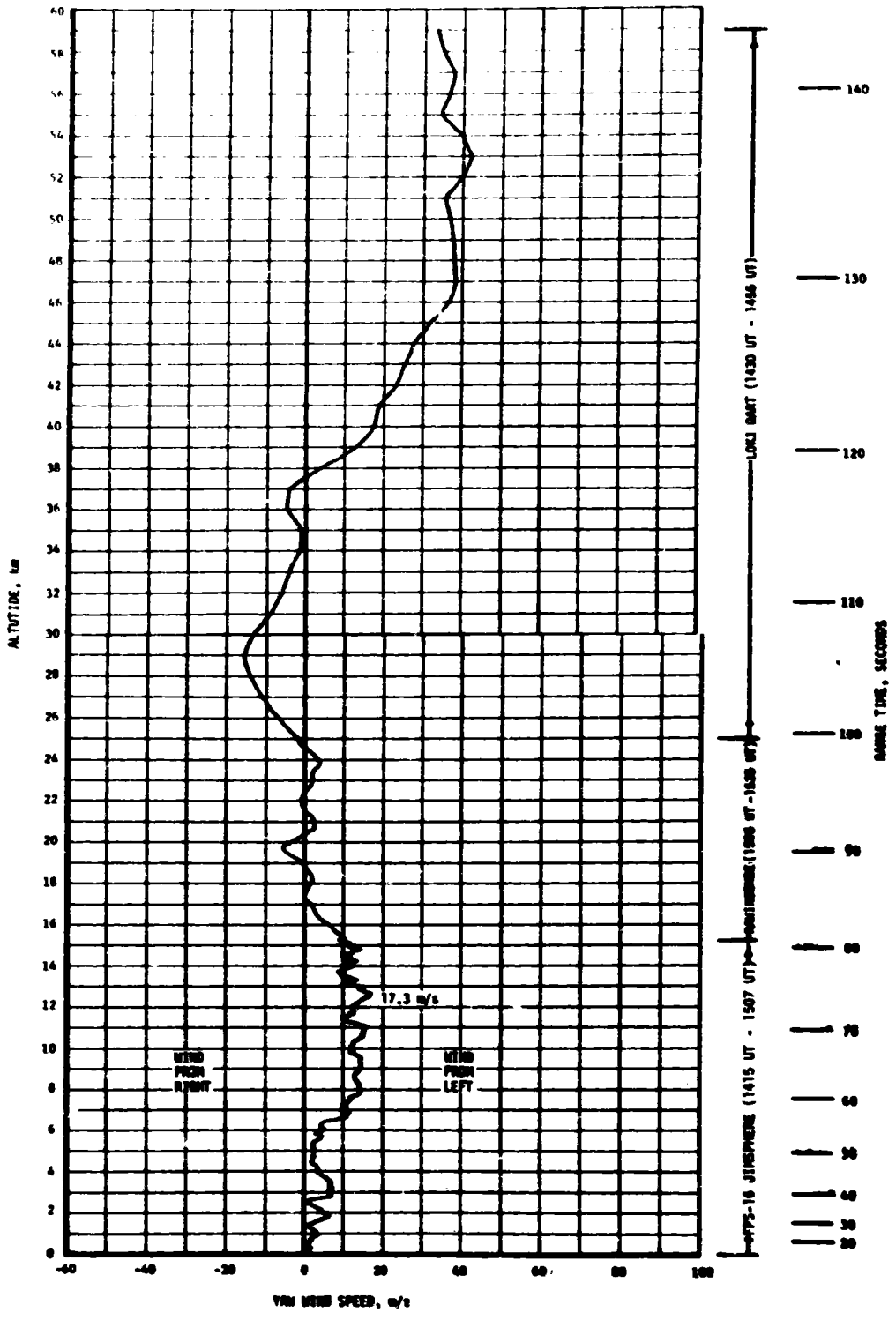


Figure A-6. Yaw Wind Velocity Component (W_z) at Launch Time of SA-208/SL-4

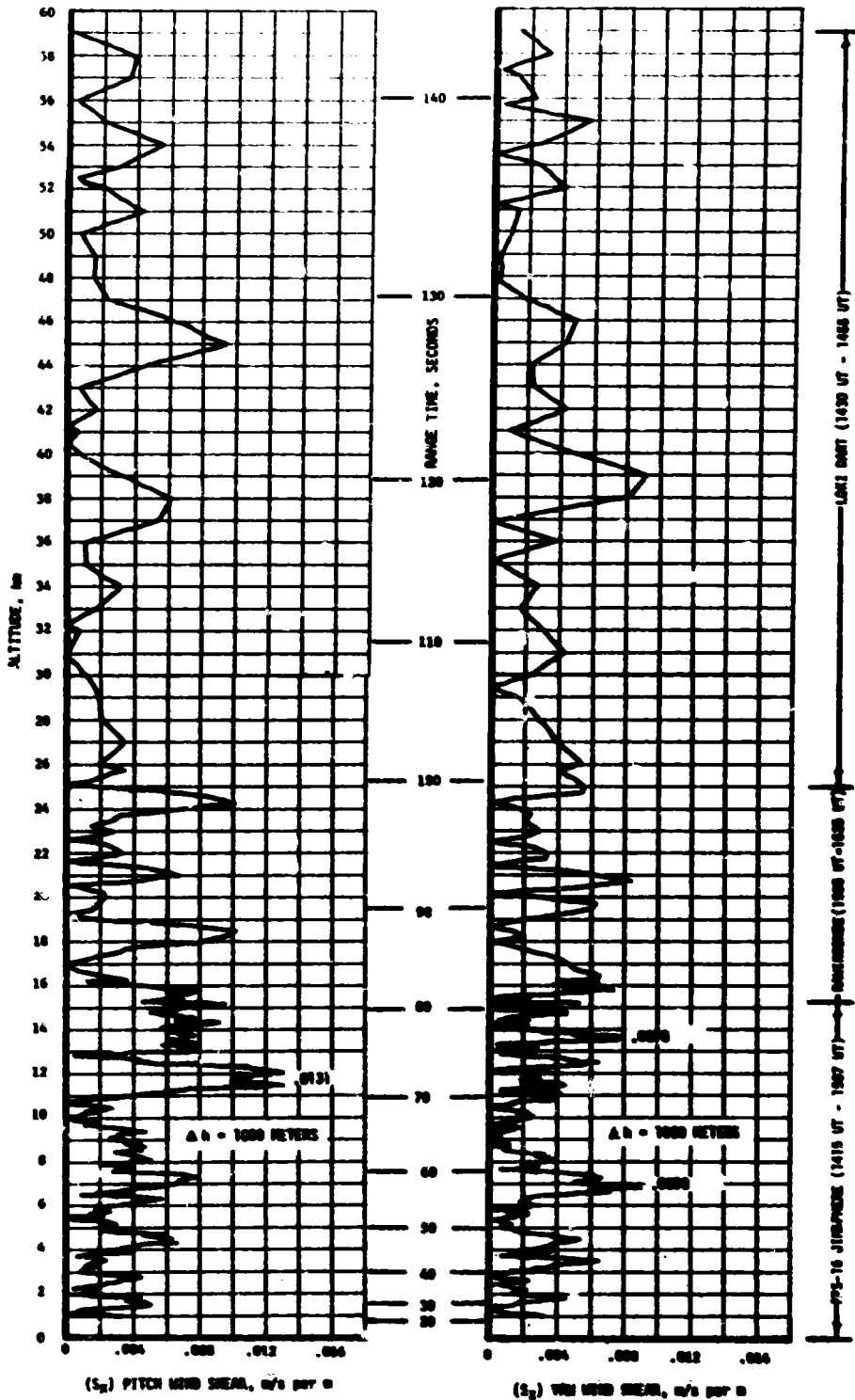


Figure A-7. Pitch (S_x) and Yaw (S_y) Component Wind Shears at Launch Time of SA-208/SL-4

Table A-4. Maximum Wind Speed in High Dynamic Pressure Region for Saturn Launch Vehicles 201 through 208

VEHICLE NUMBER	MAXIMUM WIND			MAXIMUM WIND COMPONENTS			
	SPEED m/s (knots)	DIR (deg)	ALT km (ft)	PITCH (W_x) m/s (knots)	ALT km (ft)	YAW (W_z) m/s (knots)	ALT km (ft)
SA-201	70.0 (136.1)	250	13.75 (45,100)	57.3 (111.4)	13.75 (45,100)	-43.3 (-84.2)	13.25 (43,500)
SA-203	18.0 (35.0)	312	13.00 (42,600)	11.1 (21.6)	12.50 (41,000)	16.6 (32.3)	13.25 (43,500)
SA-202	16.0 (31.1)	231	12.00 (39,400)	10.7 (20.8)	12.50 (41,000)	-15.4 (-29.9)	10.25 (33,600)
SA-204	35.0 (68.0)	288	12.00 (39,400)	32.7 (63.6)	15.25 (50,000)	20.6 (40.0)	12.00 (39,400)
SA-205	15.6 (30.3)	309	14.60 (44,500)	15.8 (30.7)	12.08 (36,800)	15.7 (30.5)	15.78 (47,500)
SA-206	42.0 (81.7)	286	13.38 (43,881)	27.9 (54.2)	14.93 (48,966)	36.3 (70.6)	13.35 (43,799)
SA-207	13.2 (25.7)	014	13.83 (45,357)	-11.7 (-22.7)	12.43 (40,764)	9.6 (18.6)	8.60 (28,215)
SA-208	43.5 (84.5)	254	12.35 (40,18)	41.1 (79.8)	12.20 (40,026)	17.3 (33.6)	12.65 (41,502)

Table A-5. Extreme Wind Shear Values in the High Dynamic Pressure Region for Saturn Launch Vehicles 201 through 208

VEHICLE NUMBER	PITCH PLANE		YAW PLANE	
	SHEAR (m/s per 1000 m)	ALTITUDE km (ft)	SHEAR (m/s per 1000 m)	ALTITUDE km (ft)
	SA-201	0.0206	16.00 (52,500)	0.0205
SA-203	0.0104	14.75 (48,400)	0.0079	14.25 (46,800)
SA-202	0.0083	13.50 (44,300)	0.0054	13.25 (43,500)
SA-204	0.0118	16.75 (55,000)	0.0116	14.00 (45,900)
SA-205	0.0113	15.78 (48,100)	0.0085	15.25 (46,500)
SA-206	0.0145	14.93 (48,966)	0.0141	14.38 (47,162)
SA-207	0.0063	10.15 (33,300)	0.0083	15.50 (50,852)
SA-208	0.0131	11.50 (37,729)	0.0078	13.53 (44,373)

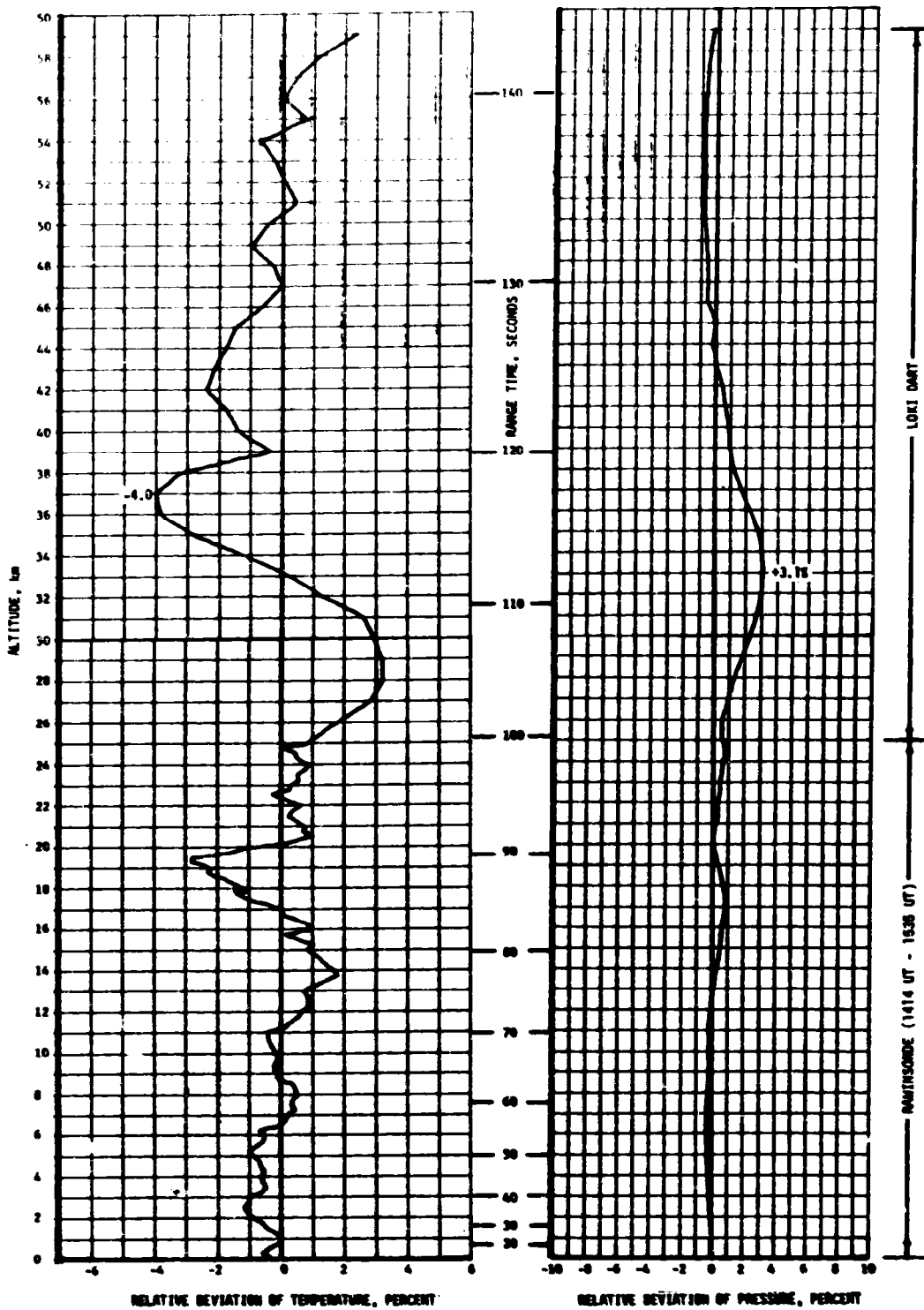


Figure A-8. Relative Deviation of Temperature and Pressure from the PRA-63 Reference Atmosphere, SA-208/SL-4

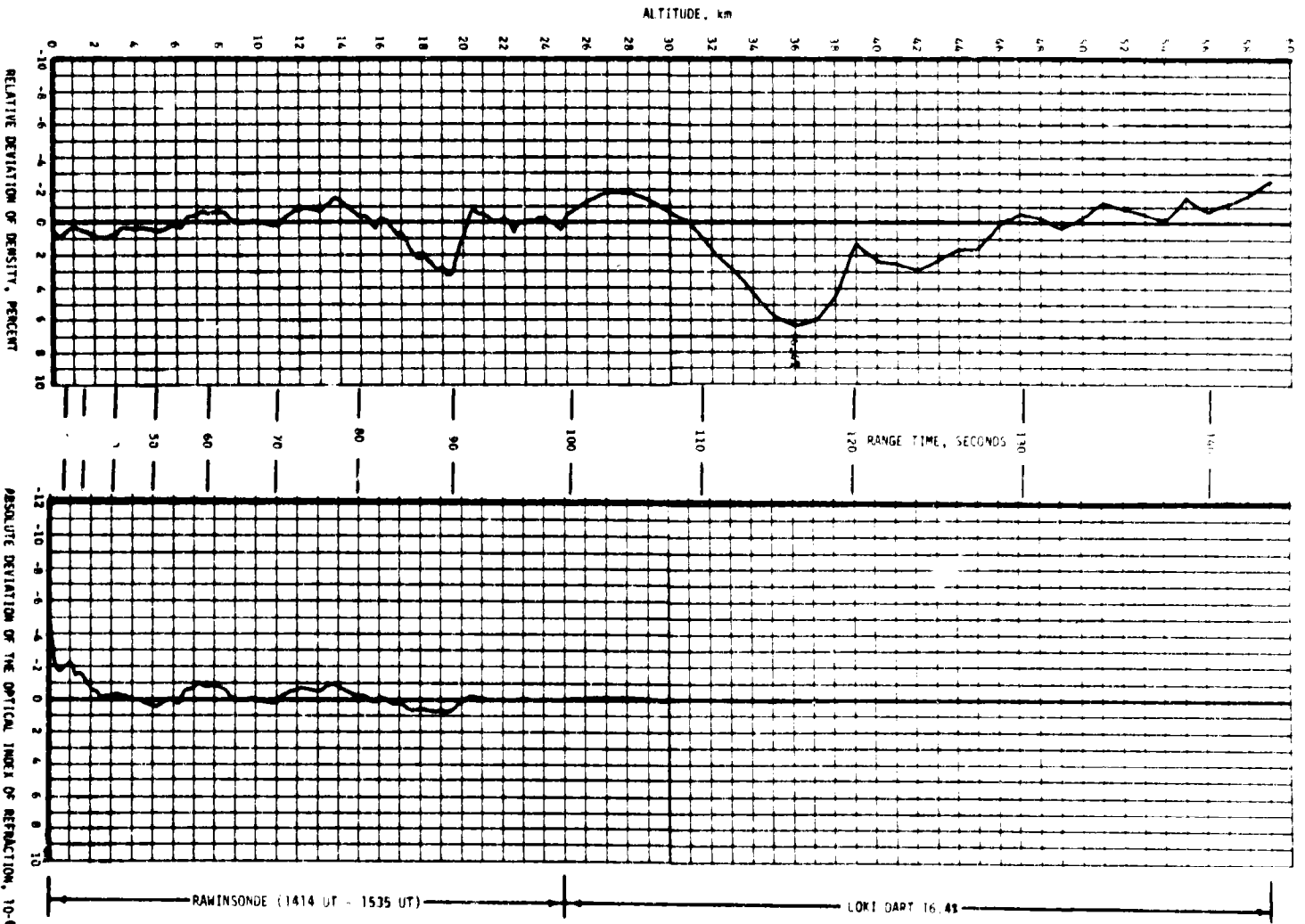


Figure A-9. Relative Deviation of Density and Absolute Deviation of the Index of Refraction from the PRA-63 Reference Atmosphere, SA-208/SL-4

A.5.1 Atmospheric Temperature

Atmospheric temperature differences were small, deviating less than 4 percent from the PRA-63 below 59 kilometers (193,567 ft) altitude. In the max Q region, temperatures did deviate to +1.78 percent of the PRA-63 value at 13.75 km (45,111 ft). Air temperatures generally deviated about the PRA-63, versus altitude, as shown in Figure A-8.

A.5.2 Atmospheric Pressure

Atmospheric pressure deviations were small in the lower levels of the atmosphere. Deviations were less than 1 percent of the PRA-63 below 27 kilometers (88,581 ft) altitude. See Figure A-8, which shows the entire pressure profile with altitude.

A.5.3 Atmospheric Density

Atmospheric density deviations were small in the lower levels, generally being within 3 percent of the PRA-63 below 33 kilometers (108,266 ft) altitude. The density deviation reached a maximum of 6.36 percent greater than the PRA-63 value at 36.00 kilometers (118,109 ft) as shown in Figure A-9.

A.5.4 Optical Index of Refraction

The Optical Index of Refraction at the surface was 4.64×10^{-6} units lower than the corresponding value of the PRA-63. The deviation then became less negative with altitude, and approximated the PRA-63 at high altitudes, as is shown in Figure A-9.

A.6 COMPARISON OF SELECTED ATMOSPHERIC DATA FOR SATURN IB LAUNCHES

A summary of the atmospheric data for each Saturn IB launch is shown in Table A-6.

Table A-6. Selected Atmospheric Observations for Saturn Launch Vehicles 201 through 208 at Kennedy Space Center, Florida

VEHICLE NUMBER	VEHICLE DATA			SURFACE DATA						INFLIGHT CONDITION		
	DATE	TIME NEAREST MINUTE	LAUNCH COMPLEX	PRESSURE N/cm ²	TEMPERATURE °C	RELATIVE HUMIDITY PERCENT	WIND*		CLOUDS	MAXIMUM WIND IN 8-16 km LAYER		
							SPEED m/s	DIR deg		ALTITUDE km	SPEED m/s	DIRECTION deg
SA-201	26 Feb 66	1112 EST	34	10.217	16.1	48	6.5	330	Clear	13.75	70.0	250
SA-203	5 Jul 66	0953 EST	37B	10.166	30.2	69	6.3	242	1/10 Cumulus 1/10 Altocumulus 1/10 Cirrus	13.00	18.0	312
SA-202	25 Aug 66	1216 EST	34	10.173	30.0	70	4.1	160	8/10 Cumulus 1/10 Cirrus	12.00	16.0	231
SA-204	22 Jan 68	1748 EST	37B	10.186	16.1	93	4.2	45	3/10 Cumulus	12.00	35.0	288
SA-205	11 Oct 68	1103 EDT	34	10.180	28.3	65	10.2	90	3/10 Cumulonimbus	14.60	15.6	309
SA-206	25 May 73	0900 EDT	39B	10.105	26.1	85	5.5 6.1	212 224	5/10 Fractocumulus 5/10 Altocumulus 1/10 Cirrus	13.38	42.0	286
SA-207	28 Jul 73	0711 EDT	39B	10.162	23.9	93	2.6 6.9	264 274	9/10 Altocumulus 5/10 Cirrus	13.83	13.2	014
SA-208	16 Nov 73	0901 EST	39B	10.186	22.2	79	3.6 3.9	202 237	Clear	12.35	43.5	254

* Instantaneous readings from charts at T-0 (unless otherwise noted) from anemometers on launch pad light poles at the following levels: Pad 34 at 19.5 m (59.4 ft), Pad 37B at 20.7 m (63.1 ft), and Pad 39B at 18.3 m (60.0 ft). Beginning with SA-206, wind measurements were required at the 161.5 m (530 ft) level from anemometer charts on the LUT. These instantaneous LUT winds are given directly under the listed pad light pole winds. Heights of anemometers are above natural grade.

APPENDIX B

SA-208 SIGNIFICANT CONFIGURATION CHANGES

B.1 INTRODUCTION

The SA-208 launch vehicle configuration was essentially the same as the SA-207 configuration with significant exceptions shown in Tables B-1 through B-3. The basic vehicle description is presented in Appendix B of the Saturn IB Launch Vehicle Flight Evaluation Report SA-206, Skylab-2 MPR-SAT-FE-73-3.

Table B-1. S-IB Significant Configuration Changes

SYSTEM	CHANGE	REASON
Structures	<p>Repair of crack in channel, upper outrigger assembly, fin position 4. Remove 1-in. x 3-3/4-in. coupon containing crack and install spacer and splice plate.</p> <p>Add reinforcing blocks at fin rear spar attachment fittings. Shim mating surfaces between fin and outrigger as required.</p> <p>Rework of fuel tanks F3 and F4</p>	<p>Crack detected on the stage at KSC during special inspection conducted after imperfection noticed in surface of same channel on stage S-IB-9. Channel is made from stress corrosion susceptible material 7178-T6 AL alloy forging. Removed cracked area to preclude propagation.</p> <p>Cracks detected in rear spar attachment fittings of all eight fins during post CDDT inspection. All eight fins replaced; reinforcing blocks added to provide fail-safe (i.e. alternate loads path) feature in event cracks occur after last preflight inspection.</p> <p>Upper bulkheads of fuel tanks F3 and F4 were re-formed pneumatically to original contour following accidental damage.</p>
Propulsion and Mechanical	<p>Reduction in fuel vent valve relief pressure and prepressurization pressure during launch operations.</p> <p>Addition of expansion loop in fuel vent sensing lines.</p>	<p>Accidental damage to upper bulkheads on fuel tanks F3 and F4 necessitated lowering relief setting from 21.0-21.5 psig to 19.0-19.1 psig to maintain an adequate structural margin. Maximum prepressurization pressure reduced from 18.5 psig to 18 psig.</p> <p>Accidental damage to upper bulkheads of fuel tanks F3 and F4 caused the bulkheads to have more deflection than normal causing a strain on the fuel vent sensing system.</p>
Instrumentation	<p>Modification of multiplexer 270 DC-DC converter. Changes include:</p> <ul style="list-style-type: none"> • Removing capacitor C-15 from the circuit • Removing capacitor C-2 from the circuit • Changing Q3 from 2N2218 to JAN2N2218A. 	<p>To improve the reliability of the DC-DC converter in the 270 multiplexer.</p>
Electrical	<p>Two plug-in type J-boxes, 9A10 and 9A11, used for interconnection of the four groups of temperature sensors, have been deleted.</p> <p>1N2150A diodes replaced in propulsion system distributor 9A1 by 51N1204A diodes.</p>	<p>Circuitry of the fire detection system has been simplified. Interconnection is accomplished in cable 9W146.</p> <p>The approved vendor for 1N2150A diodes has closed operations and the diodes are unavailable. 51N1204A diodes are used in other Saturn stages and electrical characteristics equal or exceed those of the 1N2150A.</p>

Table B-2. S-IVB Significant Configuration Changes

SYSTEM	CHANGE	REASON
Propulsion	Modifications to increase the thrust level from 225,000 pounds to 230,000 pounds. These modifications bring the S-IVB-208 J-2 engine up to the thrust level used on the S-IVB engines of AS-503 thru AS-512.	Improved performance for greater payload capability.

Table B-3. IU Significant Configuration Changes

SYSTEM	CHANGE	REASON
Structures	P-10 gas supply panel at location 14 deleted.	S-150 Experiment deleted.
Instrumentation and Communications	C-Band Transponder 601A635 moved to Panel 23 and renumbered 6U3A635.	S-150 Experiment deleted.
	S-150 experiment components listed below have been deleted: <ul style="list-style-type: none"> ● ASAP Interface Unit 603A83 ● UDAS Computer Interface Unit 603A84 ● ASAP Memory Assembly 603A85 ● ASAP DC-DC Converter 603A86 ● ASAP Tape Recorder 603A87 ● Experiment Control Distributor 603A88 ● S-150 X-Ray Sensor Unit 603A82 ● Signal Conditional Assy. 601A679 	S-150 Experiment deleted.
Environmental Control System	Re-potted GN ₂ Solenoid Valve Connector.	Prevent possible abrasion of electrical wiring.
	Sublimator vent baffle removed and P-10 gas supply system deleted.	S-150 Experiment deleted.
Flight Program		
S-150 Galactic X-Ray Experiment	Deletion of alternate sequences, maneuvers, and data dumps peculiar to the S-150 experiment	S-150 Experiment deleted.
S-16 Yaw Guidance Commands	Predetermined yaw commands will be initiated by the flight program between 10.3 and 130 seconds after liftoff.	Minimizes yaw angle of attack through maximum dynamic pressure.
S-IVB/IU De-Orbit DCS Command	The De-orbit DCS Command now consists of the following: <ul style="list-style-type: none"> ● Three Dump Options <ul style="list-style-type: none"> LOX Dump only LOX and Hydrogen Dump No Dump, Safing Sequence only ● LOX Hydrogen Dump Termination <ul style="list-style-type: none"> Dump Duration Time Change in Measured Velocity 	Expands De-orbit capability by providing additional methods for accomplishing De-orbit.
Pre-Programmed Retrograde Maneuver	At T ₄ + 700 seconds the Flight Program will command a 180 pitch and 180 degree roll maneuver.	This maneuver will decrease the possibility of venting liquid propellant overboard.

APPROVAL

SATURN IB LAUNCH VEHICLE FLIGHT EVALUATION REPORT

SA-208, SKYLAB-4

By Saturn Flight Evaluation Working Group

The information in this report has been reviewed for security classification. Review of any information concerning Department of Defense or Atomic Energy Commission programs has been made by the MSFC Security Classification Officer. The highest classification has been determined to be unclassified.

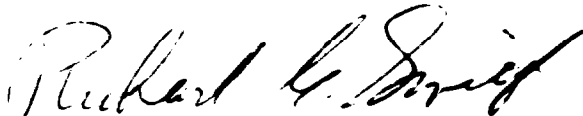


Stanley L. Fragge
Security Classification Officer

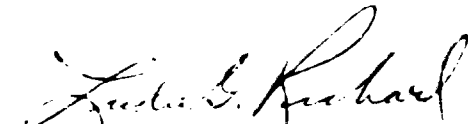
This report has been reviewed and approved for technical accuracy.



George H. McKay, Jr.
Chairman, Saturn Flight Evaluation Working Group



Richard G. Smith
Saturn Program Manager



Richard G. Smith
Director, Science and Engineering

END

DATE

FILMED

JAN 2 1975